

Universität  
Rostock



Traditio et Innovatio

# Neue CN-funktionalisierte Borat- Anionen – Anwendungen in ionischen Flüssigkeiten und Koordinationspolymeren

## Kumulative Dissertation

zur

Erlangung des akademischen Grades

*doctor rerum naturalium (Dr. rer. nat.)*

der Mathematisch-Naturwissenschaftlichen Fakultät

der Universität Rostock

vorgelegt von Markus Karsch, geb. am 06.11.1985 in Rostock

Rostock, 13.12.2013

Die vorliegende Arbeit wurde in der Zeit von Oktober 2010 bis Dezember 2013 am Institut für Chemie der Universität Rostock am Lehrstuhl für Anorganische Chemie in der Arbeitsgruppe von Prof. Dr. Axel Schulz angefertigt.

1. Gutachter: Prof. Dr. Axel Schulz

2. Gutachter: Prof. Dr. Wolfram Seidel

## **ERKLÄRUNG**

Ich versichere hiermit an Eides statt, dass ich die vorliegende Arbeit selbstständig angefertigt und ohne fremde Hilfe verfasst habe. Dazu habe ich keine außer den von mir angegebenen Hilfsmitteln und Quellen verwendet und die den benutzten Werken inhaltlich und wörtlich entnommenen Stellen als solche kenntlich gemacht.

Rostock, 13.12.2013

.....  
Markus Karsch

## **Danksagung**

Mein ganz besonderer Dank gilt Herrn Prof. Dr. Axel Schulz für die Vergabe des interessanten Themas, das in mich gesetzte Vertrauen sowie den hilfreichen und informativen Gesprächen. Zusammen mit der wissenschaftlichen Freiheit im Rahmen meines Themas gelten all diese Beiträge als wertvolle Grundlage der vorliegenden Arbeit.

Bei Herrn Dr. Jörg Harloff möchte ich mich für die Betreuung meiner Arbeit, den wissenschaftlichen Diskussionen und den Stickstoffadsorptionsmessungen bedanken.

Herrn Dr. Alexander Villinger, Herrn Christian Hering und Frau Isabel Schicht gilt ausdrücklicher Dank für die Vermessung der Einkristalle und die Verfeinerung der Röntgenstrukturen. Herrn Dr. Ronald Wustrack möchte ich für die Bereitstellung und Einrichtung benötigter Software danken.

Für die angenehme und heitere Atmosphäre sowie der hilfreichen Zusammenarbeit im Labor möchte ich mich besonders bei Herrn Thomas Jantz und Herrn Sebastian Lorenz bedanken. Meinen Dank möchte ich auch allen weiteren Mitarbeitern im Arbeitskreis Schulz für die freundliche Zusammenarbeit und der hilfreichen Unterstützung aussprechen.

Für die unvergesslichen Erlebnisse bei der Betreuung des Grundpraktikums möchte ich mich bei meinen Mitbetreuern Herrn Dr. Jörg Harloff, Frau Regina Brosin und Sebastian Lorenz bedanken.

Des Weiteren möchte ich mich bei der analytischen Abteilung des Hauses bedanken. Bei Frau Pries und Frau Duncker für die Durchführung der Elementaranalysen, bei Frau Weihs für die Anfertigung der IR-Spektren, bei Herrn Dr. Michalik, Frau Schimanski und Frau Goronzi für die Anfertigung der NMR-Spektren und bei Herrn Thomas, Herrn Ruhmann, Herrn Reiß und Herrn Dr. Ronald Wustrack für die Vermessung der Raman-Proben.

Mein persönlicher Dank geht an meine Freunde und meine Familie, die mich abseits des Studiums und der Arbeit jederzeit sowohl tatkräftig, als auch mental unterstützt haben.

## **Zusammenfassung**

In der vorliegenden Dissertation werden die Ergebnisse aus der Untersuchung der Chemie CN-funktionalisierter Borat-Anionen präsentiert. Eine Reihe an diversen Borat-Anionen mit terminalen CN-Gruppen wurde zum einen auf klassischem Wege, ausgehend von  $\text{NaBH}_4$  und unterschiedlichen aliphatischen oder aromatischen Hydroxynitrilen, synthetisiert. Zum anderen wurde eine Syntheseroute zur Darstellung von Polynitril-Anionen erfolgreich angewendet, wodurch cyanhydrin-analoge Liganden zugänglich sind. Die Synthese der ersten porösen Koordinationspolymere, basierend auf CN-funktionalisierten Borat-Anionen, wurde anhand von Kristallstrukturanalysen und Stickstoffsorptionsmessungen nachgewiesen. Durch Austausch des Natrium-Kations mit schwach koordinierenden Kationen wurde eine Reihe neuer CN-funktionalisierter ionischer Flüssigkeiten synthetisiert. Sämtliche erhaltenen Verbindungen wurden durch gängige Analysemethoden vollständig charakterisiert, wodurch die Abhängigkeit der thermischen und spektroskopischen Eigenschaften bezüglich des verwendeten Ligandensystems (Struktur-Eigenschaft-Beziehung) aufgezeigt werden konnte. Zudem wurde durch VBT-Berechnungen der Einfluss der verwendeten Liganden auf Gitterenergie, Gitterenthalpie und Standardentropie theoretisch diskutiert.

## **Summary**

This thesis presents experimental and theoretical results from the investigation of the chemistry of CN-functionalized borate-anions. Starting from  $\text{NaBH}_4$  and aliphatic or aromatic hydroxynitriles a wide range of diverse borate-anions with multiple terminal nitrile groups was synthesized. Additionally, a new synthetic route was applied generating borate anions with cyanohydrin analogue ligands. The first permanent porous coordination polymers based on CN-functionalized borate-anions were observed by X-ray diffractometry and sorption experiments. By salt-metathesis reaction with weakly coordinating cations a wide range of new CN-functionalized ionic liquids was synthesized. All new compounds were completely characterized by common analytics. A dependence of the thermal and spectroscopic characteristics according to the utilized ligand system was observed. By VBT-calculations the influence of the ligand system on the lattice potential energy, lattice enthalpy and the standard entropy was discussed.

# Inhalt

Abkürzungsverzeichnis .....	VII
Vom SI-System abweichende Einheiten .....	VII
1 Zielsetzung .....	1
2 Bisheriger Kenntnisstand .....	3
2.1 CN-basierte Addukt-Anionen.....	3
2.2 CN-funktionalisierte ionische Flüssigkeiten .....	6
2.3 CN-basierte Koordinationspolymere.....	8
3 Zusammenfassung der Ergebnisse .....	11
3.1 Synthese CN-funktionalisierter Borat-Anionen .....	11
3.2 Strukturanalytik der Natrium-Borate.....	11
3.3 Allgemeine, thermische und spektroskopische Eigenschaften der Natrium-Borate .....	11
3.4 Stickstoffsorptionsmessungen an lösungsmittelfreien Natrium-Boraten .....	24
3.5 VBT-Berechnungen der Natrium-Borate .....	25
3.6 Darstellung von Addukt-Anionen mit Tris(pentafluorphenyl)boran.....	26
3.7 Darstellung CN-funktionalisierter ionischer Flüssigkeiten .....	28
4 Literaturverzeichnis.....	31
5 Publikationen.....	35
5.1 Molecular Networks Based on CN Coordination Bonds.....	36
5.2 Tetrakis(2-cyanoethoxy)borate – An Alternative to Tetracyanidoborate-Based Ionic Liquids ..	49
5.3 Nitrile-rich Borate Anions – Application in Ionic Liquids.....	58
6 Anhang .....	84

## Abkürzungsverzeichnis

<b>BET</b>	Brunauer-Emmett-Teller	<b>RTIL</b>	<i>Room Temperature Ionic Liquid</i> (Raumtemperatur ionische Flüssigkeit)
<b>BMIm</b>	1-Butyl-3-methylimidazolium	<b>tert</b>	<i>tertiär</i>
<b>DCA</b>	Dicyanamid	<b>TCB</b>	Tetracyanidoborat
<b>DMSO</b>	Dimethylsulfoxid	<b>TCEG</b>	Tetracyanoethylenglykolat
<b>DSC</b>	<i>Differential Scanning Calometry</i> (Dynamische Differenzkalorimetrie)	<b>TCM</b>	Tricyanmethanid
<b>EMIm</b>	1-Ethyl-3-methylimidazolium	<b>TCMel</b>	Tricyanmelaminat
<b>IL</b>	<i>Ionic Liquid</i> (ionische Flüssigkeit)	<b>T<sub>G</sub></b>	Glasübergangspunkt
<b>IR</b>	Infrarot	<b>TGA</b>	Thermogravimetrische Analyse
<b>LM</b>	Lösungsmittel	<b>THF</b>	Tetrahydrofuran
<b>MMIm</b>	1-Ethyl-3-methylimidazolium	<b>T<sub>Smp</sub></b>	Schmelzpunkt
<b>NMR</b>	<i>Nuclear Magnetic Resonance</i> (Kernspinresonanzspektroskopie)	<b>T<sub>Zers</sub></b>	Zersetzungspunkt
<b>OMIm</b>	1-Octyl-3-methylimidazolium	<b>TMS</b>	Trimethylsilyl
<b>ppm</b>	<i>parts per million</i>	<b>VBT</b>	Volumenbasierte Thermodynamik
<b>RT</b>	Raumtemperatur	<b>WCC</b>	<i>Weakly Coordinating Cation</i> (schwach koordinierende Kationen)

## Vom SI-System abweichende Einheiten

Größe	Symbol	Bezeichnung	Umrechnung in SI-Einheit
Frequenz	MHz	Megahertz	1 MHz = 10 <sup>6</sup> s <sup>-1</sup>
	Hz	Hertz	1 Hz = 1 s <sup>-1</sup>
Länge	Å	Ångström	1 Å = 10 <sup>-10</sup> m
Leistung	mW	Milliwatt	1 mW = 10 <sup>-3</sup> kg·m <sup>2</sup> ·s <sup>-3</sup>
Temperatur	°C	Grad Celsius	x °C = (x + 273.15) K
Volumen	ml	Milliliter	1 ml = 1 cm <sup>3</sup> = 10 <sup>-6</sup> m <sup>3</sup>
Wärmemenge	kJ	Kilojoule	1 kJ = 10 <sup>3</sup> m <sup>2</sup> ·kg·s <sup>-2</sup>
Wellenzahl	cm <sup>-1</sup>	reziproke Zentimeter	1 cm <sup>-1</sup> = 100 m <sup>-1</sup>
	h	Stunde	1 h = 3600 s
Zeit	min	Minute	1 min = 60 s

## 1 Zielsetzung

Im Rahmen dieser Arbeit sollten unterschiedlich substituierte und mit Nitril-Gruppen funktionalisierte Anionen entsprechend eines Baukasten-Prinzips untersucht werden (Abbildung 1). Hierbei lag der Fokus auf Borat-Anionen der 2. Generation. Das bekannte Tetracyanidoborat (Anion 1. Generation) und seine Verbindungen sollten dabei als Bezugspunkte und Vergleichsverbindungen dienen.

0. Generation	1. Generation (Pseudohalogenide)	2. Generation (Spacer-Anionen)
F <sup>-</sup>	Delokalisierung	Spacer
OH <sup>-</sup>	[O–CN] <sup>-</sup>	[O–Spacer–CN] <sup>-</sup>
NH <sub>2</sub> <sup>-</sup>	[N(CN) <sub>2</sub> ] <sup>-</sup>	[N(Spacer–CN) <sub>2</sub> ] <sup>-</sup>
CH <sub>3</sub> <sup>-</sup>	[C(CN) <sub>3</sub> ] <sup>-</sup>	[C(Spacer–CN) <sub>3</sub> ] <sup>-</sup>
BH <sub>4</sub> <sup>-</sup>	[B(CN) <sub>4</sub> ] <sup>-</sup>	[B(Spacer–CN) <sub>4</sub> ] <sup>-</sup>

+ Lewis-Säuren                      + WCC                      + Metallkationen  
 ↓    ↓    ↓  
 Addukt-Anionen                      Ionische Flüssigkeiten                      Koordinationspolymere

**3. Generation**

**Abbildung 1.** Baukastenprinzip zur Darstellung großer CN-funktionalisierter Borat-Anionen und ihre Anwendungen in Addukt-Anionen, ionischen Flüssigkeiten und Koordinationspolymeren.

Durch Variation der Platzhalter-Gruppen (= *Spacer*), die zwischen dem Bor-Zentrum und den terminalen CN-Gruppen eingefügt werden, sollten so neue, vergrößerte und nitrilhaltige Anionen der 2. Generation synthetisiert werden. Analog zum [B(CN)<sub>4</sub>]<sup>-</sup> sollte untersucht werden, inwiefern sich die neuen CN-funktionalisierten Borat-Anionen für die Darstellung von Addukt-Anionen, ionischen Flüssigkeiten und Koordinationspolymeren eignen. Diese Verbindungen der 3. Generation sollten dabei durch geeignete Analysemethoden vollständig charakterisiert werden.

Durch Verwendung von sperrigen und chelatartigen Liganden sollte zudem die Stabilität der Borat-Anionen gegenüber thermischer Zersetzung bzw. Hydrolyse erhöht werden. Eine alternative Synthesemethode, analog der des Bis(oxalato)borats, zur Darstellung von cyanhydrin-substituierten Boraten sollte hierbei angewendet werden.



Die dargestellten Verbindungen sollten vollständig durch die gängigen analytischen Methoden (NMR-, IR-, Raman-Spektroskopie, Elementaranalyse, DSC/TGA) charakterisiert werden. Durch Einkristallröntgenstrukturanalysen sollten bei den synthetisierten Metallsalzen strukturelle Erkenntnisse für die Bildung poröser Koordinationspolymere gewonnen werden. Stabile Hohlraumstrukturen sollten mittels Stickstoffsorptionsmessung analysiert werden.

## 2 Bisheriger Kenntnisstand

### 2.1 CN-basierte Addukt-Anionen

Bei Addukt-Anionen handelt es sich um Anionen, die aus der Addition neutraler Lewis-Säuren zu Lewis-basischen Anionen hervorgehen. Neben Cyanid und Cyanido-Komplexanionen eignen sich auch nitrilhaltige Anionen auf Grund ihres Donor-Charakters besonders gut zur Addukt-Bildung, jedoch ist ihre Verwendung in Addukt-Anionen nicht sehr weit verbreitet. Viele Addukt-Anionen erregen Interesse als schwach koordinierende Anionen, da ihre Ladung im Vergleich zum ursprünglichen Anion über eine größere Anzahl an Atomen delokalisiert ist. Eines der ersten synthetisierten Lewis-Säure-Lewis-Base-Addukt-Anionen ist  $[\text{Al}_2\text{Cl}_7]^-$ , das als Intermediat in den Friedel-Crafts-Reaktionen auftritt, wobei dessen Nachweis erst später mittels NMR-Spektroskopie erfolgte.<sup>[1]</sup>

Erste gezielte Darstellungen solcher Addukt-Anionen erfolgten jedoch erst in den 1960er Jahren. Neben der Synthese des  $[\text{B}_2\text{F}_7]^-$  im Jahr 1965 durch Brownstein und Paasivirta<sup>[2]</sup> beschäftigten sich mehrere Arbeitsgruppen mit der Darstellung pniktogenhaltiger Addukt-Anionen.<sup>[3,4,5]</sup> Gillespie und Moss berichteten erstmals, dass sich bei der Synthese des bekannten  $[\text{SbF}_6]^-$  ein  $[\text{Sb}_2\text{F}_{11}]^-$ -Addukt-Anion bildet, wenn ein stöchiometrischer Überschuss an  $\text{SbF}_5$  zu einer HF-Lösung gegeben wird.<sup>[3]</sup> Darauf folgend wurden von Brownstein 1968 verschiedene Addukt-Anionen ausgehend von Hexafluoridopniktogenaten und Pentafluoropniktogenen synthetisiert, unter anderem  $[\text{As}_2\text{F}_{11}]^-$ ,  $[\text{AsSbF}_{11}]^-$  und  $[\text{PSbF}_{11}]^-$ .<sup>[4]</sup> Neben dem  $[\text{Sb}_2\text{F}_{11}]^-$ -Anion sind bis heute noch das  $[\text{Sb}_3\text{F}_{16}]^-$  und das  $[\text{Sb}_4\text{F}_{21}]^-$  bekannt (Abbildung 2), die als schwach koordinierende Anionen hoch reaktive Kationen stabilisieren können, wie z.B. das von Edwards *et al.* synthetisierte  $[\text{Br}_2]^+$  und das von Drews *et al.* dargestellte  $[\text{Xe}_2]^+$ .<sup>[6,7]</sup>

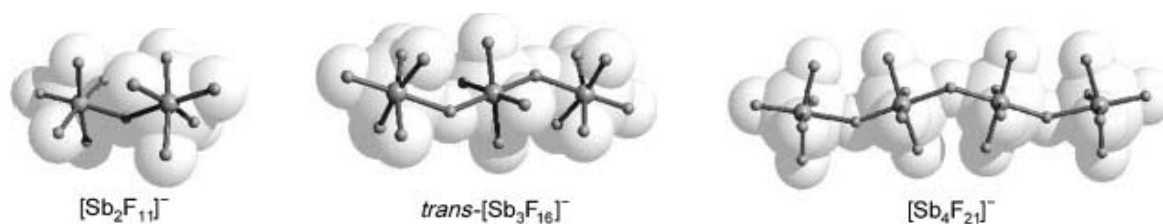


**Abbildung 2.** Molekülstrukturen der größer werdenden Antimonat-Anionen als Überlagerung von ball-and-stick- und space-filling-Darstellung.

Im Jahr 1999 veröffentlichten Bochmann *et al.* eine neue Methode zur Darstellung neuer schwach koordinierender Lewis-Säure-Base-Addukt-Anionen. Hierbei wurde als Lewis-Säure Tris(pentafluorophenyl)boran jeweils mit Cyanid und dem zweiwertigen Komplex-Anion  $[\text{Ni}(\text{CN})_4]^{2-}$  zu den entsprechenden Addukt-Anionen  $[(\text{F}_5\text{C}_6)_3\text{B}\cdot\text{CN}\cdot\text{B}(\text{C}_6\text{F}_5)_3]^-$  und  $[\text{Ni}\{\text{CN}\cdot\text{B}(\text{C}_6\text{F}_5)_3\}_4]^{2-}$  umgesetzt (Abbildung 3).<sup>[8]</sup> Bei der Aktivierung von Metallocen-Polymerisationskatalysatoren in der Ethen-Polymerisation wurden mit diesen Addukt-Anionen die bis dato höchsten „turnover number“ erzielt. Weitere Addukt-Anionen, die aus diesen Arbeiten entstanden, sind  $[(\text{F}_5\text{C}_6)_3\text{B}\cdot\mu\text{-NH}_2\cdot\text{B}(\text{C}_6\text{F}_5)_3]^-$  und  $[\text{Pd}\{\text{CN}\cdot\text{B}(\text{C}_6\text{F}_5)_3\}_4]^{2-}$ .<sup>[9,10]</sup> Einen sehr interessanten Ansatz für CN-basierte Addukt-Anionen lieferte Bochmann *et al.* 2006 mit der Darstellung des  $[\text{N}\{\text{CN}\cdot\text{B}(\text{C}_6\text{F}_5)_3\}_2]^-$ .<sup>[11]</sup> Ausgegangen wurde hierbei von Dicyanamid, welches als Pseudohalogenid sehr gut die Ladung delokalisieren kann.

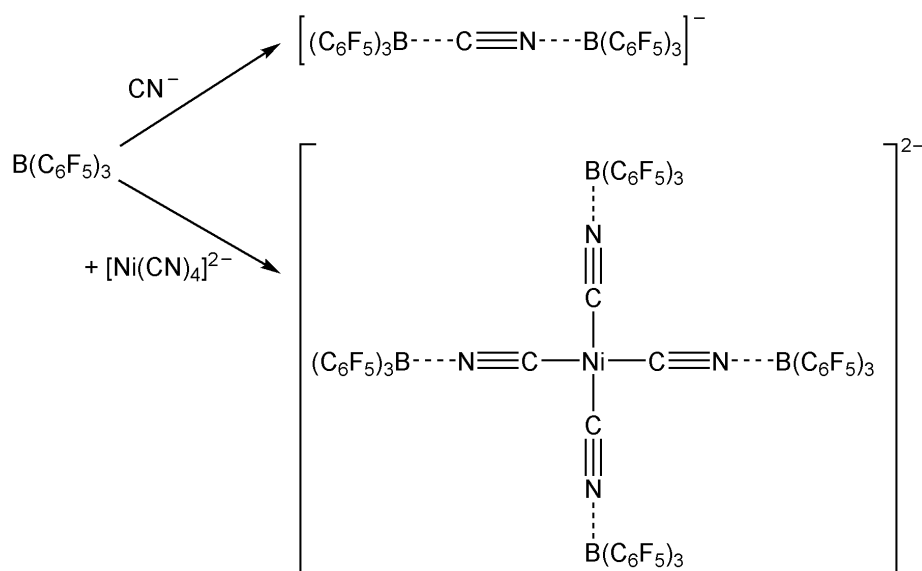


**Abbildung 3.** Übersicht zur Synthese von  $[(\text{F}_5\text{C}_6)_3\text{B}\cdot\text{CN}\cdot\text{B}(\text{C}_6\text{F}_5)_3]^-$  (oben) und  $[\text{Ni}\{\text{CN}\cdot\text{B}(\text{C}_6\text{F}_5)_3\}_4]^{2-}$  (unten).

Auf diesen Arbeiten basierend wurden 2009 von unserer Arbeitsgruppe neue schwach koordinierende Addukt-Anionen synthetisiert und publiziert.<sup>[12]</sup> Wie in Abbildung 1 dargestellt, wurden konzeptionell neue Anionen der 1. Generation zur Addukt-Bildung verwendet, die sich zusammen aus dem Grimm'schen Hydridverschiebungssatz und einer CN-Funktionalisierung ergeben. Hierbei handelte es sich neben Dicyanamid, um Tricyanmethanid und Tetracyanidoborat, welche durch Umsetzung mit  $\text{B}(\text{C}_6\text{F}_5)_3$  die entsprechenden Addukt-Anionen  $[\text{N}\{\text{CN}\cdot\text{B}(\text{C}_6\text{F}_5)_3\}_2]^-$  (DCA·2B),  $[\text{C}\{\text{CN}\cdot\text{B}(\text{C}_6\text{F}_5)_3\}_3]^-$  (TCM·3B) und  $[\text{B}\{\text{CN}\cdot\text{B}(\text{C}_6\text{F}_5)_3\}_4]^-$  (TCB·4B) bilden. Die Strukturen der resultierenden Addukt-Anionen konnten hierbei röntgenkristallografisch ermittelt werden (Abbildung 4).

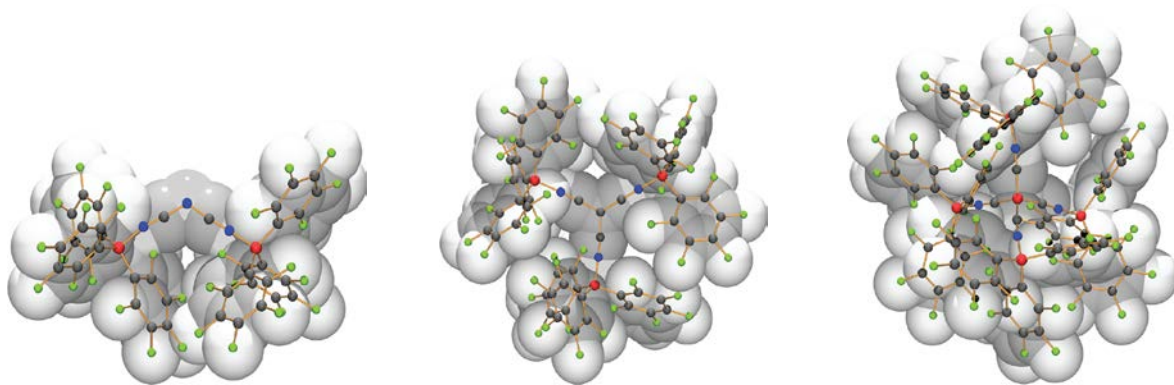


**Abbildung 4.** Molekülstruktur des [DCA·2B]<sup>-</sup>-Anions (links) in K[DCA·2B], des [TCM·3B]<sup>-</sup>-Anions (mitte) in [K(18-Krone-6)][TCM·3B] und des [TCB·4B]<sup>-</sup>-Anions (rechts) in [K(Et<sub>2</sub>O)<sub>4</sub>][TCB·4B] als Überlagerung von *ball-and-stick*- und *space-filling*-Darstellungen. Farbcode: Bor rot, Kohlenstoff dunkelgrau, Stickstoff blau, Fluor hellgrün.

In einer weiteren Arbeit aus unserer Arbeitsgruppe gelang die erfolgreiche Umsetzung des Tricyanmelaminats mit B(C<sub>6</sub>F<sub>5</sub>)<sub>3</sub> zum Tricyanmelaminat-Boran-Addukt ([TCMel·3B]<sup>-</sup>).<sup>[13]</sup> Ebenfalls sind hier die CN-Gruppen als Donor-Gruppen an der Koordination zum Boran beteiligt. Aus der röntgenkristallografischen Strukturanalyse von Na<sub>3</sub>[TCMel·3B] und MMIm<sub>3</sub>[TCMel·3B] geht jedoch hervor, dass Donor-Akzeptor-Wechselwirkungen zwischen den jeweiligen Kationen und den amidischen und aromatischen Stickstoffatomen im Anion vorliegen (Abbildung 5).

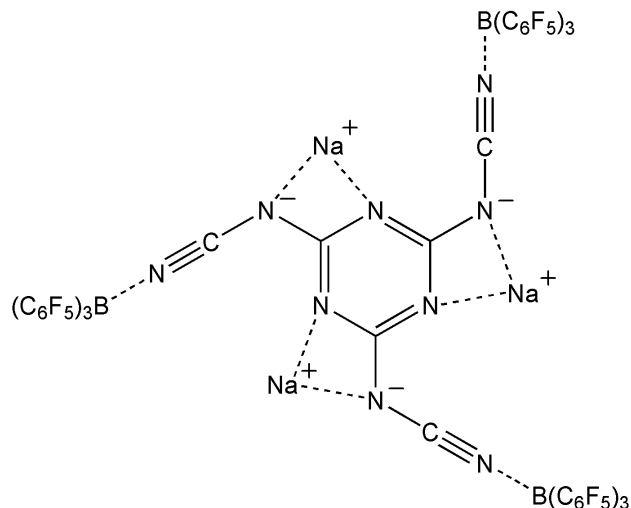


**Abbildung 5.** Koordinationsumgebung am Tricyanmelaminat-Boran-Addukt-Anion in Na<sub>3</sub>[TCMel·3B].

## 2.2 CN-funktionalisierte ionische Flüssigkeiten

Die Darstellung der ersten feuchtigkeits- und luftstabilen ionischen Flüssigkeiten führte zu einem stetigen Anstieg des Interesses an dieser Verbindungsklasse.<sup>[14]</sup> Heute lassen sich ionische Flüssigkeiten (ILs) unterteilen in klassische ILs, die einen Schmelzpunkt unterhalb des Siedepunkts von Wasser besitzen und die für viele Anwendungen bedeutenderen *Room Temperature ILs* (RTILs), die selbst noch bei Raumtemperatur flüssig sind. Durch die Kombination der Fließeigenschaften von Flüssigkeiten mit weiteren interessanten Eigenschaften, wie z.B. elektrische Leitfähigkeit, vernachlässigbarem Dampfdruck und hoher Wärmekapazität, ist der Anwendungsbereich heute weit gefächert. Einsatz finden ionische Flüssigkeiten als alternative Lösungsmittel in der sogenannten „*Green Chemistry*“ (z.B. Cellulose-Verarbeitung),<sup>[15]</sup> in der Katalyse,<sup>[16]</sup> als flüssige Wärmespeichermedien<sup>[17]</sup> und als Elektrolyte in Batterien.<sup>[18]</sup>

In Folge der sehr anwendungsbezogenen Forschung auf dem Gebiet der ionischen Flüssigkeiten wurde eine ganze Reihe an funktionalisierten ionischen Flüssigkeiten synthetisiert. Besonders die Eigenschaften CN-funktionalisierter ionischer Flüssigkeiten sind gut erforscht und ihre Anwendung als Lösungsmittel in vielen C–C-Kupplungsreaktionen, wie z.B. Heck-, Stille-, Suzuki- und Hiyama-Reaktionen<sup>[19]</sup> weitreichend untersucht. Ionische Flüssigkeiten, die diese Reaktionen im Vergleich zu ihren unfunktionalisierten Analoga weitaus effektiver machen, besitzen dabei nitril-funktionalisierte Kationen. Zwei Beispiele sollen dabei oben Genanntes verdeutlichen: CN-funktionalisierte pyridinium-basierte ILs stabilisieren zum einen Reaktionsintermediate in Glykosylierungsreaktionen (C–O-Kupplung),<sup>[20]</sup> zum anderen bilden diese durch Katalysatorimmobilisierung ein effektiveres katalytisches System in der Suzuki-Reaktion, wobei der Katalysatorkomplex weniger stark ausgewaschen wird und die Aktivität über mehrere Katalysezyklen erhalten bleibt.<sup>[19a]</sup>

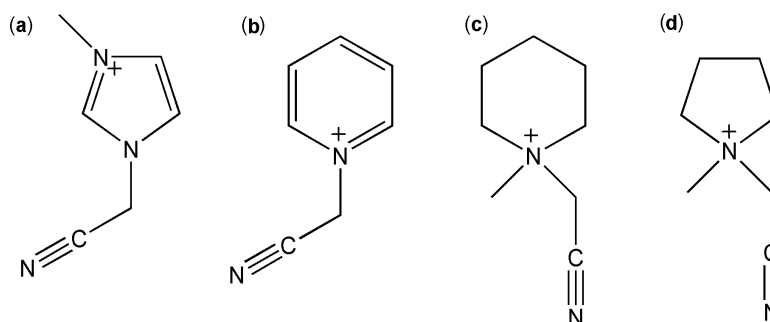


**Abbildung 6.** Ausgewählte Beispiele für CN-funktionalisierte Imidazolium- (a), Pyridinium- (b), Piperidinium- (c) und Pyrrolidinium-Kationen (d).

Mit CN-funktionalisierten Imidazolium- (a), Pyridinium- (b), Piperidinium- (c) und Pyrrolidinium-Kationen (d, Abbildung 6) sind ionische Flüssigkeiten basierend auf CN-funktionalisierten Kationen in der Literatur weitaus häufiger vertreten, während über ionische Flüssigkeiten mit CN-funktionalisierten Anionen recht wenig bekannt ist.

Eine Anwendung ist jedoch von ionischen Flüssigkeiten bekannt, die das CN-haltige 4,5-Dicyano-triazolat-Anion (e) beinhalten. Diese ionischen Flüssigkeiten, die auch „Armand’s Ligand“ genannt werden, sind effektive Stabilisierungsreagenzien für die Herstellung von verunreinigungsfreien, insbesondere chloridfreien, hoch dispersen Katalysatoren.<sup>[21]</sup> Neben dem bereits erwähnten „Armand’s Ligand“ sind noch einige weitere CN-funktionalisierte Anionen bekannt, die mit schwach koordinierenden Kationen ionische Flüssigkeiten bilden, wie z.B. Tetracyanopyrrolid (f),<sup>[22]</sup> Dicyanamid (g),<sup>[23]</sup> Tricyanmethanid (h)<sup>[24]</sup> oder Tetracyanidoborat (j)<sup>[25]</sup> (Abbildung 7). Eine Besonderheit innerhalb der CN-funktionalisierten ILs stellen die imidazolium-basierten ionischen Flüssigkeiten mit dem Tricyanmelaminat (j) als Anion dar.<sup>[13]</sup> Nach bestem Kenntnisstand handelt es sich hierbei um die ersten ionischen Flüssigkeiten mit einem dreifach negativ geladenen Anion.

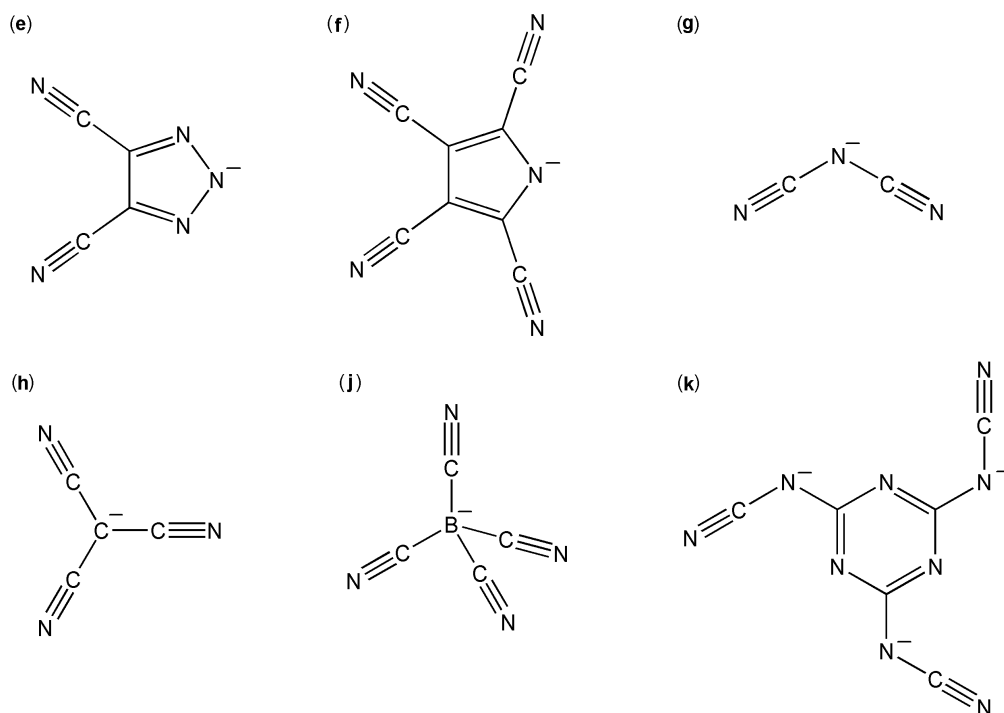


**Abbildung 7.** Für ionische Flüssigkeiten geeignete CN-funktionalisierte Anionen: 4,5-Dicyano-triazolat (e), Tetracyanopyrrolid (f), Dicyanamid (g), Tricyanmethanid (h), Tetracyanidoborat (j) und Tricyanmelaminat (k).

## 2.3 CN-basierte Koordinationspolymere

Definitionsgemäß handelt es sich bei Koordinationspolymeren um anorganische Polymere, in denen Metallzentren und Liganden durch koordinative Bindungen miteinander verbrückt sind. Die koordinativen Einheiten können sich dabei in einer, zwei oder drei Raumrichtungen erstrecken.<sup>[26]</sup> Durch Variation der Metallzentren und Liganden lassen sich interessante Polymerstrukturen aufbauen mit besonderen chemischen und physikalischen Eigenschaften. Neben ihrer hohen thermischen Stabilität können so spezifische Eigenschaften, wie beispielsweise Lumineszenz, Magnetismus und Porosität im Polymer erhalten werden. Somit eignen sich diese Koordinationspolymere auch als Materialien in LEDs (*Light-Emitting Diodes*), Supraleitern und Molekülspeichermedien.<sup>[27]</sup>

Zur Darstellung von stabilen und funktionalisierten Koordinationspolymeren haben sich hierbei Cyanid, Cyanido-Komplexe und Cyanido-Cluster als Liganden bewährt (Abbildung 8). „*Web of Knowledge*“ führt mittlerweile 604 Publikationen an, die „*Coordination Polymer*“ und „*Cyanide*“ als gemeinsames Thema besitzen. Somit soll hier nur kurz auf ausgewählte Beispiele eingegangen werden. Bezeichnend für die Vielseitigkeit der Cyanid-Liganden ist, dass Koordinationspolymere mit den drei oben erwähnten spezifischen Eigenschaften dargestellt werden können.

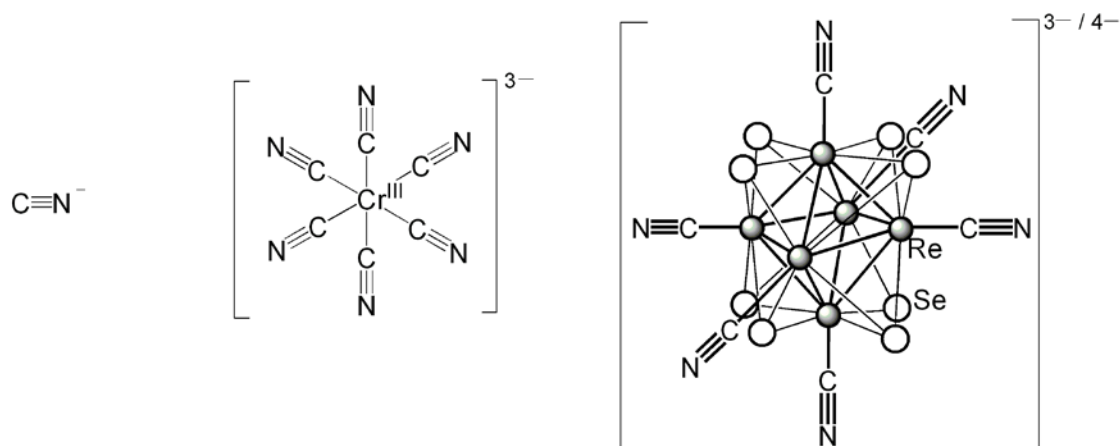


**Abbildung 8.** Ausgewählte Beispiele der drei Cyanid-basierten Liganden-Typen: Cyanid-Anion (links),  $[\text{Cr}^{\text{III}}(\text{CN})_6]^{3-}$ -Komplex-Anion (mitte) und  $[\text{Re}_6\text{Se}_8(\text{CN})_6]^{3-/4-}$ -Cluster-Anion (rechts).

Cyanid-verbrückte Kupfer-Zentren bilden Koordinationspolymere, die Lumineszenz in einem breiten spektroskopischen Bereich aufweisen, wobei Co-Liganden die Frequenz der emittierten Strahlung beeinflussen.<sup>[28]</sup> Durch Verbrückung von Übergangsmetallen (z.B. Nickel, Eisen, Chrom) mit Cyaniden konnten ferromagnetische Koordinationspolymere

synthetisiert werden. Bei einigen dieser Koordinationspolymere, die zudem permanente Porosität aufweisen, können sich Veränderungen der magnetischen Ordnung oder auch der Farbe in Abhängigkeit vom Beladungszustand mit Gastmolekülen zeigen, wie zum Beispiel bei  $\text{Co}^{\text{II}}_3[\text{Cr}^{\text{III}}(\text{CN})_6]_2$  beobachtet.<sup>[29]</sup> Um Lumineszenz und magnetische Eigenschaften in Koordinationspolymeren für Molekularsensoren zu nutzen, ist die Porosität von großer Bedeutung. Poröse Koordinationspolymere besitzen dabei auch Anwendungsmöglichkeiten in der heterogenen Katalyse, in Lösungsmittel- und Gasspeichermedien und Materialien zur molekularen Trennung.<sup>[30]</sup> Berliner Blau und seine Analoga, wie beispielsweise  $\text{Ni}_3[\text{Re}_6\text{Se}_8(\text{CN})_6]_2$ , bilden nachweislich große Hohlraumstrukturen mit permanenter Porosität und einer inneren Oberfläche von bis zu  $521 \text{ m}^2/\text{cm}^3$  aus.<sup>[31]</sup>

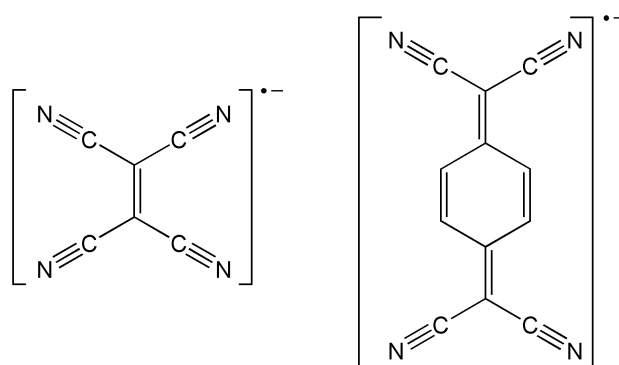


**Abbildung 9.** Schematische Darstellung der Radikal-Anionen des Tetracyanoethylens (links) und des Tetracyanochinodimethans (rechts).

Zudem ist eine große Anzahl an Koordinationspolymeren bekannt, die aus anionischen oder neutralen Polynitril-Liganden aufgebaut sind. Unter anderem finden sich in der Literatur eine Reihe an Koordinationspolymeren mit Dicyanamid<sup>[32]</sup> und Tricyanmethanid<sup>[33]</sup> als anionische Liganden. Des Weiteren sind Koordinationspolymere mit radikal-anionischen CN-Liganden, bspw. Tetracyanoethylen<sup>[34]</sup> und Tetracyanochinodimethan-Radikal-Anionen<sup>[35]</sup> (Abbildung 9), untersucht worden, die interessante elektronische und magnetische Eigenschaften besitzen. Bekanntere Vertreter von neutralen Polynitril-Liganden sind mit 4,4',4'',4'''-Tetracyanophenylmethan (**l**),<sup>[30d]</sup> 4,4',4'',4'''-Tetracyanophenylsilan (**m**),<sup>[36]</sup> 1,3,5-Tris(3-ethinylbenzonnitril)benzol (**n**),<sup>[37]</sup> 1,3,5-Tricyanobenzol (**o**),<sup>[38]</sup> 1,2,4,5-Tetracyanobenzol (**p**),<sup>[39]</sup> sowie 4,4'-Biphenyl-dicarbonitril (**q**)<sup>[40]</sup> in Abbildung 10 dargestellt. Durch Addition dieser neutralen Polynitril-Liganden zu Metallsalzen, die schwach koordinierende Anionen enthalten, lassen sich Koordinationspolymere synthetisieren, die ein kationisches Koordinationsnetzwerk besitzen.



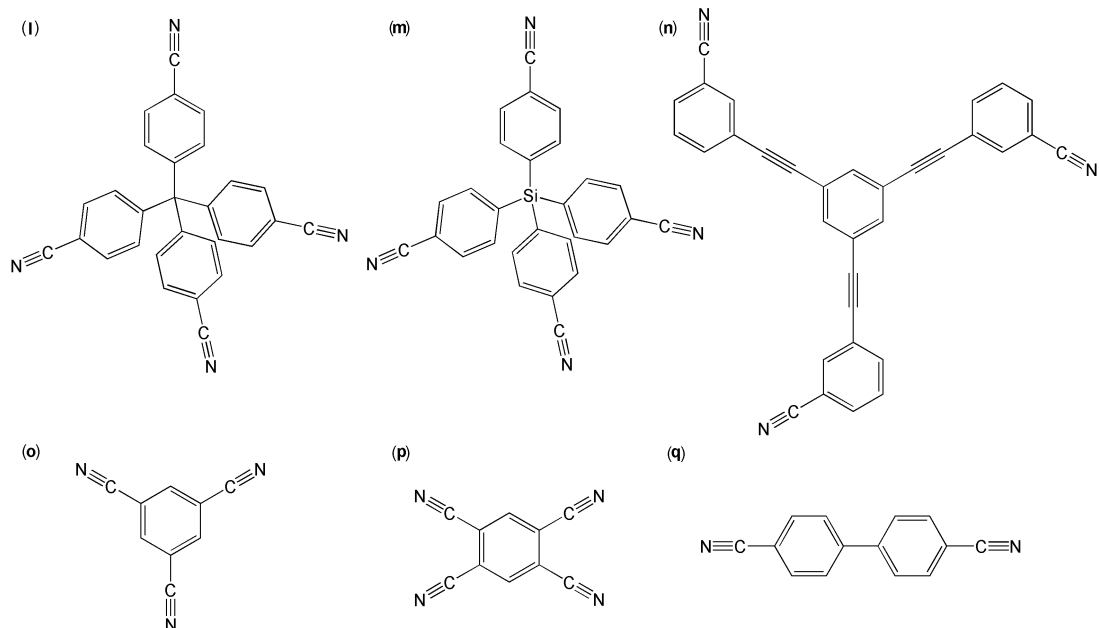


**Abbildung 10.** Darstellung ausgewählter neutraler Liganden: 4,4',4'',4'''-Tetracyanophenylmethan (**l**), 4,4',4'',4'''-Tetracyanophenylsilan (**m**), 1,3,5-Tris(3-ethynylbenzonitril)benzol (**n**), 1,3,5-Tricyanobenzol (**o**), 1,2,4,5-Tetracyanobenzol (**p**) und 4,4'-Biphenyl-dicarbonitril (**q**).

Über nitril-substituierte Borate als Liganden in Koordinationspolymeren ist hingegen recht wenig bekannt. Vom einfachsten dieser Borate, dem Tetracyanidoborat, gibt es mittlerweile eine Reihe an Metallsalzen, die auch strukturanalytisch untersucht wurden.<sup>[41]</sup> Hierbei handelt es sich um Koordinationspolymere, bei denen die terminalen CN-Gruppen starke koordinative Bindungen zu den Metallkationen ausbilden. Im lösungsmittelfreien  $\text{Na}[\text{B}(\text{CN})_4]$  konnte hierbei ein dreidimensionales Polymernetzwerk gefunden werden, wobei durch die dichte Packung aus Natrium und den relativ kleinen Anionen keine Hohlräumstrukturen ausgebildet werden (Abbildung 11).

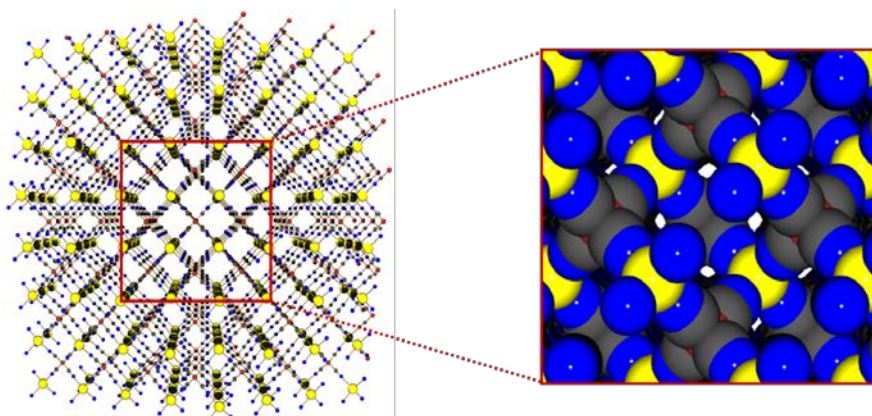


**Abbildung 11.** Links: *Ball-and-stick*-Darstellung des Netzwerks in  $\text{Na}[\text{B}(\text{CN})_4]$ . Rechts: Auszug des Netzwerks als Kalottenmodell dargestellt. Farbcode: Bor braun, Kohlenstoff dunkelgrau, Stickstoff blau, Natrium gelb.

### 3 Zusammenfassung der Ergebnisse

#### 3.1 Synthese CN-funktionalisierter Borat-Anionen

Die Darstellung diverser CN-funktionalisierter Borat-Anionen erfolgte durch Umsetzung von  $\text{NaBH}_4$  mit unterschiedlichen aliphatischen und aromatischen Hydroxynitrilen. So wurden neben den kommerziell erhältlichen 3-Hydroxypropionitril und 4-Hydroxybenzonnitril auch selbst synthetisierte Hydroxynitrile (Abbildung 12), wie 4-Hydroxy-2,3,5,6-tetrafluorbenzonnitril (**i**), 4-Hydroxy-4'-cyanobiphenyl (**ii**) und 5-Hydroxy-isophthalonitril (**iii**), verwendet.

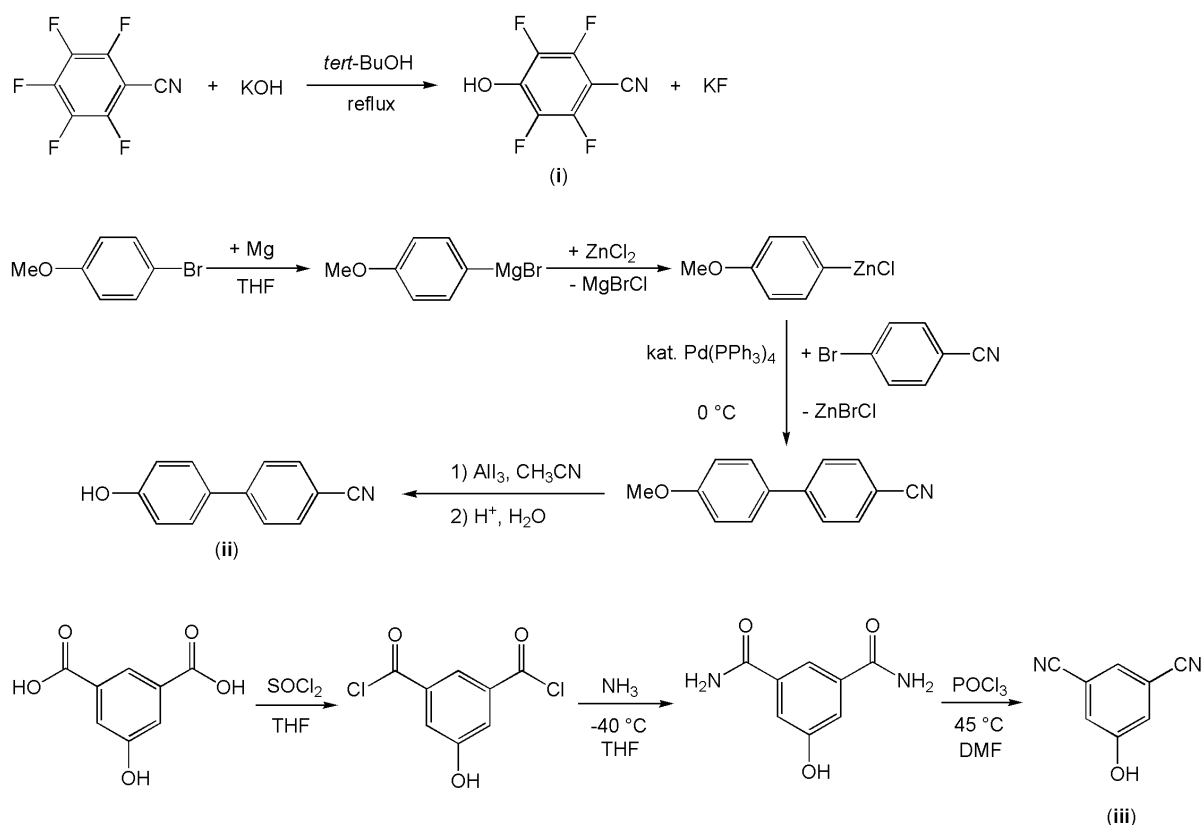


**Abbildung 12.** Synthese von 4-Hydroxy-2,3,5,6-tetrafluorbenzonnitril (**i**), 4-Hydroxy-4'-cyanobiphenyl (**ii**) und 5-Hydroxy-isophthalonitril (**iii**).

4-Hydroxy-2,3,5,6-tetrafluorbenzonnitril (**i**) konnte durch Umsetzung von Pentafluorbenzonnitril mit KOH in *tert*-BuOH in befriedigenden Ausbeuten (51 %) nach Literaturvorschrift synthetisiert werden.<sup>[42]</sup> Hierbei dient die Bildung des schwer löslichen Kaliumfluorids als Triebkraft der Reaktion. Die Darstellung von 4-Hydroxy-4'-cyanobiphenyl (**ii**) erfolgte in einer zweistufigen Reaktion mit einer Gesamtausbeute von ca. 50 % nach

Literatur.<sup>[43]</sup> Der erste Reaktionsschritt stellt dabei eine Negishi-Kupplung von 4-Bromanisol nach erfolgter Grignard-Bildung mit 4-Brombenzonnitril unter Zuhilfenahme katalytischer Mengen Pd(PPh<sub>3</sub>)<sub>4</sub> dar. Die Methyl-Gruppe vom gebildeten 4-Methoxy-4'-cyanobiphenyl wurde im zweiten Reaktionsschritt unter Lewis-sauren Bedingungen abgespalten, wobei nach wässriger Aufarbeitung 4-Hydroxy-4'-cyanobiphenyl (**ii**) erhalten werden konnte. Ausgehend von 5-Hydroxy-isophthalsäure konnte 5-Hydroxy-isophthalonitril (**iii**) in einer zweistufigen Synthese nach einer modifizierten Synthesevorschrift für die nitro-analoge Verbindung hergestellt werden.<sup>[44]</sup> Durch Behandeln der Säure mit SOCl<sub>2</sub> wurde zunächst das Säurechlorid synthetisiert und mit Ammoniak direkt weiter zum Amid umgesetzt, welches in befriedigenden Ausbeuten (52 %) erhalten wurde. Im zweiten Reaktionsschritt erfolgte die Dehydratisierung mit POCl<sub>3</sub> zum 5-Hydroxy-isophthalonitril (**iii**) in Ausbeuten bis zu 67 %.

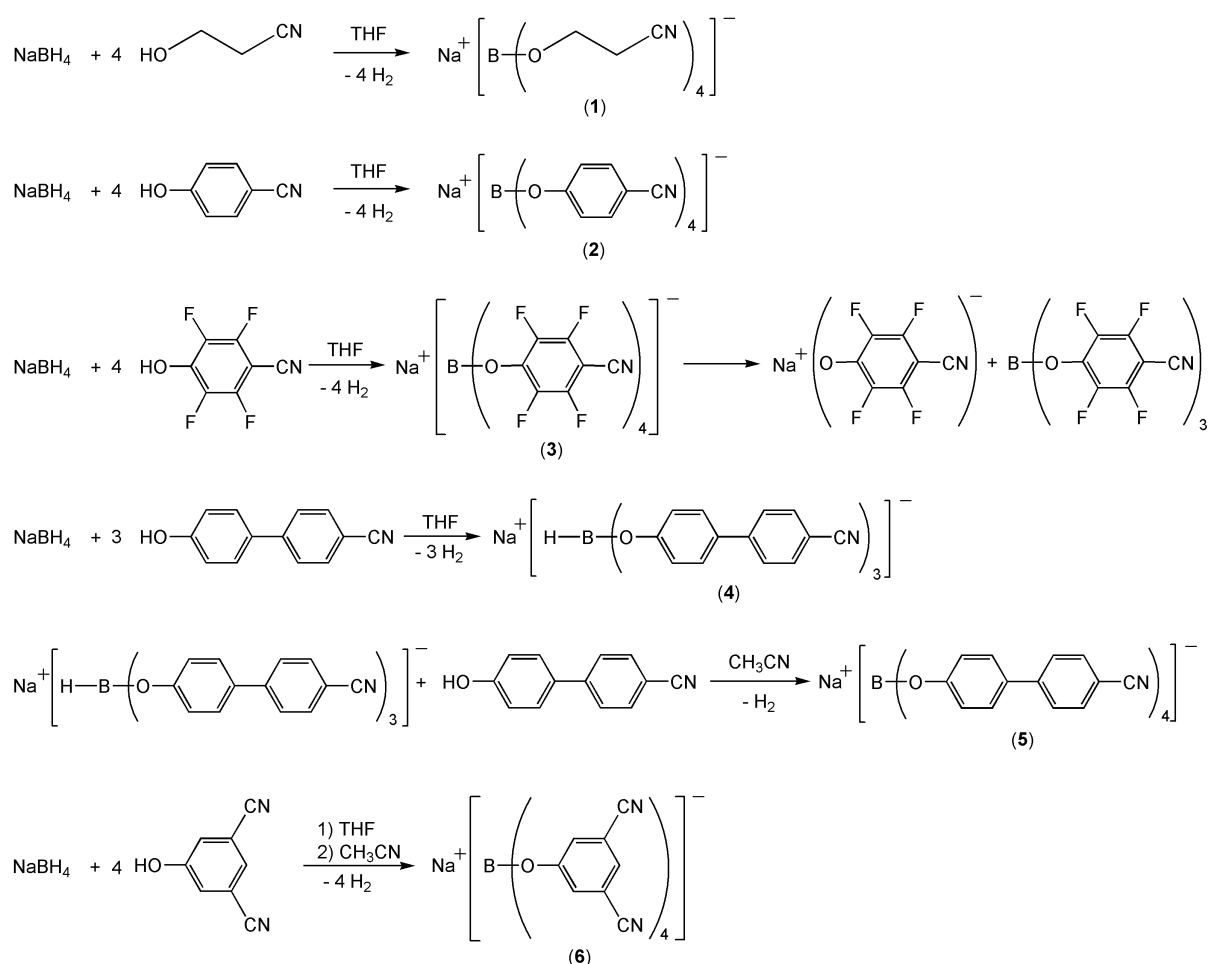


**Abbildung 13.** Synthese der Borate **1-6** durch Umsetzung von NaBH<sub>4</sub> mit den entsprechenden Hydroxynitrilen.

Die Umsetzung der unterschiedlichen Hydroxynitrile mit NaBH<sub>4</sub> erfolgte zunächst jeweils in THF (Abbildung 13). Durch vollständige Hydrid-Substitution konnten die Borate Na[B(O-

$\text{C}_2\text{H}_4\text{--CN}_4$ ] (**1**) und  $\text{Na}[\text{B}(\text{O--C}_6\text{H}_4\text{--CN})_4]$  (**2**) problemlos in THF dargestellt werden. Nach erfolgter Synthese ließ sich Borat **1** von der Reaktionslösung abfiltrieren und durch Extraktion mit  $\text{CH}_3\text{CN}$  aufarbeiten, so dass analytisch reines  $\text{Na}[\text{B}(\text{O--C}_2\text{H}_4\text{--CN})_4]$  (**1**) in Ausbeuten von 58 % erhalten wurde. Borat **2** besitzt eine bessere Löslichkeit als **1** in THF und kristallisierte aus einer heißen, stark konzentrierten THF-Lösung. Nach Abtrennen und Trocknen der Kristalle unter reduziertem Druck konnte  $\text{Na}[\text{B}(\text{O--C}_6\text{H}_4\text{--CN})_4]$  (**2**) in guten Ausbeuten (78 %) erhalten werden. Die Reaktion von  $\text{NaBH}_4$  mit 4-Hydroxy-2,3,5,6-tetrafluorbenzonnitril hingegen führte zwar zur vollständigen Substitution von Hydrid, jedoch konnte das gewünschte Borat  $\text{Na}[\text{B}(\text{O--C}_6\text{F}_4\text{--CN})_4]$  (**3**) nicht isoliert werden. Durch Kristallisationen der Reaktionsprodukte aus THF und  $\text{CH}_3\text{CN}$  wurde hingegen  $\text{Na}(\text{O--C}_6\text{F}_4\text{--CN})$  in zwei unterschiedlichen Modifikationen erhalten. Neben dem Alkoholat konnte nur das entsprechende Boran in Lösung durch NMR-Spektroskopie nachgewiesen werden. Die Umsetzung von  $\text{NaBH}_4$  mit vier Äquivalenten 4-Hydroxy-4'-cyanobiphenyl (**ii**) in THF führte hierbei nicht zur vollständigen Substitution des Hydrids mit dem Biphenoxy-Liganden. Während der Reaktion fiel das dreifach substituierte  $\text{Na}[\text{H--B}(\text{O--C}_{12}\text{H}_8\text{--CN})_3]$  (**4**) aus der Reaktionslösung aus, ohne dass eine weitere Bildung von Wasserstoff beobachtet wurde. Nach Abfiltrieren des Reaktionsproduktes und Umkristallisieren aus  $\text{CH}_3\text{CN}$  konnte **4** in Ausbeuten mit bis zu 64 % isoliert werden. Die Umsetzung von **4** mit einem Überschuss an  $\text{HO--C}_{12}\text{H}_8\text{--CN}$  (**ii**) in  $\text{CH}_3\text{CN}$  führte anschließend zur Bildung des gewünschten Borats  $\text{Na}[\text{B}(\text{O--C}_{12}\text{H}_8\text{--CN})_4]$  (**5**), das nach Aufarbeitung in guten Ausbeuten (74 %) erhalten wurde. Bei der Reaktion von  $\text{NaBH}_4$  mit  $\text{HO--C}_6\text{H}_3\text{--}(\text{CN})_2$  (**iii**) in THF konnte nur teilweise die Bildung des gewünschten  $\text{Na}[\text{B}\{\text{O--C}_6\text{H}_3\text{--}(\text{CN})_2\}_4]$  (**6**) beobachtet werden, wobei ein signifikanter Anteil als  $\text{Na}[\text{H--B}\{\text{O--C}_6\text{H}_3\text{--}(\text{CN})_2\}_3]$  beständig blieb und nur sehr langsam weiterreagierte. Nach erfolgtem Austausch des Lösungsmittels mit  $\text{CH}_3\text{CN}$  konnte eine vollständige Umsetzung zu  $\text{Na}[\text{B}\{\text{O--C}_6\text{H}_3\text{--}(\text{CN})_2\}_4]$  (**6**) erzielt werden, welches nach Umkristallisation in Ausbeuten von 63 % isoliert werden konnte.

Neben der Synthese ausgehend von  $\text{NaBH}_4$  und den Hydroxynitrilen wurde eine weitere Möglichkeit zur Darstellung CN-funktionalisierter Borate erprobt (Abbildung 15). Diese Reaktion stellt eine modifizierte Synthese des Bis(oxalato)borats aus Tetramethoxyborat und Bis(trimethylsilyl)oxalat dar.<sup>[45]</sup>

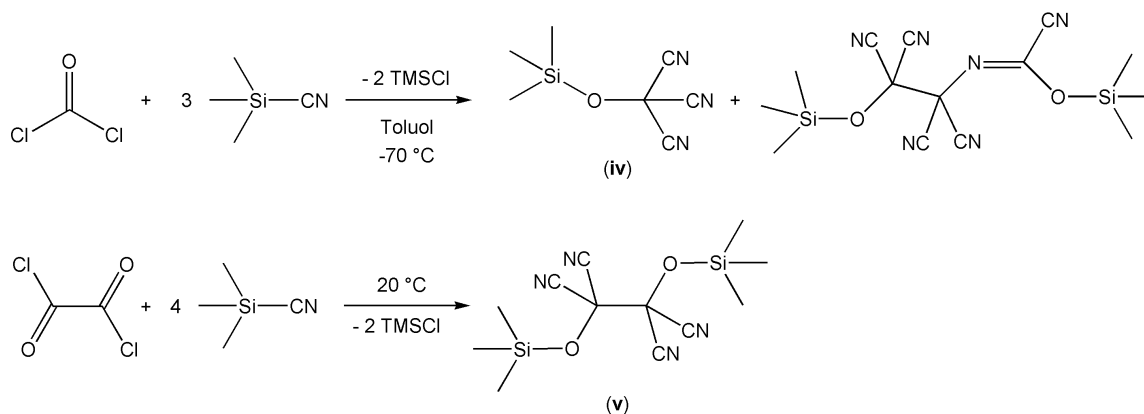


**Abbildung 14.** Synthese von Tricyano(trimethylsiloxy)methan (**iv**) und 1,1,2,2-Tetracyano-1,2-bis(trimethylsiloxy)ethan (**v**).

Als Liganden wurden Tricyano(trimethylsiloxy)methan (**iv**) und 1,1,2,2-Tetracyano-1,2-bis(trimethylsiloxy)ethan (**v**) nach Literaturvorschrift synthetisiert (Abbildung 14).<sup>[46]</sup> Tricyano(trimethylsiloxy)methan (**iv**) konnte hierbei durch Umsetzung einer Phosgen-Lösung in Toluol mit Trimethylsilylcyanid bei  $-70\text{ °C}$  synthetisiert werden. Neben dem Produkt, das durch fraktionierte Destillation in Ausbeuten bis 64 % erhalten wurde, konnte im Rückstand der Destillation ein Konstitutions-Dimer von **iv** als Nebenprodukt analysiert werden. Die Synthese von 1,1,2,2-Tetracyano-1,2-bis(trimethylsiloxy)ethan (**v**) erfolgte lösungsmittelfrei durch Reaktion von Oxalylchlorid mit Trimethylsilylcyanid bei Raumtemperatur. Das Produkt **v** kristallisierte direkt aus der Reaktionslösung und konnte nach dem Waschen mit *n*-Hexan und Sublimation in analytischer Reinheit und guten Ausbeuten (78 %) erhalten werden.

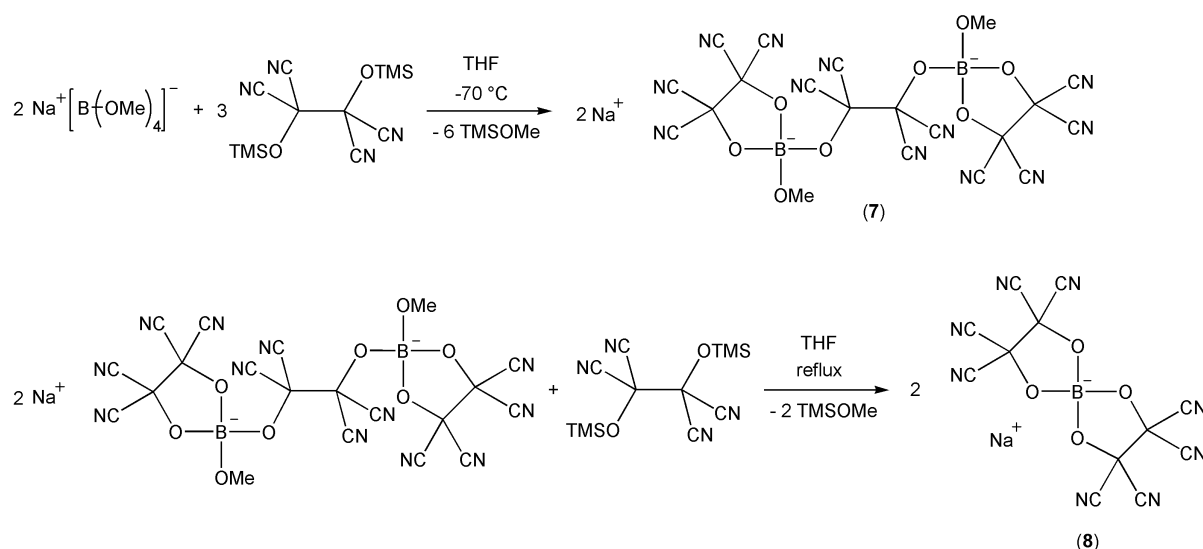


**Abbildung 15.** Synthese von Na<sub>2</sub>[B<sub>2</sub>(OMe)<sub>2</sub>(TCEG)<sub>3</sub>] (**7**) und Na[B(TCEG)<sub>2</sub>] (**8**).

Die Umsetzung von Natrium-tetramethoxyborat mit vier Äquivalenten Tricyano(trimethylsiloxy)methan (**iv**) führte zu einer Reihe an diversen Nebenprodukten. Die Reaktion wurde bei unterschiedlichen Temperaturen durchgeführt, wobei jeder Ansatz zu einem Gemisch an verschiedenen Borat-Spezies führte, wie  $^{11}\text{B}$ -NMR-Messungen ergaben. Als eines der Nebenprodukte konnte nach jeder Reaktion 1,1,2,2-Tetracyano-1,2-bis(trimethylsiloxy)ethan (**v**) gefunden werden, welches sowohl durch Einkristallröntgenstrukturanalytik als auch durch NMR-Messungen analysiert wurde.

Aus der Reaktion von Natrium-tetramethoxyborat mit dem zweizähligen Liganden 1,1,2,2-Tetracyano-1,2-bis(trimethylsiloxy)ethan (**v**) in THF bei  $-70\text{ °C}$  konnte zunächst das Diborat  $\text{Na}_2[\text{B}_2(\text{OMe})_2(\text{TCEG})_3]$  (**7**) erhalten werden, in dem jeweils ein Tetracyanoethylenglykolat-Ligand (TCEG-Ligand) chelatartig am Bor gebunden ist, während ein weiterer TCEG-Ligand beide Bor-Zentren überbrückt und eine Methoxy-Gruppe an den Bor-Zentren bestehen bleibt. Die Aufarbeitung des Diborats (**7**) erfolgte durch Umkristallisation aus THF, wonach **7** in sehr guten Ausbeuten (87 %) erhalten wurde. Die verbliebenen Methoxy-Gruppen konnten anschließend in einer Reaktion von **7** mit einem Überschuss an **v** in THF unter Rückflusserhitzen durch einen TCEG-Liganden substituiert werden, wobei sich der verbrückende TCEG-Ligand in **7** während der Reaktion zu einem Chelat-Liganden umorientiert. Nach Umkristallisation aus THF/ $\text{Et}_2\text{O}$  wurde  $\text{Na}[\text{B}(\text{TCEG})_2]$  (**8**) in Ausbeuten von 73 % erhalten.

### 3.2 Strukturanalytik der Natrium-Borate

Um den Einfluss der Liganden auf die strukturellen Eigenschaften der Koordinationspolymere zu untersuchen, wurden die Strukturen der Natrium-Borate nach kristallografischer Vermessung geeigneter Einkristalle bestimmt. Lediglich von  $\text{Na}[\text{B}(\text{O}-\text{C}_{12}\text{H}_8-\text{CN})_4]$  (**5**) konnten keine Kristalle erhalten und somit auch keine Struktur ermittelt werden.

$\text{Na}[\text{B}(\text{O}-\text{C}_2\text{H}_4-\text{CN})_4]$  (**1**) konnte sowohl aus THF als auch aus  $\text{CH}_3\text{CN}$  kristallisiert werden. Hierbei wirkt sich das Lösungsmittel nicht auf die Struktur aus, da **1** bevorzugt lösungsmittelfrei kristallisiert. Wie aus Abbildung 16 ersichtlich wird, bildet **1** ein dreidimensionales Koordinationspolymer. Das Anion koordiniert hierbei chelatartig mit jeweils zwei Sauerstoffatomen zwei Natrium-Kationen, wobei sich alternierend aus Kationen und Anionen „Zick-Zack“-Stränge bilden, die über eine  $\text{CN}\cdots\text{Na}$ -Koordination miteinander verbrückt sind. Weiterhin bleiben drei Nitril-Gruppen je Anion im Netzwerk unkoordiniert.

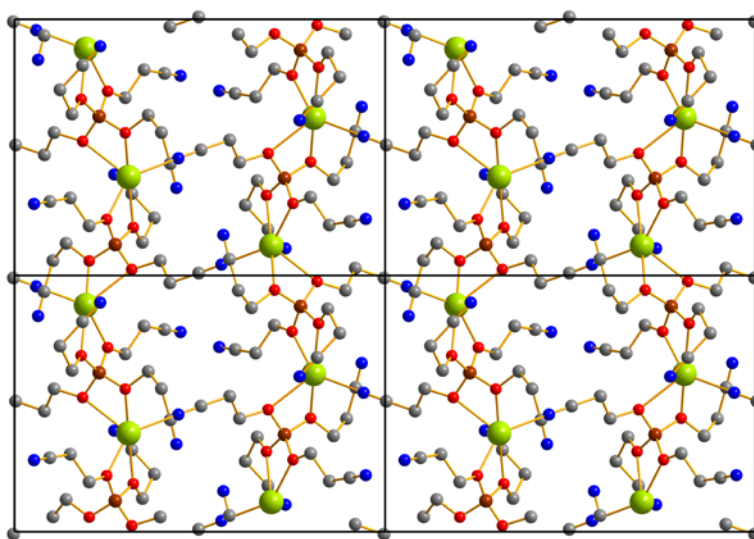


**Abbildung 16.** Elementarzelle von  $\text{Na}[\text{B}(\text{O}-\text{C}_2\text{H}_4-\text{CN})_4]$  in einer *ball-and-stick*-Darstellung. Blickrichtung entlang der *a*-Achse. Wasserstoffatome zur besseren Übersicht nicht dargestellt. Farbkodierung: C dunkelgrau, B braun, N blau, Na grün, O rot.

$\text{Na}[\text{B}(\text{O}-\text{C}_6\text{H}_4-\text{CN})_4]$  (**2**) konnte sowohl aus THF als auch aus  $\text{CH}_3\text{CN}$  kristallisiert werden, wobei das Lösungsmittel durch Solvat-Bildung einen entscheidenden Einfluss auf die Struktur hat.  $\text{Na}[\text{B}(\text{O}-\text{C}_6\text{H}_4-\text{CN})_4]\cdot 4.5\text{THF}$  kristallisiert aus THF als zweidimensionales Koordinationsnetzwerk (Abbildung 17 links), wobei die Schichten in einer ABC-Folge übereinander liegen, wie in Abbildung 17 rechts dargestellt. Die Anionen koordinieren mit

drei ihrer vier CN-Gruppen die Natrium-Kationen, wobei die oktaedrische Koordinationsumgebung an den Kationen neben den CN-Liganden zusätzlich mit THF abgesättigt ist.

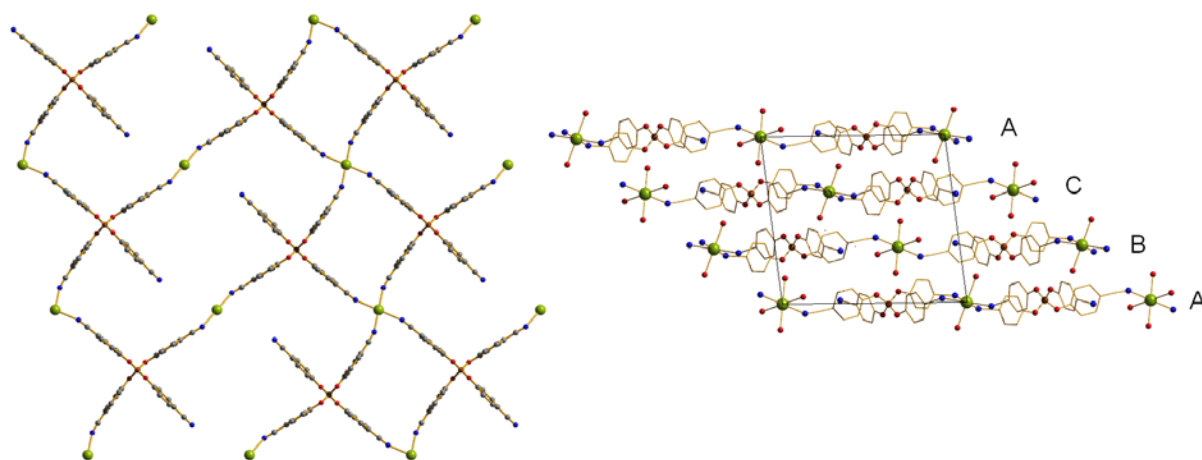


**Abbildung 17.** Links: *Ball-and-stick*-Darstellung des 2D Netzwerkes in  $\text{Na}[\text{B}(\text{O}-\text{C}_6\text{H}_4-\text{CN})_4] \cdot 4.5\text{THF}$ . Blickrichtung entlang der *b*-Achse. Zur besseren Übersicht sind THF-Moleküle und Wasserstoffatome nicht dargestellt. Rechts: *Ball-and-stick*- und *wire*-Darstellung der Schichtfolge. Zur besseren Übersicht sind die Kohlenstoffatome der THF-Moleküle und Wasserstoffatome nicht dargestellt. Blickrichtung entlang der *c*-Achse. Farbkodierung: C dunkelgrau, B braun, N blau, Na grün, O rot.

Durch Kristallisation aus  $\text{CH}_3\text{CN}$  konnte das dreidimensionale Koordinationspolymer  $\text{Na}[\text{B}(\text{O}-\text{C}_6\text{H}_4-\text{CN})_4] \cdot \text{CH}_3\text{CN}$  erhalten werden (Abbildung 18). Die Acetonitril-Moleküle (rot) diffundieren in die Poren ein, ohne stärkere Donor-Akzeptor-Wechselwirkungen zum Netzwerk (blau) einzugehen. Das Netzwerk wird durch Koordination von drei der vier CN-Gruppen des Anions zu Natrium-Kationen gebildet. Im Gegensatz zur Struktur von  $\text{Na}[\text{B}(\text{O}-\text{C}_6\text{H}_4-\text{CN})_4] \cdot 4.5\text{THF}$  koordiniert zusätzlich jedes Anion chelatartig mit zwei Sauerstoffatomen ein viertes Kation.

Das Entfernen des Lösungsmittels führte in beiden Fällen zu einem Verlust der Kristallinität, jedoch lässt sich weiterhin zwischen einem  $\alpha$ - $\text{Na}[\text{B}(\text{O}-\text{C}_6\text{H}_4-\text{CN})_4]$  (desolvatisierte Modifikation nach Kristallisation aus THF) und einem  $\beta$ - $\text{Na}[\text{B}(\text{O}-\text{C}_6\text{H}_4-\text{CN})_4]$  (desolvatisierte Modifikation nach Kristallisation aus  $\text{CH}_3\text{CN}$ ) unterscheiden, wie im folgenden Kapitel spektroskopische und thermische Analysen zeigen.



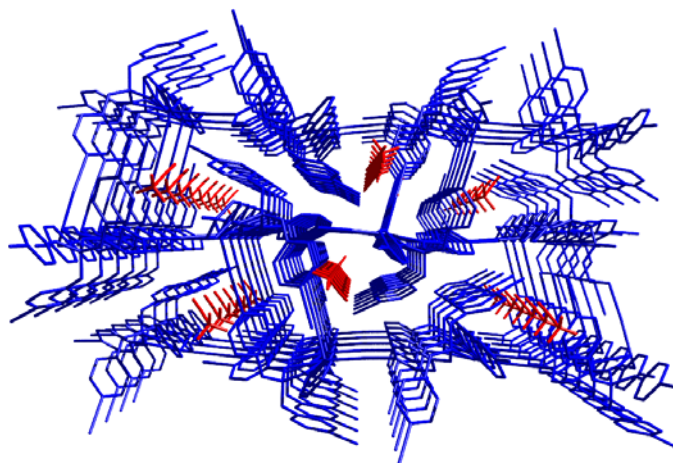


**Abbildung 18.** Wire-Darstellung des Einschusses von CH<sub>3</sub>CN (rot) in das dreidimensionale Netzwerk (blau) in Na[B(O–C<sub>6</sub>H<sub>4</sub>–CN)<sub>4</sub>]·CH<sub>3</sub>CN. Blickrichtung entlang der *c*-Achse. Wasserstoffatome des Netzwerks zur besseren Übersicht nicht dargestellt.

Durch Kristallisation von Na[H–B(O–C<sub>12</sub>H<sub>8</sub>–CN)<sub>3</sub>] (**4**) aus CH<sub>3</sub>CN wurde das dreidimensionale Koordinationspolymer Na[H–B(O–C<sub>12</sub>H<sub>8</sub>–CN)<sub>3</sub>]·3CH<sub>3</sub>CN erhalten (Abbildung 19). Das Netzwerk entsteht hierbei durch Koordination von zwei der drei CN-Gruppen zu Natrium-Kationen, während zwei weitere Natrium-Kationen chelatartig von jeweils zwei Sauerstoffatomen koordiniert werden. Interessanterweise ist ein Sauerstoffatom an beiden Chelatisierungen beteiligt. In der Kristallstruktur von **4** befinden sich zwei interpenetrierende Netzwerke, die entlang der *c*-Achse dreieckförmige, mit CH<sub>3</sub>CN-Molekülen gefüllte Poren bilden.

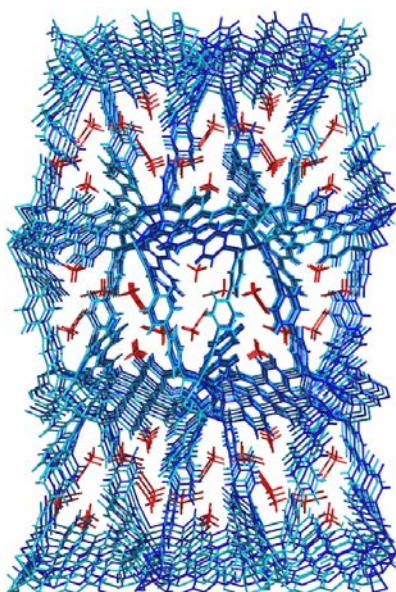


**Abbildung 19.** Wire-Darstellung des Einschusses von CH<sub>3</sub>CN (rot) in die dreidimensionalen, interpenetrierenden Netzwerke (blau und hellblau) in Na[H–B(O–C<sub>12</sub>H<sub>8</sub>–CN)<sub>3</sub>]·3CH<sub>3</sub>CN. Blickrichtung entlang der *c*-Achse.

Von  $\text{Na}[\text{B}\{\text{O}-\text{C}_6\text{H}_3-(\text{CN})_2\}_4]$  (**6**) konnte aus einem THF/ $\text{CH}_2\text{Cl}_2$ -Gemisch das zwei-dimensionale Koordinationspolymer  $\text{Na}[\text{B}\{\text{O}-\text{C}_6\text{H}_3-(\text{CN})_2\}_4]\cdot 2\text{THF}$  kristallisiert werden (Abbildung 20). Weitere Lösungsmittelmoleküle, THF- und  $\text{CH}_2\text{Cl}_2$ -Moleküle, befinden sich zudem in den quadratischen Hohlräumen ohne signifikante Donor-Akzeptor-Wechselwirkungen zum Netzwerk. Die Natrium-Kationen befinden sich in einer oktaedrischen Koordinationsumgebung mit quadratisch planarer Ausrichtung der CN-Koordinationen und zwei THF-Molekülen in trans-Position. Zwei Anionen koordinieren mit vier ihrer acht CN-Gruppen zusammen vier Natrium-Kationen, die in einer Ebene liegen, wobei jeweils ein Anion oberhalb und das andere unterhalb dieser Ebene befinden.

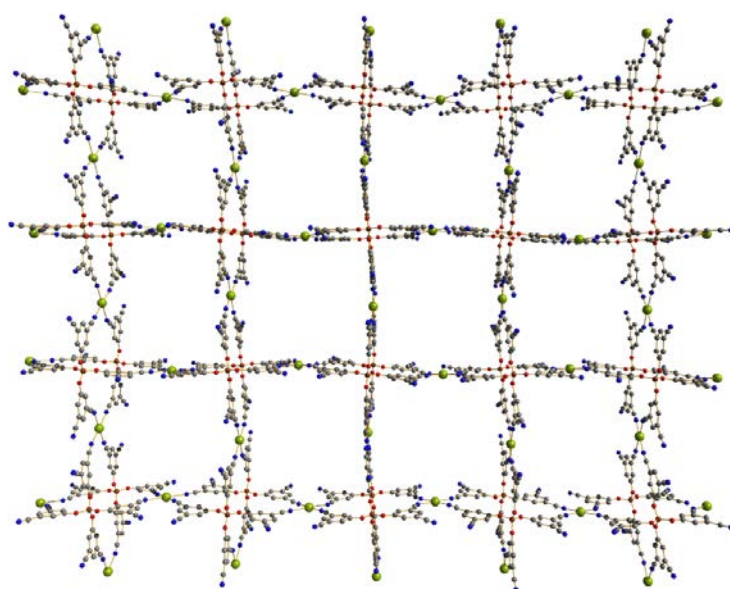


**Abbildung 20.** Ball-and-stick-Darstellung des zweidimensionalen Koordinationsnetzwerks in  $\text{Na}[\text{B}\{\text{O}-\text{C}_6\text{H}_3-(\text{CN})_2\}_4]\cdot 2\text{THF}$ . Blickrichtung entlang der  $c$ -Achse. THF/ $\text{CH}_2\text{Cl}_2$ -Moleküle und Wasserstoffatome zur besseren Übersicht nicht dargestellt. Farbkodierung: C dunkelgrau, B braun, N blau, Na grün, O rot.

Kristallisation des Diborats  $\text{Na}_2[\text{B}_2(\text{OMe})_2(\text{TCEG})_3]$  (**7**) aus einer konzentrierten THF-Lösung führte zur Bildung des Koordinationspolymers  $\text{Na}_2[\text{B}_2(\text{OMe})_2(\text{TCEG})_3]\cdot 8\text{THF}$  mit eindimensionalen Koordinationssträngen (Abbildung 21). Im Kristall befinden sich die Natrium-Kationen in einer oktaedrischen Koordinationsumgebung mit facialer CN- und THF-Koordination. Zwei der drei CN-Gruppen stammen von einem Diborat-Anion, während die dritte CN-Koordination am Kation vom nächsten Anion herrührt. Dies führt zu einer Überbrückung der Dianionen durch zwei Natrium-Kationen, welche sich in einer Raumrichtung fortsetzt.

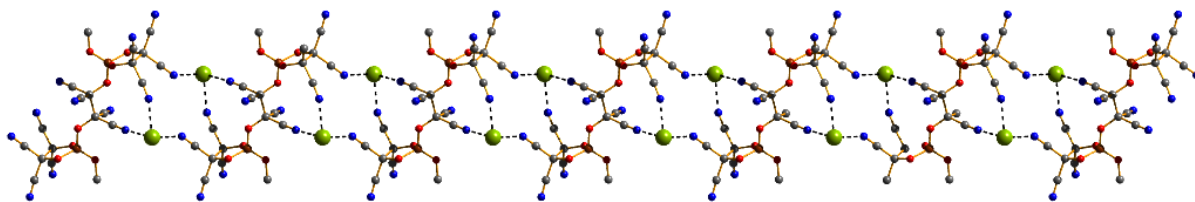


**Abbildung 21.** Ball-and-stick-Darstellung des eindimensionalen Koordinationsstrangs in  $\text{Na}_2[\text{B}_2(\text{OMe})_2(\text{TCEG})_3] \cdot 8\text{THF}$ . Blickrichtung entlang der *b*-Achse. THF-Moleküle und Wasserstoffatome zur besseren Übersicht nicht dargestellt. Farbkodierung: C dunkelgrau, B braun, N blau, Na grün, O rot.

Aus einem Gemisch von THF/Et<sub>2</sub>O konnte  $\text{Na}[\text{B}(\text{TCEG})_2]$  (**8**) als Solvat kristallisiert werden. Wie in Abbildung 22 dargestellt, bildet  $\text{Na}[\text{B}(\text{TCEG})_2] \cdot 0.85\text{THF} \cdot 0.15\text{Et}_2\text{O}$  ein dreidimensionales Koordinationsnetzwerk aus. Von den acht CN-Gruppen des Anions koordinieren fünf die Natrium-Kationen, während drei unkoordiniert bleiben. Jedes Kation wird dabei oktaedrisch von fünf Anionen durch deren CN-Gruppen und einem THF- bzw. Et<sub>2</sub>O-Molekül koordiniert. Entlang der *b*-Achse sind viereckig geformte Poren zu erkennen, in denen die THF-Moleküle Platz finden.

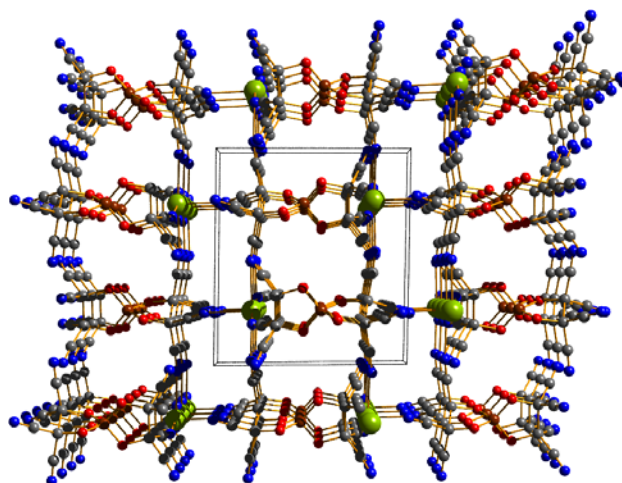


**Abbildung 22.** Ball-and-stick-Darstellung des dreidimensionalen Koordinationsnetzwerks in  $\text{Na}[\text{B}(\text{TCEG})_2] \cdot 0.85\text{THF} \cdot 0.15\text{Et}_2\text{O}$ . Blickrichtung entlang der *b*-Achse. THF- und Et<sub>2</sub>O-Moleküle zur besseren Übersicht nicht dargestellt. Farbkodierung: C dunkelgrau, B braun, N blau, Na grün, O rot.

### 3.3 Allgemeine, thermische und spektroskopische Eigenschaften der Natrium-Borate

Sämtliche Natrium-Borate zeigen eine sehr gute Löslichkeit in DMSO. Sowohl in THF als auch in CH<sub>3</sub>CN sind zudem Na[B(O–C<sub>6</sub>H<sub>4</sub>–CN)<sub>4</sub>], Na[B{O–C<sub>6</sub>H<sub>3</sub>–(CN)<sub>2</sub>]<sub>4</sub>], Na<sub>2</sub>[B<sub>2</sub>(OMe)<sub>2</sub>(TCEG)<sub>3</sub>] und Na[B(TCEG)<sub>2</sub>] gut löslich, während Na[B(O–C<sub>2</sub>H<sub>4</sub>–CN)<sub>4</sub>] in beiden Lösungsmitteln nur geringfügig löslich ist. Auffällig ist, dass Na[H–B(O–C<sub>12</sub>H<sub>8</sub>–CN)<sub>3</sub>] im Vergleich zu Na[B(O–C<sub>12</sub>H<sub>8</sub>–CN)<sub>4</sub>] deutlich schlechter in THF löslich ist, hingegen aber eine gute Löslichkeit in heißem CH<sub>3</sub>CN besitzt. Alle Natrium-Borate sind zudem nahezu unlöslich in Lösungsmitteln mit geringerer Polarität als die oben Genannten, z.B. Et<sub>2</sub>O, CH<sub>2</sub>Cl<sub>2</sub> und Toluol.

**Tabelle 1:** Thermische Analyse: Lösungsmittelverlust und Zersetzungspunkte aus TGA-Messungen von **2·4.5THF**, **2·CH<sub>3</sub>CN**, **4·3CH<sub>3</sub>CN**, **6·solvent**, **7·8THF** und **8·0.85THF·0.15Et<sub>2</sub>O**. Onset- und Peak-Temperaturen aus der Differentialkurve der TGA-Daten bestimmt.

Verbindung	Ursache	Massenverlust/ %	TGA	
			Onset/ °C	Peak/ °C
Na[B(O–C <sub>6</sub> H <sub>4</sub> –CN) <sub>4</sub> ]·4.5THF	Lösungsmittelverlust	20.8	47.9	70.7
	Lösungsmittelverlust	10.9	124.9	131.8
	Lösungsmittelverlust	4.2	145.2	160.6
	Zersetzung	32.8	420.5	454.0
Na[B(O–C <sub>6</sub> H <sub>4</sub> –CN) <sub>4</sub> ]·CH <sub>3</sub> CN	Lösungsmittelverlust	7.0	40.4	61.1
	Lösungsmittelverlust	2.1	144.3	152.2
	Zersetzung	27.4	296.4	302.5
Na[H–B(O–C <sub>12</sub> H <sub>8</sub> –CN) <sub>3</sub> ]·3CH <sub>3</sub> CN	Lösungsmittelverlust	16.2	38.9	77.7
	Zersetzung	21.3	323.4	351.2
Na[B{O–C <sub>6</sub> H <sub>3</sub> –(CN) <sub>2</sub> ] <sub>4</sub> ]·solvent	Lösungsmittelverlust	4.2	27.8	35.4
	Lösungsmittelverlust	4.2	50.9	58.4
	Lösungsmittelverlust	21.9	64.7	74.1
	Lösungsmittelverlust	8.4	91.0	98.0
	Lösungsmittelverlust	4.5	136.8	140.0
	Zersetzung	8.7	336.3	357.9
Na <sub>2</sub> [B <sub>2</sub> (OMe) <sub>2</sub> (TCEG) <sub>3</sub> ]·8THF	Lösungsmittelverlust	29.0	38.1	80.1
	Lösungsmittelverlust	22.9	119.7	149.4
	Zersetzung	21.4	208.2	-
Na[B(TCEG) <sub>2</sub> ]·0.85THF·0.15Et <sub>2</sub> O	Lösungsmittelverlust	13.4	121.0	151.4
	Zersetzung	59.4	264.5	283.9

Die kristallinen Produkte wurden durch TGA/DSC-Messungen auf ihre thermischen Eigenschaften bzw. Stabilitäten hin untersucht. Die Ergebnisse der Solvat-Verbindungen sind in Tabelle 1 dargestellt. Bei diesen konnte jeweils ein prozentualer Massenverlust festgestellt werden, welcher der Lösungsmittelmenge, berechnet aus den Ergebnissen der Röntgenstrukturanalyse, entspricht.

**Tabelle 2:** Thermische Analyse: Zersetzungspunkte ( $T_{\text{Zers}}$ ; Onset-Wert aus DSC-Messung); spektroskopische Daten: IR-, Raman-,  $^{11}\text{B}$ - und  $^{13}\text{C}$ -NMR-Daten von **1**,  $\alpha$ -**2**,  $\beta$ -**2**, **4**, **5**, **6**, **7** und **8**.

	$T_{\text{Zers}}/$ $^{\circ}\text{C}$	$^{13}\text{C}$ -NMR (CN)/ ppm	$^{11}\text{B}$ -NMR/ ppm	IR ( $\tilde{\nu}_{\text{CN}}$ )/ $\text{cm}^{-1}$	Raman( $\tilde{\nu}_{\text{CN}}$ )/ $\text{cm}^{-1}$
$\text{Na}[\text{B}(\text{O}-\text{C}_2\text{H}_4-\text{CN})_4]$	135	120.7	2.3	2250	2252
$\alpha$ - $\text{Na}[\text{B}(\text{O}-\text{C}_6\text{H}_4-\text{CN})_4]$	362	119.4	2.6	2226	2230
$\beta$ - $\text{Na}[\text{B}(\text{O}-\text{C}_6\text{H}_4-\text{CN})_4]$	292	119.5	2.6	2220, 2231	2230, 2234, 2243
$\text{Na}[\text{H}-\text{B}(\text{O}-\text{C}_{12}\text{H}_8-\text{CN})_3]$	314	119.2	4.3*	2224, 2238	2233, 2249
$\text{Na}[\text{B}(\text{O}-\text{C}_{12}\text{H}_8-\text{CN})_4]$	301	119.2	2.8	2224	2219, 2237
$\text{Na}[\text{B}\{\text{O}-\text{C}_6\text{H}_3-(\text{CN})_2\}_4]$	318	117.3	2.3	2235	2238
$\text{Na}_2[\text{B}_2(\text{OMe})_2(\text{TCEG})_3]$	209	112.3, 112.4, 113.2	7.9	2256	2274
$\text{Na}[\text{B}(\text{TCEG})_2]$	305	112.1	11.9	2254, 2271	2256, 2273

\*breites Signal

Die Zersetzungspunkte der lösungsmittelfreien Natrium-Borate liegen fast ausschließlich im Bereich von 300  $^{\circ}\text{C}$  (Tabelle 2). Ausnahmen bilden hier  $\text{Na}[\text{B}(\text{O}-\text{C}_2\text{H}_4-\text{CN})_4]$  (**1**) mit den aliphatischen Cyanoethoxy-Liganden und das Diborat  $\text{Na}_2[\text{B}_2(\text{OMe})_2(\text{TCEG})_3]$  (**8**). Die bei sehr niedrigen Temperaturen einsetzende Zersetzung von **1** wurde durch NMR-spektroskopische Analyse der entweichenden, einkondensierten Zersetzungsprodukte untersucht. Dabei wurde Acrylnitril als Zersetzungsprodukt nachgewiesen, welches nach Protonenübertragung vom  $\beta$ -Kohlenstoff auf den Sauerstoff eliminiert wird (Abbildung 23).

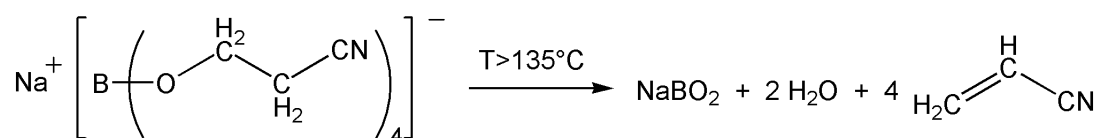


**Abbildung 23.** Thermische Zersetzung von  $\text{Na}[\text{B}(\text{O}-\text{C}_2\text{H}_4-\text{CN})_4]$ .

Durch thermische und spektroskopische Analysen lassen sich zwei Modifikationen von  $\text{Na}[\text{B}(\text{O}-\text{C}_6\text{H}_4-\text{CN})_4]$  unterscheiden. Neben dem Zersetzungspunkt, der bei  $\beta$ - $\text{Na}[\text{B}(\text{O}-\text{C}_6\text{H}_4-\text{CN})_4]$  deutlich niedriger liegt als bei  $\alpha$ - $\text{Na}[\text{B}(\text{O}-\text{C}_6\text{H}_4-\text{CN})_4]$ , lassen sich durch IR- und

Raman-Spektroskopie beim  $\beta$ -Na[B(O-C<sub>6</sub>H<sub>4</sub>-CN)<sub>4</sub>] mehr Banden für die CN-Schwingung feststellen, verglichen mit  $\alpha$ -Na[B(O-C<sub>6</sub>H<sub>4</sub>-CN)<sub>4</sub>]. Dies weist auf unterschiedliche Koordinationen an den CN-Gruppen hin, woraus sich ein struktureller Unterschied im desolvatisierten Zustand zwischen beiden Modifikationen ableiten lässt. Banden im IR- und Raman-Spektrum, die der CN-Streckschwingung zuzuordnen sind, liegen bei allen Verbindungen in einem Bereich zwischen 2219 und 2274 cm<sup>-1</sup>, der repräsentativ für diese Schwingung ist.

Die <sup>13</sup>C-NMR-Verschiebungen für die CN-Gruppen der Anionen liegen alle in einem für CN-Gruppen typischen Bereich zwischen 112 und 121 ppm. Ein signifikanter Unterschied dieser chemischen Verschiebungen ist dabei zwischen den nitrilreichen Boraten **7** und **8** (112-113 ppm) und den Boraten, die lediglich vier oder drei CN-Gruppen aufweisen, (117-121 ppm) zu erkennen. Die nitrilreichen Borate, deren CN-Gruppen in unmittelbarer Nähe zum Bor-Atom stehen, weisen ebenfalls eine deutliche Tieffeldverschiebung des <sup>11</sup>B-Signals von etwa 5 bzw. 9 ppm auf. Eine Verbreiterung der <sup>11</sup>B-Resonanz konnte beim Na[H-B(O-C<sub>12</sub>H<sub>8</sub>-CN)<sub>3</sub>] beobachtet werden, was auf eine Kopplung des Bor-Kerns mit dem direkt gebundenen (hydridischen) Wasserstoff zurückzuführen ist.

### 3.4 Stickstoffsorptionsmessungen an lösungsmittelfreien Natrium-Boraten

Für die Stickstoffsorptionsmessungen wurden desolvatisierte Proben von  $\beta$ -Na[B(O-C<sub>6</sub>H<sub>4</sub>-CN)<sub>4</sub>] (**2**) und Na[H-B(O-C<sub>12</sub>H<sub>8</sub>-CN)<sub>3</sub>] (**4**) verwendet, die in der Kristallstruktur ein von Lösungsmitteln unkoordiniertes poröses Netzwerk aufweisen. Des Weiteren wurde eine Stickstoffsorptionsmessung an einer desolvatisierten Probe von Na[B(O-C<sub>12</sub>H<sub>8</sub>-CN)<sub>4</sub>] (**5**) durchgeführt. Durch die Sorptionsmessungen konnte eine permanente Porosität in **4** nachgewiesen werden, während Proben von **2** und **5** vernachlässigbare Mengen an Stickstoff adsorbieren (Abbildung 24). Hierbei zeigt Na[H-B(O-C<sub>12</sub>H<sub>8</sub>-CN)<sub>3</sub>] eine Adsorption in Form einer Typ-I-Isotherme mit einem starken Anstieg im Bereich kleiner Partialdrücke, gefolgt von einem nur noch leichten Anstieg des adsorbierten Volumens an Stickstoff. Der Verlauf der Kurve ist dabei typisch für mikroporöse Substanzen und kann durch die Ergebnisse der Röntgenstrukturanalyse von **4**·3CH<sub>3</sub>CN belegt werden.<sup>[47]</sup> Nach Gurvich's Regel ließen sich die Porenvolumina bei  $p/p^0 = 0.95$  bestimmen, die entlang der Reihe  $0.0735 \text{ cm}^3 \cdot \text{g}^{-1}$  (**5**),  $0.0253 \text{ cm}^3 \cdot \text{g}^{-1}$  (**6**) und  $0.0094 \text{ cm}^3 \cdot \text{g}^{-1}$  (**3**) abnehmen.<sup>[48]</sup> Die spezifischen inneren Oberflächen wurden nach der BET-Theorie und einer Drei-Parameter-Anpassung berechnet. Ebenso wie die Porenvolumina nehmen die spezifischen inneren Oberflächen entlang der Reihe Na[H-B(O-C<sub>12</sub>H<sub>8</sub>-CN)<sub>3</sub>] ( $131.3 \text{ m}^2 \cdot \text{g}^{-1}$ ), Na[B(O-C<sub>12</sub>H<sub>8</sub>-CN)<sub>4</sub>] ( $17.2 \text{ m}^2 \cdot \text{g}^{-1}$ ) und Na[B(O-C<sub>6</sub>H<sub>4</sub>-CN)<sub>4</sub>] ( $7.1 \text{ m}^2 \cdot \text{g}^{-1}$ ) ab.

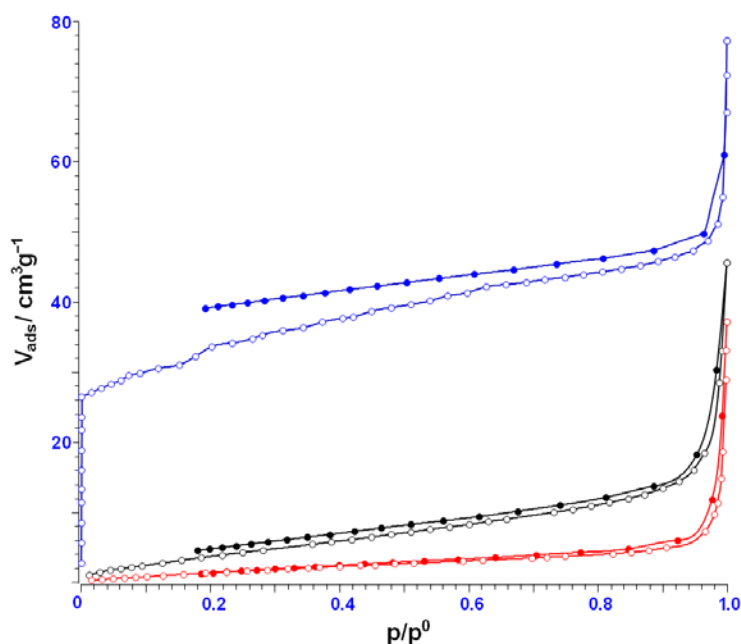


**Abbildung 24.** N<sub>2</sub>-Adsorptionsisotherme von  $\beta$ -Na[B(O-C<sub>6</sub>H<sub>4</sub>-CN)<sub>4</sub>] (rot), Na[B(O-C<sub>12</sub>H<sub>8</sub>-CN)<sub>4</sub>] (schwarz) und Na[H-B(O-C<sub>12</sub>H<sub>8</sub>-CN)<sub>3</sub>] (blau) bei  $-196 \text{ }^\circ\text{C}$ .

### 3.5 VBT-Berechnungen der Natrium-Borate

Zur Untersuchung des Einflusses der *Spacer* in den Liganden wurden VBT-Berechnungen für die synthetisierten Natrium-Borate und  $\text{Na}[\text{B}(\text{CN})_4]$  als Vergleich durchgeführt (Tabelle 3).<sup>[49,50,51]</sup> Die Anionen-Volumina vergrößern sich dabei entlang der Reihe  $[\text{B}(\text{CN})_4]^-$  ( $136.7 \text{ \AA}^3$ ) <  $[\text{B}(\text{TCEG})_2]^-$  ( $329.4 \text{ \AA}^3$ ) <  $[\text{B}(\text{O}-\text{C}_2\text{H}_4-\text{CN})_4]^-$  ( $361.6 \text{ \AA}^3$ ) <  $[\text{B}_2(\text{OMe})_2(\text{TCEG})_3]^{2-}$  ( $563.5 \text{ \AA}^3$ ) <  $[\text{B}(\text{O}-\text{C}_6\text{H}_4-\text{CN})_4]^-$  ( $571.6 \text{ \AA}^3$ ) <  $[\text{B}\{\text{O}-\text{C}_6\text{H}_3-(\text{CN})_2\}_4]^-$  ( $604.8 \text{ \AA}^3$ ) <  $[\text{H}-\text{B}(\text{O}-\text{C}_{12}\text{H}_8-\text{CN})_3]^-$  ( $737.2 \text{ \AA}^3$ ) <  $[\text{B}(\text{O}-\text{C}_{12}\text{H}_8-\text{CN})_4]^-$  ( $963.4 \text{ \AA}^3$ ). Mit wachsendem Anionen-Volumen nehmen hierbei die Gitterenergie und Gitterenthalpie ab. Eine Ausnahme stellt hierbei das Diborat  $[\text{B}_2(\text{OMe})_2(\text{TCEG})_3]^{2-}$  dar, bei dessen Berechnung der Gitterenergie und Gitterenthalpie eine höhere Ionenstärke berücksichtigt werden muss, die maßgeblich das Ergebnis beeinflusst. Die Standardentropien der Verbindungen stehen hingegen in Proportion zum molekularen Volumen und steigen dementsprechend entlang der oben genannten Reihe.

**Tabelle 3:** Anionen-Volumina der CN-funktionalisierten Borat-Anionen und thermodynamische Daten, berechnet durch volumenbasierte Thermodynamik (VBT) für die Natrium-Salze ( $V(\text{Na}^+) = 27.7 \text{ \AA}^3$ ).

	$V_{\text{anion}} (\text{\AA}^3)$	$U_{\text{pot}} (\text{kJ mol}^{-1})$	$S^\circ_{298} (\text{J K}^{-1} \text{mol}^{-1})$	$\Delta H_L (\text{kJ mol}^{-1})$
$[\text{B}(\text{CN})_4]^-$ <sup>a</sup>	136.7	540.8	225.4	542.0
$[\text{B}(\text{O}-\text{C}_2\text{H}_4-\text{CN})_4]^-$ <sup>a</sup>	361.6	427.8	531.4	431.5
$[\text{B}(\text{O}-\text{C}_6\text{H}_4-\text{CN})_4]^-$ <sup>a</sup>	571.6	383.6	816.9	384.8
$[\text{B}\{\text{O}-\text{C}_6\text{H}_3-(\text{CN})_2\}_4]^-$ <sup>a</sup>	604.8	378.5	862.1	379.7
$[\text{H}-\text{B}(\text{O}-\text{C}_{12}\text{H}_8-\text{CN})_3]^-$ <sup>a</sup>	737.2	361.4	1042.2	362.6
$[\text{B}(\text{O}-\text{C}_{12}\text{H}_8-\text{CN})_4]^-$ <sup>a</sup>	963.4	339.9	1349.7	341.1
$[\text{B}_2(\text{OMe})_2(\text{TCEG})_3]^{2-}$ <sup>b</sup>	563.5	997.3	830.5	997.3
$[\text{B}(\text{TCEG})_2]^-$ <sup>a</sup>	329.4	437.5	487.6	438.7

$$^a U_{\text{pot}} = 2 \cdot 1 \left( \frac{117.3}{\sqrt[3]{V_m}} + 51.9 \text{ kJ mol}^{-1} \right), \Delta H_L = U_{\text{pot}} + 1 \left( \frac{3}{2} - 2 \right) RT + 1 \left( \frac{6}{2} - 2 \right) RT;$$

$$^b U_{\text{pot}} = 2 \cdot 3 \left( \frac{165.3}{\sqrt[3]{V_m}} - 29.8 \text{ kJ mol}^{-1} \right), \Delta H_L = U_{\text{pot}} + 2 \left( \frac{3}{2} - 2 \right) RT + 1 \left( \frac{6}{2} - 2 \right) RT;$$

$$S^\circ_{298} = 1360V_m + 15 \text{ J K}^{-1} \text{mol}^{-1}, \text{ korrigierte Hofmann-Volumina wurden verwendet.}^{[52]}$$



### 3.6 Darstellung von Addukt-Anionen mit Tris(pentafluorphenyl)boran

Die Addukt-Anionen der synthetisierten CN-haltigen Borate sollten analog der Darstellung des  $[\text{B}\{\text{CN}\cdot\text{B}(\text{C}_6\text{F}_5)_3\}_4]^-$  durch Umsetzung mit Tris(pentafluorphenyl)boran erfolgen. Am Beispiel des  $[\text{B}(\text{O}-\text{C}_6\text{H}_4-\text{CN})_4]^-$ -Anions konnte jedoch gezeigt werden, dass die  $\text{BO}_4$ -Einheit in den Anionen eine Schwachstelle gegenüber stark Lewis-sauren Systemen darstellt. Bei der Umsetzung mit einem Überschuss an  $\text{B}(\text{C}_6\text{F}_5)_3$  wurde eine Fragmentierung des Anions durch  $^{11}\text{B}$ -NMR-Messung beobachtet, bei der, entgegen den Erwartungen, ein komplexeres Spektrum mit vier anstatt zwei Signalen erhalten wurde. Zudem konnte ein Fragment der Zersetzungsreaktion kristallisiert und durch Röntgenkristallstrukturanalyse als  $\text{Na}(\text{OEt}_2)_4[(\text{F}_5\text{C}_6)_3\text{B}\cdot\text{O}-\text{C}_6\text{H}_4-\text{CN}\cdot\text{B}(\text{C}_6\text{F}_5)_3]$  bestimmt werden (Abbildung 25).

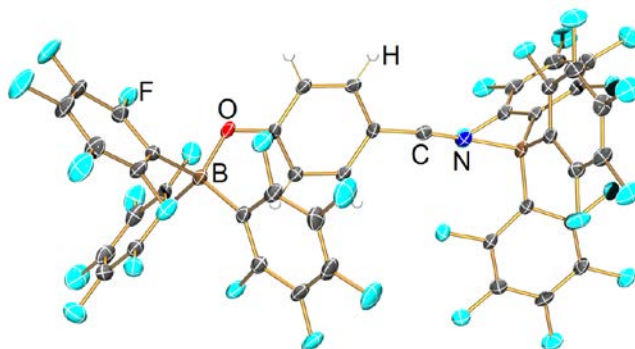
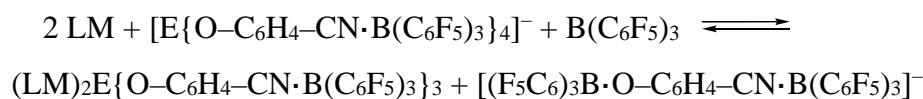


**Abbildung 25.** ORTEP-Darstellung des Anions in der Molekülstruktur von  $\text{Na}(\text{OEt}_2)_4[(\text{F}_5\text{C}_6)_3\text{B}\cdot\text{O}-\text{C}_6\text{H}_4-\text{CN}\cdot\text{B}(\text{C}_6\text{F}_5)_3]$ . Thermische Ellipsoide entsprechen 30 % Wahrscheinlichkeit bei 173 K. Farbkodierung: C dunkelgrau, H weiß, B braun, F hellblau, N blau, O rot.

Aus dieser Reaktion konnte das verbliebene neutrale Fragment zwar nicht sauber isoliert werden, jedoch gelang es aus einem analogen Ansatz mit  $[\text{Al}(\text{O}-\text{C}_6\text{H}_4-\text{CN})_4]^-$  und  $\text{B}(\text{C}_6\text{F}_5)_3$  das Lewis-saure Fragment als Lösungsmittel-Addukt  $(\text{THF})_2\text{Al}\{\text{O}-\text{C}_6\text{H}_4-\text{CN}\cdot\text{B}(\text{C}_6\text{F}_5)_3\}_3$  zu kristallisieren. Somit lassen diese strukturanalytischen und NMR-spektroskopischen Daten Rückschlüsse auf die Zersetzung ziehen, wie sie durch folgende Reaktionsgleichung im Allgemeinen für das Aluminat und Borat ( $\text{E} = \text{Al}, \text{B}$ ) beschrieben werden kann:



Die Addukt-Bildung mit  $\text{B}(\text{C}_6\text{F}_5)_3$  wurde zudem mit  $[\text{B}(\text{O}-\text{C}_2\text{H}_4-\text{CN})_4]^-$  vorgenommen, um die Stabilität der Anionen hinsichtlich der *Spacer*-Gruppen zu untersuchen. Jedoch wurde

auch bei diesem aliphatischen Ligandensystem eine Zersetzung analog der in obiger Reaktionsgleichung beschriebenen Reaktion mittels  $^{11}\text{B}$ -NMR-Spektroskopie nachgewiesen.

Die Problematik der Addukt-Bildung ist in beiden Reaktionen, dass wie beim  $[\text{B}(\text{CN})_4]^-$  ein Überschuss an  $\text{B}(\text{C}_6\text{F}_5)_3$  benötigt wird, um vierfache Addukt-Bildung zu erzielen. Jedoch führt dieser Überschuss bei Boraten mit  $\text{BO}_4$ -Zentren zur Abstraktion eines Liganden, der nach der Fragmentierung zweifach vom Boran koordiniert wird. Das Lewis-saure Fragment wird durch Donor-Akzeptor-Wechselwirkungen mit Lösungsmittelmolekülen stabilisiert, was die Rückreaktion beeinträchtigt.

### 3.7 Darstellung CN-funktionalisierter ionischer Flüssigkeiten

Bei der Synthese ionischer Flüssigkeiten mit den CN-funktionalisierten Boraten sollte zunächst ein Austausch von  $\text{Na}^+$  mit schwach koordinierenden Kationen (WCCs), z.B. Tetraalkylammonium- und 1-Alkyl-3-methylimidazolium-Kationen, erfolgen. Salzmetathese-Reaktionen der Natrium-Borate mit den Ammonium- und Imidazolium-chloriden in Acetonitril führten zu den besten Ergebnissen (Abbildung 26). Zur Darstellung der ionischen Flüssigkeiten wurden hierbei die Natrium-Salze von  $[\text{B}(\text{O}-\text{C}_2\text{H}_4-\text{CN})_4]^-$  und  $[\text{B}(\text{TCEG})_2]^-$  umgesetzt.

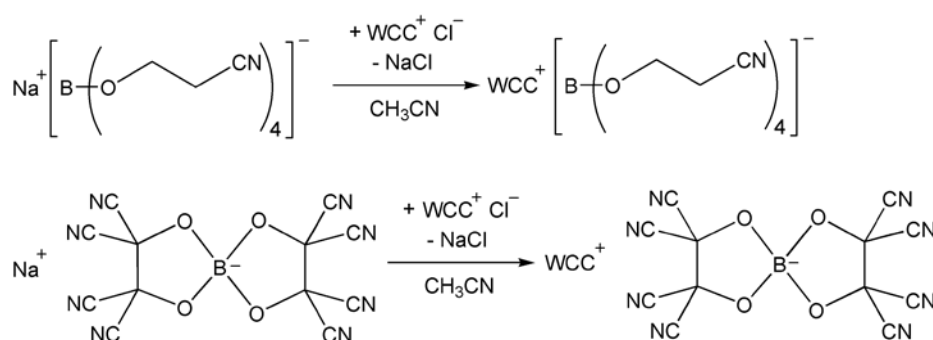


**Abbildung 26.** Darstellung von  $\text{WCC}[\text{B}(\text{O}-\text{C}_2\text{H}_4-\text{CN})_4]$  und  $\text{WCC}[\text{B}(\text{TCEG})_2]$  (WCC = EMI, BMIm, OMIm, Me<sub>4</sub>N, Et<sub>4</sub>N, Bu<sub>4</sub>N).

Nach Ausfällen und Abtrennen des in der Reaktion entstehenden Natriumchlorids sowie anschließendem Entfernen des Lösungsmittels konnten  $\text{WCC}[\text{B}(\text{O}-\text{C}_2\text{H}_4-\text{CN})_4]$  und  $\text{WCC}[\text{B}(\text{TCEG})_2]$  in sehr guten Ausbeuten (86-93 %) erhalten werden. Sämtliche Salze mit  $[\text{B}(\text{O}-\text{C}_2\text{H}_4-\text{CN})_4]^-$  als Anion konnten kristallisiert und kristallografisch vermessen werden. In Abbildung 27 ist die Struktur von  $\text{OMIm}[\text{B}(\text{O}-\text{C}_2\text{H}_4-\text{CN})_4]$  als Beispielstruktur dargestellt.

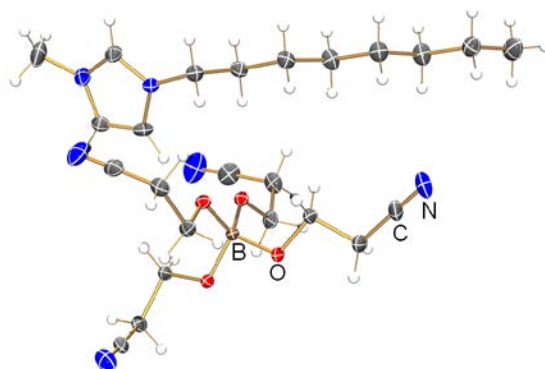


**Abbildung 27.** ORTEP-Darstellung der Molekülstruktur von  $\text{OMIm}[\text{B}(\text{O}-\text{C}_2\text{H}_4-\text{CN})_4]$ . Thermische Ellipsoide entsprechen 30 % Wahrscheinlichkeit bei 173 K. Farbkodierung: C dunkelgrau, H weiß, B braun, N blau, O rot.

Die Ergebnisse der thermischen Analysen der WCC-Borate durch DSC-Messungen dienten hierbei als Kriterium, welche Verbindungen als ionische Flüssigkeiten charakterisiert werden können. Eine Zusammenfassung der so bestimmten Schmelz- ( $T_{\text{Smp}}$ ), Glasübergangs- ( $T_{\text{G}}$ ) und Zersetzungspunkte ( $T_{\text{Zers}}$ ) ist neben den Ausbeuten in Tabelle 4 angegeben.

**Tabelle 4:** Ausbeuten, Schmelz- ( $T_{\text{Smp}}$ ; Peak-Wert), Glasübergangs- ( $T_{\text{G}}$ ; Wendepunkt der Kurve) und Zersetzungspunkte ( $T_{\text{Zers}}$ ; Onset-Wert) von WCC[B(O–C<sub>2</sub>H<sub>4</sub>–CN)<sub>4</sub>] und WCC[B(TCEG)<sub>2</sub>].

Anion	Kation	Ausbeute	$T_{\text{Smp}}/^{\circ}\text{C}$ ( $T_{\text{G}}$ )	$T_{\text{Zers}}/^{\circ}\text{C}$
[B(O–C <sub>2</sub> H <sub>4</sub> –CN) <sub>4</sub> ]	EMIm	91	39 (–5) <sup>[a]</sup>	121
	BMIm	92	41 (–15) <sup>[b]</sup>	97
	OMIm	89	47 (–40) <sup>[c]</sup>	96
	Me <sub>4</sub> N	86	87	87
	Et <sub>4</sub> N	89	26 (–40) <sup>[c]</sup>	80
	Bu <sub>4</sub> N	87	96	96
[B(TCEG) <sub>2</sub> ]	EMIm	90	66	222
	BMIm	89	45 (–34) <sup>[d]</sup>	242
	OMIm	93	(–47) <sup>[e]</sup>	257
	Me <sub>4</sub> N	88	173	270
	Et <sub>4</sub> N	91	140	248
	Bu <sub>4</sub> N	90	95	270

[a] kristallisiert nach 1 Woche bei RT, [b] kristallisiert nach 4 Wochen bei RT, [c] kristallisiert aus Lösung bei –40 °C, [d] kristallisiert durch Reiben mit Glasstab bei RT, [e] keine Kristallisation beobachtbar.

Die Verbindungen WCC[B(O–C<sub>2</sub>H<sub>4</sub>–CN)<sub>4</sub>] stellen allesamt ionische Flüssigkeiten dar, wobei mit Me<sub>4</sub>N<sup>+</sup>- und Bu<sub>4</sub>N<sup>+</sup>-Kationen Salze gebildet werden, die erst am Zersetzungspunkt zu schmelzen anfangen. Die Salze mit OMIm<sup>+</sup>- und Et<sub>4</sub>N<sup>+</sup>-Kationen konnten zwar nur aus der Lösung bei –40 °C kristallisiert werden, stellen jedoch streng betrachtet keine Raumtemperatur ionischen Flüssigkeiten dar. Beim [B(TCEG)<sub>2</sub>]<sup>–</sup>-Anion sind alle imidazoliumbasierten Verbindungen ionische Flüssigkeiten, wobei das OMIm-Salz eine Raumtemperatur ionische Flüssigkeit ist. Allgemein sinkt mit zunehmender Kettenlänge der Alkyl-Gruppen in den Ammonium-Salzen der Schmelzpunkt, so dass auch das Bu<sub>4</sub>N-Salz als ionische Flüssigkeit betrachtet werden kann.

Wie zu erwarten, traten in der Reihe der WCC[B(O–C<sub>2</sub>H<sub>4</sub>–CN)<sub>4</sub>]- und WCC[B(TCEG)<sub>2</sub>]-Verbindungen keine signifikanten Unterschiede der <sup>13</sup>C- und <sup>11</sup>B-NMR-Verschiebungen auf (Tabelle 5). Die Absorptionsbanden der CN-Streckschwingung in den IR- und Ramanspektren

befinden sich alle in einem schmalen Bereich zwischen 2240 und 2255  $\text{cm}^{-1}$ . Im Vergleich zu den Natrium-Verbindungen von  $[\text{B}(\text{O}-\text{C}_2\text{H}_4-\text{CN})_4]^-$  und  $[\text{B}(\text{TCEG})_2]^-$  sind die Banden zu kleineren Wellenzahlen verschoben, was auf schwächere Kation-Anion-Wechselwirkungen hinweist.

**Tabelle 5:** Spektroskopische Daten: IR-, Raman-,  $^{11}\text{B}$ - und  $^{13}\text{C}$ -NMR-Daten von  $\text{WCC}[\text{B}(\text{O}-\text{C}_2\text{H}_4-\text{CN})_4]$  und  $\text{WCC}[\text{B}(\text{TCEG})_2]$ .

Anion	Kation	$^{13}\text{C}$ -NMR (CN)/ ppm	$^{11}\text{B}$ -NMR/ ppm	IR ( $\tilde{\nu}_{\text{CN}}$ )/ $\text{cm}^{-1}$	Raman( $\tilde{\nu}_{\text{CN}}$ )/ $\text{cm}^{-1}$
$[\text{B}(\text{O}-\text{C}_2\text{H}_4-\text{CN})_4]$	EMIm	120.5	2.60	2240	2245
	BMIm	119.4	2.64	2245	2245
	OMIm	120.9	2.64	2243	2244
	$\text{Me}_4\text{N}$	121.0	2.39	2241	2242
	$\text{Et}_4\text{N}$	120.8	2.48	2243	2247
	$\text{Bu}_4\text{N}$	120.7	2.60	2245	2242
$[\text{B}(\text{TCEG})_2]$	EMIm	112.1	11.96	2251	2247
	BMIm	112.1	11.92	2251	2247, 2255
	OMIm	112.1	11.96	2250	2240
	$\text{Me}_4\text{N}$	112.1	11.98	2242	2243, 2253
	$\text{Et}_4\text{N}$	112.1	11.94	2248	2255
	$\text{Bu}_4\text{N}$	112.1	11.96	2250	2248

## 4 Literaturverzeichnis

---

- [1] a) C. Friedel, J. M. Crafts, *C. R. Acad. Sci.* **1877**, *84*, 1392-1395; b) H. C. Brown, H. W. Pearsall, *J. Am. Chem. Soc.* **1952**, *74*, 191-195; c) T. Matsumoto, K. Ichikawa, *J. Am. Chem. Soc.* **1984**, *106*, 4316-4320.
- [2] S. Brownstein, J. Paasivirta, *Can. J. Chem.* **1965**, *43*, 1645-1649.
- [3] R. J. Gillespie, K. C. Moss, *J. Chem. Soc. A* **1966**, 1170-1175.
- [4] S. Brownstein, *Can. J. Chem.* **1969**, *47*, 605-609.
- [5] a) K. O. Christe, W. Maya, *Inorg. Chem.* **1969**, *8*, 1253-1257; c) P. A. W. Dean, R. J. Gillespie, R. Hume, *J. Chem. Soc. D* **1969**, 990-991.
- [6] A. J. Edwards, G. R. Jones, R. J. Sills, *J. Chem. Soc., Chem. Commun.* **1968**, 1527-1528.
- [7] T. Drews, K. Seppelt, *Angew. Chem.* **1997**, *109*, 264-266; *Angew. Chem. Int. Ed. Engl.* **1997**, *36*, 273-274.
- [8] S. J. Lancaster, D. A. Walker, M. Thornton-Pett, M. Bochmann, *Chem. Commun.* **1999**, 1533-1534.
- [9] S. J. Lancaster, A. Rodriguez, A. Lara-Sanchez, M. D. Hannant, D. A. Walker, D. H. Hughes, M. Bochmann, *Organometallics* **2002**, *21*, 451-453.
- [10] J. Zhou, S. J. Lancaster, D. A. Walker, S. Beck, M. Thornton-Pett, M. Bochmann, *J. Am. Chem. Soc.* **2001**, *123*, 223-237.
- [11] M. H. Hannant, J. A. Wright, S. J. Lancaster, D. L. Hughes, P. N. Horton, M. Bochmann, *Dalton Trans.* **2006**, 2415-2426.
- [12] A. Bernsdorf, H. Brand, R. Hellmann, M. Köckerling, A. Schulz, A. Villinger, K. Voss, *J. Am. Chem. Soc.* **2009**, *131*, 8958-8970.
- [13] K. Voss, M. Becker, A. Villinger, V. N. Emelyanenko, R. Hellmann, B. Kirchner, F. Uhlig, S. P. Verevkin, A. Schulz, *Chem. Eur. J.* **2011**, *17*, 13526-13537.
- [14] J. S. Wilkes, *Green Chemistry* **2002**, *4*, 73-80.
- [15] R. P. Swatloski, S. K. Spear, J. D. Holbrey, R. D. Rogers, *J. Am. Chem. Soc.* **2002**, *124*, 4974-4975.
- [16] D. Zhao, M. Wu, Y. Kou, E. Min, *Catal. Today* **2002**, *74*, 157-189.
- [17] a) M. E. Van Valkenburg, R. L. Vaughn, M. Williams, J. S. Wilkes, *Thermochim. Acta* **2005**, *425*, 181-188; b) M. Zhang, R. G. Reddy, *ECS Trans.* **2007**, *2*, 27-34.
- [18] N. Madriaa, T. A. Arunkumar, N. G. Nair, A. Vadapalli, Y.-W. Huang, S. C. Jones, V. P. Reddy, *J. Power Sources* **2013**, *234*, 277-284.

- 
- [19] a) D. Zhao, Z. Fei, T. J. Geldbach, R. Scopelliti, P. J. Dyson, *J. Am. Chem. Soc.* **2004**, *126*, 15876-15882; b) Z. Fei, D. Zhao, D. Pieraccini, W. H. Ang, T. J. Geldbach, R. Scopelliti, C. Chiappe, P. J. Dyson, *Organometallics* **2007**, *26*, 1588-1598; c) C. Premi, N. Jain, *Eur. J. Org. Chem.* **2013**, *78*, 5493-5499; d) C. Chiappe, D. Pieraccini, D. Zhao, Z. Fei, P. J. Dyson, *Adv. Synth. Catal.* **2006**, *348*, 68-74.
- [20] K. Sasaki, S. Matsumura, K. Toshima, *Tetrahedron Lett.* **2004**, *45*, 7043-7047.
- [21] H. Bönnemann, R. Brinkmann, S. Kinge, T. O. Ely, M. Armand, *Fuell Cells* **2004**, *4*, 289-296.
- [22] M. Becker, J. Harloff, T. Jantz, A. Schulz, A. Villinger, *Eur. J. Inorg. Chem.* **2012**, *34*, 5658-5667.
- [23] D. R. MacFarlane, S. A. Forsyth, J. Golding, G. B. Deacon, *Green Chemistry* **2002**, *4*, 444-448.
- [24] C. Täschler, C. Zur Täschler, A. Breuer, F. Previdoli, *WO 2006/021390 A1* **2006**.
- [25] U. Welz-Biermann, N. Ignatjev, E. Bernhardt, M. Finze, H. Willner, *German Pat. DE 10306617/A1* **2004**.
- [26] S. R. Batten, N. R. Champness, X.-M. Chen, J. Garcia-Martinez, S. Kitagawa, L. Öhrström, M. O'Keeffe, M. P. Suh, J. Reedijk, *Pure Appl. Chem.* **2013**, *85*, 1715-1724.
- [27] a) B. Chen, Y. Yang, F. Zapata, G. Lin, G. Qian, E. B. Lobkovsky, *Adv. Mater.* **2007**, *19*, 1693-1696; b) S. M. Holmes, G. S. Girolami, *J. Am. Chem. Soc.* **1999**, *121*, 5593-5594; c) V. Niel, J. M. Martinez-Agudo, M. C. Muñoz, A. B. Gaspar, J. A. Real, *Inorg. Chem.* **2001**, *40*, 3838-3839; d) S. Kitagawa, R. Kitaura, S. Noro, *Angew. Chem.* **2004**, *116*, 2388-2430; *Angew. Chem. Int. Ed.* **2004**, *43*, 2334-2375.
- [28] M. D. Dembo, L. E. Dunaway, J. S. Jones, E. A. Lepekhina, S. M. McCullough, J. L. Ming, X. Li, F. Baril-Robert, H. H. Patterson, C. A. Bayse, R. D. Pike, *Inorg. Chim. Acta* **2010**, *364*, 102-114.
- [29] a) Y. Sato, S. Ohkoshi, K. Arai, M. Tozawa, K. Hashimoto, *J. Am. Chem. Soc.* **2003**, *125*, 14590-14595; b) S. Ohkoshi, K. Arai, Y. Sato, K. Hashimoto, *Nat. Mater.* **2004**, *3*, 857-861; c) B. Nowicka, M. Rams, K. Stadnicka, B. Sieklucka, *Inorg. Chem.* **2007**, *46*, 8123-8125.
- [30] a) G. J. Halder, C. J. Kepert, B. Moubaraki, K. S. Murray, J. D. Cashion, *Science* **2002**, *298*, 1762-1765; b) K. Biradha, M. Fujita, *Angew. Chem.* **2002**, *114*, 3542-3545; *Angew. Chem. Int. Ed.* **2002**, *41*, 3392-3395; c) K. W. Chapman, P. J. Chupas, E. R.

- 
- Maxey, J. W. Richardson, *Chem. Commun.* **2006**, 4013-4015; d) B. F. Hoskins, R. Robson, *J. Am. Chem. Soc.* **1989**, *111*, 5962-5964.
- [31] M. V. Bennett, L. G. Beauvais, M. P. Shores, J. R. Long, *J. Am. Chem. Soc.* **2001**, *123*, 8022-8032.
- [32] a) S. R. Batten, P. Jensen, B. Moubaraki, K. S. Murray, R. Robson, *Chem. Commun.* **1998**, 439-440; b) P. Jensen, S. R. Batten, G. D. Fallon, B. Moubaraki, K. S. Murray, D. J. Price, *Chem. Commun.* **1999**, 177-178; c) S. R. Marshall, C. D. Incarvito, J. L. Manson, A. L. Rheingold, J. S. Miller, *Inorg. Chem.* **2000**, *39*, 1969-1973; d) Z.-M. Wang, B.-W. Sun, J. Luo, S. Gao, C.-S. Liao, C.-H. Yan, Y. Li, *Inorg. Chim. Acta* **2002**, *332*, 127-134.
- [33] a) S. R. Batten, B. F. Hoskins, B. Moubaraki, K. S. Murray, R. Robson, *J. Chem. Soc., Dalton Trans.* **1999**, 2977-2986; b) P. Jensen, D. J. Price, S. R. Batten, B. Moubaraki, K. S. Murray, *Chem. Eur. J.* **2000**, *6*, 3186-3195.
- [34] a) J. M. Manriquez, G. T. Yee, R. S. McLean, A. J. Epstein, J. S. Miller, *Science* **1991**, *252*, 1415-1417; b) J. S. Miller, J. C. Calabrese, R. S. McLean, A. J. Epstein, *Adv. Mater.* **1992**, *4*, 498-501; c) F. A. Cotton, Y. Kim, *J. Am. Chem. Soc.*, **1993**, *115*, 8511-8512; d) J. S. Miller, C. Vazquez, N. L. Jones, R. S. McLean, A. J. Epstein, *J. Mater. Chem.* **1995**, *5*, 707-711.
- [35] a) L. Shields, *J. Chem. Soc., Faraday Trans. 2* **1985**, *81*, 1-9; b) S. Shimomura, R. Matsuda, T. Tsujino, T. Kawamura, S. Kitagawa, *J. Am. Chem. Soc.* **2006**, *128*, 16416-16417; c) H. Miyasaka, C. S. Campos-Fernández, R. Clérac, K. R. Dunbar, *Angew. Chem.* **2000**, *112*, 3989-3993; *Angew. Chem. Int. Ed.* **2000**, *39*, 3831-3835.
- [36] F.-Q. Liu, T. D. Tilley, *Inorg. Chem.* **1997**, *36*, 5090-5096.
- [37] D. Venkataraman, G. B. Gardner, S. Lee, J. S. Moore, *J. Am. Chem. Soc.* **1995**, *117*, 11600-11601.
- [38] G. B. Gardner, D. Venkataraman, J. S. Moore, S. Lee, *Nature* **1995**, *374*, 792-795.
- [39] L. Carlucci, G. Ciani, D. W. v. Gudenberg, D. M. Proserpio, *New J. Chem.* **1999**, *23*, 397-402.
- [40] K. A. Hirsch, S. R. Wilson, J. S. Moore, *Chem. Eur. J.* **1997**, *3*, 765-771.
- [41] a) E. Bernhardt, G. Henkel, H. Willner, *Z. Anorg. Allg. Chem.* **2000**, *626*, 560-568; b) T. Küppers, E. Bernhardt, H. Willner, H. W. Rohm, M. Köckerling, *Inorg. Chem.* **2005**, *44*, 1015-1022; c) C. Nitschke, M. Köckerling, *Z. Anorg. Allg. Chem.* **2009**, *635*, 503-507.
- [42] J. M. Birchall, R. N. Haszeldine, M. E. Jones, *J. Chem. Soc. C* **1971**, 1343-1348.



- 
- [43] B. Heinrich, D. Guillon, *Mol. Cryst. Liq. Cryst.* **1995**, 268, 21-43.
- [44] a) M. Mazik, W. Sicking, *Chem. Eur. J.* **2001**, 7, 664-670; b) W. Thiel, R. Mayer, E.-A. Jauer, H. Modrow, H. Dost, *J. f. prakt. Chemie* **1986**, 328, 497-514.
- [45] C. A. Angell, W. Xu, US2004/0034253 A1 **2004**.
- [46] W. Lidy, W. Sundermeyer, *Chem. Ber.* **1973**, 106, 587-593.
- [47] K. S.W. Sing, D. H. Everett, R. A. W. Haul, L. Mouscou, R. A. Pierotti, J. Rouquerol, T. Siemieniewska, *Pure Appl. Chem.* **1985**, 57, 603-619.
- [48] a) F. Rouquerol, J. Rouquerol, K. S. W. Sing, *Adsorption by Powders and Porous Solids*, Academic Press, UK **1999**; b) S. Lowell, J. Shields, M. A. Thomas, M. Thommes, *Characterization of Porous Solids and Powders: Surface Area, Pore Size and Density*, Springer, Netherlands **2004**.
- [49] D. W. M. Hofmann, *Acta Cryst.* **2002**, B58, 489-493.
- [50] a) V. M. Goldschmidt, *Chem. Ber.* **1927**, 60, 1263-1296; b) R. D. Shannon, *Acta Cryst.* **1976**, A32, 751-767; c) L. Glasser, H. D. B. Jenkins, *Inorg. Chem.* **2008**, 47, 6195-6202.
- [51] a) H. D. B. Jenkins, L. Glasser, T. M. Klapötke, M.-J. Crawford, K. K. Bhasin, J. Lee, G. J. Schrobilgen, L. S. Sunderlin, J. F. Liebman, *Inorg. Chem.* **2004**, 43, 6238-6248; b) H. D. Jenkins, J. F. Liebman, *Inorg. Chem.* **2005**, 44, 6359-6372.
- [52] U. Preiss, J. M. Slattery, I. Krossing, *Ind. Eng. Chem. Res.* **2009**, 48, 2290-2296.

## **5 Publikationen**

Die im vorhergehenden Kapitel zusammengefassten Ergebnisse stellen Auszüge eigener Publikationen dar. Im aktuellen Kapitel sind die bereits veröffentlichten Publikationen bzw. das Manuskript der angenommenen Publikation enthalten. Der eigene Beitrag zu den betreffenden Publikationen ist jeweils angegeben.

## 5.1 Molecular Networks Based on CN Coordination Bonds

Markus Karsch, Henrik Lund, Axel Schulz, Alexander Villinger, Karsten Voss.

*Eur. J. Inorg. Chem.* **2012**, 5542-5553.

Der Großteil der experimentellen Arbeiten wurde in dieser Publikation von mir durchgeführt. Die in dieser Arbeit erstmalig publizierten Verbindungen  $\text{Li}[\text{Al}(\text{O}-\text{C}_6\text{H}_4-\text{CN})_4]$ ,  $\text{Na}[\text{B}(\text{O}-\text{C}_6\text{H}_4-\text{CN})_4]$ ,  $\text{Li}[\text{Al}(\text{O}-\text{C}_6\text{F}_4-\text{CN})_4]$ ,  $\text{Na}(\text{O}-\text{C}_6\text{F}_4-\text{CN})$ ,  $\text{Na}[(\text{F}_5\text{C}_6)_3\text{B}\cdot\text{O}-\text{C}_6\text{H}_4-\text{CN}\cdot\text{B}(\text{C}_6\text{F}_5)_3]$ ,  $\text{Na}[(\text{F}_5\text{C}_6)_3\text{B}\cdot\text{O}-\text{C}_6\text{F}_4-\text{CN}\cdot\text{B}(\text{C}_6\text{F}_5)_3]$  und  $\text{Li}[\text{NC}-\text{C}_6\text{F}_4-\text{O}-\text{Al}\{\text{O}-\text{C}_6\text{F}_4-\text{CN}\cdot\text{B}(\text{C}_6\text{F}_5)_3\}_3]$  wurden von mir synthetisiert und vollständig charakterisiert. Die Verbindungen  $\text{Li}[\text{Al}(\text{O}-\text{C}_6\text{F}_4-\text{CN})_4]$ ,  $\text{Na}(\text{O}-\text{C}_6\text{F}_4-\text{CN})$  (2 Modifikationen),  $\text{Na}[(\text{F}_5\text{C}_6)_3\text{B}\cdot\text{O}-\text{C}_6\text{H}_4-\text{CN}\cdot\text{B}(\text{C}_6\text{F}_5)_3]$ ,  $\text{Na}[(\text{F}_5\text{C}_6)_3\text{B}\cdot\text{O}-\text{C}_6\text{F}_4-\text{CN}\cdot\text{B}(\text{C}_6\text{F}_5)_3]$  und  $\text{Li}[\text{NC}-\text{C}_6\text{F}_4-\text{O}-\text{Al}\{\text{O}-\text{C}_6\text{F}_4-\text{CN}\cdot\text{B}(\text{C}_6\text{F}_5)_3\}_3]$  konnte ich für strukturanalytische Zwecke kristallisieren.

Bei der Publikation habe ich als Co-Autor mitgewirkt. Die Synthesen der Verbindungen und die analytischen Daten wurden von mir im Supporting zusammengefasst. Zudem habe ich an den Korrekturen zu dem Manuskript mitgewirkt. Der eigene Anteil liegt bei ca. 60 %.

## Molecular Networks Based on CN Coordination Bonds

Markus Karsch,<sup>[a]</sup> Henrik Lund,<sup>[a]</sup> Axel Schulz,<sup>\*[a,b]</sup> Alexander Villinger,<sup>[a]</sup> and Karsten Voss<sup>[a]</sup>

**Keywords:** Coordination polymers / Aluminates / Borates / Silver / Copper / Bridging ligands

This study examines the use of tetrahedral  $[E(O-C_6X_4-CN)_4]^-$  anions ( $E = B, Al; X = H, F$ ), which can be synthesized from the reaction of tetrahedral  $NaBH_4/LiAlH_4$  and  $HO-C_6X_4-CN$ , as anionic linkers for the generation of 2D and 3D crystalline coordination polymer networks. Such polymer networks were obtained by the connection of tetrahedral *p*-cyanophenoxy aluminate or borate linkers with monocationic metal centers such as  $Li^+$ ,  $Na^+$ ,  $Ag^+$ , and  $Cu^+$ . These studies are specifically focused on the synthesis, structure, and stability of such polymers. Additionally, the perfluorinated  $O-C_6F_4-CN$  linker was used to study electronic influences. Salts

bearing the perfluorinated  $[E(O-C_6F_4-CN)_4]^-$  anion decompose into  $E(O-C_6F_4-CN)_3$  and  $[O-C_6F_4-CN]^-$ , which is also observed when a Lewis acid such as  $B(C_6F_5)_3$  is added. Moreover, addition of  $B(C_6F_5)_3$  leads to the formation of molecular-ion pairs because the cyano groups are now either completely or partly blocked. The structures of  $M[Al(O-C_6H_4-CN)_4]$  ( $M = Li, Ag, Cu$ ),  $Na[B(O-C_6H_4-CN)_4]$ , and  $Li[Al(O-C_6F_4-CN)_4]$  as well as of the decomposition products  $Na(O-C_6F_4-CN)$ ,  $(THF)Al[O-C_6H_4-CN \cdot B(C_6F_5)_3]_3$  ( $THF =$  tetrahydrofuran),  $Na[(F_5C_6)_3B \cdot O-C_6H_4-CN \cdot B(C_6F_5)_3]$ , and  $Li[NC-C_6F_4-O-Al(O-C_6F_4-CN \cdot B(C_6F_5)_3)_3]$  are discussed.

### Introduction

The directed synthesis of coordination polymers<sup>[1]</sup> with two- or three-dimensional framework structures can be achieved through the connection of molecular building blocks through hydrogen bonds,<sup>[2,3]</sup> donor–acceptor bonds,<sup>[4]</sup> halogen bonds,<sup>[5]</sup> metal–metal,<sup>[6]</sup>  $CH-\pi$ ,<sup>[7]</sup> and  $\pi-\pi$  interactions.<sup>[8]</sup> The synthesis and characterization of infinite two- and three-dimensional networks has been an area of rapid growth, because many applications of their useful electronic, magnetic, optical, and catalytic properties are expected.

Coordination polymers are composed of connectors and linkers.<sup>[1]</sup> We decided to study tetraphenoxaluminates and borates of the type  $[E(O-C_6X_4-CN)_4]^-$  ( $E = B, Al; X = H, F$ ) with one cyano group as binding site per phenoxy group as linker. Transition-metal ions such as silver or copper ions are often utilized as versatile connectors in the construction of coordination polymers. Depending on the metal and its oxidation state, different coordination numbers and geometries, such as linear, tetrahedral, square planar, square pyramidal, trigonal bipyramidal, octahedral, etc. are obtained.<sup>[1]</sup> Tetraphenoxaluminates and borates<sup>[9,10]</sup> and also

their fluorinated analogs<sup>[11]</sup> have been studied and widely applied, for example, in catalysis, however, to the best of our knowledge the cyano-substituted anions are not known yet. The only known cyanoborates and aluminates are of the type  $[B(C_6H_4-CN)_4]^-$ <sup>[12]</sup> and  $[B(CN)_4]^-$ .<sup>[13]</sup> In addition, there is a great wealth of compounds based on polycyanometallates,<sup>[4b,14]</sup>  $[C(CN)_3]^-$ ,<sup>[15]</sup> or  $Si(p-C_6H_4-CN)_4$ .<sup>[16]</sup>

Herein, we describe crystalline coordination polymer networks that were obtained through the connection of tetrahedral *p*-cyanophenoxy aluminate or borate linkers with monocationic transition metal center such as  $Ag^+$  and  $Cu^+$ . A common feature of these supramolecular polymers is the presence of dative  $M-NC$  bonds ( $M = Ag, Cu$ ), which are crucial structure-directing elements in addition to the tetrahedral  $[E(O-C_6X_4-CN)_4]^-$  building block.

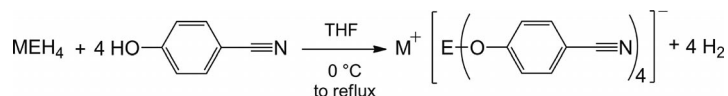
### Results and Discussion

Ligands, such as *p*-cyanophenoxy linkers, with the potential for supplemental Lewis base interactions are finding increasing utility for the stabilization of electrophilic metal centers (metal = alkali, Cu, Ag, etc.).<sup>[17]</sup> For the synthesis of salts bearing the aluminate and borate anions,  $[E(O-C_6H_4-CN)_4]^-$  ( $E = Al, B$ ),  $LiAlH_4$  and  $NaBH_4$  were treated with four equivalents of 4-hydroxybenzonnitrile,  $HO-C_6H_4-CN$ , at low temperatures in tetrahydrofuran (THF, Scheme 1). The resulting solution was heated to reflux for two hours. After filtration and removal of the solvent in vacuo, a colorless solid was obtained, which was washed with  $Et_2O$  to remove the excess 4-hydroxybenzonnitrile. In both cases, the pure  $Li[Al(O-C_6H_4-CN)_4]$  (1) or  $Na[B(O-$

[a] Institut für Chemie, Universität Rostock, Albert-Einstein-Str. 3a, 18059 Rostock, Germany  
Fax: +49-381-498-6381  
E-mail: axel.schulz@uni-rostock.de  
Homepage: <http://www.schulz.chemie.uni-rostock.de/>

[b] Leibniz Institut für Katalyse, Albert-Einstein-Str. 29a, 18059 Rostock, Germany  
Fax: +49-381-498-6381

Supporting information for this article is available on the WWW under <http://dx.doi.org/10.1002/ejic.201200427>.

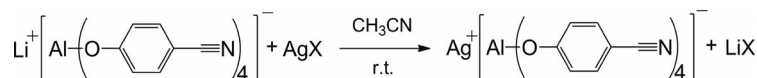
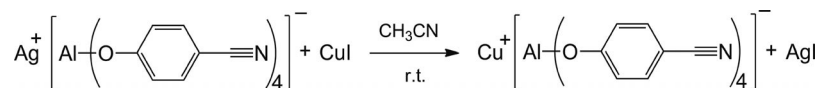
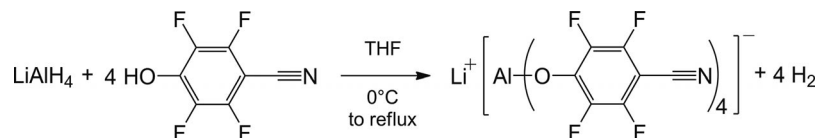
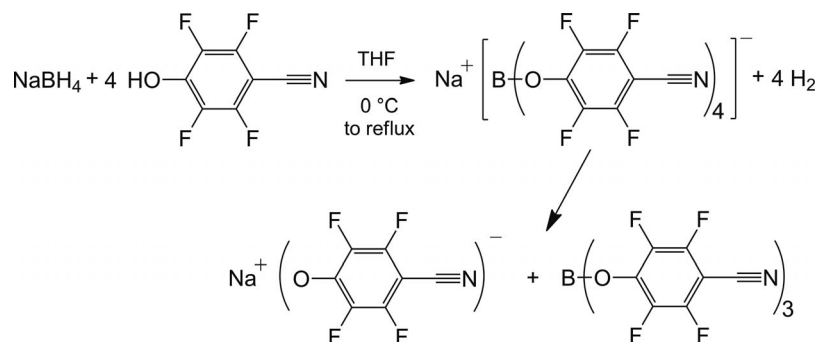
Scheme 1. Synthesis of  $\text{Li}[\text{Al}(\text{O}-\text{C}_6\text{H}_4-\text{CN})_4]$  (**1**) and  $\text{Na}[\text{B}(\text{O}-\text{C}_6\text{H}_4-\text{CN})_4]$  (**2**).

$\text{C}_6\text{H}_4-\text{CN})_4]$  salt (**2**) was obtained in yields between 60–70%.  $\text{Li}[\text{Al}(\text{O}-\text{C}_6\text{H}_4-\text{CN})_4]$  (**1**) is highly soluble in THF and acetonitrile, whereas  $\text{Na}[\text{B}(\text{O}-\text{C}_6\text{H}_4-\text{CN})_4]$  (**2**) is slightly less soluble. Both salts are almost insoluble in  $\text{CH}_2\text{Cl}_2$  and aromatic solvents such as benzene or toluene.

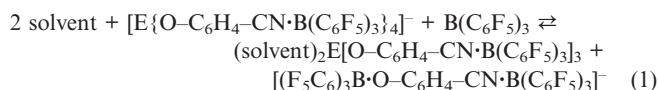
By utilizing salt metathesis reactions with different silver salts  $\text{AgX}$  ( $\text{X} = \text{NO}_3^-$ ,  $\text{CF}_3\text{COO}^-$ ,  $\text{CF}_3\text{SO}_3^-$ ), the exchange of the  $\text{Li}^+$  ions by  $\text{Ag}^+$  ions was achieved (Scheme 2) to afford  $\text{Ag}[\text{Al}(\text{O}-\text{C}_6\text{H}_4-\text{CN})_4]$  (**3**) in yields between 40–50%. The copper salt  $\text{Cu}[\text{Al}(\text{O}-\text{C}_6\text{H}_4-\text{CN})_4]$  (**4**) was obtained in the reaction of  $\text{Ag}[\text{Al}(\text{O}-\text{C}_6\text{H}_4-\text{CN})_4]$  with  $\text{CuI}$ , which, unlike  $\text{AgI}$ , is soluble in acetonitrile (50% yield, Scheme 3). In comparison to the lithium salt, the  $\text{M}[\text{Al}(\text{O}-\text{C}_6\text{H}_4-\text{CN})_4]$  salts ( $\text{M} = \text{Ag}, \text{Cu}$ ) are also very good soluble in acetonitrile but considerably less soluble in THF. Whereas the silver and lithium salt can be crystallized as solvent-free species, solvent molecules occupy the voids in the copper species.

In a second series of experiments, we tried to synthesize the analogous perfluorinated salts  $\text{Li}[\text{E}(\text{O}-\text{C}_6\text{F}_4-\text{CN})_4]$  ( $\text{E} = \text{B}, \text{Al}$ ). Although the aluminate salt  $\text{Li}[\text{Al}(\text{O}-\text{C}_6\text{F}_4-$

$\text{CN})_4]$  (**5**) is easily generated in good yields (51%) by utilizing 4-cyano-2,3,5,6-tetrafluorophenol,  $\text{HO}-\text{C}_6\text{F}_4-\text{CN}$ , as shown in Scheme 4, in the reaction of  $\text{NaBH}_4$  with  $\text{HO}-\text{C}_6\text{F}_4-\text{CN}$  in acetonitrile only the formation of  $\text{Na}(\text{O}-\text{C}_6\text{F}_4-\text{CN})$  (**6**), the free acid  $\text{B}(\text{O}-\text{C}_6\text{F}_4-\text{CN})_3$ , and molecular hydrogen (Scheme 5) is observed. If the  $\text{Na}^+$  ion is not stabilized by significant donor–acceptor interactions as in compounds **1–5**, the “naked”  $\text{Na}^+$  ion seems to be the stronger Lewis acid, which results in the abstraction of  $\text{O}-\text{C}_6\text{F}_4-\text{CN}^-$  from the  $[\text{B}(\text{O}-\text{C}_6\text{F}_4-\text{CN})_4]^-$  ion and yields  $\text{Na}(\text{O}-\text{C}_6\text{F}_4-\text{CN})$  and  $\text{B}(\text{O}-\text{C}_6\text{F}_4-\text{CN})_3$ . Obviously, the driving force for the formation of **6** is the instability of the  $[\text{B}(\text{O}-\text{C}_6\text{F}_4-\text{CN})_4]^-$  anion towards strong electrophilic ions. The whole process can formally be regarded as a Lewis acid/Lewis base reaction. A similar Lewis acid/Lewis base reaction is assumed to occur for weakly coordinating anions of the type  $[\text{Al}(\text{OR}^F)_4]^-$  or  $[\text{B}(\text{C}_6\text{F}_5)_4]^-$  in the presence of very electrophilic cations, in which the decomposition is initiated either by ligand ( $\text{R}^F\text{O}^-$ ,<sup>[18,19]</sup>  $\text{C}_6\text{F}_5^-$ )<sup>[20]</sup> or fluoride ion abstraction.<sup>[21]</sup>

Scheme 2. Synthesis of  $\text{Ag}[\text{Al}(\text{O}-\text{C}_6\text{H}_4-\text{CN})_4]$  (**3**).Scheme 3. Synthesis of  $\text{Cu}[\text{Al}(\text{O}-\text{C}_6\text{H}_4-\text{CN})_4]$  (**4**).Scheme 4. Synthesis of  $\text{Li}[\text{Al}(\text{O}-\text{C}_6\text{F}_4-\text{CN})_4]$  (**5**).Scheme 5. Synthesis of  $\text{Na}(\text{O}-\text{C}_6\text{F}_4-\text{CN})$  (**6**).

Finally, we studied the stability of salts bearing the  $[E(O-C_6X_4-CN)_4]^-$  anion towards strong Lewis acids such as  $B(C_6F_5)_3$ . The idea was to see if either the very bulky adduct anions<sup>[22–25]</sup> of the type  $[E(O-C_6X_4-CN \cdot B(C_6F_5)_3)_4]^-$  are formed or if Lewis acid assisted degradation occurs leading to the formation of  $M[O-C_6X_4-CN \cdot B(C_6F_5)_3]$ . The reaction of  $Li[Al(O-C_6H_4-CN)_4]$  with an excess of  $B(C_6F_5)_3$  led to the isolation of the solvent-stabilized Lewis acids  $(THF)_2Al[O-C_6H_4-CN \cdot B(C_6F_5)_3]_3$  (**7**) and  $Li[(F_5C_6)_3B \cdot O-C_6H_4-CN \cdot B(C_6F_5)_3]$  [Equation (1)]; and the addition of  $B(C_6F_5)_3$  to a solution of  $Na[B(O-C_6H_4-CN)_4]$  gave  $Na[(F_5C_6)_3B \cdot O-C_6H_4-CN \cdot B(C_6F_5)_3]$  (**8a**) as confirmed by X-ray structure analysis. In the latter case, it can be assumed that the free acid  $(Et_2O)_2B[O-C_6H_4-CN \cdot B(C_6F_5)_3]$  is also formed; however, this could not be isolated [Equation (1)]. Only when  $Li[Al(O-C_6F_4-CN)_4]$  was treated with  $B(C_6F_5)_3$ , was no decomposition observed, however, the tri-adduct  $Li[(NC-C_6F_4-O)Al\{O-C_6F_4-CN \cdot B(C_6F_5)_3\}_3]$  (**9**) and not the tetra-adduct was obtained as shown by X-ray structure analysis.



## Properties

Salts bearing the  $[E(O-C_6X_4-CN)_4]^-$  anion ( $E = B, Al$ ;  $X = H, F$ ) are neither air- nor considerably moisture-sensitive. They dissolve in solvents such as  $CH_3CN$  or THF but not in  $CH_2Cl_2$  or benzene. They slowly decompose in water with the formation of the free alcohol  $HO-C_6X_4-CN$  and  $B_2O_3 \cdot nH_2O$  and  $Al_2O_3 \cdot nH_2O$  as shown by  $^1H$ ,  $^{19}F$ , and  $^{11}B$  NMR studies. All mentioned  $[E(O-C_6X_4-CN)_4]^-$  salts are easily prepared in bulk and are indefinitely stable when stored in a sealed tube in the dark (silver salts). All considered salts bearing the  $[E(O-C_6X_4-CN)_4]^-$  ion are thermally stable up to at least 270 °C (Table 1). The thermal stabilities nicely correlate with the trends found for  $M[B(CN)_4]$  ( $M = Li$  500,  $Cu$  470,  $Ag$  440 °C).<sup>[26]</sup> The decomposition products were analyzed by powder XRD (PXRD) measurements and were identified as  $LiAlO_2$  (for **1**),  $NaBO_2$  (for **2**),  $Ag$  (for **3**), and a mixture of  $Cu_2O$ ,  $CuO$ , and  $Cu$  (for **4**).

Table 1. Thermal analysis: melting and decomposition points (from DSC measurements); spectroscopic data: IR, Raman, and  $^{13}C$  NMR spectroscopic data of  $HO-C_6X_4-CN$  ( $X = H, F$ ) based species along with the data of free *p*-cyanophenols.

	M.p. [°C]	$^{13}C$ NMR $\delta_{(CN)}$ [ppm]	IR $\nu_{CN}$ [ $cm^{-1}$ ]	Raman $\nu_{CN}$ [ $cm^{-1}$ ]
$HO-C_6H_4-CN$	113	119.6	2231 (s)	2239(10)
$HO-C_6F_4-CN$	268	107.8	2252 (s)	2267(1), 2252(10)
$Li[Al(O-C_6H_4-CN)_4]$ ( <b>1</b> )	349 <sup>[a]</sup>	120.8	2236 (s)	2244(2), 2235(10), 2217(4)
$Na[B(O-C_6H_4-CN)_4]$ ( <b>2</b> )	362 <sup>[a]</sup>	119.4	2226 (m)	2230(10)
$Ag[Al(O-C_6H_4-CN)_4]$ ( <b>3</b> )	243 <sup>[a]</sup>	120.7	2223 (s)	2244(10)
$Cu[Al(O-C_6H_4-CN)_4]$ ( <b>4</b> )	281 <sup>[a]</sup>	120.9	2231 (m)	2235(10), 2181(1)
$Li[Al(O-C_6F_4-CN)_4]$ ( <b>5</b> )	271	109.7	2256 (m)	2266(10)
$Na(O-C_6F_4-CN)$ ( <b>6</b> )	367	113.0	2253 (s)	2252(10)
$(thf)_2Al[O-C_6H_4-CN \cdot B(C_6F_5)_3]_3$ ( <b>7</b> )	137 <sup>[a]</sup>	115.6	2307 (s)	2312(10)
$Na[(F_5C_6)_3B \cdot O-C_6H_4-CN \cdot B(C_6F_5)_3]$ ( <b>8a</b> )	155	114.7	2309 (s)	2312(10)
$Li[(NC-C_6F_4-O)Al\{O-C_6F_4-CN \cdot B(C_6F_5)_3\}_3]$ ( <b>9</b> )	319 <sup>[a]</sup>	114.8	2318 (m), 2263 (w)	2324(10)

[a] Decomposition temperature.

## Spectroscopic Studies

The  $^{13}C$  NMR spectroscopic data along with the IR/Raman data for the compounds described in this work are listed in Table 1. The IR and Raman data of all considered CN-group-containing anions in Table 1 show sharp bands in the expected 2220–2320  $cm^{-1}$  region, which can be assigned to the  $\nu_{CN}$  stretching frequencies. Interestingly, there is almost no difference between free  $HO-C_6X_4-CN$  ( $X = H$ : 2231;  $X = F$ : 2252  $cm^{-1}$ ) and the metal salts containing the  $[E(O-C_6X_4-CN)_4]^-$  ion (shift < 10  $cm^{-1}$ ;  $X = H$ : 2223–2236;  $X = F$ : 2252–2256  $cm^{-1}$ ). On the contrary, the coordination of a Lewis acid such as  $B(C_6F_5)_3$  to a  $NC-R$  species causes a significant band shift to higher wave numbers ( $\Delta\nu = 76$  in **7**, 78 in **8a**, and 66  $cm^{-1}$  in **9**).<sup>[27]</sup> For the  $B(C_6F_5)_3$  adducts,  $^{11}B$  spectroscopy is also particularly well suited to distinguish between three-coordinate borane and the four-coordinate boron found in the Lewis acid–base adducts for which the  $^{11}B$  resonance (**7**: –11.8, **8**: –10.1, and **9**: –8.5 ppm) is shifted to lower frequency with respect to free  $B(C_6F_5)_3$  by more than 65 ppm [cf.  $B(C_6F_5)_3$  in  $CD_2Cl_2$ : 59.1 ppm].<sup>[28–33]</sup>

## X-ray Structure Analysis

The structures of compounds **1–9** have been determined. Tables 2 and 3 present the X-ray crystallographic data of species **1–5**, **7**, and **8a**. X-ray quality crystals of all considered species were selected in Kel-F-oil (Riedel-de Haën) or Fomblin YR-1800 (Alfa Aesar) at ambient temperature. All samples were cooled to –100(2) °C during the measurement. More details are found in the Supporting Information.

### *Li[Al(O-C<sub>6</sub>H<sub>4</sub>-CN)<sub>4</sub>]* (**1**)

Crystals suitable for X-ray crystallographic analysis were obtained by adding three drops of  $CH_2Cl_2$  to a saturated THF solution of **1** and storing it at 7 °C for 2 d. Complex **1** crystallized as colorless blocks in the tetragonal space group  $I\bar{4}$  with two formula units per unit cell. Both metal ions have a tetrahedral coordination environment and all *p*-cyanophenoxy linker molecules (tetrahedrally attached to Al atoms through O atoms and to Li atoms through N

Table 2. Crystallographic details of Li[Al(O–C<sub>6</sub>H<sub>4</sub>–CN)<sub>4</sub>] (1), Na[B(O–C<sub>6</sub>H<sub>4</sub>–CN)<sub>4</sub>] (2), Ag[Al(O–C<sub>6</sub>H<sub>4</sub>–CN)<sub>4</sub>] (3).

	1	2	3
Empirical formula	C <sub>28</sub> H <sub>16</sub> AlLiN <sub>4</sub> O <sub>4</sub>	C <sub>46</sub> H <sub>52</sub> BN <sub>4</sub> NaO <sub>8.5</sub>	C <sub>28</sub> H <sub>16</sub> AgAlN <sub>4</sub> O <sub>4</sub>
Formula weight. [g mol <sup>-1</sup> ]	506.37	830.72	607.3
Color	colorless	colorless	colorless
Crystal system	tetragonal	triclinic	tetragonal
Space group	<i>I</i> $\bar{4}$	<i>P</i> 1	<i>I</i> $\bar{4}$
<i>a</i> [Å]	6.9524(8)	11.3778(4)	6.9541(3)
<i>b</i> [Å]	6.95424(8)	14.5700(6)	6.9541(3)
<i>c</i> [Å]	25.457(7)	14.8545(6)	26.2002(15)
$\alpha$ [°]	90	83.928(2)	90
$\beta$ [°]	90	76.016(2)	90
$\gamma$ [°]	90	70.325(2)	90
<i>V</i> [Å <sup>3</sup> ]	1230.5(4)	2249.2(2)	1267.0(1)
<i>Z</i>	2	2	2
$\mu$ [mm <sup>-1</sup> ]	0.13	0.09	0.87
$\lambda$ Mo- <i>K</i> $\alpha$ [Å]	0.71073	0.71073	0.71073
<i>T</i> [K]	173	173	173
Measured reflections	4206	38231	5766
Independent reflections	2153	11158	2274
Reflections with <i>I</i> > 2 $\sigma$ ( <i>I</i> )	2053	7149	2167
<i>R</i> <sub>int</sub>	0.03	0.044	0.022
<i>F</i> (000)	520	880	1480
<i>R</i> <sub>1</sub> { <i>R</i> [ <i>F</i> <sub>2</sub> > 2 $\sigma$ ( <i>F</i> <sub>2</sub> )]}	0.036	0.067	0.026
<i>wR</i> <sub>2</sub> (all data)	0.091	0.204	0.048
Goof	1.08	0.99	1.002
Parameters	87	644	87

Table 3. Crystallographic details of Cu[Al(O–C<sub>6</sub>H<sub>4</sub>–CN)<sub>4</sub>] $\cdot$ 2CH<sub>2</sub>Cl<sub>2</sub> (4), Li[Al(O–C<sub>6</sub>F<sub>4</sub>–CN)<sub>4</sub>] (5), and (THF)<sub>2</sub>Al[O–C<sub>6</sub>H<sub>4</sub>–CN $\cdot$ B(C<sub>6</sub>F<sub>5</sub>)<sub>3</sub>]<sub>3</sub> (7).

	4	5	7
Empirical formula	C <sub>30</sub> H <sub>20</sub> AlCl <sub>4</sub> CuN <sub>4</sub> O <sub>4</sub>	C <sub>48</sub> H <sub>40.8</sub> AlF <sub>16</sub> LiN <sub>4</sub> O <sub>9</sub>	C <sub>83.5</sub> H <sub>29</sub> AlClB <sub>3</sub> F <sub>45</sub> N <sub>3</sub> O <sub>5</sub>
Formula weight [g mol <sup>-1</sup> ]	732.82	1155.55	2103.96
Color	colorless	colorless	colorless
Cryst. system	monoclinic	monoclinic	triclinic
Space group	<i>P</i> 2 <sub>1</sub> / <i>c</i>	<i>C</i> 2/ <i>c</i>	<i>P</i> $\bar{1}$
<i>a</i> [Å]	12.4486(6)	23.49(2)	16.921(9)
<i>b</i> [Å]	15.0360(6)	13.024(9)	17.643(9)
<i>c</i> [Å]	16.5961(7)	33.99(2)	18.37(1)
$\alpha$ [°]	90	90	62.08(2)
$\beta$ [°]	92.074(2)	98.59(2)	62.87(2)
$\gamma$ [°]	90	90	83.93(2)
<i>V</i> [Å <sup>3</sup> ]	3104.4 (2)	10280(12)	4271(4)
<i>Z</i>	4	8	2
$\mu$ [mm <sup>-1</sup> ]	1.12	0.16	0.21
$\lambda$ Mo- <i>K</i> $\alpha$ [Å]	0.71073	0.71073	0.71073
<i>T</i> [K]	173	173	173
Measured reflections	36748	43873	71398
Independent reflections	7508	11625	20425
Reflections with <i>I</i> > 2 $\sigma$ ( <i>I</i> )	4900	6878	11411
<i>R</i> <sub>int</sub>	0.058	0.032	0.041
<i>F</i> (000)	1480	4710	2082
<i>R</i> <sub>1</sub> { <i>R</i> [ <i>F</i> <sub>2</sub> > 2 $\sigma$ ( <i>F</i> <sub>2</sub> )]}	0.043	0.051	0.055
<i>wR</i> <sub>2</sub> (all data)	0.110	0.138	0.174
Goof	1.06	1.05	0.99
Parameters	442	846	1365

atoms) bridge the two metal ions to form a 3D framework structure as shown in Figures 1 and 2. Each nitrile group in the structure is coordinated to a lithium atom with a Li–N length of 2.054(1) Å (cf.  $\Sigma r_{\text{cov}} = 2.05$  Å) and an Al–O bond length of 1.7329(9) (cf.  $\Sigma r_{\text{cov}} = 1.89$  Å).<sup>[34]</sup> These values are similar to those observed for phenoxyaluminates and lithium nitrile complexes.<sup>[35]</sup> Both the AlO<sub>4</sub> tetrahedron

and the LiN<sub>4</sub> moiety are slightly distorted with one smaller [N1–Li1–N1' 106.78(3) and O1'–Al1–O1 107.43(3)°] and one larger angle [N1'–Li1–N1'' 115.00(6) and O1'–Al1–O1'' 113.63(7)°]. Whereas the LiN<sub>4</sub> tetrahedra are almost linearly attached to the phenoxy linker [C7–N1–Li1 160.0(1)°], the AlO<sub>4</sub> tetrahedra display a bent structure [C1–O1–Al1 134.20(8)°].



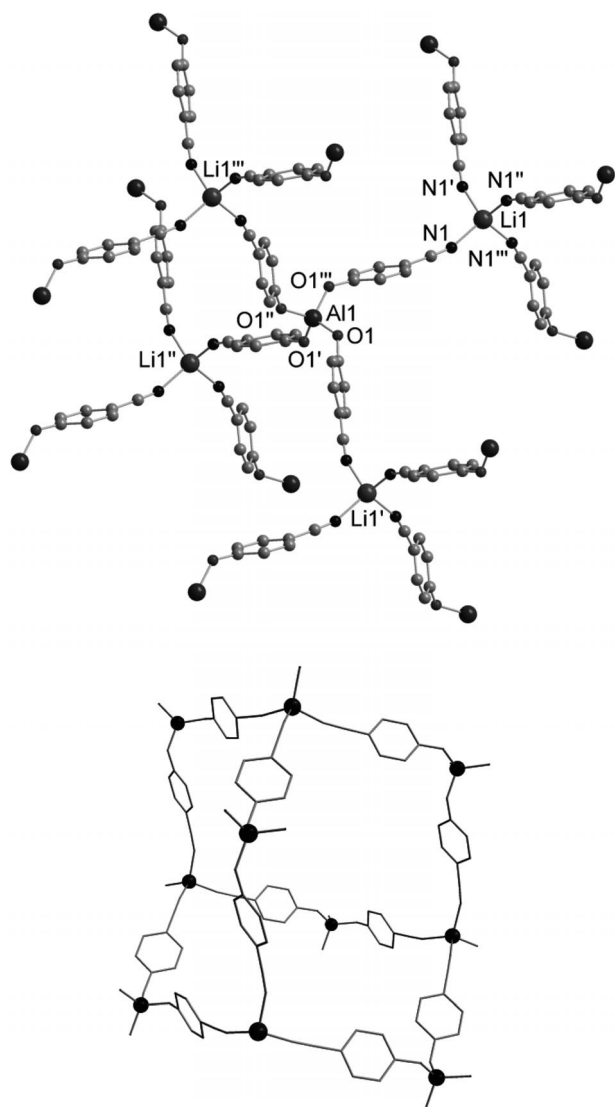


Figure 1. Top: Ball-and-stick drawing of the local environment about the tetrahedral centers in **1** (hydrogen atoms omitted for clarity). Selected bond lengths [Å] and angles [°]: Al1–O1 1.7329(9), O1–C1 1.338(1), C7–N1 1.149(2), N1–Li1 2.054(1); O1'–Al1–O1 107.43(3), O1'–Al1–O1'' 113.63(7), N1–Li1–N1' 106.78(3), N1'–Li1–N1'' 115.00(6), C1–O1–Al1 134.20(8), C7–N1–Li1 160.0(1). Bottom: adamantane structural motif in **1**.

A closer look at the 3D network of **1** revealed a highly interpenetrated structure, which does not possess large free channels or pores. It consists of five independent infinite frameworks, each with diamond-like topology (Figure 2). The interpenetrated framework of **1** is related to some classic inorganic frameworks, as it features the adamantane structural motif known from diamondlike frameworks such as that of zinc cyanide, which consists of two independent infinite frameworks, each with diamondlike topology.<sup>[36]</sup> Interpenetrating diamond-related nets with  $n = 5$  ( $n =$  number of nets) have been described for adamantane-1,3,5,7-tetracarboxylic acid,<sup>[37]</sup>  $[\text{Cu}(\text{L})_2](\text{BF}_4)$  ( $\text{L} = 1,4\text{-dicyanobenzene}$ )<sup>[38]</sup> and  $[\text{Cu}(\text{bpe})_2](\text{BF}_4)$  [with  $\text{CH}_3\text{CN}$  or  $\text{CH}_2\text{Cl}_2$  as guest molecules, bpe = 1,4-bis(4-pyridyl)butadiyne].<sup>[39]</sup>

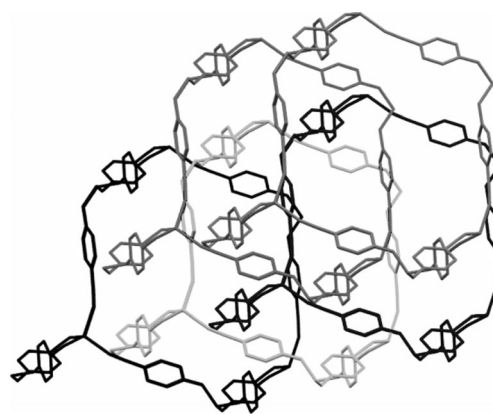


Figure 2. Five interpenetrating diamond-like frameworks in the structure of **1** showing the translational relationship between independent nets.

An inherent feature of such entangled interpenetrated structures is that they can be disentangled only by breaking internal connections.<sup>[1a]</sup> Furthermore,  $\text{N}_2$  sorption measurements with compound **1** did not show significant permanent porosity (approximately  $4 \text{ m}^2 \text{ g}^{-1}$  of BET surface). The structural collapse seems to occur in one step at  $349^\circ\text{C}$  upon thermal treatment and results in the formation of  $\text{LiAlO}_2$ .

#### *Ag[Al(O-C6H4-CN)4] (3)*

Compound **3** crystallizes isostructurally to compound **1** with very similar cell parameters [cf. Li: 6.9524(8), 6.9524(8), 25.457(7) vs. Ag: 6.9541(3), 6.9541(3), 26.200(2) Å; Table 2]. Only the  $c$  axis is slightly elongated. All the structural features discussed before for compound **1**

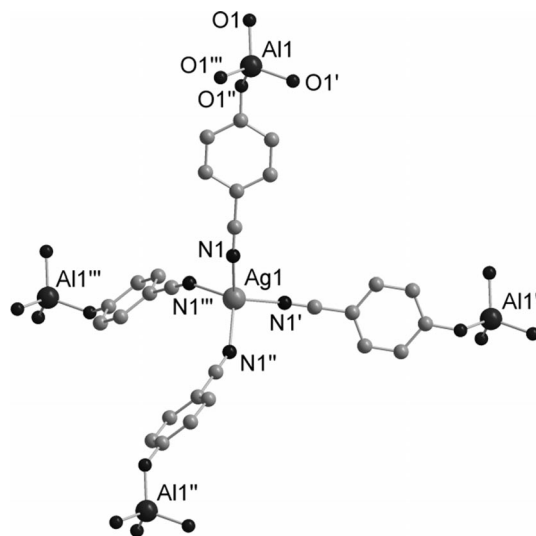


Figure 3. Ball-and-stick drawing of the local environment about the tetrahedral centers in **3** (hydrogen atoms omitted for clarity). Selected bond lengths [Å] and angles [°]: Ag1–N1 2.286(2), Al1–O1 1.736(1), N1–C7 1.144(3); N1'–Ag1–N1 117.76(7), N1'–Ag1–N1'' 105.49(3), O1''–Al1–O1 112.7(1), O1'–Al1–O1 107.89(5), C7–N1–Ag1 154.0(2), C1–O1–Al1 131.4(1).



(Figure 1) are similarly found in the silver salt (Figure 3). Only slight differences arise from the longer Ag–N bond length of 2.286(2) compared to 2.054(1) Å for Li–N in **1**; the Al–O distances are essentially identical and the angles are also very similar.

#### $\text{Cu}[\text{Al}(\text{O}-\text{C}_6\text{H}_4-\text{CN})_4] \cdot 2\text{CH}_2\text{Cl}_2$ (**4**)

Single crystals of **4** were grown by slow vapor diffusion of  $\text{CH}_2\text{Cl}_2$  into a saturated acetonitrile solution of the compound overnight at ambient temperature. In contrast to the isostructural complexes **1** and **3**, the copper salt crystallizes in the monoclinic space group  $P2_1/c$  with four formula units per unit cell. Again, both metal centers sit in a slightly distorted tetrahedral environment (Figure 4, top) with an

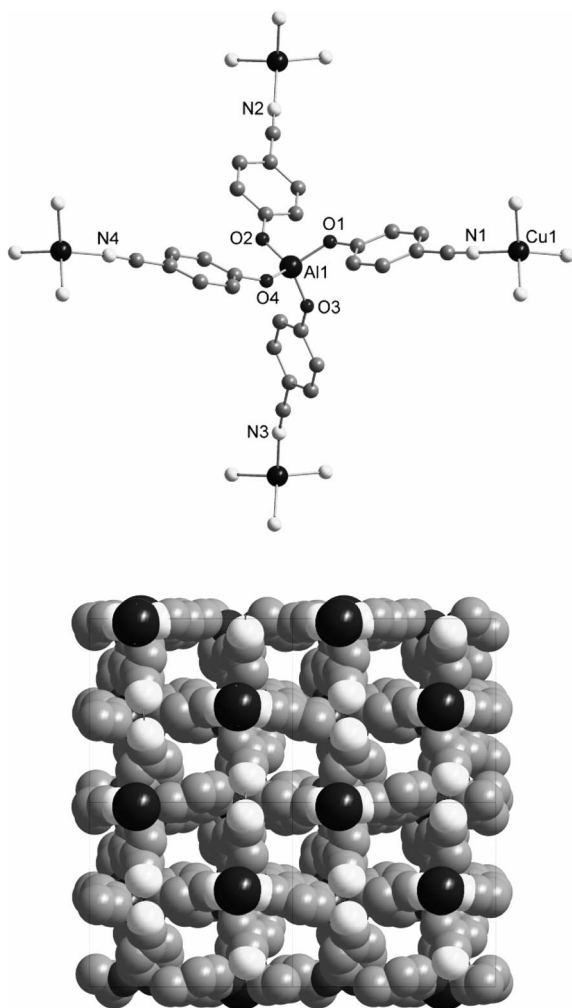


Figure 4. Top: Ball-and-stick drawing of the local environment about the tetrahedral centers in **4** (hydrogen atoms omitted for clarity). Selected bond lengths [Å] and angles [°]: Al1–O2 1.735(2), Al1–O4 1.735(2), Al1–O1 1.739(2), Al1–O3 1.722(2), Cu1–N1 1.975(2), Cu1–N2 2.018(2), Cu1–N3 1.992(2), Cu1–N4 1.996(2); N1–Cu1–N3 110.1(1), N1–Cu1–N4 118.07(9), N3–Cu1–N4 101.55(9), N1–Cu1–N2 105.10(9), N3–Cu1–N2 111.68(9), N4–Cu1–N2 110.53(9), O3–Al1–O2 115.55(9), O3–Al1–O4 107.38(9), O2–Al1–O4 108.39(9), O3–Al1–O1 105.25(9), O2–Al1–O1 108.42(9), O4–Al1–O1 111.90(9). Bottom: space filling model of a section of **4**, view along *a* axis, disordered solvent molecules ( $\text{CH}_2\text{Cl}_2$ ) inside the pores are omitted for clarity.

average Cu–N distance of 1.995 Å {cf. 1.979 Å in  $[\text{Cu}_2(1,2,4,5\text{-tetracyanobenzene})_3](\text{PF}_6)_2(\text{Me}_2\text{CO})_4$  or 1.977 Å in  $[\text{Cu}[\text{B}(\text{CN})_4]^{2-}]^{26}$  and 1.732 Å for the Al–O bond lengths [cf. 1.733 and 1.736(1) Å in compounds **1** and **3**, respectively]. The solid-state structure possesses relatively large cavities despite fourfold interpenetration (see Supporting Information Figure S2), and the cavities are filled by two solvent molecules per formula unit. As illustrated in Figure 4 (bottom), the major difference in the solid-state structure of **4** compared to the those of compounds **1** and **2** arises from the smaller degree of interpenetration in **4** leading to larger voids, which are filled with disordered  $\text{CH}_2\text{Cl}_2$  solvent molecules. Thermogravimetric analysis (TGA) indicates that the solvent can be fully removed at 90 °C. However, removal of the solvent leads to a loss of crystallinity (single-crystal integrity is not maintained), as evidenced by powder X-ray diffraction analysis (see Supporting Information). No specific surface could be found by nitrogen sorption experiments of the desolvated compound.

#### $\text{Na}[\text{B}(\text{O}-\text{C}_6\text{H}_4-\text{CN})_4] \cdot 8\text{THF}$ (**2**)

Crystals suitable for X-ray crystallographic analysis were obtained by adding three drops of  $\text{CH}_2\text{Cl}_2$  to a saturated THF solution and storing it at ambient temperature. Complex **2** crystallizes in the triclinic space group  $P\bar{1}$  with two formula units per unit cell. As the  $\text{Na}^+$  ions prefer an octahedral rather than a tetrahedral coordination sphere (in contrast to  $\text{Li}^+$  or  $\text{Cu}^+$ , see above), the coordination sphere around the sodium ions is either composed of four square planar arranged N atoms of the *p*-cyanophenoxy linker and two O atoms of THF molecules (Na1) with a linear O5–Na1–O5' moiety (180.0°) or two N atoms of the *p*-cyanophenoxy linker (N4–Na2–N4' 180.0°) and four square planar arranged O atoms of THF molecules as observed for Na2 (Figure 5, top). The boron atom is in a distorted tetrahedral environment with an average O–B–O angle of 108.8°. Interestingly, only three of the *p*-cyanophenoxy linkers act as bridging ligands between both metal ions and the fourth remains uncoordinated (N1 in Figure 5). Obviously, no stable network can be composed with octahedral  $\text{Na}^+$  ions and a tetrahedral  $\text{BO}_4$  building block in the presence of a donating solvent such as THF. Thus a 2D network with three different parallel layers is formed as depicted in Figure 5 (bottom). In addition to the six coordinated THF molecules, two further uncoordinated THF molecules per unit cell are found between these layers. The average B–O distance is 1.466 Å, which is slightly longer than the sum of the covalent radii (1.38 Å).<sup>34</sup> The C–N distance of the uncoordinated CN group is slightly shorter than those that are attached to  $\text{Na}^+$  ions [1.137(3) vs. 1.143(3), 1.141(2), and 1.148(2) Å].

#### $[\text{Li}(\text{THF})_{3.6}(\text{Et}_2\text{O})_{0.4}][(\text{THF})\text{Al}(\text{O}-\text{C}_6\text{F}_4-\text{CN})_4]$ (**5**)

Crystals of **5** were obtained by a slow diffusion method.  $\text{Et}_2\text{O}$  was layered above a saturated THF solution of **5**, stored at –30 °C, and after one day crystals had formed near the original solvent interface. Complex **5** crystallized as colorless prisms in the monoclinic space group  $C2/c$  with

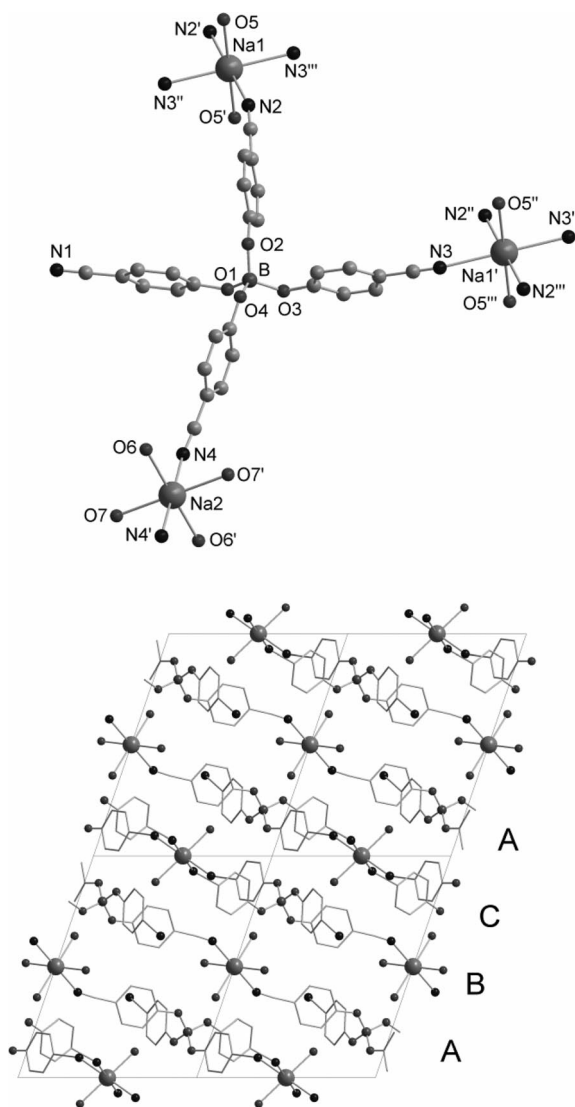


Figure 5. Top: Ball-and-stick drawing of the local environment about the tetrahedral centers in **2** (hydrogen atoms omitted for clarity, only the O atoms of the coordinated THF molecules are shown). Selected bond lengths [Å] and angles [°]: B–O1 1.463(2), B–O4 1.467(2), B–O2 1.467(2), B–O3 1.468(2), N2–Na1 2.443(2), N3–Na1 2.572(2), N4–Na2 2.541(2), Na1–O5 2.375(1), Na2–O6 2.419(5), N1–C7 1.137(3), N2–C14 1.143(3), N3–C21 1.141(2), N4–C28 1.148(2), Na2–O7 2.44(1); O1–B–O4 114.7(1), O1–B–O2 113.9(2), O4–B–O2 100.5(1), O1–B–O3 101.0(1), O4–B–O3 113.6(2), O2–B–O3 113.7(1), O5'–Na1–O5 180.00(9), O5–Na1–N2 86.50(6), O5–Na1–N2' 93.50(6), O5–Na1–N2 93.50(6), O5–Na1–N2 86.50(6), N2'–Na1–N2 180.0(1), O5–Na1–N3 93.86(5), O5–Na1–N3 86.14(5), N2–Na1–N3 83.34(6), N2–Na1–N3 96.66(6), O5–Na1–N3 86.14(5), N2–Na1–N3 96.66(6), N3–Na1–N3' 180.0(1), O6–Na2–O6' 180.0(1), O6–Na2–O7 92.7(4), O6–Na2–O7 87.3(4), O7–Na2–O7' 180.000(2). Bottom: view along *c* axis displaying parallel layers (A, B, C) of the 2D network (hydrogen atoms and all uncoordinated THF molecules omitted for clarity, only O atoms of coordinating THF molecules are shown).

eight crystallographically equivalent  $[\text{Li}(\text{THF})_{3.6}(\text{Et}_2\text{O})_{0.4}] - [(\text{THF})\text{Al}(\text{O}-\text{C}_6\text{F}_4-\text{CN})_4]$  asymmetric units per unit cell. As illustrated in Figure 6, the asymmetric unit consists of the separated complex ion pair  $[\text{Li}(\text{THF})_{3.6}(\text{Et}_2\text{O})_{0.4}]^+$  and  $[(\text{THF})\text{Al}(\text{O}-\text{C}_6\text{F}_4-\text{CN})_4]^-$ , which display no significant in-

teractions since all CN groups remain uncoordinated. The  $\text{Li}^+$  ion is tetrahedrally surrounded exclusively by either THF or  $\text{Et}_2\text{O}$  molecules. Hence, no network is formed. Obviously, perfluorination at the phenyl rings results in a dramatic decrease of the basicity of the CN groups; therefore, the  $\text{Li}^+$  ions favor coordination by solvent molecules. The positions of four THF molecules in **5** were found to be disordered and were split in two parts. The occupancy of each part was refined freely (for details see Supporting Information). The position of the fifth THF molecule in **5** was found to be partially displaced by  $\text{Et}_2\text{O}$  and was split in two parts. The occupancy of each part was refined freely (THF/ $\text{Et}_2\text{O}$ : 0.606(7)/0.394(7)).

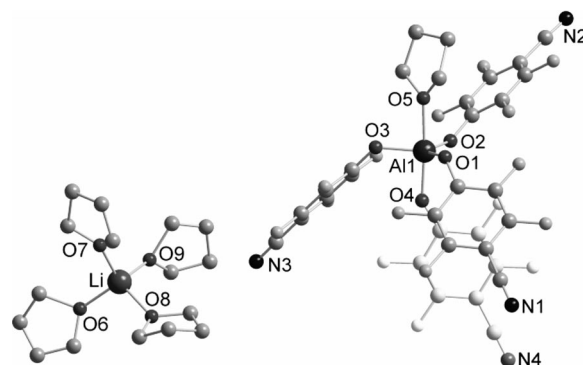


Figure 6. Ball-and-stick drawing of the asymmetric unit in **5** (hydrogen atoms omitted for clarity, disorder not shown). Selected bond lengths [Å] and angles [°]: Al1–O2 1.765(2), Al1–O1 1.766(2), Al1–O3 1.771(2), Al1–O4 1.821(2), Al1–O5 1.966(2), N1–C7 1.138(3), N2–C14 1.136(3), N3–C21 1.135(3), N4–C28 1.137(3); O2–Al1–O1 122.46(9), O2–Al1–O3 116.49(9), O1–Al1–O3 120.17(9), O2–Al1–O4 92.55(8), O1–Al1–O4 95.97(8), O3–Al1–O4 90.63(9), O2–Al1–O5 90.15(8), O1–Al1–O5 84.84(7), O3–Al1–O5 85.76(9), O4–Al1–O5 176.19(8), C1–O1–Al1 132.3(2), C8–O2–Al1 141.3(2), C15–O3–Al1 129.2(2), C22–O4–Al1 147.3(2).

Probably the most interesting feature of the molecular structure of **5** is the pentacoordination feature of the  $\text{Al}^{3+}$  in the complex anion, which displays a distorted trigonal bipyramidal arrangement of the O atoms around the  $\text{Al}^{3+}$  center. The one coordinating THF molecule adopts an apical position with an O4–Al1–O5 angle of 176.19(8)°. As expected the Al–O<sub>ax</sub> bond lengths [Al1–O4 1.821(2) and Al1–O5 1.966(2) Å] are considerably elongated compared to the Al–O<sub>eq</sub> bond lengths [Al1–O2 1.765(2), Al1–O1 1.766(2), and Al1–O3 1.771(2) Å]. In contrast to compounds **1–4**, the perfluorinated *p*-cyanophenoxy linker,  $-\text{O}-\text{C}_6\text{F}_4-\text{CN}$ , is considerably less basic and thus allows pentacoordination at the  $\text{Al}^{3+}$  center and prevents the cyano groups from coordinating to the  $\text{Li}^+$  ion. Moreover, the perfluorinated *p*-cyanophenoxy linker does not provide sufficient steric hindrance to prevent solvent coordination. The oxygen-pentacoordinate aluminate is well known and can be found in aluminium containing alcoholates<sup>[40]</sup> or can be achieved by additional solvent coordination.<sup>[41]</sup> Furthermore, pentacoordination by nitrogen and oxygen containing ligands is known.<sup>[42]</sup>

*Na(O-C<sub>6</sub>F<sub>4</sub>-CN)·3THF and Na(O-C<sub>6</sub>F<sub>4</sub>-CN)·nCH<sub>3</sub>CN*

Crystals of Na(O-C<sub>6</sub>F<sub>4</sub>-CN) were obtained from THF (**6a**) and CH<sub>3</sub>CN (**6b**) solutions. As the X-ray data sets for both species were rather poor, the structural details cannot be discussed in detail, but the data allowed us to establish the connectivity as displayed in Figures 7 and 8. In **6a** the oxygen atom of the -O-C<sub>6</sub>F<sub>4</sub>-CN linker bridges two Na<sup>+</sup>

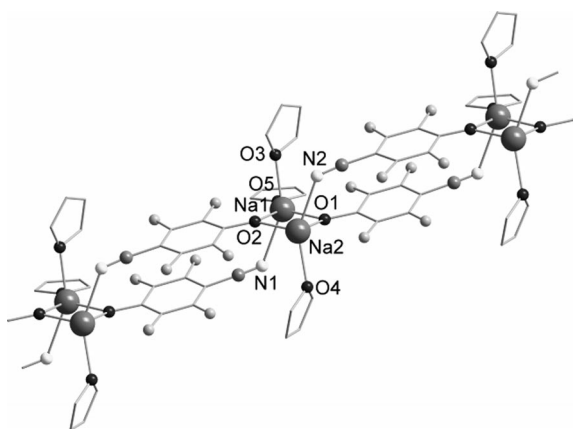


Figure 7. Drawing of the chains in **6a** (hydrogen atoms omitted for clarity, disorder not shown).

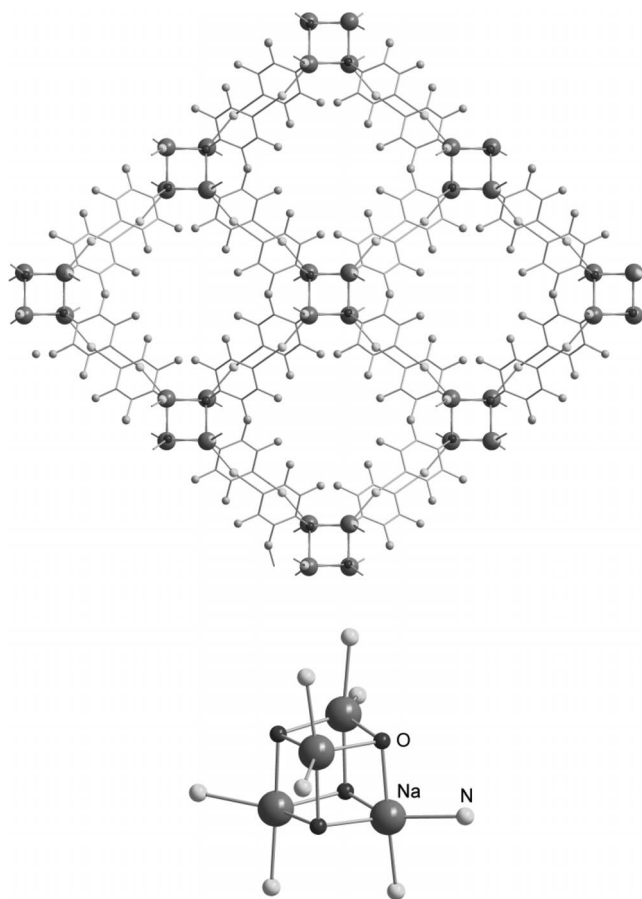


Figure 8. Top: view along the *a* axis of the 3D network in **6b**; bottom: Na<sub>4</sub>O<sub>4</sub> cube in **6b**, each Na<sup>+</sup> center is attached to one N atom of the phenoxy linker and one of the CH<sub>3</sub>CN molecule.

ions thus forming chains of planar Na<sub>2</sub>O<sub>2</sub> rings connected by two perfluorinated *p*-cyanophenoxy linkers. In **6b**, the oxygen of the perfluorinated *p*-cyanophenoxy coordinates in a μ<sup>3</sup> coordination mode to three adjacent Na<sup>+</sup> ions resulting in the formation of a distorted Na<sub>4</sub>O<sub>4</sub> cube (Figure 8 bottom). These cubes are linked by the nitrogen and oxygen atoms of the *p*-cyanophenoxy linker leading to the formation of 3D network with channels and voids as illustrated in Figure 8 (top). Moreover, one CH<sub>3</sub>CN solvent molecule is attached to each Na<sup>+</sup> center.

*(THF)<sub>2</sub>Al{O-C<sub>6</sub>H<sub>4</sub>-CN·B(C<sub>6</sub>F<sub>5</sub>)<sub>3</sub>}<sub>3</sub> (7)*

Compound **7** crystallizes in the triclinic space group *P* $\bar{1}$  with two formula units per unit cell. There are no significant interactions between adjacent (THF)<sub>2</sub>Al{O-C<sub>6</sub>H<sub>4</sub>-CN·B(C<sub>6</sub>F<sub>5</sub>)<sub>3</sub>}<sub>3</sub> molecules. As shown in Figure 9, species **7** can be considered as a solvent-stabilized Al{O-C<sub>6</sub>H<sub>4</sub>-CN·B(C<sub>6</sub>F<sub>5</sub>)<sub>3</sub>}<sub>3</sub> Lewis acid with a trigonal pyramidal coordinated Al center with O<sub>eq</sub>-Al-O<sub>eq</sub> angles close to 120° [O1-Al1-O3 118.85(9), O1-Al1-O2 121.53(9), O3-Al1-O2 119.58(9)°] and an almost linear O<sub>ax</sub>-Al-O<sub>ax</sub> unit [O5-Al1-O4 177.70(8)°]. Both THF solvent molecules occupy axial positions, and the B(C<sub>6</sub>F<sub>5</sub>)<sub>3</sub> molecules are attached to the N atom of the cyano group thus preventing the formation of 2D or 3D networks. The average Al-O<sub>eq</sub> bond length is 1.742 Å (cf. Al-O<sub>ax</sub> 1.976 Å).

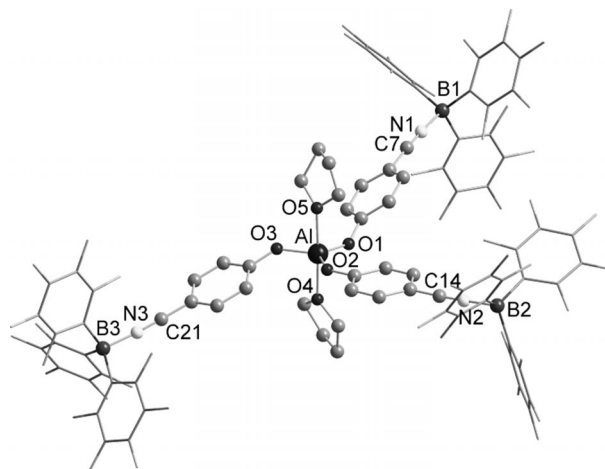


Figure 9. Drawing of the molecular structure of **7** (hydrogen atoms omitted for clarity). Selected bond lengths [Å] and angles [°]: Al1-O1 1.722(2), Al1-O3 1.748(2), Al1-O2 1.755(2), Al1-O4 1.986(2), Al1-O5 1.965(2), N1-C7 1.137(3), N2-C14 1.142(3), N3-C21 1.139(3), N1-B1 1.588(4), N2-B2 1.581(3), N3-B3 1.574(3); O1-Al1-O3 118.85(9), O1-Al1-O2 121.53(9), O3-Al1-O2 119.58(9), O1-Al1-O5 92.1(1), O3-Al1-O5 88.30(9), O2-Al1-O5 91.63(9), O1-Al1-O4 88.5(1), O3-Al1-O4 89.47(8), O2-Al1-O4 89.94(8), O5-Al1-O4 177.70(8), C7-N1-B1 176.7(2), C14-N2-B2 177.3(2), C21-N3-B3 175.5(2).

*[Na(Et<sub>2</sub>O)<sub>4</sub>][(C<sub>6</sub>F<sub>5</sub>)<sub>3</sub>B-NC-C<sub>6</sub>H<sub>4</sub>-O-B(C<sub>6</sub>F<sub>5</sub>)<sub>3</sub>] (8a), [Na(Et<sub>2</sub>O)<sub>4</sub>][(C<sub>6</sub>F<sub>5</sub>)<sub>3</sub>B-NC-C<sub>6</sub>F<sub>4</sub>-O-B(C<sub>6</sub>F<sub>5</sub>)<sub>3</sub>] (8b),<sup>1431</sup> and Li[(NC-C<sub>6</sub>F<sub>4</sub>-O)Al{O-C<sub>6</sub>F<sub>4</sub>-CN·B(C<sub>6</sub>F<sub>5</sub>)<sub>3</sub>}<sub>3</sub>] (9)*

Compounds **8a**, **8b**, and **9** crystallize as ion pairs. As the X-ray data sets for **8b** and **9** were rather poor, structural details cannot be discussed in detail. The connectivity of all



three species is displayed in Figures 10 (anions of **8a** and **8b**) and 11 (ion pair in **9**). Whereas no significant cation⋯anion interactions are observed for **8**, in **9** the  $[\text{Li}(\text{Et}_2\text{O})_3]^+$  ion is strongly coordinated to one unblocked cyano group of the  $[(\text{NC}-\text{C}_6\text{F}_4-\text{O})\text{Al}\{\text{O}-\text{C}_6\text{F}_4-\text{CN}\cdot\text{B}(\text{C}_6\text{F}_5)_3\}_3]$  anion. However, there are no interactions between the ion pairs of **9** worthy of discussion. For both species, the metal ions as well as the Al and B centers are tetrahedrally coordinated. (Figure 11).

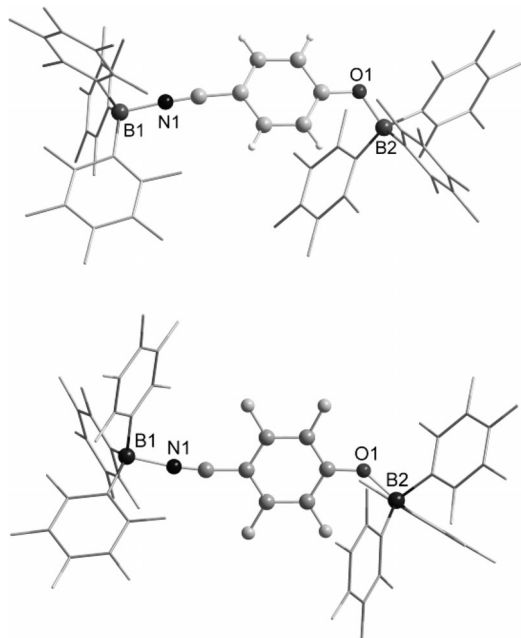


Figure 10. Drawing of the molecular structures of the anion in **8a** (top) and **8b** (bottom).

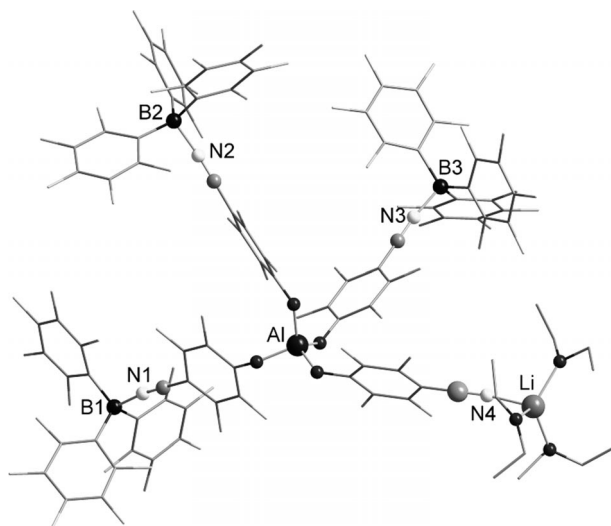


Figure 11. Drawing of the molecular structure of **9**.

## Conclusions

Crystalline coordination polymer networks were obtained by connection of *p*-cyanophenoxy linker units, tetra-

hedrally attached to either aluminium or boron, with monocationic metal centers (M) such as  $\text{Li}^+$ ,  $\text{Na}^+$ ,  $\text{Ag}^+$ , and  $\text{Cu}^+$ . An interesting common feature of these supramolecular polymers is the presence of dative metal–nitrogen bonds as crucial structure-directing elements besides the tetrahedral  $[\text{E}(\text{O}-\text{C}_6\text{H}_4-\text{CN})_4]^-$  (E = Al, B) anion. Utilizing the perfluorinated  $\text{O}-\text{C}_6\text{F}_4-\text{CN}$  linker leads to a decrease in the stability of the  $[\text{E}(\text{O}-\text{C}_6\text{H}_4-\text{CN})_4]^-$  anion with respect to decomposition into  $\text{E}(\text{O}-\text{C}_6\text{H}_4-\text{CN})_3$  and  $(\text{O}-\text{C}_6\text{H}_4-\text{CN})^-$ , which is also observed when a Lewis acid such as  $\text{B}(\text{C}_6\text{F}_5)_3$  is added. Moreover, addition of  $\text{B}(\text{C}_6\text{F}_5)_3$  leads to the formation of molecular ion pairs because now the cyano groups are either completely or partly blocked.

## Experimental Section

**General Information:** All manipulations were carried out under oxygen- and moisture-free conditions under argon using standard Schlenk or drybox techniques.

Dichloromethane and acetonitrile were heated to reflux over  $\text{CaH}_2$ ; tetrahydrofuran and  $\text{Et}_2\text{O}$  were dried with  $\text{Na}/\text{benzophenone}$  and freshly distilled prior to use. Lithium aluminium hydride (Alfa Aesar) was purified by recrystallization from  $\text{Et}_2\text{O}$  prior to use. 4-Hydroxybenzotrile (Merck) was sublimated in vacuo at  $60^\circ\text{C}$  prior use.  $\text{AgNO}_3$  (VEB Arzneimittelwerk, Dresden) was recrystallized from water, powdered, and dried in vacuo for 10 h.  $\text{NaBH}_4$  (Merck) and  $\text{KOH}$  (VWR) were used as received.  $^1\text{H}$ ,  $^{11}\text{B}$  and  $^{13}\text{C}$  NMR spectra were obtained with Bruker Avance 250 (250 MHz) and Avance 300 (300 MHz) spectrometers and were referenced externally.  $\text{CD}_2\text{Cl}_2$  and  $\text{CDCl}_3$  were dried with  $\text{P}_4\text{O}_{10}$ ,  $[\text{D}_6]\text{DMSO}$  and  $\text{CD}_3\text{CN}$  were dried with  $\text{CaH}_2$ , and  $\text{C}_6\text{D}_6$  was dried with sodium. FTIR spectra were obtained with a Nicolet 380 FTIR spectrometer with a Smart Orbit attenuated total reflectance (ATR) device. Raman spectra were obtained with a Bruker Vertex 70 FTIR spectrometer with a RAM II FT-Raman module equipped with a Nd:YAG laser (1064 nm) or Kaiser Optical Systems RXN1-785 nm microprobe. CHN analyses were conducted with an Analysator Flash EA 1112 instrument from Thermo Quest or C/H/N/S-Mikroanalysator TruSpec-932 instrument from Leco. Differential scanning calorimetry (DSC) measurements were obtained with a Mettler-Toledo 823e instrument (heating rate  $5^\circ\text{C}/\text{min}$ ). Thermogravimetric analysis (TGA) measurements were performed with a Setaram LapSys 1600 TGA-DSC under an argon atmosphere (heating rate  $5^\circ\text{C}/\text{min}$ ). Nitrogen sorption experiments were performed at  $-192^\circ\text{C}$  with a Thermo Sorptomatic 1990 instrument.

**X-ray Structure Determination:** X-ray quality crystals were selected in Fomblin YR-1800 perfluoroether (Alfa Aesar) at ambient temperatures. The samples were cooled to 173(2) K during measurement. The data were collected with a Bruker Apex Kappa-II CCD diffractometer using graphite monochromated  $\text{Mo}-K_\alpha$  radiation ( $\lambda = 0.71073 \text{ \AA}$ ). The structures were solved by direct methods (SHELXS-97) and refined by full-matrix least-squares procedures (SHELXL-97). Semi-empirical absorption corrections were applied (SADABS). All non-hydrogen atoms were refined anisotropically, hydrogen atoms were included in the refinement at calculated positions using a riding model.

**XRD:** Powder XRD patterns were collected with a Stoe Stadi P diffractometer using a position sensitive detector and germanium-monochromatized  $\text{Cu}-K_\alpha$  radiation ( $\lambda = 1.5406 \text{ \AA}$ ) at ambient temperature.

Syntheses<sup>[44]</sup>

**Li[Al(O-C<sub>6</sub>H<sub>4</sub>-CN)<sub>4</sub>] (1):** 4-Hydroxybenzotrile (2 g, 17 mmol, 4.25 equiv.) dissolved in THF (18 mL) was added slowly to a stirred solution of activated LiAlH<sub>4</sub> (0.152 g, 4 mmol, 1 equiv.) in THF (24 mL) at 0 °C. The resulting solution was heated to reflux for two hours. The solution was filtered, and the solvent was removed in vacuo to yield a colorless solid. This crude product was washed two times with Et<sub>2</sub>O (10 mL) to remove the excess 4-hydroxybenzotrile. The pure product was dried for three hours in vacuo at 70 °C; yield 1.32 g (65%). M.p. (DSC): (onset) 349.4 °C, (peak) 353.9 °C. C<sub>28</sub>H<sub>16</sub>AlLiN<sub>4</sub>O<sub>4</sub> (506.37): calcd. C 66.41, H 3.18, N 11.06; found C 65.35, H 3.54, N 10.68. <sup>1</sup>H NMR (CD<sub>3</sub>CN, 300 MHz, 25 °C): δ = 7.49–7.42 (m, 8 H, CH–C–CN), 6.90–8.84 (m, 8 H, CH–C–O) ppm. <sup>13</sup>C NMR (CD<sub>3</sub>CN, 300 MHz, 25 °C): δ = 164.9 (s, 1 C, CO), 135.0 (s, 1 C, C–C–CN), 121.1 (s, 1 C, CN), 120.8 (s, 1 C, C–C–O), 101.4 (s, 1 C, C–CN) ppm.

**Na[B(O-C<sub>6</sub>H<sub>4</sub>-CN)<sub>4</sub>] (2):** 4-Hydroxybenzotrile (2.728 g, 23 mmol, 4.25 equiv.) dissolved in THF (18 mL) was rapidly added to a stirred suspension of NaBH<sub>4</sub> (0.205 g, 5.4 mmol, 1 equiv.) in THF (24 mL) at 0 °C. The resulting suspension was heated to reflux for three hours. A colorless solid was obtained after filtration and removal of the solvent in vacuo. This crude product was washed two times with Et<sub>2</sub>O (10 mL) to remove the excess 4-hydroxybenzotrile. The pure product was dried for six hours in vacuo at 70 °C; yield 1.56 g (67%); decomp. (DSC): (onset) 362.1 °C. C<sub>28</sub>H<sub>16</sub>B N<sub>4</sub>NaO<sub>4</sub> (506.26): calcd. C 66.43, H 3.19, N 11.07; found C 66.10, H 3.39, N 10.25. <sup>1</sup>H NMR ([d<sub>6</sub>]DMSO, 300 MHz, 25 °C): δ = 7.55–7.45 (m, 8 H, CH–CCN), 7.12–7.04 (m, 8 H, CH–C–O) ppm. <sup>13</sup>C NMR (CD<sub>3</sub>CN, 250 MHz, 25 °C): δ = 165.3 (s, 1 C, CO), 133.1 (s, 1 C, C–C–CN), 119.4 (s, 1 C, CN), 119.1 (s, 1 C, C–C–O), 100.6 (s, 1 C, C–CN) ppm. <sup>11</sup>B NMR (CD<sub>3</sub>CN, 300 MHz, 25 °C): δ = 2.55 (s) ppm.

**Ag[Al(O-C<sub>6</sub>H<sub>4</sub>-CN)<sub>4</sub>] (3):** Lithium tetrakis-(4-cyanophenyl)aluminate (4 mmol, 2.0255 g) and silver triflate (4.5 mmol, 1.1562 g) were each dissolved in acetonitrile (40 mL). The silver salt solution was added to the stirred aluminate solution through a dropping funnel at ambient temperature. The turbid deep red solution was filtered, and the volume of the solvent was reduced to ca. 40 mL and filtered again. The microcrystalline product was crystallized overnight in a freezer at –30 °C from the clear red solution. The solvent was removed by decantation and the product was dried in vacuo for 2 h. After powdering and drying again for 2 h in high vacuum a light red-gray powder was obtained; yield 1.038 g (42.71% with respect to Al); decomp. (DSC): (onset) 243 °C. C<sub>28</sub>H<sub>16</sub>AlAgN<sub>4</sub>O<sub>4</sub> (607.31): calcd. C 55.38, H 2.66, N 9.23; found C 54.57, H 2.49, N 8.84. <sup>1</sup>H NMR (CD<sub>3</sub>CN, 300 MHz, 25 °C): δ = 7.50–7.42 (m, 8 H, CH–C–CN), δ = 6.89–6.81 (m, 8 H, CH–C–O) ppm. <sup>13</sup>C NMR (CD<sub>3</sub>CN, 300 MHz, 25 °C): δ = 164.6 (s, 1 C, CO), 135.0 (s, 1 C, C–C–CN), 120.7 (s, 1 C, CN), 119.7 (s, 1 C, C–C–O), 101.6 (s, 1 C, C–CN) ppm.

**Cu[Al(O-C<sub>6</sub>H<sub>4</sub>-CN)<sub>4</sub>] (4):** A solution of Ag[Al(O-C<sub>6</sub>H<sub>4</sub>-CN)<sub>4</sub>] (607.3 mg, 1 mmol) in acetonitrile (40 mL) was added to a stirred yellow colored solution of CuI (190.4 mg, 1 mmol) in acetonitrile (15 mL) at ambient temperature. A white precipitate was formed, and the solution turned slightly green. The reaction mixture was allowed to stir for ten minutes, and the precipitate was allowed to settle out. The solution was filtered and the residue was washed with acetonitrile (15 mL). The solution was filtered again, and the solvent was removed under reduced pressure. The white solid was dried for twelve hours at ambient temperature to yield the desired product (316.6 mg, 51% yield). Dec (DSC): (Onset) 281 °C. C<sub>28</sub>H<sub>16</sub>AlCuN<sub>4</sub>O<sub>4</sub> (562.89): calcd. C 59.74, H 2.86, N 9.95; found

C 58.84, H 3.44, N 9.65. <sup>1</sup>H NMR (CD<sub>3</sub>CN, 250 MHz, 25 °C): δ = 7.50–7.41 (m, 8 H, CH–C–CN), 6.90–6.82 (m, 8 H, CH–C–O) ppm. <sup>13</sup>C NMR (CD<sub>3</sub>CN, 250 MHz, 25 °C): δ = 164.9 (s, 1 C, CO), 135.0 (s, 1 C, C–C–CN), 121.1 (s, 1 C, CN), 120.7 (s, 1 C, C–C–O), 101.4 (s, 1 C, C–CN) ppm.

**Li[Al(O-C<sub>6</sub>F<sub>4</sub>-CN)<sub>4</sub>] (5):** 4-Hydroxy-2,3,5,6-tetrafluorobenzotrile (5.52 g, 28.87 mmol, 4.2 equiv.) dissolved in THF (18 mL) was added slowly to a stirred solution of activated LiAlH<sub>4</sub> (0.26 g, 6.87 mmol, 1 equiv.) in THF (24 mL) at 0 °C. The resulting solution was heated to reflux for two hours. The solution was filtered, and the solvent was removed in vacuo to yield the desired product as a colorless solid. This crude product was washed two times with CH<sub>2</sub>Cl<sub>2</sub> (10 mL) to remove the excess 4-hydroxy-2,3,5,6-tetrafluorobenzotrile. The pure product was dried for ten hours in vacuo at 80 °C; yield 3.5 g (64.16%). M.p. (DSC): (onset) 271.2 °C, (peak) 281.4 °C; dec. (onset) 361 °C. C<sub>28</sub>AlF<sub>16</sub>LiN<sub>4</sub>O<sub>4</sub> (794.23): calcd. C 42.34, N 7.05; found C 42.15, N 6.75. <sup>13</sup>C NMR (CD<sub>3</sub>CN, 300 MHz, 25 °C): δ = 149.1 (dm, <sup>1</sup>J<sub>C,F</sub> = 251.7 Hz, 1 C, CF–CO), 145.2 (m, 1 C, CO), 141.2 (dm, <sup>1</sup>J<sub>C,F</sub> = 242.2 Hz, 1 C, CF–CCN), 109.7 (t, <sup>3</sup>J<sub>C,F</sub> = 3.6 Hz, 1 C, CN), 84.9 (m, 1 C, C–CN) ppm. <sup>19</sup>F NMR (CD<sub>3</sub>CN, 282.4 MHz, 25 °C): δ = –139.1 (d, <sup>1</sup>J<sub>C,F</sub> = 11.23 Hz, 8 F), –161.4 (d, <sup>1</sup>J<sub>C,F</sub> = 14.83 Hz, 8 F) ppm.

**Na(O-C<sub>6</sub>F<sub>4</sub>-CN) (6):** To a stirred suspension of NaBH<sub>4</sub> (0.257 g, 6.75 mmol, 1 equiv.) in THF (24 mL), cooled to 0 °C, 4-hydroxy-2,3,5,6-tetrafluorobenzotrile (5.435 g, 28.5 mmol, 4.2 equiv.) dissolved in freshly distilled THF (18 mL) was added. The resulting suspension was heated to reflux for three hours. The suspension was filtered, and the solvent was removed in vacuo to give a colorless solid. The solid was washed two times with freshly distilled Et<sub>2</sub>O (10 mL) to remove the excess 4-hydroxy-2,3,5,6-tetrafluorobenzotrile; decomp. (DSC): (onset) 366.56 °C, (peak) 371.11 °C. C<sub>7</sub>F<sub>4</sub>NNaO (213.07): calcd. C 39.46, N 6.57; found C 39.40, N 6.20. <sup>13</sup>C NMR ([D<sub>6</sub>]DMSO, 75.5 MHz, 25 °C): δ = 153.7 (d, <sup>1</sup>J<sub>C,F</sub> = 260.4 Hz, 2 C, C–CO), 146.9 (tt, <sup>2</sup>J<sub>C,F</sub> = 13.9, <sup>3</sup>J<sub>C,F</sub> = 4.5 Hz, 1 C, CO), 140.3 (d, <sup>1</sup>J<sub>C,F</sub> = 247.6 Hz, 2 C, C–CN), 112.7 (t, <sup>3</sup>J<sub>C,F</sub> = 3.77 Hz, 1 C, CN), 63.4 (t, <sup>2</sup>J<sub>C,F</sub> = 18.1 Hz, 1 C, C–CN). <sup>19</sup>F NMR ([D<sub>6</sub>]DMSO, 282.4 MHz, 25 °C, ppm): δ = –144.8 (m, 2 F), –167.7 (m, 2 F) ppm.

**(THF)Al{O-C<sub>6</sub>H<sub>4</sub>-CN·B(C<sub>6</sub>F<sub>5</sub>)<sub>3</sub>}<sub>3</sub> (7):** To a stirred solution of B(C<sub>6</sub>F<sub>5</sub>)<sub>3</sub> (2.56 g, 5 mmol, 5 equiv.) in THF (50 mL), solid Li[Al(O-C<sub>6</sub>H<sub>4</sub>-CN)] (0.505 g, 1 mmol, 1 equiv.) was added in one portion and the resulting solution was stirred overnight. Removal of the solvent yielded a colorless solid, which was washed two times with *n*-hexane (50 mL). The residual *n*-hexane was removed in vacuo, and the solid was dissolved in Et<sub>2</sub>O (20 mL). The resulting solution was filtered and concentrated to 6 mL. Storage over 48 h at 7 °C resulted in the precipitation of (THF)<sub>2</sub>Al{O-C<sub>6</sub>H<sub>4</sub>-CN·B(C<sub>6</sub>F<sub>5</sub>)<sub>3</sub>}<sub>3</sub>; yield 0.6 g (31%). For analytical experiments the solid was dried in vacuo for six hours at 70 °C and (THF)Al{O-C<sub>6</sub>H<sub>4</sub>-CN·B(C<sub>6</sub>F<sub>5</sub>)<sub>3</sub>}<sub>3</sub> was obtained; decomp. (DSC): (onset) 136.8 °C. C<sub>79</sub>H<sub>20</sub>AlB<sub>3</sub>F<sub>45</sub>N<sub>3</sub>O<sub>4</sub> (1989.37): calcd. C 47.70, H 1.01, N 2.11; found C 47.43, H 1.33, N 1.71. <sup>1</sup>H NMR (CDCl<sub>3</sub>, 300 MHz, 25 °C): δ = 7.54–7.48 (m, 6 H, CH–C–CN), 6.77–6.71 (m, 6 H, CH–CO) ppm. <sup>13</sup>C NMR (CDCl<sub>3</sub>, 300 MHz, 25 °C): δ = 166.4 (s, 3 C, CO), 147.2 (m, 6 C, CF–CB), 139.7 (m, 3 C, CF–CF–CB), 136.3 (m, 6 C, CF–CF–CB), 136.0 (s, 6 C, CH–C–CN), 120.4 (s, 6 C, CH–CO), 115.6 (s, 3 C, CN), 114.9 (br., 3 C, C–B), 92.2 (s, 3 C, C–CN) ppm. <sup>19</sup>F NMR (CDCl<sub>3</sub>, 282 MHz, 25 °C): δ = –135.1 to –135.2 (m, 6 F, CF–CB), –157.9 (t, <sup>3</sup>J<sub>F,F</sub> = 20.3 Hz, 3 F, CF–CF–CF–CB), –164.7 to –164.8 (m, 6 F, CF–CF–CB) ppm. <sup>11</sup>B NMR (CDCl<sub>3</sub>, 96 MHz, 25 °C): δ = –11.7 (s, 3 B) ppm.

**Na[(F<sub>5</sub>C<sub>6</sub>)<sub>3</sub>B·O-C<sub>6</sub>H<sub>4</sub>-CN·B(C<sub>6</sub>F<sub>5</sub>)<sub>3</sub>] (8a):** A Schlenk flask was loaded with B(C<sub>6</sub>F<sub>5</sub>)<sub>3</sub> (2.56 g, 5 mmol, 5 equiv.) and Na[B(O-C<sub>6</sub>H<sub>4</sub>-CN)] (0.505 g, 1 mmol, 1 equiv.). To this mixture Et<sub>2</sub>O (50 mL) was added to obtain a suspension. The suspension was stirred overnight and a colorless solution was obtained. After removal of the solvent in vacuo a solid was obtained, which was washed three times with *n*-hexane (20 mL). The residual *n*-hexane was removed in vacuo, and the solid was dissolved in Et<sub>2</sub>O (15 mL). The resulting solution was filtered and concentrated to 5 mL. Colorless crystals of [Na(Et<sub>2</sub>O)<sub>4</sub>][(F<sub>5</sub>C<sub>6</sub>)<sub>3</sub>B·O-C<sub>6</sub>H<sub>4</sub>-CN·B(C<sub>6</sub>F<sub>5</sub>)<sub>3</sub>] suitable for X-ray crystallographic analysis were grown by storage at -30 °C overnight. The crystallized product was dried in vacuo for six hours at 70 °C to give the solvent-free product Na[(F<sub>5</sub>C<sub>6</sub>)<sub>3</sub>B·O-C<sub>6</sub>H<sub>4</sub>-CN·B(C<sub>6</sub>F<sub>5</sub>)<sub>3</sub>] for analytical experiments; yield 0.25 g (21%). M.p. (DSC): (onset) 154.7 °C, (peak) 164.4 °C; dec. (onset) 303.9 °C. C<sub>51</sub>H<sub>28</sub>B<sub>2</sub>F<sub>30</sub>NNaO<sub>5</sub> (1349.3): calcd. C 45.40, H 2.09, N 1.04; found C 45.22, H 1.46, N 1.04. <sup>1</sup>H NMR (CDCl<sub>3</sub>, 300 MHz, 25 °C, ppm): δ = 7.71–7.47 (m, CH-C-CN, 2 H), 6.96–7.78 (m, 2 H, CH-CO). <sup>13</sup>C NMR (CDCl<sub>3</sub>, 300 MHz, 25 °C, ppm): δ = 163.5 (s, 1C, C-O), 148.0 (m, 12C, CF-CB), 139.5 (m, CF-CF-CB, 6C), 137.4 (m, 12C, CF-CF-CB), 136.6 (s, 2C, CH-C-CN), 117.8 (s, 2C, CH-CO), 115.0 (br., 6C, C-B), 114.7 (s, 1C, CN), 96.3 (s, 1C, C-CN). <sup>19</sup>F NMR (CDCl<sub>3</sub>, 300 MHz, 25 °C): δ = -134.4 to -134.5 (m, 12 F, CF-CB), -156.2 (t, 6 F, CF-CF-CB, <sup>3</sup>J<sub>FF</sub> = 19.3 Hz), -163.2 to -163.4 (m, 12 F, CF-CF-CB). <sup>11</sup>B NMR (CDCl<sub>3</sub>, 300 MHz, 25 °C): δ = -11.7 (s, 1B, B-NC), -2.9 (s, 1B, B-O).

**Li[NC-C<sub>6</sub>F<sub>4</sub>-O-Al{O-C<sub>6</sub>F<sub>4</sub>-CN·B(C<sub>6</sub>F<sub>5</sub>)<sub>3</sub>}<sub>3</sub>] (9):** A Schlenk flask was loaded with B(C<sub>6</sub>F<sub>5</sub>)<sub>3</sub> (1.03 g, 2 mmol, 4 equiv.) and Li[Al(O-C<sub>6</sub>F<sub>4</sub>-CN)] (0.4 g, 0.5 mmol, 1 equiv.). To this mixture Et<sub>2</sub>O (25 mL) was added to obtain a suspension. The suspension was stirred overnight and a colorless solution was obtained. The solution was filtered and the volume of the solvent reduced to 10 mL. Storage at -40 °C overnight gave colorless crystals of [(Et<sub>2</sub>O)<sub>3</sub>Li]([NC-C<sub>6</sub>F<sub>4</sub>-O)Al{O-C<sub>6</sub>F<sub>4</sub>-CN·B(C<sub>6</sub>F<sub>5</sub>)<sub>3</sub>}<sub>3</sub>) suitable for X-ray crystallographic analysis. The crystallized product was dried in vacuo for six hours at 70 °C to give the solvent-free product Li([NC-C<sub>6</sub>F<sub>4</sub>-O)Al{O-C<sub>6</sub>F<sub>4</sub>-CN·B(C<sub>6</sub>F<sub>5</sub>)<sub>3</sub>}<sub>3</sub>) for analytical experiments; yield 0.86 g (74%); decomp. (DSC): (onset) 318.7 °C. C<sub>82</sub>AlB<sub>3</sub>F<sub>61</sub>LiN<sub>4</sub>O<sub>4</sub> (2330.17): calcd. C 42.27, N 2.40; found C 41.92, N 1.81. <sup>13</sup>C NMR (CDCl<sub>3</sub>, 300 MHz, 25 °C, ppm): δ = 151.23 (m, 1C, CF-C-CN), 149.83 (m, CO), 148.24 (dm, CF-C-B), 145.93 (dm, CF-CF-CB), 142.87 (m, CF-CO), 137.53 (dm, CF-CF-CB), 107.92 (m, CN). <sup>19</sup>F NMR (CDCl<sub>3</sub>, 300 MHz, 25 °C, ppm): δ = -130.93 (s), -133.78 (s), -155.82 (s), -156.46 (s), -163.19 (s). <sup>11</sup>B NMR (CDCl<sub>3</sub>, 300 MHz, 25 °C): δ = 2.5 to -41.5 (br).

CCDC-901962 (for 1), -901963 (for 5), -901964 (for 3), -901965 (for 4), -901966 (for 7), -901967 (for 2) contain the supplementary crystallographic data for this paper. These data can be obtained free of charge from The Cambridge Crystallographic Data Centre via [www.ccdc.cam.ac.uk/data\\_request/cif](http://www.ccdc.cam.ac.uk/data_request/cif).

**Supporting Information** (see footnote on the first page of this article): Details of crystallography experiments, figure showing the interpenetration in the solid state structure of 4, IR and Raman spectroscopic data.

## Acknowledgments

Financial support by the Deutsche Forschungsgemeinschaft (DFG) is gratefully acknowledged. We are indebted to Martin Ruhmann (University of Rostock) and Johannes Thomas (University of Rostock) for the measurement of Raman spectra.

- [1] For overviews, see: a) S. R. Batten, R. Robson, *Angew. Chem.* **1998**, *110*, 1558; *Angew. Chem. Int. Ed.* **1998**, *37*, 1460–1494; b) B. Moulton, M. J. Zaworotko, *Chem. Rev.* **2001**, *101*, 1629–1658; c) S. Kitagawa, R. Kitaura, S.-i. Noro, *Angew. Chem.* **2004**, *116*, 2388–2430; *Angew. Chem. Int. Ed.* **2004**, *43*, 2334–2375; d) R. Robson, in: *Comprehensive Supramolecular Chemistry*, vol. 6 (Eds.: J. L. Atwood, J. E. D. Davies, D. D. MacNicol, F. Vögtle, F. Toda, R. Bishop), Pergamon, Oxford, UK, **1996**, pp. 733–755.
- [2] a) C. B. Aakeroy, K. R. Seddon, *Chem. Soc. Rev.* **1993**, *22*, 397–407; b) O. Ermer, A. Eling, *J. Chem. Soc. Perkin Trans. 2* **1994**, 925–944; c) P. Brunet, M. Simard, J. D. Wuest, *J. Am. Chem. Soc.* **1997**, *119*, 2737–2738; d) D. S. Reddy, D. C. Craig, G. R. Desiraju, *J. Chem. Soc., Chem. Commun.* **1995**, 339–340; e) V. A. Russell, M. D. Ward, *Chem. Mater.* **1996**, *8*, 1654–1666; f) K. Kobayashi, K. Endo, Y. Aoyama, H. Masuda, *Tetrahedron Lett.* **1993**, *34*, 7929–7932; g) K. Endo, T. Sawaki, M. Koyanagi, K. Kobayashi, H. Masuda, Y. Aoyama, *J. Am. Chem. Soc.* **1995**, *117*, 8341–8352; h) M. Mitsumi, J. Toyoda, K. Nakasuji, *Inorg. Chem.* **1995**, *34*, 3367–3370; i) S. Subramanian, M. J. Zaworotko, *Coord. Chem. Rev.* **1994**, *137*, 357–401.
- [3] a) C. B. Aakeroy, N. R. Champness, C. Janiak, *CrystEngComm* **2010**, *12*, 22–43; b) G. R. Desiraju, *Angew. Chem.* **2007**, *119*, 8492; *Angew. Chem. Int. Ed.* **2007**, *46*, 8342–8356; c) D. Braga, L. Brammer, N. R. Champness, *CrystEngComm* **2005**, *7*, 1–19.
- [4] a) C. Janiak, J. K. Vieth, *New J. Chem.* **2010**, *34*, 2366–2388, and references cited therein b) B. Sieklucka, R. Podgajny, T. Korzeniak, B. Nowicka, D. Pinkowicz, M. Koziel, *Eur. J. Inorg. Chem.* **2011**, *3*, 305–326.
- [5] a) M. Fourmigu, *Curr. Opin. Solid State Mater. Sci.* **2009**, *13*, 36–45; b) P. Metrangolo, T. Pilati, G. Terraneo, S. Biella, G. Resnati, *CrystEngComm* **2009**, *11*, 1187–1196; c) L. Brammer, G. M. Espallargas, S. Libri, *CrystEngComm* **2008**, *10*, 1712–1727; d) P. Metrangolo, F. Meyer, T. Pilati, G. Resnati, G. Terraneo, *Angew. Chem.* **2008**, *120*, 6206; *Angew. Chem. Int. Ed.* **2008**, *47*, 6114–6127.
- [6] M. J. Katz, K. Sakai, D. B. Leznoff, *Chem. Soc. Rev.* **2008**, *37*, 1884–1895.
- [7] M. Nishio, *CrystEngComm* **2004**, *6*, 130–158.
- [8] C. A. Hunter, K. R. Lawson, J. Perkins, C. J. Urch, *J. Chem. Soc. Perkin Trans. 2* **2001**, 651–669.
- [9] I. Alkorta, O. Picazo, J. Elguero, *Tetrahedron: Asymmetry* **2005**, *16*, 755–760.
- [10] M. T. Mock, R. G. Potter, D. M. Camaioni, J. Li, W. G. Dougherty, W. S. Kassel, B. Twamley, D. L. DuBois, *J. Am. Chem. Soc.* **2009**, *131*, 14454–14465.
- [11] a) M. M. Aminia, M. Sharbatdaran, M. Mirzaee, P. Mirzaei, *Polyhedron* **2006**, *25*, 3231–3237; b) S. HePmanek, O. Kpiz, J. Fusek, Z. Cerny, B. Casensky, *J. Chem. Soc. Perkin Trans. 2* **1989**, 987; c) R.-M. Ho, T.-C. Wang, C.-C. Lin, T.-L. Yu, *Macromolecules* **2007**, *40*, 2814–2821; d) D. S. McGuinness, A. J. Rucklidge, R. P. Tooze, A. M. Slawin, *Organometallics* **2007**, *26*, 2561–2569; e) K. Tabatabaeian, M. Mamaghani, A. Pourahamad, *Russ. J. Org. Chem.* **2001**, *37*, 1287–1288; f) S. Gou, J. Wang, X. Liu, W. Wang, F.-X. Chen, X. Feng, *Adv. Synth. Catal.* **2007**, *349*, 343–349; g) E. Keller, N. Veldman, A. L. Spek, B. L. Feringa, *Tetrahedron: Asymmetry* **1997**, *8*, 3403–3413.
- [12] N. Malek, T. Maris, M. Simard, J. D. Wuest, *J. Am. Chem. Soc.* **2005**, *127*, 5910–5916.
- [13] E. Bernhardt, G. Henkel, H. Willner, *Z. Anorg. Allg. Chem.* **2000**, *626*, 560–568.
- [14] a) Y. Y. Karabach, M. Fatima, C. Guedes da Silva, M. N. Kopylovich, B. Gil-Hernandez, J. Sanchiz, A. M. Kirillov, A. J. L. Pombeiro, *Inorg. Chem.* **2010**, *49*, 11096–11105; b) H. Dan, S. Nishikiori, O. Yamamuro, *Dalton Trans.* **2011**, *40*, 1168–1174; c) P. K. Thallapally, R. Kishan Motkuri, C. A. Fernandez, B. P. McGrail, G. S. Behrooz, *Inorg. Chem.* **2010**, *49*, 4909–4915; d)



- B. F. Hoskins, R. Robson, *J. Am. Chem. Soc.* **1990**, *112*, 1546–1554.
- [15] a) S. R. Batten, B. F. Hoskins, R. Robson, *New J. Chem.* **1998**, *22*, 173–175; b) B. F. Abrahams, S. R. Batten, B. F. Hoskins, R. Robson, *Inorg. Chem.* **2003**, *42*, 2654–2664.
- [16] a) F.-Q. Liu, T. D. Tilley, *Inorg. Chem.* **1997**, *36*, 5090–5096; b) F.-Q. Liu, T. D. Tilley, *Chem. Commun.* **1998**, 103–104.
- [17] a) F. Fahra Jr., R. T. Iwamoto, *Inorg. Chem.* **1965**, *4*, 844–848; b) D. T. Cromer, A. C. Larson, *Acta Crystallogr., Sect. B* **1972**, *28*, 1052–1058; c) L. Carlucci, G. Ciani, D. W. v. Gudenberg, D. M. Proserpio, *New J. Chem.* **1999**, *23*, 397–402.
- [18] a) I. Krossing, A. Reisinger, *Coord. Chem. Rev.* **2006**, *250*, 2721; b) M. Gonsior, I. Krossing, L. Müller, I. Raabe, M. Jansen, L. Van Wullen, *Chem. Eur. J.* **2002**, *8*, 4475; c) I. Krossing, *J. Chem. Soc., Dalton Trans.* **2002**, *4*, 500; d) I. Krossing, I. Raabe, *Chem. Eur. J.* **2004**, *10*, 5017.
- [19] M. Kuprat, R. Kuzora, M. Lehmann, A. Schulz, A. Villinger, R. Wustrack, *J. Organomet. Chem.* **2010**, *695*, 1006–1011.
- [20] M. Kuprat, M. Lehmann, A. Schulz, A. Villinger, *Organometallics* **2010**, *29*, 1421–1427.
- [21] F. Ibad, P. Langer, A. Schulz, A. Villinger, *J. Am. Chem. Soc.* **2011**, *133*, 21016–21027.
- [22] a) J. Zhou, S. J. Lancaster, D. A. Walker, S. Beck, M. Thornton-Pett, M. Bochmann, *J. Am. Chem. Soc.* **2001**, *123*, 223; b) S. J. Lancaster, D. A. Walker, S. Beck, M. Thornton-Pett, M. Bochmann, *Chem. Commun.* **1999**, 1533; c) R. E. LaPointe, WO 99/42467, **1999**.
- [23] D. Vagedes, G. Erker, R. Fröhlich, *J. Organomet. Chem.* **2002**, *641*, 148.
- [24] R. E. LaPointe, G. R. Roof, K. A. Abboud, J. Klosin, *J. Am. Chem. Soc.* **2000**, *122*, 9560.
- [25] a) A. Bernsdorf, H. Brand, R. Hellmann, M. Köckerling, A. Schulz, A. Villinger, K. Voss, *J. Am. Chem. Soc.* **2009**, *131*, 8958–8970; b) M. Becker, A. Schulz, A. Villinger, K. Voss, *RSC Adv.* **2011**, *1*, 128–134; c) J. M. Birchall, R. N. Haszeldine, M. E. Jones, *J. Chem. Soc. C* **1971**, 1343–1348; d) A. G. Massey, A. J. Park, *J. Organomet. Chem.* **1964**, *2*, 245–250; e) N. Malek, T. Maris, M. Simard, J. D. Wuest, *J. Am. Chem. Soc.* **2004**, *127*, 5910–5916.
- [26] a) M. Munakata, G. L. Ning, T. Kuroda-Sowa, M. Maekawa, Y. Suenaga, T. Horino, *Inorg. Chem.* **1998**, *37*, 5651–5656; b) T. Küppers, E. Bernhardt, H. Willner, H. W. Rohm, M. Köckerling, *Inorg. Chem.* **2005**, *44*, 1015–1022.
- [27] H. Jacobsen, H. Berke, S. Doering, G. Kehr, G. Erker, R. Froehlich, O. Meyer, *Organometallics* **1999**, *18*, 1724.
- [28] I. C. Veil, S. I. Pascu, M. L. H. Green, J. C. Green, R. E. Schilling, G. D. W. Anderson, L. H. Rees, *Dalton Trans.* **2003**, 2550.
- [29] A. A. Danopoulos, J. R. Galsworthy, M. L. H. Green, S. Caf-ferkey, L. H. Doerrer, M. B. Hursthouse, *Chem. Commun.* **1998**, 2529.
- [30] L. H. Doerrer, J. R. Galsworthy, M. L. H. Green, M. A. Leech, M. Mueller, *J. Chem. Soc., Dalton Trans.* **1998**, 3191.
- [31] L. H. Doerrer, J. R. Galsworthy, M. L. H. Green, M. A. Leech, *J. Chem. Soc., Dalton Trans.* **1998**, 2483.
- [32] L. H. Doerrer, A. J. Graham, M. L. H. Green, *J. Chem. Soc., Dalton Trans.* **1998**, 3941.
- [33] L. H. Doerrer, M. L. H. Green, *J. Chem. Soc., Dalton Trans.* **1999**, 4325.
- [34] P. Pykkö, M. Atsumi, *Chem. Eur. J.* **2009**, *15*, 12770–12779.
- [35] a) B. F. Straub, M. Wrede, K. Schmid, F. Rominger, *Eur. J. Inorg. Chem.* **2010**, *13*, 1907–1911; b) M. L. Cole, D. E. Hibbs, C. Jones, P. C. Junk, N. A. Smithies, *Inorg. Chim. Acta* **2005**, *358*, 102–108; c) D. M. Seo, P. D. Boyle, W. A. Henderson, *Acta Crystallogr., Sect. E* **2011**, *67*, m1148; d) H. Wang, H. Li, B. Xue, Z. Wang, Q. Meng, L. Chen, *J. Am. Chem. Soc.* **2005**, *127*, 6394–6401.
- [36] a) B. F. Hoskins, R. Robson, *J. Am. Chem. Soc.* **1990**, *112*, 1546–1554; b) H. S. Zhdanov, *Acad. Sci. URSS* **1941**, *31*, 352–354; c) T. Kitazawa, S. Nishikiori, R. Kuroda, T. Iwamoto, *J. Chem. Soc., Dalton Trans.* **1994**, 1029–1036.
- [37] O. Ermer, *J. Am. Chem. Soc.* **1988**, *110*, 3747–3754.
- [38] R. Robson, B. F. Abrahams, S. R. Batten, R. W. Gable, B. F. Hoskins, J. Liu, in: *Supramolecular Architecture: Synthetic Control in Thin Films and Solids* (Ed.: T. Bein), American Chemical Society, Washington DC, **1992**, p. 256–273.
- [39] A. J. Blake, N. R. Champness, S. S. M. Chung, W.-S. Li, M. Schroder, *Chem. Commun.* **1997**, 1005–1006.
- [40] a) J. Pauls, B. Neumüller, *Z. Anorg. Allg. Chem.* **2000**, *626*, 270–279; b) J. Pauls, S. Chitsaz, B. Neumüller, *Phosphorus Sulfur Silicon Relat. Elem.* **2001**, *168*, 233–238; c) L. Dostál, R. Jambor, I. Cisařová, J. Merna, J. Holěček, *Appl. Organomet. Chem.* **2007**, *21*, 688–693.
- [41] W. Ziemkowska, A. Kubiak, S. Kucharski, R. Woźniak, R. Anulewicz-Ostrowska, *Polyhedron* **2007**, *26*, 1436–1444.
- [42] W. Su, Y. Kim, A. Ellern, I. A. Guzei, J. G. Verkade, *J. Am. Chem. Soc.* **2006**, *128*, 13727–13735.
- [43] Fluorinated species **8b** was prepared for comparison from Na[O–C<sub>6</sub>F<sub>4</sub>–CN] and B(C<sub>6</sub>F<sub>5</sub>)<sub>3</sub>.
- [44] IR and Raman data can be found in the Supporting Information.

Received: April 29, 2012

Published Online: September 25, 2012

## **5.2 Tetrakis(2-cyanoethoxy)borate – An Alternative to Tetracyanidoborate-Based Ionic Liquids**

Jörg Harloff, Markus Karsch, Henrik Lund, Axel Schulz, Alexander Villinger.

*Eur. J. Inorg. Chem.* **2013**, 4243-4250.

In dieser Publikation wurden sämtliche experimentellen Arbeiten von mir durchgeführt. Die in der Arbeit erstmalig publizierten Verbindungen wurden von mir synthetisiert und vollständig charakterisiert. Sämtliche Verbindungen wurden von mir für die Röntgenstrukturanalytik kristallisiert.

Das vorliegende Manuskript zur Publikation wurde von mir als Erstautor verfasst. Die Darstellungen der Verbindungen und die analytischen Daten wurden von mir im Supporting zusammengefasst. Zudem habe ich an den Korrekturen zu dem Manuskript mitgewirkt. Der eigene Anteil liegt bei ca. 85 %.



DOI:10.1002/ejic.201300228

## Tetrakis(2-cyanoethoxy)borate – An Alternative to Tetracyanidoborate-Based Ionic Liquids

Jörg Harloff,<sup>[a]</sup> Markus Karsch,<sup>[a]</sup> Henrik Lund,<sup>[a]</sup> Axel Schulz,<sup>\*,[a,b]</sup> and Alexander Villinger<sup>[a]</sup>

**Keywords:** Ionic liquids / Coordination chemistry / Anions / Borates

This study examines the synthesis and properties of salts of the new tetrahedral  $[\text{B}(\text{O}-\text{C}_2\text{H}_4-\text{CN})_4]^-$  anion, which can be synthesized by the reaction of tetrahedral  $\text{NaBH}_4$  and  $\text{HO}-\text{C}_2\text{H}_4-\text{CN}$  followed by salt metathesis. The structures of

$\text{M}[\text{B}(\text{O}-\text{C}_2\text{H}_4-\text{CN})_4]$  [ $\text{M} = \text{Na}$ , 1-ethyl-3-methylimidazolium (EMIm), 1-butyl-3-methylimidazolium (BMIm), 1-octyl-3-methylimidazolium (OMIm),  $\text{Me}_4\text{N}$ ,  $\text{Et}_4\text{N}$ , and  $\text{Bu}_4\text{N}$ ] as well as the thermal decomposition products are discussed.

### Introduction

Recent developments in the synthesis and applications of ionic liquids (ILs) have led to functionalized ILs with a great number of applications in increasingly diverse fields.<sup>[1,2]</sup> For example, ILs have attracted attention as alternative solvents in green chemistry, catalysis, materials science, and separation technology. In turn, such applications have promoted the design and synthesis of many new ILs, especially functionalized ILs.<sup>[3]</sup> For example, CN-functionalized pyridinium based ILs were found to (1) generate a more effective catalytic system in the Heck reaction by catalyst immobilization or (2) stabilize reaction intermediates in glycosidation reactions (C–O coupling).<sup>[4]</sup> In both examples, CN groups were introduced in the cations, which has been the common method of CN functionalization as found in CN-functionalized imidazolium,<sup>[5]</sup> pyridinium, pyrrolidinium, and piperidinium cations.<sup>[6]</sup> Much less is known about ILs containing CN-functionalized anions.<sup>[7]</sup> We have recently studied the synthesis and properties of CN-functionalized borate/aluminate based ILs with anions of the type  $[\text{E}(\text{O}-\text{C}_6\text{X}_4-\text{CN})_4]^-$  ( $\text{E} = \text{B}, \text{Al}$ ;  $\text{X} = \text{H}, \text{F}$ )<sup>[8]</sup> and tetracyanopyrrolide-based ILs.<sup>[9]</sup> Tetraphenoxaluminates and -borates<sup>[10,11]</sup> and their fluorinated analogues<sup>[12]</sup> have been studied and widely applied, for example, in catalysis; however, to the best of our knowledge cyano-substituted anions of the type  $[\text{B}(\text{O}-\text{C}_n\text{H}_{2n}-\text{CN})_4]^-$  ( $n = 2, 3$ , etc.) with alkyl chains are not known yet. The only known cyanoborates

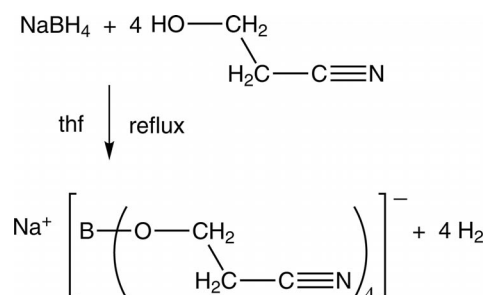
and -aluminates are of the type  $[\text{B}(\text{C}_6\text{H}_4-\text{CN})_4]^-$ ,<sup>[13]</sup> and  $[\text{B}(\text{CN})_4]^-$ <sup>[14]</sup> or with the mentioned *para*-cyanophenoxy ligands. Furthermore, there is a great wealth of compounds based on polycyanometallates,<sup>[4b,15]</sup>  $[\text{C}(\text{CN})_3]^-$ ,<sup>[16]</sup> or  $\text{Si}(\text{p}-\text{C}_6\text{H}_4-\text{CN})_4$ .<sup>[17]</sup>

Herein, we describe the synthesis, structure, and physical properties of ILs bearing the new  $[\text{B}(\text{O}-\text{C}_2\text{H}_4-\text{CN})_4]^-$  anion.

### Results and Discussion

#### Synthesis

Although ligands with the potential for supplemental Lewis base interactions such as those with *para*-cyanophenoxy linkers are finding increasing utility for the stabilization of electrophilic metal centers (e.g., metal = alkali, Cu, Ag), CN-functionalized alkyl chains have not been used so far.<sup>[8,18]</sup> For the synthesis of salts of the borate anion  $[\text{B}(\text{O}-\text{C}_2\text{H}_4-\text{CN})_4]^-$ ,  $\text{NaBH}_4$  was treated with five equivalents (1 equiv. excess) of 3-hydroxypropionitrile,  $\text{HO}-\text{C}_2\text{H}_4-\text{CN}$ , at ambient temperatures in tetrahydrofuran (THF, Scheme 1). Complete hydrogen release was obtained after the reaction mixture had been heated to reflux in THF for



Scheme 1. Synthesis of **1**.

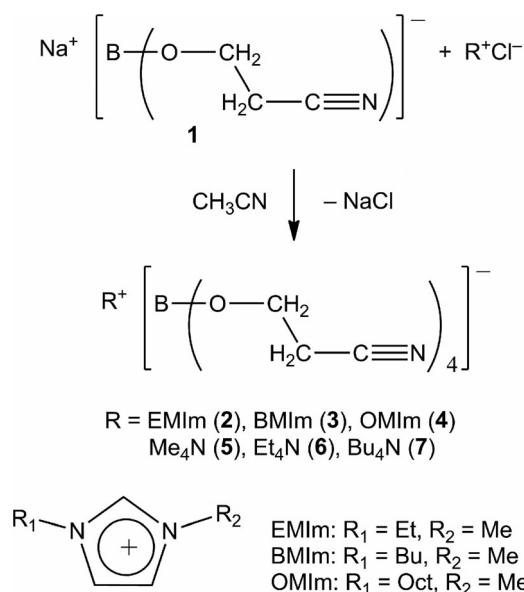
[a] Institut für Chemie, Universität Rostock, Albert-Einstein-Str. 3a, 18059 Rostock, Germany  
Fax: +49-381-498-6381  
E-mail: axel.schulz@uni-rostock.de  
Homepage: <http://www.schulz.chemie.uni-rostock.de/>

[b] Leibniz Institut für Katalyse, Albert-Einstein-Str. 29a, 18059 Rostock, Germany  
Fax: +49-381-498-6381

Supporting information for this article is available on the WWW under <http://dx.doi.org/10.1002/ejic.201300228>

6 h. The precipitate was collected by filtration, washed with  $\text{CH}_2\text{Cl}_2$ , and recrystallized from  $\text{CH}_3\text{CN}$  to afford colorless, crystalline  $\text{Na}[\text{B}(\text{O}-\text{C}_2\text{H}_4-\text{CN})_4]$  (**1**) in good yield (50–60%).

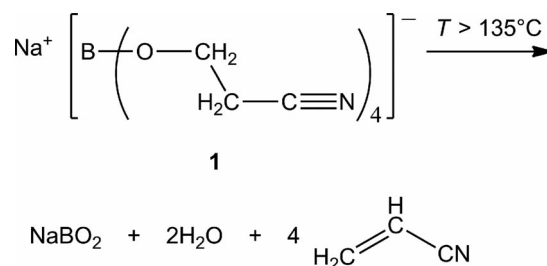
By salt metathesis reactions of  $\text{Na}[\text{B}(\text{O}-\text{C}_2\text{H}_4-\text{CN})_4]$ , the exchange of the  $\text{Na}^+$  ion by several imidazolium and ammonium  $\text{M}^+$  ions was achieved to afford  $\text{M}[\text{B}(\text{O}-\text{C}_2\text{H}_4-\text{CN})_4]$  [ $\text{M} = 1$ -ethyl-3-methylimidazolium (EMIm), 1-butyl-3-methylimidazolium (BMIm), 1-octyl-3-methylimidazolium (OMIm),  $\text{Me}_4\text{N}$ ,  $\text{Et}_4\text{N}$ ,  $\text{Bu}_4\text{N}$ ; **2–7**] in yields of 86–92% (Scheme 2). The best approach for such a metathesis reaction is the treatment of  $\text{Na}[\text{B}(\text{O}-\text{C}_2\text{H}_4-\text{CN})_4]$  (1.1 equiv.) suspended in  $\text{CH}_3\text{CN}$  with the imidazolium or ammonium chloride (1 equiv.) dissolved in  $\text{CH}_3\text{CN}$ . After the mixtures had been heated to reflux for 3 h, the precipitated  $\text{NaCl}$  and excess  $\text{Na}[\text{B}(\text{O}-\text{C}_2\text{H}_4-\text{CN})_4]$  were removed by filtration, and the solvent was removed in vacuo. The crude products were dissolved in  $\text{CH}_2\text{Cl}_2$ , filtered, and the solvent of the filtrate was evaporated in vacuo. The products were dried in vacuo for 3 h at 60 °C.



Scheme 2. Synthesis of imidazolium and ammonium salts bearing the  $[\text{B}(\text{O}-\text{C}_2\text{H}_4-\text{CN})_4]^-$  ion.

## Properties

Sodium salt **1** is almost insoluble in  $\text{CH}_2\text{Cl}_2$  and aromatic solvents such as benzene or toluene but slightly soluble in  $\text{CH}_3\text{CN}$ . Compound **1** can be prepared in bulk, is hygroscopic, and decomposes at temperatures over 135 °C. Thermogravimetric analysis (TGA) measurements, mass spectrometry, and NMR studies revealed the release of acrylonitrile at temperatures above 135 °C. In addition to acrylonitrile, water and  $\text{NaBO}_2$  are formed in the decomposition process as illustrated in Scheme 3. All ammonium and imidazolium salts bearing the  $[\text{B}(\text{O}-\text{C}_2\text{H}_4-\text{CN})_4]^-$  anion are moisture- and considerably air-sensitive. They dissolve in solvents such as  $\text{CH}_3\text{CN}$ , THF,  $\text{CH}_2\text{Cl}_2$ , but not in  $\text{Et}_2\text{O}$  or benzene. They slowly decompose in water with the formation of the free alcohol  $\text{HO}-\text{C}_2\text{H}_4-\text{CN}$  and  $\text{B}_2\text{O}_3 \cdot n\text{H}_2\text{O}$  as shown by  $^1\text{H}$ ,  $^{13}\text{C}$ , and  $^{11}\text{B}$  NMR studies. All mentioned  $[\text{B}(\text{O}-\text{C}_2\text{H}_4-\text{CN})_4]^-$  salts are easily prepared in bulk and are infinitely stable when stored in a sealed tube. All considered ammonium and imidazolium salts bearing the  $[\text{B}(\text{O}-\text{C}_2\text{H}_4-\text{CN})_4]^-$  ion are thermally stable to more than 80 °C (Table 1). Well-defined reversible melting points are not observed. Although **5** and **7** decompose at their melting points, crystals of **2–4** and **6** melt upon heating, but form frozen undercooled melts when the temperature is decreased (Table 1), and a glass transition is observed. Compound **4** and **6** in particular can be referred to as room temperature stable ionic liquids with glass transition temperatures of ca.  $-40$  °C.<sup>[19,20]</sup>



Scheme 3. Decomposition of **1**.

## Spectroscopic Studies

The  $^{13}\text{C}$  and  $^{11}\text{B}$  NMR spectroscopic data along with IR/Raman data for compounds described in this work are

Table 1. Thermal analysis: melting and decomposition points [from differential scanning calorimetry (DSC) measurements]; spectroscopic data: IR, Raman, and  $^{13}\text{C}$  NMR spectroscopic data of **1–7** and free  $\text{HO}-\text{C}_2\text{H}_4-\text{CN}$ .

	$T(T_{\text{glass}})$ [°C]	$T_{\text{dec}}^{\text{[a]}}$ [°C]	$^{13}\text{C}$ NMR $\delta_{\text{CN}}$ [ppm]	$^{11}\text{B}$ NMR $\delta$ [ppm]	IR $\nu_{\text{CN}}$ [ $\text{cm}^{-1}$ ]	Raman $\nu_{\text{CN}}$ [ $\text{cm}^{-1}$ ]
$\text{HO}-\text{C}_2\text{H}_4-\text{CN}$	−46	–	118.6	–	2261	2252
<b>1</b>	–	135	120.7	2.32	2258, 2248	2247
<b>2</b>	39 (−5) <sup>[b]</sup>	121	120.5	2.60	2240	2245
<b>3</b>	41 (−15) <sup>[b]</sup>	97	119.4	2.64	2245	2245
<b>4</b>	47 (−40) <sup>[c]</sup>	96	120.9	2.64	2243	2244
<b>5</b>	87	87	121.0	2.39	2241	2242
<b>6</b>	26 (−40) <sup>[c]</sup>	80	120.8	2.48	2243	2247
<b>7</b>	96	96	120.7	2.60	2245	2242

[a] Decomposition temperature. [b] Forms a glass that slowly crystallizes after 7 (**2**) or 28 d (**3**). [c] Does not crystallize within six weeks. Crystals were obtained from a THF solution at  $-80$  °C.

listed in Table 1. The IR and Raman data of all considered CN-group-containing anions in Table 1 show sharp bands in the expected region 2240–2258 cm<sup>-1</sup>, which can be assigned to  $\nu_{\text{CN}}$  stretching. Interestingly, the differences between the band of free HO–C<sub>2</sub>H<sub>4</sub>–CN (2261 cm<sup>-1</sup>) and those of the sodium salt **1** as well as **2–7** are rather small. The  $\nu_{\text{CN}}$  stretching bands of the ammonium and imidazolium salts (**2–7**) are found at slightly lower wavenumbers. The <sup>13</sup>C NMR resonance of the cyano groups in [B(O–C<sub>2</sub>H<sub>4</sub>–CN)<sub>4</sub>]<sup>-</sup> are detected at slightly lower field than that of HO–C<sub>2</sub>H<sub>4</sub>–CN and are in the range  $\delta = 118$ –121 ppm. Typically for borate anions, a rather sharp <sup>11</sup>B NMR resonance is found for the [B(O–C<sub>2</sub>H<sub>4</sub>–CN)<sub>4</sub>]<sup>-</sup> ion at 2.3–2.6 ppm.

### X-ray Structure Analysis

The structures of compounds **1–7** have been determined, and their X-ray crystallographic data are presented in Tables 2 and 3. Selected bond lengths and angles are listed in Table 4. X-ray quality crystals of all considered species were selected in Kel-F-oil (Riedel deHaen) or Fomblin YR-1800 (Alfa Aesar) at ambient temperature. All samples were cooled to –100(2) °C during the measurement. More details are found in the Supporting Information.

#### Na[B(O–C<sub>2</sub>H<sub>4</sub>–CN)<sub>4</sub>] (**1**)

Crystals of **1** suitable for X-ray crystallographic analysis were obtained by recrystallization from a hot saturated acetonitrile solution. Sodium salt **1** crystallized as colorless blocks in the orthorhombic space group *P*2<sub>1</sub>2<sub>1</sub>2<sub>1</sub> with four formula units per unit cell. The Flack parameter is close to

zero, and the crystallization of **1** in a non-centrosymmetric space group is probably because of some polar packing within the network (see below). The problem of packing in non-centrosymmetric space groups has been addressed in a series of paper by Janiak et al.,<sup>[21]</sup> in which non-centrosymmetric or even chiral packing was traced to strong intermolecular, chain, or layer hydrogen bonding or molecules with the same orientation along one axis.

There are strong cation⋯anion interactions as depicted in Figures 1 and 2. The Na ions are in a distorted squared pyramidal environment and interact with three adjacent borate anions through two chelating oxygen atoms of two borate anions and a nitrogen atom of the third borate anion (Figure 1). The Na–O distances are 2.3013(9), 2.4005(8), 2.3418(8), and 2.5459(9) Å [cf.  $\Sigma r_{\text{cov}}(\text{Na–O}) = 2.18$  Å,  $\Sigma r_{\text{vdW}}(\text{Na}⋯\text{O}) = 3.77$ ],<sup>[22]</sup> and the Na–N distance of 2.509(1) Å is considerably longer than the sum of the covalent radii,  $\Sigma r_{\text{cov}}(\text{Na–N}) = 2.26$  Å.<sup>[22]</sup> In addition, a further close contact between the sodium ion and N3 is found [3.264(2) Å], which lies well within the sum of their van der Waals radii [ $\Sigma r_{\text{vdW}}(\text{Na}⋯\text{N}) = 3.82$  Å].<sup>[23]</sup> With this interaction included, a 5+1 coordination describes best the situation around the Na<sup>+</sup> ion.

The B atom of the anion is in a tetrahedral coordination environment but only one of the four cyano linkers (tetrahedrally attached to the B atom through an O atom and to Na ion through a N atom) bridges the B and Na atoms to form a 3D framework structure as shown in Figure 3. The B–O bond lengths are 1.462–1.472 Å [cf.  $\Sigma r_{\text{cov}}(\text{B–O}) = 1.48$  Å].<sup>[22]</sup> These values are similar to those of phenoxyborates and lithium nitrile complexes.<sup>[24]</sup> The tetrahedron of the BO<sub>4</sub> moiety is slightly distorted with two smaller [O2–

Table 2. Crystallographic details of **1–3**.

	<b>1</b> <sup>[a]</sup>	<b>2</b>	<b>3</b>
Formula	C <sub>12</sub> H <sub>16</sub> BN <sub>4</sub> NaO <sub>4</sub>	C <sub>18</sub> H <sub>27</sub> BN <sub>6</sub> O <sub>4</sub>	C <sub>20</sub> H <sub>31</sub> BN <sub>6</sub> O <sub>4</sub>
Formula weight [g mol <sup>-1</sup> ]	314.09	402.27	430.32
Color	colorless	colorless	colorless
Crystal system	orthorhombic	monoclinic	monoclinic
Space group	<i>P</i> 2 <sub>1</sub> 2 <sub>1</sub> 2 <sub>1</sub>	<i>P</i> 2 <sub>1</sub> / <i>n</i>	<i>P</i> 2 <sub>1</sub> / <i>c</i>
<i>a</i> [Å]	8.6005 (3)	9.5305 (4)	18.426 (1)
<i>b</i> [Å]	11.2286 (4)	14.6660 (6)	16.3189 (9)
<i>c</i> [Å]	16.2283 (5)	15.7521 (7)	18.427 (1)
$\alpha$ [°]	90	90	90
$\beta$ [°]	90	93.236 (2)	116.873 (3)
$\gamma$ [°]	90	90	90
<i>V</i> [Å <sup>3</sup> ]	1567.19 (9)	2198.23 (16)	4942.4 (5)
<i>Z</i>	4	4	8
$\mu$ [mm <sup>-1</sup> ]	0.12	0.09	0.08
$\lambda$ (Mo– <i>K</i> $\alpha$ ) [Å]	0.71073	0.71073	0.71073
<i>T</i> [K]	173(2)	173(2)	173(2)
Measured reflections	15052	24720	54453
Independent reflections	5513	5297	11311
Reflections with <i>I</i> > 2 $\sigma$ ( <i>I</i> )	4913	4030	6265
<i>R</i> <sub>int</sub>	0.016	0.035	0.071
<i>F</i> (000)	656	856	1840
<i>R</i> <sub>1</sub> [ <i>R</i> ( <i>F</i> <sub>2</sub> > 2 $\sigma$ ( <i>F</i> <sub>2</sub> ))]	0.038	0.048	0.051
<i>wR</i> <sub>2</sub> (all data)	0.107	0.133	0.123
GooF	1.06	1.09	0.95
Parameters	199	276	594

[a] Flack parameter –0.1(2).<sup>[25]</sup>

Table 3. Crystallographic details of 4–7.

	4	5	6	7
Formula	C <sub>24</sub> H <sub>39</sub> BN <sub>6</sub> O <sub>4</sub>	C <sub>16</sub> H <sub>28</sub> BN <sub>5</sub> O <sub>4</sub>	C <sub>20</sub> H <sub>36</sub> BN <sub>5</sub> O <sub>4</sub>	C <sub>28</sub> H <sub>52</sub> BN <sub>5</sub> O <sub>4</sub>
Formula weight [g mol <sup>-1</sup> ]	486.42	365.24	421.35	533.56
Color	colorless	colorless	colorless	colorless
Crystal system	monoclinic	monoclinic	monoclinic	monoclinic
Space group	<i>P2<sub>1</sub>/c</i>	<i>P2<sub>1</sub>/n</i>	<i>P2<sub>1</sub>/c</i>	<i>P2<sub>1</sub>/c</i>
<i>a</i> [Å]	17.3769 (9)	9.819 (2)	14.7265 (9)	18.5879 (7)
<i>b</i> [Å]	9.5184 (4)	8.340 (2)	8.7969 (5)	9.4625 (4)
<i>c</i> [Å]	16.9209 (8)	13.154 (3)	18.9127 (10)	18.6960 (7)
<i>α</i> [°]	90	90	90	90
<i>β</i> [°]	92.064 (2)	109.064 (9)	96.376 (2)	95.834 (2)
<i>γ</i> [°]	90	90	90	90
<i>V</i> [Å <sup>3</sup> ]	2796.9 (2)	1018.2 (4)	2434.9 (2)	3271.4 (2)
<i>Z</i>	4	2	4	4
<i>μ</i> [mm <sup>-1</sup> ]	0.08	0.09	0.08	0.07
<i>λ</i> (Mo- <i>K<sub>α</sub></i> ) [Å]	0.71073	0.71073	0.71073	0.71073
<i>T</i> [K]	173(2)	173(2)	173(2)	173(2)
Measured reflections	38933	11216	25828	45069
Independent reflections	10116	2961	6453	8695
Reflections with <i>I</i> > 2σ( <i>I</i> )	7118	2072	4142	6153
<i>R</i> <sub>int</sub>	0.032	0.039	0.071	0.034
<i>F</i> (000)	1048	392	912	1168
<i>R</i> <sub>1</sub> [ <i>R</i> [ <i>F</i> <sub>2</sub> > 2σ( <i>F</i> <sub>2</sub> )]]	0.048	0.044	0.048	0.046
<i>wR</i> <sub>2</sub> (all data)	0.148	0.113	0.137	0.141
Goof	1.10	1.03	1.05	1.09
Parameters	331	131	356	385

 Table 4. Selected bond lengths [Å] and angles [°] of the [B(O–C<sub>2</sub>H<sub>4</sub>–CN)<sub>4</sub>]<sup>-</sup> ion in 2–7.

	2	3	4	5	6	7
B–O	1.459(2)	1.473(2)	1.464(1)	1.475(1)	1.468(2)	1.475(1)
	1.465(2)	1.468(2)	1.465(1)	1.475(1)	1.466(2)	1.472(1)
	1.465(2)	1.467(2)	1.465(1)	1.476(1)	1.476(2)	1.472(1)
	1.476(2)	1.467(2)	1.472(1)	1.476(1)	1.467(2)	1.467(1)
C–N	1.142(2)	1.156(3)	1.134(2)	1.147(2)	1.120(5)	1.159(5)
	1.139(2)	1.133(2)	1.139(2)	1.143(2)	1.136(2)	1.139(2)
	1.137(2)	1.143(3)	1.143(2)	1.147(2)	1.146(4)	1.143(2)
	1.139(2)	1.140(2)	1.139(2)	1.143(2)	1.137(2)	1.137(2)
O–B–O	114.0(1)	113.4(1)	113.24(7)	102.96(4)	112.4(1)	112.14(8)
	113.4(1)	113.6(1)	112.93(7)	113.3(1)	111.7(1)	112.86(8)
	102.6(1)	101.3(1)	102.12(7)	112.64(4)	103.96(9)	103.79(7)
C–C–N	178.8(2)	178.8(2)	178.0(1)	178.8(1)	178.6(6)	177.5(6)
	178.7(2)	179.8(2)	178.9(2)	178.8(1)	178.9(2)	178.9(1)
	178.2 (2)	178.5(4)	178.8(1)	177.7(1)	168.9(5)	179.0(2)
	177.9(2)	178.7(2)	178.2(1)	177.7(1)	179.4(2)	179.4(1)

B1–O1 99.51(7), O3–B1–O4 101.46(7)°] and four larger angles [O3–B1–O1 114.05(9), O4–B1–O1 113.80(9), O3–B1–O2 113.90(9), O4–B1–O2 114.80(9)°]. The achiral (isolated) borate anion becomes chiral in the sodium salt (**1**), and the boron atom becomes the stereogenic center upon metal coordination. The BO<sub>4</sub> tetrahedron displays a bent structure (C–O–B angles 114–120°). Each BO<sub>4</sub> tetrahedron links two Na<sup>+</sup> ions to form zigzag chains with B1⋯Na⋯B1' angles of 140.4° and Na1⋯B⋯Na1' angles of 108.4°. As one of the four nitrile groups is also involved in coordination, these zigzag chains are interconnected to form a highly complex 3D network with polar packing along the (polar) *b* axis (Figure 3). Interestingly, three nitrile groups are not

involved in the coordination and might be used as coordinating sites in follow-up chemistry.

#### *M*[B(O–C<sub>2</sub>H<sub>4</sub>–CN)<sub>4</sub>] (*M* = EMIm, BMIm, OMIm, Me<sub>4</sub>N, Et<sub>4</sub>N, Bu<sub>4</sub>N; 2–7)

Compounds **2–7** crystallize in the space group *P2<sub>1</sub>/n* (**2** and **5**) or *P2<sub>1</sub>/c* (**3**, **4**, **6**, and **7**) as colorless crystals. There are no significant cation⋯anion contacts in the solid-state structures of **2–7**. Therefore, the molecular structural data of the [B(O–C<sub>2</sub>H<sub>4</sub>–CN)<sub>4</sub>]<sup>-</sup> ions are quite similar as shown in Table 2. The molecular structure of one example of M[B(O–C<sub>2</sub>H<sub>4</sub>–CN)<sub>4</sub>] (*M* = EMIm) is depicted in Figure 4.



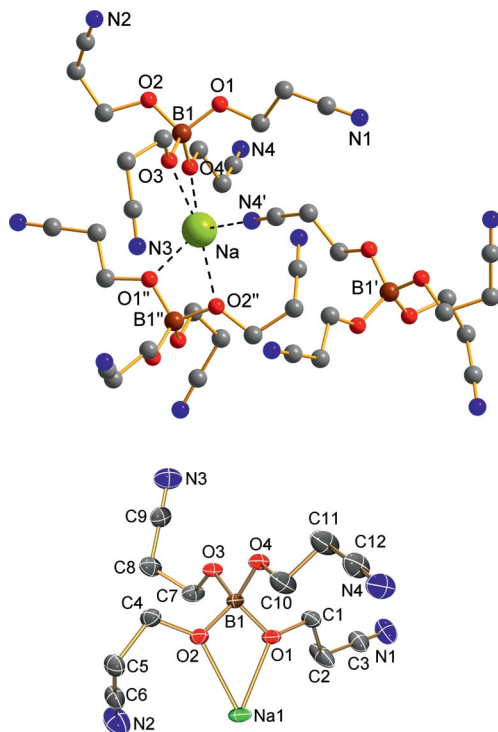


Figure 1. Top: Ball-and-stick drawing of the local environment of the Na centers in **1**. Bottom: ORTEP representation of the asymmetric unit. Thermal ellipsoids with 50% probability at 173 K. Hydrogen atoms omitted for clarity. Selected bond lengths [Å] and angles [°]: Na1–O1 2.3013(9), Na1–O2 2.4005(8), Na1–O3' 2.3418(8), Na1–O4' 2.5459(9), Na1–N4'' 2.509(1), Na1...N3 3.264(2); O1–Na1–O2 57.03(3), O3'–Na1–O4' 55.10(3), O1–Na1–N4'' 141.27(4), O2–Na1–N4'' 94.93(4), O3'–Na1–N4'' 89.15(4), N4''–Na1–O4' 119.54(4). Symmetry codes: (')  $-x + 1, y - 1/2, -z + 1/2$ ; (')'  $x + 1/2, -y + 3/2, -z$ ; (')''  $-x + 1, y + 1/2, -z + 1/2$ ; (iv)  $x - 1/2, -y + 3/2, -z$ .

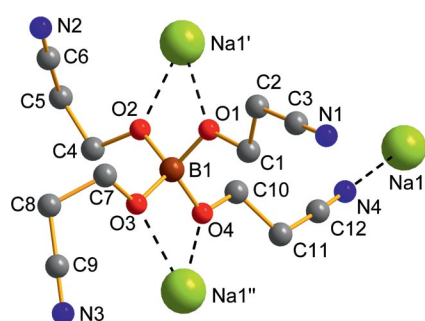


Figure 2. Ball-and-stick drawing of the local environment about the anion centers in **1** (hydrogen atoms omitted for clarity). Selected bond lengths [Å] and angles [°]: B1–O1 1.472(1), B1–O2 1.471(1), B1–O3 1.462(1), B1–O4 1.467(1); O2–B1–O1 99.51(7), O3–B1–O1 114.05(9), O4–B1–O1 113.80(9), O3–B1–O2 113.90(9), O4–B1–O2 114.80(9), O3–B1–O4 101.46(7).

Without any coordination to the cation, the B atom of the anion is distorted and is tetrahedrally coordinated with two larger and one smaller O–B–O angles (Table 2). The average B–O bond lengths are 1.470 Å. The CN group is almost linearly bound to the ethylene unit (average  $\langle \text{CCN} \rangle$  178.2°) and has an average CN bond length of 1.141 Å.

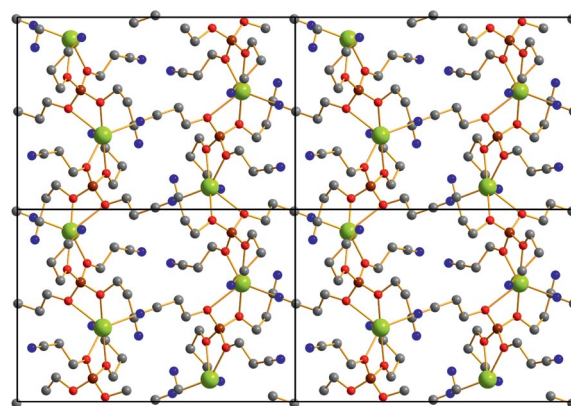


Figure 3. Top: Unit cell of **1** with a view along the *a* axis. Bottom: View along (*a* + *c*) axis displaying helical chains along the *b* axis, which illustrates the polar packing along the *b* axis (BO<sub>4</sub> unit shown as tetrahedron, C atoms as wire model, intermolecular Na<sup>+</sup>...NC interactions are shown in light blue).

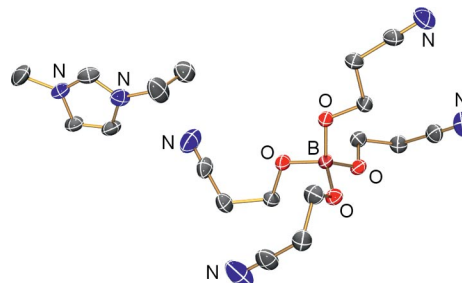


Figure 4. ORTEP drawing of the molecular crystal structure of **2**. Thermal ellipsoids with 50% probability at 173 K.

## Thermodynamics

The principles of volume-based thermodynamics (VBT), introduced by Jenkins, Glasser and Passmore, have been utilized to estimate the lattice potential energy ( $U_{\text{POT}}$ ), lattice enthalpy ( $\Delta H_L$ ), and the standard entropy ( $S_{298}^\circ$  in  $\text{J mol}^{-1} \text{K}^{-1}$  at 298.15 K and 101 kPa) of the new  $\text{M}^+\text{X}^-$  salts ( $\text{M} = \text{Na}, \text{EMIm}, \text{BMIm}, \text{OMIm}, \text{Me}_4\text{N}, \text{Et}_4\text{N}, \text{Bu}_4\text{N}$ ) from their molecular volume (Table 5).<sup>[26,27]</sup> To gain insight into the influence of the anion, we have also studied differently substituted cyano borate salts derived from  $\{\text{B}[\text{O}(\text{CH}_2)_n\text{CN}]_4\}^-$  ( $n = 0, 1, 2, 3$ ), and the data for  $[\text{B}(\text{CN})_4]^-$  is included for comparison.<sup>[28]</sup> The ion volumes were calculated from the average atomic volumes by summing the vol-

Table 5. Ionic volumes of cyano-substituted borate anions and thermodynamic data derived from VBT<sup>[a]</sup> for the sodium salts [ $V(\text{Na}^+) = 27.7 \text{ \AA}^3$ ].

	$[\text{B}(\text{CN})_4]^-$	$[\text{B}(\text{OCN})_4]^-$	$[\text{B}(\text{OCH}_2\text{CN})_4]^-$	$[\text{B}(\text{OC}_2\text{H}_4\text{CN})_4]^-$	$[\text{B}(\text{OC}_3\text{H}_6\text{CN})_4]^-$
$V_{\text{anion}} [\text{\AA}^3]$	136.7	179.8	270.7	361.6	452.6
$U_{\text{pot}} [\text{kJ mol}^{-1}]$	540.8	506.4	458.7	427.8	405.4
$S_{298}^\circ [\text{J K}^{-1} \text{mol}^{-1}]$	225.4	284.0	407.7	531.4	655.0
$\Delta H_{\text{L}} [\text{kJ mol}^{-1}]$	543.6	509.5	462.2	431.5	409.3

$$[\text{a}] U_{\text{POT}} = 2 \left( \frac{117.3}{\sqrt[3]{V_m}} + 51.9 \text{ kJ mol}^{-1} \right), \quad S_{298}^\circ = 1360V_m + 15 \text{ J K}^{-1} \text{mol}^{-1}$$

Corrected Hofmann's volumina are used<sup>[30]</sup>

ume contributions from each atom in the molecular formula as described by Hofmann (Table 5).<sup>[29]</sup> Krossing et al. found that  $V_{\text{Hofmann}}$  correlates linearly with the experimental cation volumes according to  $V_{\text{exp}} = 0.964V_{\text{Hofmann}} - 7 \text{ \AA}^3$  and for the anion according to  $V_{\text{exp}} = 0.946V_{\text{Hofmann}} + 27 \text{ \AA}^3$ .<sup>[30]</sup> The Hofmann approach is not always the best method for the estimation of volumes. For instance, the anion and cation volumes are equal as no charge considerations are made. The isomegetic rule of Jenkins and Liebman can be referred to as the theoretical basis of the Hofmann approach. The isomegetic rule offers another approach to the calculation of ion volumes.<sup>[27]</sup>

#### Anion Size and Lattice Enthalpies

As expected, the anion volumes increase along the series  $[\text{B}(\text{CN})_4]^-$  (116) <  $[\text{B}(\text{OCN})_4]^-$  (161) <  $[\text{B}(\text{O}-\text{CH}_2-\text{CN})_4]^-$  (258) <  $[\text{B}(\text{O}-\text{C}_2\text{H}_4-\text{CN})_4]^-$  (354) <  $[\text{B}(\text{O}-\text{C}_3\text{H}_6-\text{CN})_4]^-$  (450  $\text{\AA}^3$ ). Each methylene group contributes to the ion volume by about 90  $\text{\AA}^3$ . Only  $[\text{B}(\text{CN})_4]^-$  and now  $[\text{B}(\text{O}-\text{C}_2\text{H}_4-\text{CN})_4]^-$  are experimentally known. For  $\text{Na}[\text{B}(\text{O}-\text{CH}_2-\text{CN})_4]$ , the anion volume can be derived from the X-ray crystallography data. With a cell volume of 1567.19(9)  $\text{\AA}^3$ ,  $Z = 4$  and  $V(\text{Na}^+) = 18.1 \text{ \AA}^3$ ,<sup>[30]</sup> an anion volume  $V\{[\text{B}(\text{O}-$

$\text{CH}_2-\text{CN})_4]\} = 373.7 \text{ \AA}^3$  is calculated, in reasonable accord with the volume derived by the Hofmann approach (361.6  $\text{\AA}^3$ , Table 5). As expected the largest lattice potential energy of 540.8  $\text{kJ mol}^{-1}$  was found for  $[\text{B}(\text{CN})_4]^-$ , followed by 506.4 for  $[\text{B}(\text{OCN})_4]^-$ , 458.7 for  $[\text{B}(\text{O}-\text{CH}_2-\text{CN})_4]^-$ , and 427.8  $\text{kJ mol}^{-1}$  for  $[\text{B}(\text{O}-\text{C}_2\text{H}_4-\text{CN})_4]^-$ . As  $n$  in  $\{[\text{B}(\text{O}-\text{CH}_2)_n-\text{CN})_4]\}^-$  increases, the lattice enthalpy decreases. Although  $[\text{B}(\text{CN})_4]^-$  is much smaller and rather rigid it is considerably robust, whereas the large  $[\text{B}(\text{O}-\text{C}_2\text{H}_4-\text{CN})_4]^-$  anion (Figure 5) is less robust, for example, with respect to water, but is highly flexible, and, thus, allows unusual coordination modes. Moreover, a much better solubility in organic solvents is found for salts bearing the  $[\text{B}(\text{O}-\text{C}_2\text{H}_4-\text{CN})_4]^-$  ion compared to  $[\text{B}(\text{CN})_4]^-$  salts in accord with the smaller lattice energies.

#### Cation Size and Lattice Enthalpies

Let us compare the influence of the cation in salts of the type  $\text{M}^+\text{X}^-$  [ $\text{M} = \text{EMIm}$  (2),  $\text{BMIm}$  (3),  $\text{OMIm}$  (4),  $\text{Me}_4\text{N}$  (5),  $\text{Et}_4\text{N}$  (6), and  $\text{Bu}_4\text{N}$  (7), see Table 6]. The cation volume increases along the imidazolium salt series  $\text{EMIm}$  (149.9) <  $\text{BMIm}$  (196.2) <  $\text{OMIm}$  (288.8  $\text{\AA}^3$ ) and along the ammonium salt series  $\text{Me}_4\text{N}$  (116.6) <  $\text{Et}_4\text{N}$  (209.3) <  $\text{Bu}_4\text{N}$  (394.6  $\text{\AA}^3$ ). Compared to the sodium salt, the lattice (427.3  $\text{kJ mol}^{-1}$ ) potential energy decreases by 32.9 (2), 41.3 (3), and 55.5  $\text{kJ mol}^{-1}$  (4). The calculated values for the ammonium salts show an energy decrease of similar magnitude (5: 26.3, 6: 43.5, and 7: 68.8  $\text{kJ mol}^{-1}$ ).

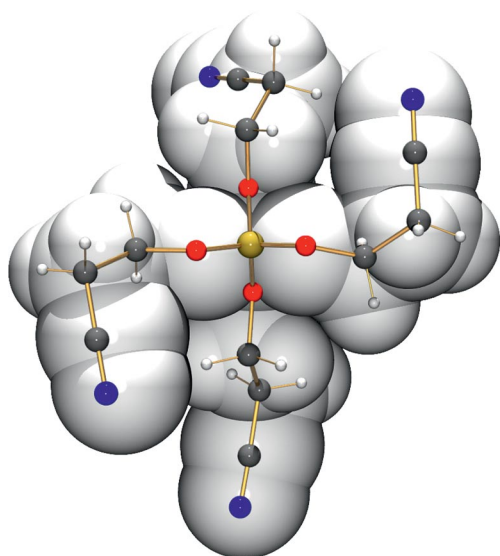


Figure 5. Molecular structure of the  $[\text{B}(\text{O}-\text{C}_2\text{H}_4-\text{CN})_4]^-$  anion in 2 as a superposition of ball-and-stick and space-filling models. Color code: B brown, O red, N blue, C dark grey, H light grey.

Table 6. Cationic volumes of 2–7 and thermodynamic data derived from VBT<sup>[a]</sup>.

	2	3	4	5	6	7
$V_{\text{cat}} [\text{\AA}^3]$	149.8	196.2	288.8	116.6	209.3	394.6
$U_{\text{pot}} [\text{kJ mol}^{-1}]$	397.2	388.8	374.6	403.8	386.6	361.3
$S_{298}^\circ [\text{J K}^{-1} \text{mol}^{-1}]$	710.6	773.6	899.6	665.4	791.4	1043.5
$\Delta H_{\text{L}} [\text{kJ mol}^{-1}]$	401.1	392.8	378.7	407.7	390.6	365.5

$$[\text{a}] U_{\text{POT}} = 2 \left( \frac{117.3}{\sqrt[3]{V_m}} + 51.9 \text{ kJ mol}^{-1} \right),$$

$$S_{298}^\circ = 1360V_m + 15 \text{ J K}^{-1} \text{mol}^{-1}$$

Corrected Hofmann's volumina are used<sup>[30]</sup>

## Conclusions

Crystalline supramolecular networks were obtained by the connection of a 3-hydroxy-propionitrile linker tetrahedrally attached to a boron atom with a monocationic metal center such as Na<sup>+</sup>. Similar results are expected for other metal salts bearing the new [B(O–C<sub>2</sub>H<sub>4</sub>–CN)<sub>4</sub>]<sup>−</sup> ion. An interesting common feature of such coordination polymers is the presence of dative metal–nitrogen bonds as crucial structure-directing elements in addition to the tetrahedral [B(O–C<sub>2</sub>H<sub>4</sub>–CN)<sub>4</sub>]<sup>−</sup> anion. By salt metathesis reactions of Na[B(O–C<sub>2</sub>H<sub>4</sub>–CN)<sub>4</sub>], the exchange of the Na<sup>+</sup> ion by several imidazolium and ammonium M<sup>+</sup> ions was achieved to afford M[B(O–C<sub>2</sub>H<sub>4</sub>–CN)<sub>4</sub>] (M = EMIm, BMIm, OMIm, Me<sub>4</sub>N, Et<sub>4</sub>N, Bu<sub>4</sub>N), which represent ionic liquids with no cation⋯anion interactions in the solid state as shown by single-crystal X-ray studies.

## Experimental Section

**General Information:** All manipulations were carried out under oxygen- and moisture-free conditions under argon by using standard Schlenk or drybox techniques.

Dichloromethane and acetonitrile were heated to reflux over CaH<sub>2</sub>, tetrahydrofuran and Et<sub>2</sub>O were dried with Na/benzophenone and freshly distilled prior to use. 3-Hydroxypropionitrile (ABCR) was distilled in vacuo at 60 °C prior to use. The imidazolium salts (ABCR), ammonium salts (Merck), and NaBH<sub>4</sub> (Merck) were used as received.

**NMR:** <sup>1</sup>H, <sup>11</sup>B, and <sup>13</sup>C spectra were obtained with a Bruker AVANCE 250 (250 MHz) or AVANCE 300 (300 MHz) spectrometer and were referenced externally. CDCl<sub>3</sub> and [D<sub>6</sub>]DMSO were dried with CaH<sub>2</sub>.

**IR:** A Nicolet 380 FTIR spectrometer with a Smart Orbit attenuated total reflectance (ATR) device was used.

**Raman:** A Bruker VERTEX 70 FTIR spectrometer equipped with a RAM II FT-Raman module and a Nd:YAG laser (1064 nm) or a Kaiser Optical Systems RXN1–785 nm was used.

**CHN analyses:** An Analysator Flash EA 1112 instrument from Thermo Quest or a C/H/N/S-Mikronalytator TruSpec-932 instrument from Leco was used.

**DSC:** A DSC 823e calorimeter from Mettler–Toledo (heating rate 5 °C/min) was used. A sample of ca. 3–5 mg was placed in an aluminum crucible. The closed crucible was placed in the furnace. The closed furnace was flushed with nitrogen and the sample was measured at a heating rate of 5 °C per minute. The heat flow was calculated based on a two point calibration (melting points of In and Zn) by using the Mettler–Toledo STARe Software.

**TGA Measurements:** TGA was done with a Setaram LapSys 1600 TGA–DSC instrument under an argon atmosphere (heating rate 5 °C/min).

**X-ray Structure Determination:** X-ray quality crystals were selected in Fomblin YR-1800 perfluoroether (Alfa Aesar) at ambient temperatures. The samples were cooled to 173(2) K during measurement. The data were collected with a Bruker Apex Kappa-II CCD diffractometer with graphite-monochromated Mo–K<sub>α</sub> radiation (λ = 0.71073 Å). The structures were solved by direct methods (SHELXS-97) and refined by full-matrix least-squares procedures

(SHELXL-97). Semi-empirical absorption corrections were applied (SADABS). All non-hydrogen atoms were refined anisotropically, and hydrogen atoms were included in the refinement at calculated positions by using a riding model.

The position of an ethyl group in the imidazolium cation in **2** was found to be disordered and was split in two parts. The occupancy of each part was refined freely [C16/C17: 0.659(8)/0.341(8)].

The position of a butyl group in the imidazolium cation in **3** was found to be disordered and was split in two parts. The occupancy of each part was refined freely [C36/C37/C38/C39: 0.991(3)/0.089(3)]. The positions of two propionitrile groups in the borate anions in **3** were found to be disordered and were split in two parts. The occupancy of each part was refined freely [C8/C9/N3: 0.868(8)/0.132(8), C22/C23/C24: 0.845(3)/0.155(3)].

The position of a propionitrile group in the borate anion in **4** was found to be disordered and was split in two parts. The occupancy of each part was refined freely [C1/C2/C3/N1: 0.924(2)/0.076(2)].

The position of a methyl group in the ammonium cation in **5** was found to be disordered and was split in two parts. The occupancy of each part was refined freely (C7: 0.5/0.5).

The positions of all four ethyl groups in the ammonium cation in **6** were found to be disordered and were split in two parts. The occupancy of each part was refined freely [C13/C14/C15/C16/C17/C18/C19/C20: 0.934(1)/0.066(1)]. The positions of two propionitrile groups in the borate anion in **6** were found to be disordered and were split in two parts. The occupancy of each part was refined freely [C2/C3/N1: 0.501(3)/0.499(3), C8/C9/N3: 0.523(3)/0.477(3)].

The positions of two propionitrile groups in the borate anion in **7** were found to be disordered and were split in two parts. The occupancy of each part was refined freely [C1/C2/C3: 0.661(3)/0.339(3), C7/C8/C9: 0.904(2)/0.096(2)].

**Synthesis of Na[B(O–C<sub>2</sub>H<sub>4</sub>–CN)<sub>4</sub>] (**1**):** To a stirred suspension of NaBH<sub>4</sub> (0.711 g, 18.8 mmol, 1 equiv.) in THF (40 mL), a mixture of HO–C<sub>2</sub>H<sub>4</sub>–CN (6.748 g, 94.8 mmol, 5 equiv.) in THF (10 mL) was added dropwise. The resulting suspension was heated to reflux with an oil bath (95 °C) for 6 h until hydrogen formation faded. The precipitate was collected by filtration and washed with CH<sub>2</sub>Cl<sub>2</sub> (3 × 10 mL). The crude product was dried in vacuo for 2 h at 90 °C. The product was purified for analytical experiments by extraction with CH<sub>3</sub>CN, yield 3.4 g (58%).

**General Procedure for the Synthesis of Imidazolium and Ammonium Salts:** A Schlenk-flask was loaded with Na[B(O–C<sub>2</sub>H<sub>4</sub>–CN)<sub>4</sub>] (6.6 mmol, 1.1 equiv.) suspended in CH<sub>3</sub>CN (15 mL). The imidazolium or ammonium chloride (6 mmol, 1 equiv.) was dissolved in CH<sub>3</sub>CN (10 mL) and added to this suspension. The mixture was heated to reflux for 3 h, the precipitated NaCl and excess Na[B(O–C<sub>2</sub>H<sub>4</sub>–CN)<sub>4</sub>] were removed by filtration, and the solvent was removed in vacuo. The crude products were dissolved in CH<sub>2</sub>Cl<sub>2</sub>, filtered, and the solvent of the filtrate was evaporated in vacuo. The products were dried in vacuo for 3 h at 60 °C, yields 86–92%.

**Supporting Information** (see footnote on the first page of this article): Analytical details for all compounds.

## Acknowledgments

Financial support by the Deutsche Forschungsgemeinschaft (DFG) is gratefully acknowledged. We are indebted to Martin Ruhmann (University Rostock) and Johannes Thomas (University Rostock) for the measurement of Raman spectra. The authors thank one reviewer of this article for most valuable comments.



- [1] J. S. Wilkes, *Green Chem.* **2002**, *4*, 73.
- [2] X. Li, D. Zhao, Z. Fei, L. Wang, *Sci. China Ser. B* **2006**, *49*, 385.
- [3] a) V. N. Emel'yanenko, S. P. Verevkin, A. Heintz, R. J. Fouston, A. Deyko, P. Licence, R. G. Jones, K. Voß, A. Schulz, *J. Phys. Chem. B* **2009**, *113*, 9871; b) A. Schulz, H. Brand, A. Villinger, *Chem. Asian J.* **2009**, *4*, 1588.
- [4] a) J.-C. Xiao, J. M. Shreeve, *J. Org. Chem.* **2005**, *70*, 3072; b) D. Zhao, Z. Fei, T. J. Geldbach, R. Scopelliti, P. J. Dyson, *J. Am. Chem. Soc.* **2004**, *126*, 15876; c) T. J. Geldbach, P. J. Dyson, *J. Am. Chem. Soc.* **2004**, *126*, 8114; d) K. Sasaki, S. Matsumura, K. J. Toshima, *Tetrahedron Lett.* **2004**, *45*, 7043.
- [5] D. Zhao, Z. Fei, R. Scopelliti, P. J. Dyson, *Inorg. Chem.* **2004**, *43*, 2197.
- [6] K. Chellappan Lethesh, K. Van Hecke, L. Van Meervelt, P. Nockemann, B. Kirchner, S. Zahn, T. N. Parac-Vogt, W. Dehaen, K. Binnemans, *J. Phys. Chem. B* **2011**, *115*, 8424.
- [7] a) Y. Yoshida, M. Kondo, G. Saito, *J. Phys. Chem. B* **2009**, *113*, 8960; b) D. Zhao, Z. Fei, C. A. Ohlin, G. Laurency, P. J. Dyson, *Chem. Commun.* **2004**, 2500.
- [8] M. Karsch, H. Lund, A. Schulz, A. Villinger, K. Voss, *Eur. J. Inorg. Chem.* **2012**, 5542.
- [9] M. Becker, J. Harloff, T. Jantz, A. Schulz, A. Villinger, *Eur. J. Inorg. Chem.* **2012**, 5658.
- [10] I. Alkorta, O. Picazo, J. Elguero, *Tetrahedron: Asymmetry* **2005**, *16*, 755.
- [11] M. T. Mock, R. G. Potter, D. M. Camaioni, J. Li, W. G. Dougherty, W. S. Kassel, B. Twamley, D. L. DuBois, *J. Am. Chem. Soc.* **2009**, *131*, 14454.
- [12] a) M. M. Aminia, M. Sharbatdaran, M. Mirzaee, P. Mirzaei, *Polyhedron* **2006**, *25*, 3231; b) S. Herfánek, O. Kříž, J. Fusek, Z. Černý, B. Čáslavský, *J. Chem. Soc. Perkin Trans. 2* **1989**, 987; c) R.-M. Ho, T.-C. Wang, C.-C. Lin, T.-L. Yu, *Macromolecules* **2007**, *40*, 2814; d) D. S. McGuinness, A. J. Rucklidge, R. P. Tooze, A. M. Slawin, *Z. Organometallics* **2007**, *26*, 2561; e) K. Tabatabaieian, M. Mamaghani, A. Pourahamad, *Russ. J. Org. Chem.* **2001**, *37*, 1287; f) S. Gou, J. Wang, X. Liu, W. Wang, F.-X. Chen, X. Feng, *Adv. Synth. Catal.* **2007**, *349*, 343; g) E. Keller, N. Veldman, A. L. Spek, B. L. Feringa, *Tetrahedron: Asymmetry* **1997**, *8*, 3403.
- [13] N. Malek, T. Maris, M. Simard, J. D. Wuest, *J. Am. Chem. Soc.* **2005**, *127*, 5910.
- [14] E. Bernhardt, G. Henkel, H. Willner, *Z. Anorg. Allg. Chem.* **2000**, *626*, 560.
- [15] a) Y. Y. Karabach, M. Fatima, C. Guedes da Silva, M. N. Kopylovich, B. Gil-Hernández, J. Sanchiz, A. M. Kirillov, A. J. L. Pombeiro, *Inorg. Chem.* **2010**, *49*, 11096; b) H. Dan, S. Nishikiori, O. Yamamuro, *Dalton Trans.* **2011**, *40*, 1168; c) P. K. Thallapally, R. Kishan Motkuri, C. A. Fernandez, B. P. McGrail, G. S. Behrooz, *Inorg. Chem.* **2010**, *49*, 4909; d) B. F. Hoskins, R. Robson, *J. Am. Chem. Soc.* **1990**, *112*, 1546.
- [16] a) S. R. Batten, B. F. Hoskins, R. Robson, *New J. Chem.* **1998**, *22*, 173; b) B. F. Abrahams, S. R. Batten, B. F. Hoskins, R. Robson, *Inorg. Chem.* **2003**, *42*, 2654.
- [17] a) F.-Q. Liu, T. D. Tilley, *Inorg. Chem.* **1997**, *36*, 5090; b) F.-Q. Liu, T. D. Tilley, *Chem. Commun.* **1998**, 103.
- [18] a) F. Fakra Jr., R. T. Iwamoto, *Inorg. Chem.* **1965**, *4*, 844; b) D. T. Cromer, A. C. Larson, *Acta Crystallogr., Sect. B* **1972**, *28*, 1052; c) L. Carlucci, G. Ciani, D. W. v. Gudenberg, D. M. Proserpio, *New J. Chem.* **1999**, *23*, 397.
- [19] Reviews: a) I. Krossing, I. Raabe, *Angew. Chem.* **2004**, *116*, 2116; *Angew. Chem. Int. Ed.* **2004**, *43*, 2066; b) C. Reed, *Acc. Chem. Res.* **1998**, *31*, 133; c) S. H. Strauss, *Chem. Rev.* **1993**, *93*, 927 and references cited therein.
- [20] P. Wasserscheid, T. Welton, *Ionic Liquids in Synthesis*, Wiley-VCH, Weinheim, Germany, **2003**.
- [21] a) B. Gil-Hernández, J. K. Maclaren, H. A. Höpfe, J. Pasán, J. Sanchiz, C. Janiak, *CrystEngComm* **2012**, *14*, 2635; B. Gil-Hernández, H. A. Höpfe, J. K. Vieth, J. Sanchiz, C. Janiak, *Chem. Commun.* **2010**, *46*, 8270; b) A. Chamayou, M. A. Neelakantan, S. Thalamuthu, C. Janiak, *Inorg. Chim. Acta* **2011**, *365*, 447; c) C. Janiak, A.-C. Chamayou, A. K. M. R. Uddin, M. Uddin, K. S. Hagen, M. Enamullah, *Dalton Trans.* **2009**, 3698; d) M. Enamullah, A. Sharmin, M. Hasegawa, T. Hoshi, A.-C. Chamayou, C. Janiak, *Eur. J. Inorg. Chem.* **2006**, 2146.
- [22] P. Pykkö, M. Atsumi, *Chem. Eur. J.* **2009**, *15*, 12770.
- [23] M. Mantina, A. C. Chamberlin, R. Valero, C. J. Cramer, D. G. Truhlar, *J. Phys. Chem. A* **2009**, *113*, 5806.
- [24] a) B. F. Straub, M. Wrede, K. Schmid, F. Rominger, *Eur. J. Inorg. Chem.* **2010**, 1907; b) M. L. Cole, D. E. Hibbs, C. Jones, P. C. Junk, N. A. Smithies, *Inorg. Chim. Acta* **2005**, *358*, 102; c) D. M. Seo, P. D. Boyle, W. A. Henderson, *Acta Crystallogr., Sect. E* **2011**, *67*, m1148; d) H. Wang, H. Li, B. Xue, Z. Wang, Q. Meng, L. Chen, *J. Am. Chem. Soc.* **2005**, *127*, 6394.
- [25] a) H. D. Flack, M. Sadki, A. L. Thompson, D. J. Watkin, *Acta Crystallogr., Sect. A* **2011**, *67*, 21; b) H. D. Flack, G. Bernardinelli, *Chirality* **2008**, *20*, 681; c) H. D. Flack, G. Bernardinelli, *Acta Crystallogr., Sect. A* **1999**, *55*, 908.
- [26] a) V. M. Goldschmidt, *Ber. Dtsch. Chem. Ges.* **1927**, *60*, 1263; b) R. D. Shannon, *Acta Crystallogr., Sect. A* **1976**, *32*, 751; c) L. Glasser, H. D. B. Jenkins, *Inorg. Chem.* **2008**, *47*, 6195.
- [27] a) H. D. B. Jenkins, L. Glasser, T. M. Klapötke, M.-J. Crawford, K. K. Bhasin, J. Lee, G. J. Schrobilgen, L. S. Sunderlin, J. F. Liebman, *Inorg. Chem.* **2004**, *43*, 6238; b) H. D. Jenkins, J. F. Liebman, *Inorg. Chem.* **2005**, *44*, 6359.
- [28] A. Bernsdorf, H. Brand, R. Hellmann, M. Köckerling, A. Schulz, A. Villinger, K. Voss, *J. Am. Chem. Soc.* **2009**, *131*, 8958.
- [29] D. W. M. Hofmann, *Acta Crystallogr., Sect. B* **2002**, *58*, 489.
- [30] U. Preiss, J. M. Slattery, I. Krossing, *Ind. Eng. Chem. Res.* **2009**, *48*, 2290.

Received: February 18, 2013  
Published Online: June 21, 2013



### 5.3 Nitrile-rich Borate Anions - Application in Ionic Liquids

Jörg Harloff, Markus Karsch, Axel Schulz, Alexander Villinger.

*Eur. J. Inorg. Chem.* **2013**, angenommen.

In dieser Publikation wurden sämtliche experimentellen Arbeiten von mir durchgeführt. Die in der Arbeit erstmalig publizierten Verbindungen wurden von mir synthetisiert und vollständig charakterisiert. Sämtliche Verbindungen, von denen im Manuskript die Kristallstruktur beschrieben ist, wurden von mir für die Röntgenstrukturanalytik kristallisiert.

Das vorliegende Manuskript zur Publikation wurde von mir als Erstautor verfasst. Zudem wurde von mir ein Supporting verfasst, das sämtliche Darstellungen der Verbindungen und die analytischen Daten beinhaltet. Der eigene Anteil liegt bei ca. 85 %.

## Nitrile-rich Borate Anions – Application in Ionic Liquids

Jörg Harloff,<sup>[a]</sup> Markus Karsch,<sup>[a]</sup> Axel Schulz,<sup>[a,b]\*</sup> Alexander Villinger<sup>[a]</sup>

**Abstract.** The novel cyano-rich borate anion  $[\text{B}(\text{tceg})_2]^-$  (tceg = tetracyanoethylene glycolate) has been synthesized in a two step reaction from  $\text{Na}[\text{B}(\text{OMe})_4]$  with two equivalents of the cyanohydrin analogue  $\text{Me}_3\text{SiO}-\text{C}_2(\text{CN})_4-\text{OSiMe}_3$ . The structures of the starting materials, an isolated intermediate  $\text{Na}_2[\text{B}_2(\text{OMe})_2(\text{tceg})_3]$  and  $\text{Na}[\text{B}(\text{tceg})_2]$  are discussed. Thermal studies of  $\text{WCC}[\text{B}(\text{tceg})_2]$  (WCC = 1-ethyl-3-methylimidazolium (EMIm), 1-butyl-3-methylimidazolium (BMIm), 1-octyl-3-methylimidazolium (OMIm),  $\text{Me}_4\text{N}$ ,  $\text{Et}_4\text{N}$ , and  $\text{Bu}_4\text{N}$ ), synthesized by salt metathesis, showed ionic liquid properties of the compounds with EMIm, BMIm, OMIm and  $\text{Bu}_4\text{N}$ . The synthesis, structure and analytical results of  $\text{Me}_3\text{SiO}-\text{C}(\text{CN})_3$  are discussed as well as the results of its conversion with  $\text{Na}[\text{B}(\text{OMe})_4]$ .

**Keywords:** borates / coordination chemistry / cyanohydrins / cyanidoborates / ionic liquids / structure

[a] Institut für Chemie  
Universität Rostock  
18059 Rostock, A.-Einstein-Str. 3a  
Fax: (+)49-(0)381/498-6381  
E-mail: axel.schulz@uni-rostock.de

[b] Leibniz-Institut für Katalyse e.V.  
18059 Rostock, A.-Einstein-Str. 29a  
Fax: (+)49-(0)381/498-6381

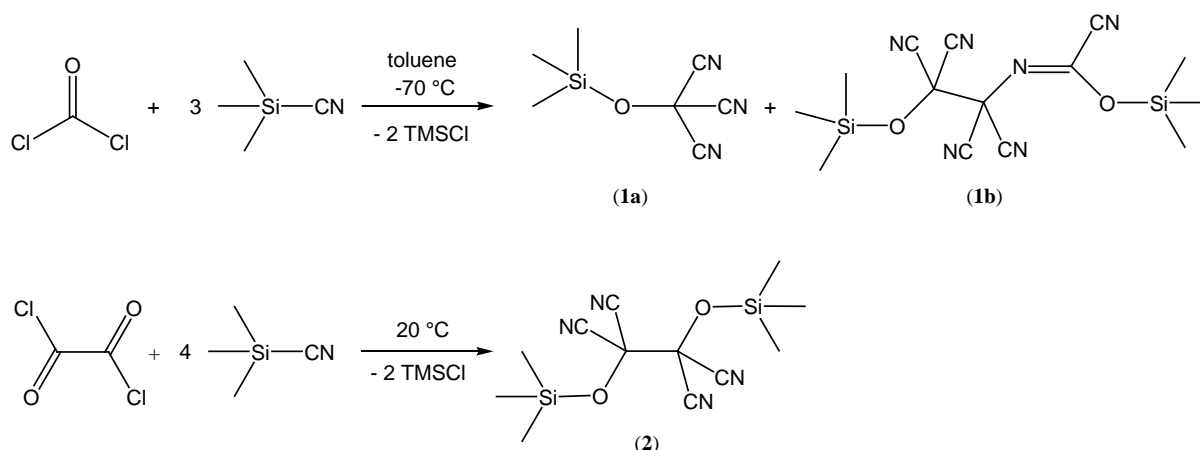
## Introduction

Since the first syntheses of moisture and air stable ionic liquids (ILs) have been reported the interest in new ILs and their applications in diverse fields were promoted.<sup>[1]</sup> In general ILs are suitable as alternative solvents in green chemistry (e.g. cellulose processing),<sup>[2]</sup> liquid thermal storage media,<sup>[3]</sup> catalysis<sup>[4]</sup> and electrolytes in batteries.<sup>[5]</sup> The preparation of “task-specific” ILs by incorporating functionalized groups to ILs led to new facilities in the application as solvents for chemical reactions.<sup>[6]</sup> In particular the characteristics of CN-functionalized ILs are well studied and investigated in many catalytic C–C-coupling reactions, e.g. Heck, Stille, Suzuki and Hiyama reactions.<sup>[7]</sup> Ionic Liquids, that make these types of reactions more effective, contain CN functionalized cations, that stabilize the active catalyst. It was found that CN functionalized pyridinium based ILs (i) generate a more effective catalytic system in the Heck reaction by catalyst immobilization<sup>[7]</sup> or (ii) stabilize reaction intermediates in glycosidation reactions (C–O coupling).<sup>[8]</sup> Apart from cations bearing the nitrile group, which are used to be the common way of CN functionalization as found in CN functionalized imidazolium-, pyridinium-, pyrrolidinium- and piperidinium-cations, there is much less known about ILs containing CN functionalized anions. For the best of our knowledge there is only one application reported for ILs bearing CN modified anions. In material surface science the so called “Armand’s ligand”, an IL containing the CN functionalized anion 4,5-dicyano triazole, can be used as an effective stabilizing agent for the preparation of impurity free and highly dispersed catalysts.<sup>[9]</sup> We have recently studied the synthesis and properties of CN functionalized borate/aluminate based ILs with anions of the type  $[E(O-C_6X_4-CN)_4]^-$  (E = B, Al; X = H, F),<sup>[10]</sup>  $[B(O-C_2H_4-CN)_4]^-$ <sup>[11]</sup> and tetracyanopyrrolides based ILs.<sup>[12]</sup> Tetraphenoxyaluminates and -borates<sup>[13,14]</sup> and also their fluorinated analogues<sup>[15]</sup> have been studied and widely applied *e.g.* in catalysis. However, to the best of our knowledge CN functionalized borates of the type  $[B(\eta^2-O_2C_6(CN)_nH_{4-n})_2]^-$  ( $n = 1, 2, 3, 4$ ) or  $[B\{\eta^2-O_2C_n(CN)_{2n}\}_2]^-$  ( $n = 2, 3, \text{etc.}$ ) with arylic or alkylic chelating ligands are not known yet. The only known cyano-borates are of the type  $[B(C_6H_4-CN)_4]^-$ ,<sup>[16]</sup> and  $[B(CN)_4]^-$ <sup>[17]</sup> or with the mentioned para-cyano-phenoxy ligands. Besides there is a great wealth of compounds based on polycyanometallates,<sup>[18]</sup>  $[C(CN)_3]^-$ <sup>[19]</sup> or  $Si(p-C_6H_4-CN)_4$ .<sup>[20]</sup>

Herein we describe the synthesis, structure and physical properties of salts bearing the novel nitrile-rich  $[B_2(OMe)_2(tceg)_3]^{2-}$  diborate anion,  $[B(tceg)_2]^-$  anion and its starting compound. The synthesis and physical properties of the ionic liquids containing the  $[B(tceg)_2]^-$  anion are discussed.

## Results and Discussion

**Synthesis.** The most common synthetic routes to borates are the treatment of  $\text{NaBH}_4$  with 4 equivalents of the desired alcohol<sup>[10,11]</sup> or the conversion of boronic acid with 3 equivalents of the alcohol and 1 equivalent of the alcoholate.<sup>[21]</sup> For the synthesis of nitrile rich borate anions a modified synthetic route according to the preparation of bis(oxalate)borate was successfully applied.<sup>[22]</sup> This synthetic route allows the application of trimethylsilyl cyanohydrins, which are more stable towards the elimination of  $\text{Me}_3\text{SiCN}$  according to their hydrogen analogues. As starting materials two *O*-(trimethylsilyl)cyanohydrins were synthesized according to literature (Scheme 1).<sup>[23]</sup> For the synthesis of tricyano(trimethylsiloxy)methane,  $\text{Me}_3\text{SiO}-\text{C}(\text{CN})_3$  (**1a**), a phosgene solution in toluene was treated with 3 equivalents of trimethylsilyl cyanide at  $-70^\circ\text{C}$ . After fractional distillation **1a** was obtained in yields up to 64 % as colorless oil. The byproduct  $\text{Me}_3\text{SiO}-\text{C}_2(\text{CN})_4-\text{N}=\text{C}(\text{CN})-\text{OSiMe}_3$  (**1b**), a dimer of **1a**, crystallized from the residual red oil and was analyzed by single crystal X-ray diffraction. 1,1,2,2-tetracyano-1,2-bis(trimethylsiloxy)ethane (**2**) was obtained by solvent free conversion of 4 equivalents of trimethylsilyl cyanide with oxalyl chloride. The precipitated crystals were filtered off, washed with *n*-hexane and sublimated at  $10^{-3}$  mbar and  $60^\circ\text{C}$  affording crystalline  $\text{Me}_3\text{SiO}-\text{C}_2(\text{CN})_4-\text{OSiMe}_3$  in good yields (70-78 %).

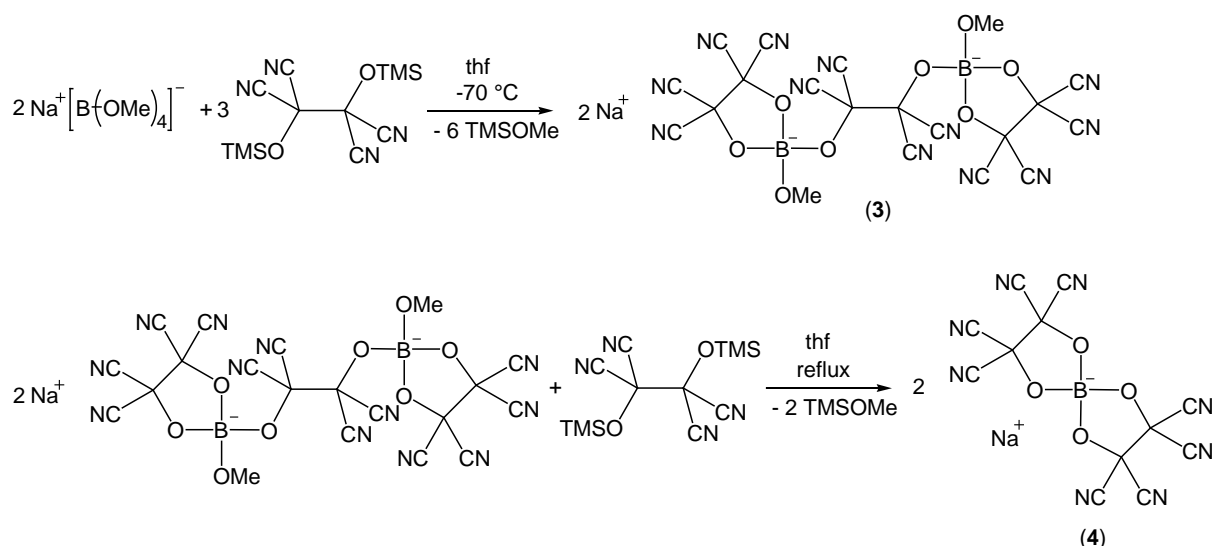


**Scheme 1.** Syntheses of  $\text{Me}_3\text{SiO}-\text{C}(\text{CN})_3$  (**1a**),  $\text{Me}_3\text{SiO}-\text{C}_2(\text{CN})_4-\text{N}=\text{C}(\text{CN})-\text{OSiMe}_3$  (**1b**) and  $\text{Me}_3\text{SiO}-\text{C}_2(\text{CN})_4-\text{OSiMe}_3$  (**2**).

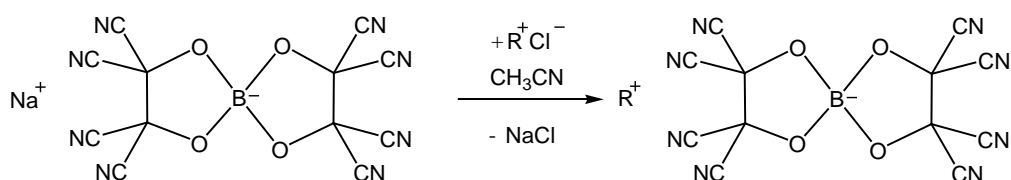
In the reaction of  $\text{Na}[\text{B}(\text{OMe})_4]$  with 4 equivalents of  $\text{Me}_3\text{SiO}-\text{C}(\text{CN})_3$  (**1a**) lead to a mixture of many species, amongst them traces of the desired  $\text{Na}[\text{B}(\text{O}-\text{C}(\text{CN})_3)_4]$ . The reaction was performed at different temperatures ranging from  $-100^\circ\text{C}$  to reflux conditions. Every approach resulted in a complex mixture of different borate species as indicated by  $^{11}\text{B}$  NMR experiments. Three different borates were obtained with  $^{11}\text{B}$  signals at 8.1, 8.7 and 13.4 ppm

after reactions at temperatures between  $-100\text{ }^{\circ}\text{C}$  and  $-70\text{ }^{\circ}\text{C}$  for several hours and slow warm up to room temperature. Reactions at room temperature to reflux conditions turned out in four different borate species with  $^{11}\text{B}$  signals at 0.4, 6.7, 11.5 and 17.3 ppm. A reason for the formation of different borate products could be that  $\text{Me}_3\text{SiO}-\text{C}(\text{CN})_3$  is unstable at elevated temperatures in the presence of the borate. A crystalline solid was obtained that sublimated from the product mixture after drying *in vacuo*. Interestingly, data obtained from X-ray structure analysis, as well as NMR experiments, revealed the formation of  $\text{Me}_3\text{SiO}-\text{C}_2(\text{CN})_4-\text{OSiMe}_3$  (**2**) from two molecules of **1a** after elimination of a CN group per molecule. However, the existence of cyanogen in solution could not be confirmed by  $^{13}\text{C}$  NMR experiments. It should be noted that compound **2** is easily obtained from oxalyl chloride and  $\text{Me}_3\text{SiCN}$  (see above, Scheme 1).

We therefore changed the synthetic procedure applying lower temperatures and  $\text{Me}_3\text{SiO}-\text{C}_2(\text{CN})_4-\text{OSiMe}_3$  instead of  $\text{Me}_3\text{SiO}-\text{C}(\text{CN})_3$ . Thus we were able to synthesize  $\text{Na}[\text{B}(\text{tceg})_2]$  from  $\text{Na}[\text{B}(\text{OMe})_4]$  and **2** in a two step reaction (Scheme 2). In the first reaction step 2.5 equivalents (1 equivalent excess) of **2** were dissolved in thf and added to a solution of  $\text{Na}[\text{B}(\text{OMe})_4]$  in thf at  $-70\text{ }^{\circ}\text{C}$  to avoid the formation of by-products. After stirring for 2 days the  $[\text{B}(\text{OMe})_4]^-$  was fully converted to  $\text{Na}_2[\text{B}_2(\text{OMe})_2(\text{tceg})_3]$  (**3**) bearing a diborate dianion bridged by a tetracyanoethylene glycolate group. After removal of the solvent, washing with  $\text{CH}_2\text{Cl}_2$ , recrystallizing from thf/ $\text{CH}_2\text{Cl}_2$  and drying *in vacuo* at  $120\text{ }^{\circ}\text{C}$  for 2 hours colorless and solvent free **3** was obtained in good yields (87 %). This intermediate **3** was reacted with 2 equivalents (1 equivalent excess) of **2** in thf under refluxing for 18 hours to substitute the residual methyl groups with tetracyanoethylene groups to give  $\text{Na}[\text{B}(\text{tceg})_2]$  (**4**). After removing the solvent *in vacuo* the excess of **2** was removed by washing with  $\text{CH}_2\text{Cl}_2$ . The raw product was crystallized from thf/ $\text{Et}_2\text{O}$  and dried *in vacuo* at  $120\text{ }^{\circ}\text{C}$  for 2 hours resulting in colorless and solvent free **4** with yields up to 73 %.



**Scheme 2.** Synthesis of  $\text{Na}_2[\text{B}_2(\text{OMe})_2(\text{tceg})_3]$  (**3**) and  $\text{Na}[\text{B}(\text{tceg})_2]$  (**4**).



(R = EMIm (**5**), BMIm (**6**), OMIm (**7**),  $\text{Me}_4\text{N}$  (**8**),  $\text{Et}_4\text{N}$  (**9**),  $\text{Bu}_4\text{N}$  (**10**))

**Scheme 3.** Synthesis of imidazolium and ammonium salts bearing  $[\text{B}(\text{tceg})_2]^-$  anion.

Starting from  $\text{Na}[\text{B}(\text{tceg})_2]$  the exchange of  $\text{Na}^+$  by several imidazolium and ammonium ions was achieved by salt metathesis reaction affording  $\text{WCC}[\text{B}(\text{tceg})_2]$  (WCC = 1-ethyl-3-methylimidazolium (EMIm, **5**), 1-butyl-3-methylimidazolium (BMIm, **6**), 1-octyl-3-methylimidazolium (OMIm, **7**),  $\text{Me}_4\text{N}$  (**8**),  $\text{Et}_4\text{N}$  (**9**), and  $\text{Bu}_4\text{N}$  (**10**) in yields between 88-93% (Scheme 3). The best result for the metathesis reaction was obtained by dissolving  $\text{Na}[\text{B}(\text{tceg})_2]$  (1.1 equiv.) and the imidazolium or ammonium chlorides (1 equiv.) in  $\text{CH}_3\text{CN}$  and stirring at room temperature over night. In the case of  $[\text{Me}_4\text{N}]\text{Cl}$ , which was suspended in  $\text{CH}_3\text{CN}$ , the borate in  $\text{CH}_3\text{CN}$  was added to the ammonium salt and the suspension was heated to reflux for 3 h. The resulting suspension of  $\text{NaCl}$  in  $\text{CH}_3\text{CN}$  was filtered and the solvent was removed *in vacuo*. The excess of  $\text{Na}[\text{B}(\text{tceg})_2]$  was removed by dissolving the product in 5 ml  $\text{CH}_2\text{Cl}_2$  and filtering off the sodium borate. After evaporation of the solvents *in vacuo* the products were dried *in vacuo* for 2 h at  $80^\circ\text{C}$ .

**Properties.** The starting materials **1a** and **2** are soluble in almost every organic solvent while the solubility decreases with the polarity of the solvent. Compound **2** is less soluble in cold *n*-hexane and can be recrystallized from a hot solution in *n*-hexane. While **1a** is a colorless liquid with a melting point at  $-14.5\text{ }^{\circ}\text{C}$ , compound **2** is a colorless crystalline solid with a melting point at  $122.1\text{ }^{\circ}\text{C}$ . Sodium salts **3** and **4** are almost insoluble in  $\text{Et}_2\text{O}$ ,  $\text{CH}_2\text{Cl}_2$  and aromatic solvents such as benzene or toluene but they show a very good solubility in thf,  $\text{CH}_3\text{CN}$  and DMSO. Compounds **3** and **4**, as well as the starting materials  $\text{Na}[\text{B}(\text{OMe})_4]$  and **2**, can be prepared in bulk and are hygroscopic. They precipitate often as solvates, which, however, can easily be removed by prolonged thermal treatment *in vacuo*. Diborate **3** and all mentioned salts bearing the  $[\text{B}(\text{tceg})_2]^-$  anion decompose slowly in water under formation of HCN within two days. As shown by  $^{11}\text{B}$  NMR studies, slow hydrolysis of **3** affords  $\text{B}_2\text{O}_3 \cdot n\text{H}_2\text{O}$ , while the decomposition of borate **4** in water gives three different unidentified boron containing decomposition products. Data of DSC measurements of the solvent free sodium compounds revealed that the thermal stability of **4** ( $T_{\text{Dec}} = 305\text{ }^{\circ}\text{C}$ ) is higher than that of diborate **3** ( $T_{\text{Dec}} = 209\text{ }^{\circ}\text{C}$ ). Data of TGA/DSC measurements of the solvated crystalline sodium compounds show a decrease of the decomposition points up to  $35\text{ }^{\circ}\text{C}$  (Table 1).

**Table 1.** Thermal analysis: Desolvation and decomposition points from TGA/DSC measurements of **3·8thf** and **4·0.85thf·0.15Et<sub>2</sub>O**. Onset and peak temperatures determined from the derivative curve from the TG data.

Compound	Explanation	Mass loss (%)	TGA		DSC	
			Onset ( $^{\circ}\text{C}$ )	Peak ( $^{\circ}\text{C}$ )	Onset ( $^{\circ}\text{C}$ )	Peak ( $^{\circ}\text{C}$ )
<b>3·8thf</b>	solvent loss <sup>[a]</sup>	29.0	38.1	80.1	47.4	79.6
	solvent loss <sup>[a]</sup>	22.9	119.7	149.4	115.8	144.0
	decomposition	21.4	208.2	-	182.8	230.8
<b>4·0.85thf·0.15Et<sub>2</sub>O</b>	solvent loss <sup>[b]</sup>	13.4	121.0	151.4	119.2	152.5
	decomposition	59.4	264.5	283.9	270.5	284.9

<sup>[a]</sup> A total loss of about 8 thf molecules was observed.

<sup>[b]</sup> A total loss of about 0.8 solvent molecules was observed.

All mentioned  $[\text{B}(\text{tceg})_2]^-$  salts with weakly coordinating cations (wcc) can be easily prepared in bulk and are infinitely stable if they are stored in sealed tubes. Beside thf,  $\text{CH}_3\text{CN}$  and DMSO they are also well soluble in  $\text{CH}_2\text{Cl}_2$ . All considered ammonium and imidazolium salts bearing the  $[\text{B}(\text{tceg})_2]^-$  ion are thermally stable up to over  $222\text{ }^{\circ}\text{C}$  (Table 2). Except for the OMIIm salt, all measured melting points are above room temperature. However,

[B(tceg)<sub>2</sub>]<sup>-</sup> forms with EMIm, BMIm, OMIm and Bu<sub>4</sub>N ionic liquids with melting points below 100 °C. For the imidazolium salts **5-7** well defined reversible melting points are not observed, although melting points of slowly grown crystals of **5** and **6** could be measured. Under argon the BMIm and OMIm salt were found to have a stable sub-cooled liquid phase at room temperature, while the EMIm salt recrystallizes within one hour. The BMIm salt slowly recrystallizes under air condition or under argon by scratching the flask with a glass rod at the argon-substance surface.

**Table 2.** Thermal analysis: Melting and decomposition points (from DSC measurements); spectroscopic data: IR, Raman, and <sup>13</sup>C NMR data of **1-10**.

	T <sub>mp</sub> /°C (T <sub>glass</sub> )	T <sub>dec</sub> /°C	<sup>13</sup> C NMR/ppm CN	<sup>11</sup> B NMR/ppm	IR/cm <sup>-1</sup> ν <sub>CN</sub>	Raman/cm <sup>-1</sup> ν <sub>CN</sub>
<b>1a</b>	-14.5	-	109.00	-	2250	2252
<b>2</b>	122.1	-	110.97	-	2251	2238, 2248
<b>3</b>	-	208.6	112.31, 112.37, 113.16	7.89	2256	2274
<b>4</b>	-	304.8	112.12	11.94	2254, 2271	2256, 2273
<b>5</b>	66.4	222.3	112.12	11.96	2251	2247
<b>6</b>	45.4 (-34.3)	241.5	112.13	11.92	2251	2247, 2255
<b>7</b>	(-46.8)	257.1	112.11	11.96	2250	2240
<b>8</b>	172.6	270.3	112.13	11.98	2242	2243, 2253
<b>9</b>	140.0	248.3	112.13	11.94	2248	2255
<b>10</b>	95.0	270.0	112.13	11.96	2250	2248

**Spectroscopic studies.** <sup>13</sup>C and <sup>11</sup>B NMR data along with IR/Raman data for compounds described in this work are listed in Table 2. The IR and Raman data of all considered CN group containing compounds show bands in the expected region between 2238-2273 cm<sup>-1</sup>, which can be assigned to the ν<sub>CN</sub> stretching frequencies. The solvent free Na[B(tceg)<sub>2</sub>] exhibits two different ν<sub>CN</sub> stretching frequencies for the uncoordinated and the sodium coordinated cyano group in both the IR and Raman spectra. Interestingly, all bands of the ν<sub>CN</sub> stretching frequencies appear with weak absorptions in IR. The <sup>13</sup>C NMR resonance of the cyano groups in the starting materials are detected slightly upfield shifted (109-111 ppm) than those in the borates (112-113 ppm). There are three resonance signals detected in <sup>13</sup>C NMR experiments for the CN groups in diborate **3**. One of the resonances can be assigned to the four equivalent cyano groups in the bridging moiety (-O-C(CN)<sub>2</sub>-C(CN)<sub>2</sub>-O-), while the two



chelating ligands, also bearing four equivalent CN groups each, give rise to another two resonances, which appear at slightly different shifts. For the diborate **3**, a rather sharp  $^{11}\text{B}$  resonance is found at 7.89 ppm and for the salts with  $[\text{B}(\text{tceg})_2]^-$  at 11.92-11.96 ppm.

**X-ray structure analysis.** The structures of compounds **1-4** have been determined. Tables 3 and 4 present the X-ray crystallographic data of species **1-4**. Selected distances and angles are listed in Table 5. X-ray quality crystals of all considered species were selected in Kel-F-oil (Riedel deHaen) or Fomblin YR-1800 (Alfa Aesar) at ambient temperature. All samples were cooled to  $-100(2)$  °C during the measurement. More details are found in the supporting information file.

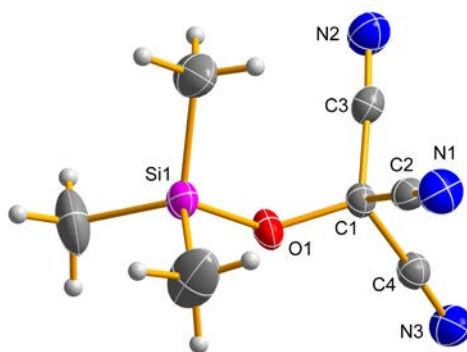


**Figure 1.** ORTEP drawing of the molecular structure of **1a**. Thermal ellipsoids with 50% probability at 173 K. Selected bond lengths (Å) and angles (°): Si1–O1 1.712(1), O1–C1 1.377(2), N1–C2 1.138(2), N2–C3 1.136(2), N3–C4 1.137(2); C1–O1–Si1 129.85(9).

$\text{Me}_3\text{SiO}-\text{C}(\text{CN})_3$  (**1a**). Crystals suitable for X-ray crystallography were obtained by storage of the pure liquid compound at  $-80$  °C for 1 hour. Tricyano(trimethylsiloxy)methane **1a** crystallized as colorless blocks in the triclinic space group  $P-1$ . Three formula units make up the asymmetric unit and six molecules take place in the unit cell. Only one independent molecule of **1a** is depicted in Figure 1 since the structural parameters are all very similar. The molecules contain a bent structure with C–O–Si angles between  $129.85(9)$ - $131.54(9)$ °. The CN groups with average CN bond lengths of  $1.137$  Å are lying well within the sum of the covalent radii for CN triple bonds,  $\Sigma r_{\text{cov}}(\text{C}\equiv\text{N}) = 1.14$  Å.<sup>[24]</sup>

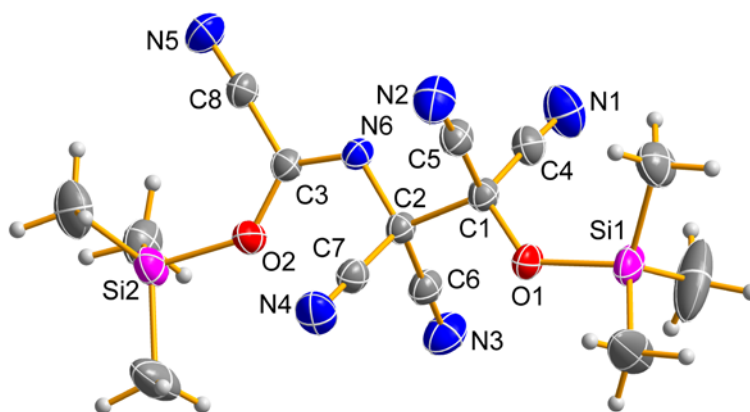


**Figure 2.** ORTEP drawing of the molecular structure of **1b**. Thermal ellipsoids with 50% probability at 173 K. Selected bond lengths (Å) and angles (°): N1–C4 1.137(2), N2–C5 1.137(2), N3–C6 1.140(2), N4–C7 1.133(2), N5–C8 1.139(2), N6–C2 1.455(2), N6–C3 1.268(2), O1–C1 1.373(2), O2–C3 1.313(2), Si1–O1 1.710(1), Si2–O2 1.724(1); C1–O1–Si1 128.5(1), C3–O2–Si2 133.9(1), C2–N6–C3 117.2(1), O2–C3–N6 125.5(2), O2–C3–C8 117.9(1), N6–C3–C8 116.7(1).

$Me_3SiO-C_2(CN)_4-N=C(CN)-OSiMe_3$  (**1b**). After distillation of **1a** few colorless crystals of **1b**, suitable for X-ray crystallographic analysis, were obtained from the residual red oil. **1b** might be considered as a dimer of **1a**, where two cyano groups were shifted from one molecule to the second and there added to one cyano carbon atom, while the residue of the first molecule forms a double bond to the cyano nitrogen atom of species two. It is assumed that the dimer was formed during the reaction since no dimerisation was observed after storage of **1a** for several months. **1b** crystallized as colorless needles in the orthorhombic space group *Pbca* with eight formula units per unit cell. There are no significant interactions between the molecules in the solid state. The most interesting structural feature of **1b** is the planar trans bent arrangement of the Si–O1–C1–C2–N6–C3–O2–Si2 skeleton. While the cyano group C8–N5 is also part of this plane the other four CN groups are out of this plane. As mentioned above N6 forms a double bond to C3 (1.268(2) Å, cf.  $\Sigma r_{cov}(C=N) = 1.27$  Å)<sup>[24]</sup> and a single bond to C2 (N6–C2 1.455(2), cf.  $\Sigma r_{cov}(C-N) = 1.46$  Å). The average bond length of the cyano groups is 1.137 Å in accord with the sum of the covalent radii for CN triple bonds (vide supra).

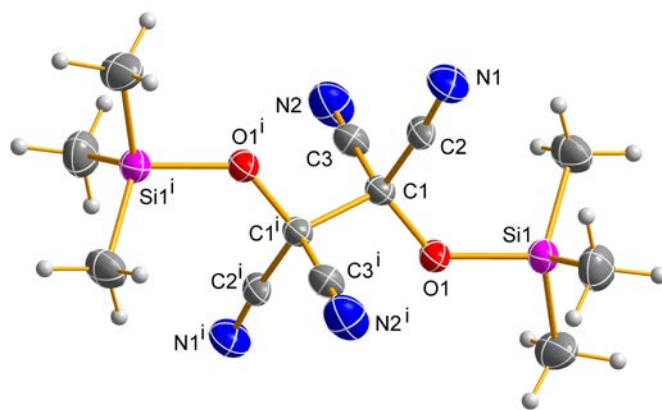


**Figure 3.** ORTEP drawing of the molecular structure of **2**. Thermal ellipsoids with 50% probability at 173 K. Selected bond lengths (Å) and angles (°): O1–Si1 1.7038(7), C2A–N1A 1.16(1), C3A–N2A 1.13(1), C1A–O1 1.372(1), C1A–C2A 1.47(1), C1A–C3A 1.491(3), C1A–C1A<sup>i</sup> 1.573(3), C4–Si1 1.840(1), C5–Si1 1.850(1), C6–Si1 1.851(1); N1A–C2A–C1A 175.1(7), N2A–C3A–C1A 177.6(5), C1A–O1–Si1 130.52(7), O1–C1A–C1A<sup>i</sup> 107.8(2), O1–C1A–C2A 111.3(3), O1–C1A–C3A 111.0(1). Symmetry code: (i)  $-x+1, -y+1, -z+1$ . Disorder not shown.

$\text{Me}_3\text{SiO}-\text{C}_2(\text{CN})_4-\text{OSiMe}_3$  (**2**). Crystals suitable for X-ray crystallographic analysis were obtained after sublimation as colorless blocks.  $\text{Me}_3\text{SiO}-\text{C}_2(\text{CN})_4-\text{OSiMe}_3$  crystallized in the monoclinic space group  $P2_1/c$  with two molecules per unit cell (Figure 3). The asymmetric unit consists half of a molecule that was found to be partially disordered. Here are no significant intermolecular interactions. With respect to the center of inversion (in the middle of the C1–C1<sup>i</sup> bond) the OSiMe<sub>3</sub>-groups were found in an anti conformation (O1–C1–C1<sup>i</sup>–O1<sup>i</sup> 180°). The C1–C1<sup>i</sup> bond length amounts to 1.573(3) Å which corresponds to a slightly elongated C–C single bond ( $\Sigma r_{\text{cov}}(\text{C}-\text{C}) = 1.50$  Å).<sup>[24]</sup> All CN distances lie in the expected range with 1.13(1)-1.16(1) Å (cf.  $\Sigma r_{\text{cov}}(\text{C}\equiv\text{N}) = 1.14$  Å).<sup>[24]</sup>

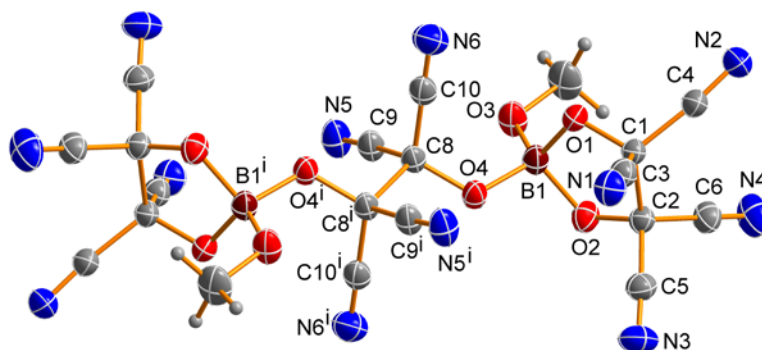


**Figure 4.** ORTEP drawing of the molecular structure of the anion in **3·8thf**. Thermal ellipsoids with 50% probability at 173 K. Selected bond lengths (Å) and angles (°): B1–O1 1.495(2), B1–O2 1.483(2), B1–O3 1.404(2), B1–O4 1.478(2), N1–C3 1.140(2), N2–C4 1.137(2), N3–C5 1.135(2), N4–C6 1.137(2), N5–C9 1.137(2), N6–C10 1.137(2), C1–C2 1.628(2), C8–C8<sup>i</sup> 1.584(2); O1–B1–O2 102.9(1), O1–B1–O3 112.1(1), O1–B1–O4 111.1(1), O2–B1–O3 115.3(1), O2–B1–O4 105.9(1), O3–B1–O4 109.4(1), B1–O1–C1 112.8(1), B1–O2–C2 113.1(1), B1–O3–C7 116.66(1), B1–O4–C8 121.2(1); B1–O1–C1–C2 10.20(1), O1–C1–C2–O2 –2.7(1), C1–C2–O2–B1 –5.8(1), C2–O2–B1–O1 11.5(1), O2–B1–O1–C1 –13.5(1). Symmetry code: (i)  $-x+1, -y, -z$ .

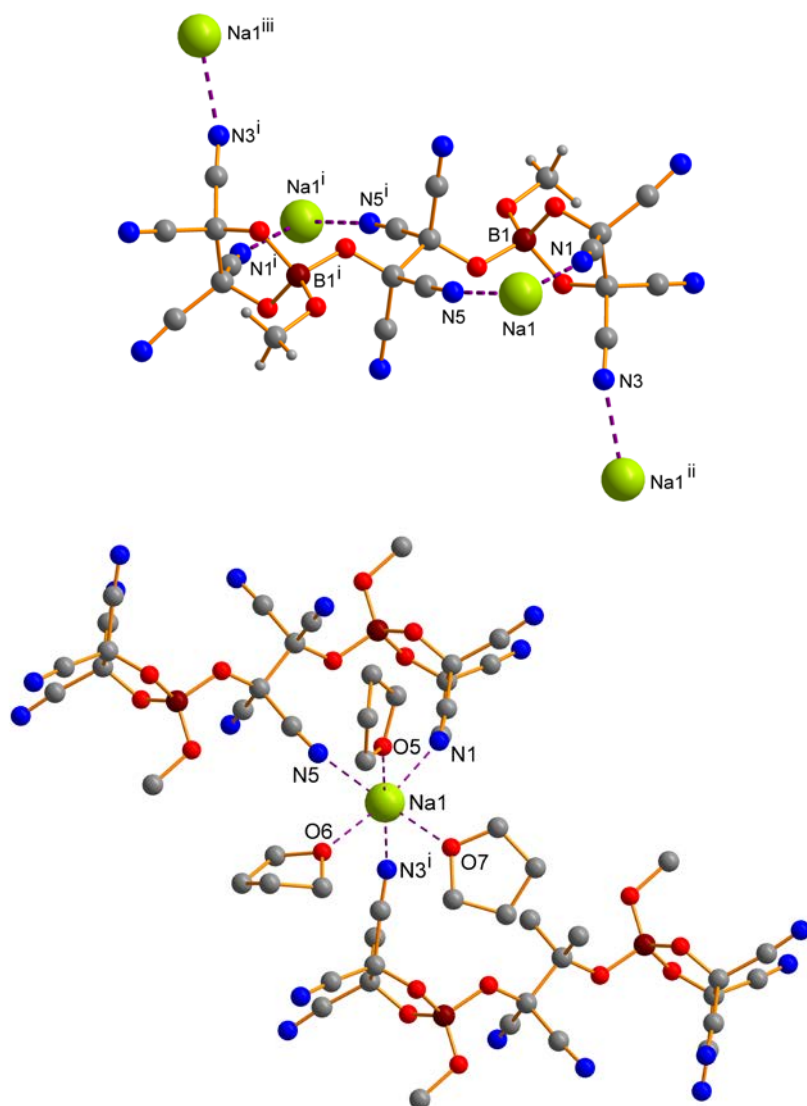


**Figure 5.** Top: Ball-and-stick drawing of the local environment around the anion center in **3·8thf**. Symmetry codes: (i)  $-x+1, -y, -z$ ; (ii)  $2-x, -y, -z$ ; (iii)  $-1+x, y, z$ ; Bottom: Ball-and-stick drawing of the local environment about the sodium centers in **3·8thf** (Hydrogen atoms omitted for clarity). Selected bond lengths (Å) and angles (°): Na1···O5 2.329(1), Na1···O7 2.339(1), Na1···O6 2.365(1), Na1···N1 2.525(1), Na1···N3<sup>i</sup> 2.516(1), Na1···N5 2.522(1); O5···Na1···O6 91.35(6), O5···Na1···O7 92.90(6), O5···Na1···N1 87.76(5), O5···Na1···N3<sup>i</sup> 174.50(6), O5···Na1···N5 89.92(6), O6···Na1···O7 94.70(5), O6···Na1···N1 169.84(5), O6···Na1···N3<sup>i</sup> 84.65(5), O6···Na1···N5 89.31(5), O7···Na1···N1 95.45(5), O7···Na1···N3<sup>i</sup> 83.68(5), O7···Na1···N5 175.04(6), N1···Na1···N3<sup>i</sup> 96.83(5), N1···Na1···N5 80.58(5), N3<sup>i</sup>···Na1···N5 93.80(5), C3···N1···Na1 155.0(1), C5<sup>i</sup>···N3<sup>i</sup>···Na1 144.3(1), C9···N5···Na1 171.9(1). Symmetry code: (i)  $-x+2, -y, -z$ .

*Na*<sub>2</sub>[*B*<sub>2</sub>(*OMe*)<sub>2</sub>(*tceg*)<sub>3</sub>]*·8thf* (**3·8thf**). Crystals suitable for single crystal X-ray diffraction were obtained from a hot saturated thf solution after storage for 1 hour at room temperature. Sodium diborate **3·8thf** crystallized as colorless blocks in the triclinic space group *P*-1 with two formula units per unit cell. As shown in Figure 4, the diborate anion of **3·8thf** is a centrosymmetric dimer composed of BO<sub>4</sub> tetrahedra which are bridged by one O4–C8–C8<sup>i</sup>–O4<sup>i</sup> moiety forming a planar trend bent chain with a C–C single bond (1.584(2) Å). Each boron centre is further bound by one *tceg* ligand in a chelating coordination mode and one

Me<sub>3</sub>SiO group is still attached. While the four cyano groups of the bridging *tceg* ligand are arranged in a staggered fashion, the cyano groups of both terminal *tceg* chelate ligands adopt an eclipsed conformation. The B–O bond lengths with values between 1.404 - 1.495 Å (cf.  $\Sigma r_{\text{cov}}(\text{B–O}) = 1.48 \text{ \AA}$ ) are comparable to those observed for alkoxy- and phenoxyborates.<sup>[10,11]</sup> The tetrahedron of the BO<sub>4</sub> moiety is slightly distorted with three smaller (102.9(1), 105.9(1) and 109.4(1)°) and three larger (112.1(1), 111.1(1) and 115.3(1)°) O–B–O angles. The chelating linker forms with the boron a five membered BO<sub>2</sub>C<sub>2</sub> ring that is nearly planar with torsion angles between 10.20(1) - -13.5(1)°. As depicted in Figures 5 and 6 there are strong interactions between the cations and anions, however, only half of the cyano groups of the anion are involved in the coordination to four sodium cations, with two CN groups bridged by a Na<sup>+</sup> ion (N5/N1 and N5<sup>i</sup>/N1<sup>i</sup>; Na1⋯N1 2.525(1) and Na1⋯N5 2.522(1)) while N3 and N3<sup>i</sup> (Na1⋯N3<sup>i</sup> 2.516(1)) act as monodentate ligand. All other CN groups remain uncoordinated. Each Na<sup>+</sup> cation is coordinated octahedrally by three thf solvent molecules and three cyano groups, whereby two CN (N1/N5) groups stem from the same anion thus forming a formal 11-membered metalla heterocycle. These coordination modes results in the formation of 1d coordination polymer with a double stranded zig-zag chains along the *b*-axis (Figure 6). The octahedral environment at the sodium cation is slightly distorted with Ligand⋯Na<sup>+</sup>⋯Ligand angles between 84.65(5) and 96.83(5)°.

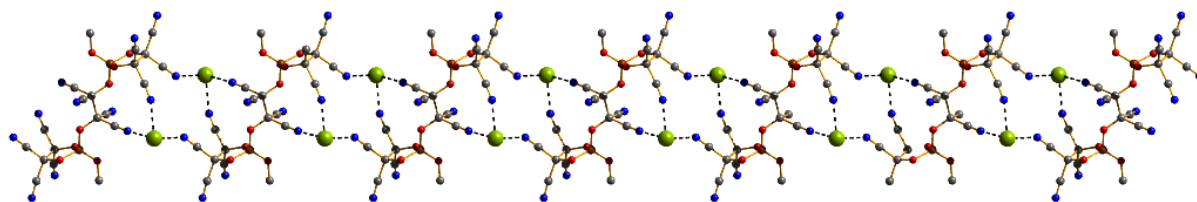


**Figure 6.** One dimensional extension of the Coordination chain in **3**. View along *b*-axis.

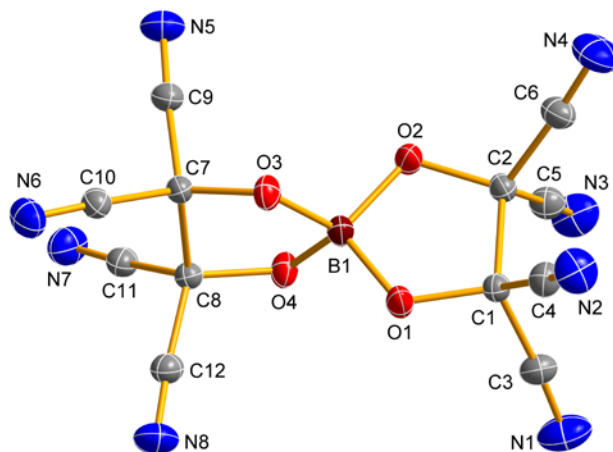


**Figure 7.** ORTEP drawing of the molecular structure of the anion in **4·0.85thf·0.15Et<sub>2</sub>O**. Thermal ellipsoids with 50% probability at 173 K. Selected bond lengths (Å) and angles (°): B1–O1 1.461(1), B1–O2 1.458(1), B1–O3 1.473(1), B1–O4 1.479(1), C1–O1 1.372(1), C2–O2 1.373(1), C7–O3 1.374(1), C8–O4 1.375(1), C3–N1 1.136(2), C4–N2 1.139(1), C5–N3 1.139(1), C6–N4 1.138(2), C9–N5 1.138(1), C10–N6 1.140(1), C11–N7 1.137(1), C12–N8 1.137(1), C1–C2 1.628(1), C1–C3 1.484(1), O1–B1–O2 104.90(8), O1–B1–O3 109.46(8), O1–B1–O4 114.31(9), O2–B1–O3 114.23(9), O2–B1–O4 109.74(8), O3–B1–O4 104.47(8), B1–O1–C1 112.65(8), B1–O2–C2 112.62(8), B1–O3–C7 109.15(7), B1–O4–C8 108.91(7), O1–C1–C2 104.43(7), O2–C2–C1 104.49(7), O3–C7–C8 102.21(7), O4–C8–C7 102.10(7), O1–C1–C2–O2 0.7(1), C1–C2–O2–B1 –6.5(1), C2–O2–B1–O1 9.7(1), O2–B1–O1–C1 –9.2(1), B1–O1–C1–O2 5.4(1), O3–C7–C8–O4 –36.49(9), C7–C8–O4–B1 29.5(1), C8–O4–B1–O3 –13.2(1), O4–B1–O3–C7 –12.4(1), B1–O3–C7–C8 29.09(9).

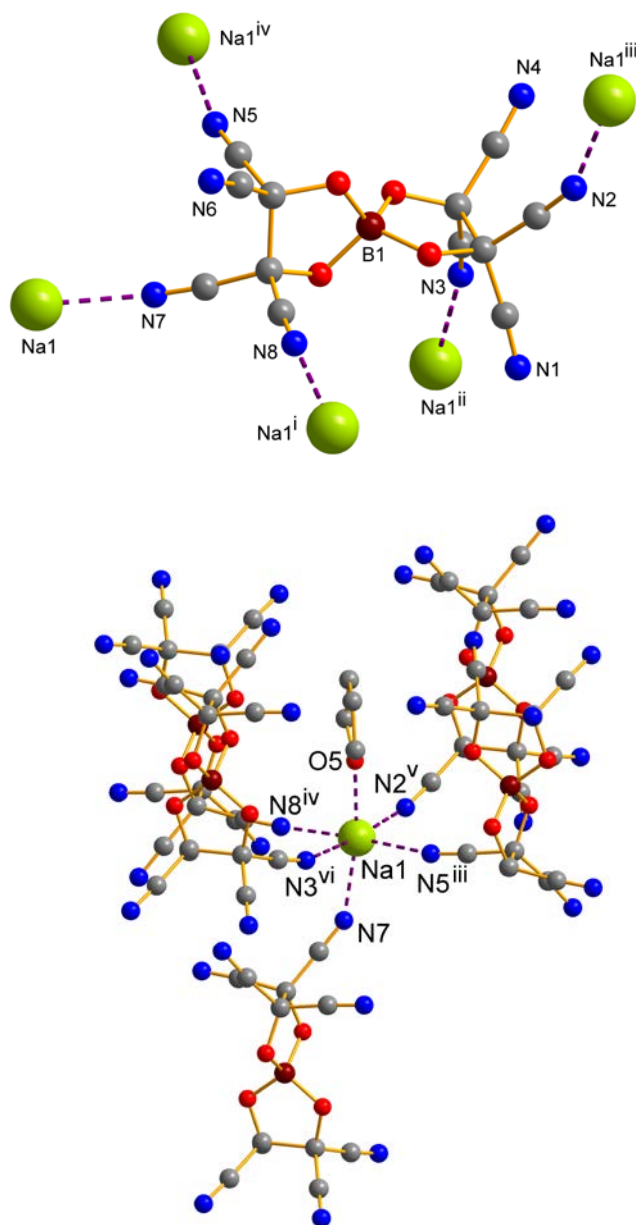


**Figure 8.** Top: Ball-and-stick drawing of the local environment of the anion Symmetry codes: (i)  $-x+2, -y, -z$ ; (ii)  $x+1, y, z$ ; (iii)  $x+1, y+1, z$ ; (iv)  $-x+2, -y, -z+1$ ; Bottom: Ball-and-stick drawing of the local environment of the  $\text{Na}^+$  ion in **4·0.85thf·0.15Et<sub>2</sub>O** (Hydrogen atoms omitted for clarity). Selected bond lengths (Å) and angles (°):  $\text{N2}\cdots\text{Na1}^{\text{iii}}$  2.487(1),  $\text{N3}\cdots\text{Na1}^{\text{ii}}$  2.563(1),  $\text{N5}\cdots\text{Na1}^{\text{iv}}$  2.525(1),  $\text{N7}\cdots\text{Na1}$  2.451(1),  $\text{N8}\cdots\text{Na1}^{\text{i}}$  2.555(1),  $\text{Na1}\cdots\text{O5A}$  2.307(7),  $\text{O5A}\cdots\text{Na1}\cdots\text{N2}^{\text{v}}$  86.5(4),  $\text{O5A}\cdots\text{Na1}\cdots\text{N3}^{\text{vi}}$  87.7(4),  $\text{O5A}\cdots\text{Na1}\cdots\text{N5}^{\text{iii}}$  90.8(4),  $\text{O5A}\cdots\text{Na1}\cdots\text{N7}$  168.6(5),  $\text{O5A}\cdots\text{Na1}\cdots\text{N8}^{\text{iv}}$  92.2(4),  $\text{N2}^{\text{v}}\cdots\text{Na1}\cdots\text{N3}^{\text{vi}}$  174.13(4),  $\text{N2}^{\text{v}}\cdots\text{Na1}\cdots\text{N5}^{\text{iii}}$  89.83(4),  $\text{N2}^{\text{v}}\cdots\text{Na1}\cdots\text{N7}$  103.69(4),  $\text{N2}^{\text{v}}\cdots\text{Na1}\cdots\text{N8}^{\text{iv}}$  91.36(4),  $\text{N3}^{\text{vi}}\cdots\text{Na1}\cdots\text{N5}^{\text{iii}}$  90.50(4),  $\text{N3}^{\text{vi}}\cdots\text{Na1}\cdots\text{N7}$  82.14(4),  $\text{N3}^{\text{vi}}\cdots\text{Na1}\cdots\text{N8}^{\text{iv}}$  88.61(4),  $\text{N5}^{\text{iii}}\cdots\text{Na1}\cdots\text{N7}$  94.29(4),  $\text{N5}^{\text{iii}}\cdots\text{Na1}\cdots\text{N8}^{\text{iv}}$  176.89(4),  $\text{N7}\cdots\text{Na1}\cdots\text{N8}^{\text{iv}}$  82.64(4),  $\text{C4}\cdots\text{N2}\cdots\text{Na1}^{\text{i}}$  154.44(1),  $\text{C5}\cdots\text{N3}\cdots\text{Na1}^{\text{ii}}$  162.31(1),  $\text{C9}\cdots\text{N5}\cdots\text{Na1}^{\text{iii}}$  167.25(9),  $\text{C12}\cdots\text{N7}\cdots\text{Na1}$  147.7(1),  $\text{C11}\cdots\text{N8}\cdots\text{Na1}^{\text{iv}}$  169.13(9). Symmetry codes: (iii)  $-x+2, -y, -z+1$ ; (iv)  $-x+2, -y, -z$ ; (v)  $x-1, y+1, z$ ; (vi)  $x-1, y, z$ .

$\text{Na}[B(\text{tceg})_2]\cdot 0.85\text{thf}\cdot 0.15\text{Et}_2\text{O}$  (**4·0.85thf·0.15Et<sub>2</sub>O**) crystallized from a saturated solution in thf after addition of Et<sub>2</sub>O and storage at room temperature over night. Sodium borate **4·0.85thf·0.15Et<sub>2</sub>O** crystallized in the triclinic space group *P*-1 with two formula units per unit cell. The boron center is coordinated by two *tceg* ligands forming two five membered



rings with the chelating ligands (Figure 7). The  $\text{BO}_4$  tetrahedron is slightly distorted with three smaller (104.47(8), 104.90(8), 109.46(8)) and three slightly larger (109.74(8), 114.23(9), 114.31(9)) angles. While one of them is nearly planar with torsion angles of the ring members up to maximal  $9.7^\circ$  the second one shows a significant twisting with a torsion angle of  $36.49(9)^\circ$ . In the crystal structure there are significant cation $\cdots$ anion interactions via dative bonds from the cyano groups to the sodium cation as shown in Figure 8. A distorted octahedral coordination environment (with angles between  $82.14(4)$  and  $103.69(4)^\circ$ ) consisting of five anions and a solvent molecule was found at the sodium cation. The position of a thf molecule at  $\text{Na}^+$  is disordered and partially substituted by  $\text{Et}_2\text{O}$ . The  $\text{Na}\cdots\text{N}$  distances range from 2.487(1) to 2.563(1) Å resulting in an average  $\text{Na}\cdots\text{N}$  distance of 2.516 Å. Only five CN groups of the anion are involved in coordination of the cations in a monodentate fashion, while three remain uncoordinated. The large number of coordinating cyano groups at the sodium leads to a coordination polymer with a three dimensional extension as displayed in Figure 9.

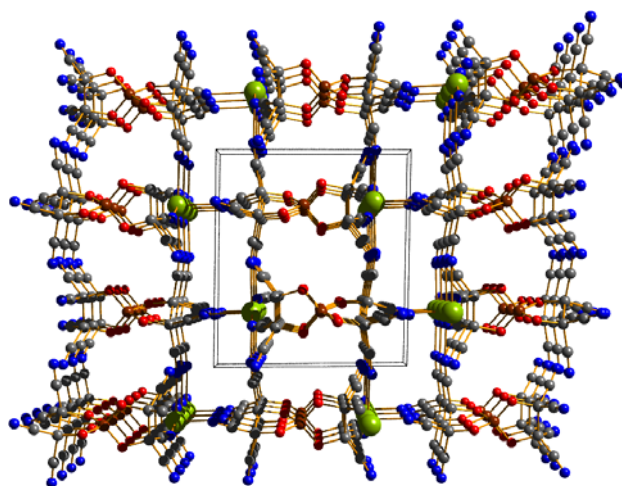


**Figure 9.** Coordination network of the crystal structure of  $4\cdot 0.85\text{thf}\cdot 0.15\text{Et}_2\text{O}$ . Solvent molecules omitted for clarity. View along  $b$ -axis.



**Table 3.** Crystallographic details of Me<sub>3</sub>SiO–C(CN)<sub>3</sub> (**1a**), Me<sub>3</sub>SiO–C<sub>2</sub>(CN)<sub>4</sub>–N=C(CN)–OSiMe<sub>3</sub> (**1b**) and Me<sub>3</sub>SiO–C<sub>2</sub>(CN)<sub>4</sub>–OSiMe<sub>3</sub> (**2**).

	<b>1a</b>	<b>1b</b>	<b>2</b>
Chem. Formula	C <sub>7</sub> H <sub>9</sub> N <sub>3</sub> OSi	C <sub>14</sub> H <sub>18</sub> N <sub>6</sub> O <sub>2</sub> Si <sub>2</sub>	C <sub>12</sub> H <sub>18</sub> N <sub>4</sub> O <sub>2</sub> Si <sub>2</sub>
Form. Wght. [g·mol <sup>-1</sup> ]	179.26	358.52	306.48
Colour	colourless	colourless	colourless
Cryst. System	triclinic	orthorhombic	monoclinic
Space Group	<i>P</i> -1	<i>Pbca</i>	<i>P</i> 2 <sub>1</sub> / <i>c</i>
a [Å]	12.2738(9)	12.853(2)	6.7485(3)
b [Å]	12.6750(9)	11.383(1)	9.2162(4)
c [Å]	12.6752(9)	28.696(3)	14.2026(5)
α [°]	60.459(4)	90	90
β [°]	74.995(4)	90	99.272(2)
γ [°]	61.370(3)	90	90
V [Å <sup>3</sup> ]	1505.1(2)	4198.4(9)	871.80(6)
Z	6	8	2
μ [mm <sup>-1</sup> ]	0.19	0.19	0.21
λ <sub>MoKα</sub> [Å]	0.71073	0.71073	0.71073
T [K]	173	173	173
Measured Reflections	49331	59243	13662
Independent Reflections	10417	6116	2524
Reflections with I > 2σ(I)	6250	3995	2169
R <sub>int</sub>	0.068	0.075	0.039
F(000)	564	1504	324
R <sub>1</sub> (R[F <sub>2</sub> > 2σ(F <sub>2</sub> )])	0.048	0.047	0.032
wR <sub>2</sub> (all data)	0.122	0.126	0.094
GooF	1.02	1.01	1.07
Parameters	334	230	134

**Table 4.** Crystallographic details of Na<sub>2</sub>[B<sub>2</sub>(OMe)<sub>2</sub>(tceg)<sub>3</sub>] $\cdot$ 8thf (**3 $\cdot$ 8thf**) and Na[B(tceg)<sub>2</sub>] $\cdot$ 0.85thf $\cdot$ 0.15Et<sub>2</sub>O (**4 $\cdot$ 0.85thf $\cdot$ 0.15Et<sub>2</sub>O**).

	<b>3<math>\cdot</math>8thf</b>	<b>4<math>\cdot</math>0.85thf<math>\cdot</math>0.15Et<sub>2</sub>O</b>
Chem. Formula	C <sub>52</sub> H <sub>70</sub> B <sub>2</sub> N <sub>12</sub> Na <sub>2</sub> O <sub>16</sub>	C <sub>16</sub> H <sub>8.3</sub> BN <sub>8</sub> NaO <sub>5</sub>
Form. Wght. [g $\cdot$ mol <sup>-1</sup> ]	1186.80	426.40
Colour	colourless	colourless
Cryst. System	triclinic	triclinic
Space Group	<i>P</i> -1	<i>P</i> -1
a [Å]	11.1767(4)	9.8393(1)
b [Å]	11.5888(4)	10.3900(1)
c [Å]	13.2737(5)	10.9953(2)
$\alpha$ [°]	69.329(2)	77.597(1)
$\beta$ [°]	78.908(2)	88.540(1)
$\gamma$ [°]	80.219(2)	78.030(1)
V [Å <sup>3</sup> ]	1568.8(1)	1073.73(2)
Z	2	2
$\mu$ [mm <sup>-1</sup> ]	0.11	0.12
$\lambda_{\text{MoK}\alpha}$ [Å]	0.71073	0.71073
T [K]	173	173
Measured Reflections	43231	35882
Independent Reflections	8743	7748
Reflections with I > 2 $\sigma$ (I)	6862	5605
R <sub>int.</sub>	0.040	0.026
F(000)	626	433
R <sub>1</sub> (R[F <sub>2</sub> > 2 $\sigma$ (F <sub>2</sub> )])	0.051	0.043
wR <sub>2</sub> (all data)	0.147	0.114
GooF	1.03	1.02
Parameters	531	345

**Table 5.** Selected structural data of ligand, intermediate and product. Distances in Å, angles in °.

Compound	B-O	O-B-O	C-N	C-C-N	O-C-C-O
<b>2</b>	-	-	1.16(1)	175.1(7)	-180
			1.13(1)	177.6(5)	
<b>3·8thf</b>	1.495(2)	102.9(1)	1.140(2)	174.7(2)	-2.7(1)
	1.483(2)	112.1(1)	1.137(2)	174.0(2)	-180
	1.404(2)	111.1(1)	1.135(2)	175.3(2)	
	1.478(2)	115.3(1)	1.137(2)	174.2(2)	
		105.9(1)	1.137(2)	176.2(1)	
		109.4(1)	1.137(2)	178.3(2)	
<b>4·thf</b>	1.461(1)	104.90(8)	1.136(2)	175.5(1)	0.7(1)
	1.458(1)	109.46(8)	1.139(1)	174.6(1)	-36.49(9)
	1.473(1)	114.31(9)	1.139(1)	176.0(1)	
	1.458(1)	114.23(9)	1.138(2)	176.2(1)	
	1.458(1)		1.138(1)	176.7(1)	
	1.473(1)		1.140(1)	173.5(1)	
	1.458(1)		1.137(1)	174.4(1)	
	1.473(1)		1.137(1)	175.9(1)	

**Thermodynamics.** The lattice potential energy ( $U_{\text{POT}}$ ), lattice enthalpy ( $\Delta H_L$ ) and the standard entropy ( $S^{\circ}_{298}$  in  $\text{J mol}^{-1} \text{K}^{-1}$  at 298.15 K and 101 kPa) of the new  $\text{M}^+_n\text{X}^-$  salts ( $\text{M} = \text{Na}, \text{EMIm}, \text{BMIm}, \text{OMIm}, \text{Me}_4\text{N}, \text{Et}_4\text{N}, \text{Bu}_4\text{N}; n = 1, 2$ ) were estimated from its molecular volume using the principles of Volume-Based Thermodynamics (VBT), introduced by Jenkins, Glasser and Passmore (Table 6).<sup>[25,26]</sup> To clarify the influence of the anion we have studied the sodium diborate **3** and sodium borate **4** including the data of the starting borate  $[\text{B}(\text{OMe})_4]^-$ , a hypothetical intermediate  $[\text{B}(\text{OMe})_2(\text{tceg})]^-$  and the well studied  $[\text{B}(\text{CN})_4]^-$  for comparison.<sup>[27]</sup> The ion volumes were calculated from the average atomic volumes by summing the volume contributions from each atom in the molecular formula as described by Hofmann (Table 6).<sup>[28]</sup> Krossing *et al.* found that  $V_{\text{Hofmann}}$  correlates linearly with the experimental cation volumes according to  $V_{\text{exp}} = 0.964V_{\text{Hofmann}} - 7 \text{ \AA}^3$  and for the anion according to  $0.946V_{\text{Hofmann}} + 27 \text{ \AA}^3$ .<sup>[29]</sup> Hofmann's approach is not always the best method for the estimation of volumes. For instance the anion and cation volumes are equal since no charge considerations are made. Jenkins and Liebman's isomegetic rule can be referred to as

the theoretical basis of Hofmann's approach. The isomegetic rule's different approach offers another way to ion volumes.<sup>[25]</sup>

*Anion size and lattice enthalpies.* The anion volumes increase along the series  $[\text{B}(\text{CN})_4]^-$  ( $137 \text{ \AA}^3$ ) <  $[\text{B}(\text{OMe})_4]^-$  ( $193 \text{ \AA}^3$ ) <  $[\text{B}(\text{OMe})_2(\text{tceg})]^-$  ( $261 \text{ \AA}^3$ ) <  $[\text{B}(\text{tceg})_2]^-$  ( $329 \text{ \AA}^3$ ) and  $[\text{B}_2(\text{OMe})_2(\text{tceg})_3]^-$  ( $564 \text{ \AA}^3$ ). Each substitution of two methyl groups with a tetracyanoethylene unit leads to an increasing of the anion volume by  $68 \text{ \AA}^3$ . It is notable that the anion volume of the diborate in **3** with  $564 \text{ \AA}^3$  is considerably smaller than the sum of the anion volumes of two borates  $[\text{B}(\text{OMe})_2(\text{tceg})]^-$  plus the substitution of two methyl groups with a tetracyanoethylene group ( $2 \times 261 \text{ \AA}^3 + 68 \text{ \AA}^3 = 590 \text{ \AA}^3$ ). For comparison with the theoretical values the anion volumes for the diborate **3** and the borate **4** were derived from X-ray crystal data. An anion volume for the diborate in **3** of  $672.5 \text{ \AA}^3$  is calculated from the cell volume  $V = 1568.8(1) \text{ \AA}^3$  subtracting the volume of eight thf molecules ( $V(\text{thf}) = 107.5 \text{ \AA}^3$ ) and two sodium cations ( $V(\text{Na}^+) = 18.1 \text{ \AA}^3$ ). With a cell volume of  $1073.7 \text{ \AA}^3$  and  $Z = 2$ , considering the volume of a thf molecule and the sodium cation, an anion volume  $V([\text{B}(\text{tceg})_2]^-) = 393.2 \text{ \AA}^3$  is calculated. The differences between the anion volumes based on Hofmann's approach and the calculations from the X-ray data are estimated to be ca. 19.5 % and can be explained with the disorder of the thf molecules in the crystal structures, which takes more space than calculated for thf. As expected the cumulating substitution of methyl groups by tetracyanoethylene groups results in a decrease of the lattice potential energy regarding to the enlargement of the anions with the exception of the diborate. Although the anion volume of the diborate was estimated to be the largest, the lattice potential energy is also the largest of all here studied anions, which can be referred to the larger coulomb interaction as the dianion forms salts of the type  $\text{M}^+_2\text{X}^{2-}$  resulting in a higher ionic strength.

*Cation size and lattice enthalpies.* The influence of the cations can be shown by opposing the lattice potential energies of the  $\text{M}^+\text{X}^-$  salts ( $\text{M} = \text{EMIm}$  (**5**),  $\text{BMIm}$  (**6**),  $\text{OMIm}$  (**7**),  $\text{Me}_4\text{N}$  (**8**),  $\text{Et}_4\text{N}$  (**9**), and  $\text{Bu}_4\text{N}$  (**10**), see Table 7) with the results of the sodium salt **4**. The lattice potential energies of the imidazolium salts decrease from the sodium salt ( $329.4 \text{ kJ mol}^{-1}$ ) by  $33.9 \text{ kJ mol}^{-1}$  (**5**),  $43.0 \text{ kJ mol}^{-1}$  (**6**), and  $58.3 \text{ kJ mol}^{-1}$  (**7**), while the calculated values of the ammonia salts decrease in a similar range (**8**:  $26.3 \text{ kJ mol}^{-1}$ , **9**:  $43.5 \text{ kJ mol}^{-1}$  and **10**:  $68.8 \text{ kJ mol}^{-1}$ ). The cation volume increases along the imidazolium salt series  $\text{EMIM}$  ( $149.9 \text{ \AA}^3$ ) <  $\text{BMIM}$  ( $196.2 \text{ \AA}^3$ ) <  $\text{OMIM}$  ( $288.8 \text{ \AA}^3$ ) and along the ammonium salt series  $\text{Me}_4\text{N}$  ( $116.6 \text{ \AA}^3$ ) <  $\text{Et}_4\text{N}$  ( $209.3 \text{ \AA}^3$ ) <  $\text{Bu}_4\text{N}$  ( $394.6 \text{ \AA}^3$ ).

**Table 6.** Ionic volumes of cyano-substituted borate anions and thermodynamic data derived from volume-based thermodynamics (VBT) for the sodium salts ( $V(\text{Na}^+) = 18.1 \text{ \AA}^3$ ).

	$V_{\text{anion}} (\text{\AA}^3)$	$U_{\text{pot}} (\text{kJ mol}^{-1})$	$S_{298}^\circ (\text{J K}^{-1} \text{mol}^{-1})$	$\Delta H_L (\text{kJ mol}^{-1})$
$[\text{B}(\text{CN})_4]^-$ <sup>a</sup>	136.7	540.8	225.4	542.0
$[\text{B}(\text{OMe})_4]^-$ <sup>a</sup>	192.8	497.9	301.8	499.2
$[\text{B}(\text{OMe})_2(\text{tceg})]^-$ <sup>a</sup>	261.0	462.8	394.6	464.0
$[\text{B}_2(\text{OMe})_2(\text{tceg})_3]^{2-}$ ( <b>3</b> ) <sup>b</sup>	563.5	997.3	830.5	997.3
$[\text{B}(\text{tceg})_2]^-$ ( <b>4</b> ) <sup>a</sup>	329.4	437.5	487.6	438.7

$$^a U_{\text{POT}} = 2 \cdot 1 \left( \frac{117.3}{\sqrt[3]{V_m}} + 51.9 \text{ kJ mol}^{-1} \right), \Delta H_L = U_{\text{POT}} + 1 \left( \frac{3}{2} - 2 \right) RT + 1 \left( \frac{6}{2} - 2 \right) RT ;$$

$$^b U_{\text{POT}} = 2 \cdot 3 \left( \frac{165.3}{\sqrt[3]{V_m}} - 29.8 \text{ kJ mol}^{-1} \right), \Delta H_L = U_{\text{POT}} + 2 \left( \frac{3}{2} - 2 \right) RT + 1 \left( \frac{6}{2} - 2 \right) RT ;$$

$$S_{298}^\circ = 1360V_m + 15 \text{ J K}^{-1} \text{mol}^{-1}, \text{ corrected Hoffmann's volumina are used.}^{[52]}$$

**Table 7.** Ionic volumes of **5-10** and thermodynamic data derived from volume-based thermodynamics (VBT)<sup>a</sup> for the  $[\text{B}(\text{tceg})_2]^-$ .

	<b>5</b>	<b>6</b>	<b>7</b>	<b>8</b>	<b>9</b>	<b>10</b>
$V_{\text{cat}} (\text{\AA}^3)$	149.8	196.2	288.8	116.6	209.3	394.6
$U_{\text{pot}} (\text{kJ mol}^{-1})$	403.6	394.5	379.2	410.9	392.1	365.1
$S_{298}^\circ (\text{J K}^{-1} \text{mol}^{-1})$	666.7	729.8	855.8	621.6	747.6	999.64
$\Delta H_L (\text{kJ mol}^{-1})$	408.5	399.4	384.1	415.8	397.1	370.0

$$^a U_{\text{POT}} = 2 \left( \frac{117.3}{\sqrt[3]{V_m}} + 51.9 \text{ kJ mol}^{-1} \right), \Delta H_L = U_{\text{POT}} + 1 \left( \frac{6}{2} - 2 \right) RT + 1 \left( \frac{6}{2} - 2 \right) RT, S_{298}^\circ = 1360V_m + 15 \text{ J K}^{-1} \text{mol}^{-1};$$

corrected Hoffmann's volumina are used.<sup>[52]</sup>

## Conclusions

An alternative synthesis method was applied for the formation of novel cyano functionalized borate anions by reacting trimethylsilyl substituted cyanohydrins with  $\text{Na}[\text{B}(\text{OMe})_4]$ . This offers a new approach to novel nitrile-rich borates that were not accessible from cyanohydrins. The molecular structures of two already known trimethylsilyl-substituted cyanohydrins were analysed by X-ray crystallography for the first time. Coordination polymer networks were obtained from the sodium salts of  $[\text{B}(\text{tceg})_2]^-$  (3D network) with the chelating linker attached twice and the diborate  $[\text{B}_2(\text{OMe})_2(\text{tceg})_3]^-$  (double-stranded chain) containing a residual methyl group at each  $\text{BO}_4$  moieties and a bridging tetracyanoethylene group. The

cyano groups were found as a dominant structure-directing unit by formation of strong dative metal...nitrogen ( $M \cdots NC$ ) bonds. Novel nitrile-rich ionic liquids of the type  $M[B(\text{tceg})_2]$  ( $M = \text{EMIm, BMIm, OMIm, Me}_4\text{N, Et}_4\text{N, Bu}_4\text{N}$ ) were obtained via salt metathesis reaction starting from  $\text{Na}[B(\text{tceg})_2]$  exchanging  $\text{Na}^+$  by several imidazolium and ammonium cations. Thermal studies via DSC revealed that  $[B(\text{tceg})_2]^-$  is suitable for the formation of ionic liquids. It was found that with OMIm as counterion a room temperature ionic liquid can be synthesized, whereas utilizing BMIm as counter ion in combination with the novel  $[B(\text{tceg})_2]^-$  anion leads to a sub-cooled liquid.

## Experimental

**General Information.** All manipulations were carried out under oxygen- and moisture-free conditions under argon using standard Schlenk or drybox techniques.

Dichloromethane and acetonitrile were refluxed over  $\text{CaH}_2$  and freshly distilled prior to use. Tetrahydrofuran, toluene and  $\text{Et}_2\text{O}$  were dried over  $\text{Na/benzophenone}$ , *n*-hexane was refluxed over  $\text{Na/benzophenone/diglyme}$  and freshly distilled prior to use. A solution of phosgene in toluene (20 %, Sigma Aldrich), the imidazolium salts (ABCR), the ammonium salts (Merck) and  $\text{NaBH}_4$  (Merck) were used as received. Oxalyl chloride (Alfa Aesar) and trimethylsilyl cyanide (Lonza) were distilled under argon atmosphere and stored in Schlenk flasks. Methanol was dried by addition of small amounts of  $\text{Na}$  and distilled under argon atmosphere.

**NMR:**  $^1\text{H}$ ,  $^{11}\text{B}$  and  $^{13}\text{C}$  spectra were obtained on Bruker AVANCE 250 (250 MHz), AVANCE 300 (300 MHz) spectrometer and were referenced externally.  $\text{CDCl}_3$  and  $\text{DMSO-d}_6$  were dried over  $\text{CaH}_2$ .

**IR:** Nicolet 380 FT-IR with a Smart Orbit ATR device was used.

**Raman:** Bruker VERTEX 70 FT-IR with RAM II FT-Raman module, equipped with a Nd:YAG laser (1064 nm), or Kaiser Optical Systems RXN1-785 nm was used.

**CHN analyses:** Analysator Flash EA 1112 from Thermo Quest, or C/H/N/S-Mikronalysator TruSpec-932 from Leco were used. Elemental analysis of nitrile rich compounds often leads to decreasing results of the C- and N-values, due to incomplete or slow combustion. In addition all these compounds are rather hygroscopic.

**DSC:** DSC 823e from Mettler-Toledo (Heating-rate 5 °C/min) was used. A sample of approximately 3 to 5 mg was placed in an aluminium crucible. The closed crucible was placed in the furnace. The closed furnace was flushed with nitrogen and the sample was measured using a heating rate of 5 °C per minute. The heat flow is calculated based on a two point calibration (melting points of In and Zn) using the Mettler-Toledo STARE Software.

Decomposition Temperatures in the experimental part are in relation to the measurements done this way.

**TGA-Measurement** was done on Setaram LapSys 1600 TGA-DSC under argon atmosphere (Heating-rate 5 °C/min).

**X-ray Structure Determination:** X-ray quality crystals were selected in Fomblin YR-1800 perfluoroether (Alfa Aesar) at ambient temperatures. The samples were cooled to 173(2) K during measurement. The data were collected on a Bruker Apex Kappa-II CCD diffractometer using graphite-monochromated  $\text{Mo K}_\alpha$  radiation ( $\lambda = 0.71073 \text{ \AA}$ ). The structures were solved by direct methods (*SHELXS-97*) and refined by full-matrix least squares procedures (*SHELXL-97*). Semi-empirical absorption corrections were applied (SADABS). All non hydrogen atoms were refined anisotropically, hydrogen atoms were included in the refinement at calculated positions using a riding model.

The position of a trimethylsilyl group in **1b** was found to be disordered and was split in two parts. The occupancy of each part was refined freely (C9/C10/C11: 0.834(7)/0.166(7)).

The position of the tetracyanoethylene group in **2** was found to be disordered and was split in two parts. The occupancy of each part was refined freely (C1/C2/C3/N1/N2: 0.662(5)/0.338(5)).

The position of a thf molecule in **3-8thf** was found to be disordered and was split in two parts. The occupancy of each part was refined freely (C15/C16/C17/C18: 0.637(8)/0.363(8)). The positions of two thf molecules in **3-8thf**

were found to be disordered and were split in three parts. The occupancy of each part was refined freely (C11/C12/C13/C14: 0.430(4)/0.313(8)/0.257(7), C19/C20/C21/C22: 0.668(3)/0.185(4)/0.147(4)).

The position of a thf molecule in **4·0.85thf·0.15Et<sub>2</sub>O** was found to be disordered and partially displaced by Et<sub>2</sub>O and was split in five parts. The occupancy of each part was refined freely (O5/C13/C14/C15/C16: 0.346(3)/0.180(6)/0.148(4)/0.181(7)/0.146(2)).

**Synthesis of Me<sub>3</sub>SiO–C(CN)<sub>3</sub> (1a).** Trimethylsilyl cyanide (20 g, 201.6 mmol, 3 equiv.) was placed into a Schlenk flask and dissolved in 25 ml toluene. A magnetic stirrer was added and the mixture was cooled to –70 °C. A dropping funnel was loaded with a phosgene solution (20 % in toluene, 33.3 g, 67.3 mmol, 1 equiv.), then placed on top of the flask and the phosgene solution was added dropwise to the trimethylsilyl cyanide. The reaction mixture was stirred at –70 °C for 1 hour and then allowed to warm up to room temperature. The volatile compounds were condensed into another flask *in vacuo*. At reduced pressure (70 mbar) toluene was removed from this mixture. Distillation of the residue at 15 mbar and 60 °C gives the colourless, liquid product **1a**. After distillation of **1a** few crystals of **1b** were obtained from a residual red oil. Yield: 7.68 g (64 %). **T<sub>Mp</sub>** –14.5 °C. **Anal. calc. % (found):** C, 46.90 (46.26); H, 5.06 (4.67); N, 23.44 (22.65). **<sup>1</sup>H NMR** (CDCl<sub>3</sub>, 300 MHz, 25 °C, ppm): δ = 0.49 (s, –Si–CH<sub>3</sub>, 9H). **<sup>13</sup>C NMR** (CDCl<sub>3</sub>, 250 MHz, 25 °C, ppm): δ = 109.00 (s, –CN, 3C); 51.74 (s, –C–CN, 1C); 0.19 (s, –Si–CH<sub>3</sub>, 3C). **<sup>29</sup>Si NMR** (CDCl<sub>3</sub>, 300 MHz, 25 °C, ppm): δ = 38.0 (s, –Si–CH<sub>3</sub>). **IR** (ATR, cm<sup>–1</sup>):  $\tilde{\nu}$  = 2967 (w), 2250 (m), 1417 (w), 1275 (m), 1261 (s), 1139 (vs), 1057 (s), 1026 (s), 845 (vs), 760 (s), 732 (m), 695 (m), 657 (m), 634 (s), 560 (m). **Raman** (473 nm, 6 mW, 25 °C, 8 scans, cm<sup>–1</sup>):  $\tilde{\nu}$  = 2975 (3), 2967 (3), 2909 (10), 2252 (9), 1416 (1), 1247 (1), 1149 (1), 1142 (1), 1061 (1), 1003 (1), 956 (1), 857 (1), 812 (1), 796 (1), 788 (1), 763 (1), 699 (1), 636 (8), 585 (3), 449 (3), 312 (1), 293 (1), 236 (1), 222 (2), 186 (2), 127 (10), 79 (1).

**Synthesis of Me<sub>3</sub>SiO–C<sub>2</sub>(CN)<sub>4</sub>–N=C(CN)–OSiMe<sub>3</sub> (1b).** After distillation of **1a** few crystals of **1b** were obtained from a residual red oil. Some crystals were taken for X-ray crystallography. The red oil coexisting beside the remaining crystals was tried to wash off with small amounts of *n*-hexane, according to the procedure for **2**. Unfortunately also the crystals of **1b** dissolved in *n*-hexane and no recrystallization was obtained after removal of the solvent. The impurities did not allow a reliable correlation of the signals in <sup>1</sup>H, <sup>13</sup>C and <sup>29</sup>Si NMR of the mixture.

**Synthesis of Me<sub>3</sub>SiO–C<sub>2</sub>(CN)<sub>4</sub>–OSiMe<sub>3</sub> (2).** Trimethylsilyl cyanide (25 g, 252 mmol, 4 equiv.) and a magnetic stirrer were placed into a Schlenk flask. A dropping funnel was installed on top of the flask and loaded with oxalyl chloride (8.02 g, 63 mmol, 1 equiv.). The oxalyl chloride was added slowly under stirring. The reaction mixture was kept at ambient temperature with an ice bath during addition. After the oxalyl chloride was added the mixture was stirred over night. A white crystalline precipitate was formed and filtered off. The filtrate was stored at room temperature for 3 days to obtain more crystallized product from the mother liquor that was filtered off. Once more the mother liquor was stored for 3 days and the crystallized product was filtered off. The crude product was washed with 20 ml cooled *n*-hexane and sublimated at 10<sup>–3</sup> mbar heated with a hot water bath. After sublimation the white crystalline 1,1,2,2-tetracyano-1,2-bis(trimethylsiloxy)ethane was obtained. Yield: 15.06 g (78 %). **T<sub>Mp</sub>** 122.1 °C. **Anal. calc. % (found):** C, 47.03 (46.99); H, 5.92 (6.07); N, 18.28 (17.91). **<sup>1</sup>H NMR** (CDCl<sub>3</sub>, 300 MHz, 25 °C, ppm): δ = 0.47 (s, –Si–CH<sub>3</sub>, 18H). **<sup>13</sup>C NMR** (CDCl<sub>3</sub>, 300 MHz, 25 °C, ppm): δ = 110.97 (s, –CN, 4C); 70.15 (s, –C–CN, 2C); 0.18 (s, –Si–CH<sub>3</sub>, 6C). **<sup>29</sup>Si NMR** (CDCl<sub>3</sub>, 300 MHz, 25 °C, ppm): δ = 36.8 (s, –Si–CH<sub>3</sub>). **IR** (ATR, cm<sup>–1</sup>):  $\tilde{\nu}$  = 2251 (m), 1456 (w), 1417 (m), 1258 (s), 1251 (s), 1175 (vs), 1064 (m), 1018 (s), 899 (s), 838 (vs), 759 (s), 710 (s), 693 (s), 664 (m), 628 (s), 571 (s). **Raman** (784 nm, 65 mW, 25 °C, 4 scans, cm<sup>–1</sup>):  $\tilde{\nu}$  = 2972 (1), 2906 (4), 2248 (2), 2238 (2), 1412 (1), 1273 (1), 1260 (1), 1172 (1), 1071 (3), 875 (1), 851 (1), 827 (1), 763 (1), 757 (1), 704 (1), 694 (1), 634 (8), 579 (5), 561 (2), 491 (1), 461 (1), 313 (2), 302 (1), 284 (2), 248 (4), 219 (3), 175 (5), 144 (10), 125 (7), 103 (1), 67 (2).

**Synthesis of Na<sub>2</sub>[B<sub>2</sub>(OMe)<sub>2</sub>(tceg)<sub>3</sub>] (3).** A magnetic stirrer and sodium tetra-methoxy-borate (3 g, 19 mmol, 1 equiv.) were placed into a Schlenk flask, dissolved in 50 ml thf and cooled to –70 °C. On top of the flask a dropping funnel was installed and loaded with a solution of 1,1,2,2-tetracyano-1,2-bis(trimethylsiloxy)ethane (14.55 g, 47.5 mmol, 2.5 equiv.) in 60 ml thf. The 1,1,2,2-tetracyano-1,2-bis(trimethylsiloxy)ethane was added dropwise under stirring. The reaction mixture was stirred at –70 °C for 2 hours and then allowed to warm up to room temperature. After stirring for 24 hours the solvent was removed *in vacuo*. The resulting solid was washed two times with 20 ml CH<sub>2</sub>Cl<sub>2</sub> and dried *in vacuo*. The raw product was dissolved in 10 ml thf and 50 ml CH<sub>2</sub>Cl<sub>2</sub> was added to form a colourless precipitate. The precipitate was filtered off and dried at 10<sup>–3</sup> mbar and 120 °C for 2 hours to give the solvent free diborate. Yield: 5.04 g (87 %). **T<sub>Dec</sub>** 208.6 °C. **Anal. calc. % (found):** C, 39.38 (39.91); H, 0.99 (1.99); N, 27.56 (24.95). **<sup>1</sup>H NMR** (DMSO-*d*<sub>6</sub>, 250 MHz, 25 °C, ppm): δ = 3.19 (s, –O–CH<sub>3</sub>, 6H). **<sup>13</sup>C NMR** (DMSO-*d*<sub>6</sub>, 250 MHz, 25 °C, ppm): δ = 113.16 (s, –CN, 4C); 112.37 (s, –CN, 4C); 112.31 (s, –

$\underline{\text{CN}}$ , 4C); 72.31 (s,  $-\underline{\text{C}}-\text{CN}$ , 4C); 69.78 (s,  $-\underline{\text{C}}-\text{CN}$ , 2C); 49.09 (s,  $-\text{O}-\underline{\text{C}}\text{H}_3$ , 2C).  $^{11}\text{B}$  NMR (DMSO- $d_6$ , 250 MHz, 25°C):  $\delta$  = 7.89 (s). IR (ATR,  $\text{cm}^{-1}$ ):  $\tilde{\nu}$  = 2987 (w), 2948 (w), 2916 (w), 2849 (w), 2256 (w), 1626 (w), 1466 (w), 1244 (m), 1231 (m), 1196 (m), 1148 (vs), 1091 (s), 1032 (vs), 1016 (vs), 951 (vs), 900 (s), 864 (s), 762 (m), 699 (m), 682 (m), 655 (m), 563 (m), 544 (m). Raman (784 nm, 65 mW, 25 °C, 5 scans,  $\text{cm}^{-1}$ ):  $\tilde{\nu}$  = 2274 (10), 1475 (2), 1262 (1), 1191 (1), 1152 (1), 1101 (1), 1045 (1), 979 (3), 963 (3), 934 (2), 905 (1), 729 (1), 663 (3), 636 (2), 618 (2), 589 (2), 510 (2), 481 (3), 438 (4), 367 (1), 335 (1), 289 (2), 243 (1), 203 (4), 161 (8).

**Synthesis of Na[B(tceg) $_2$ ] (4).** The diborate **3** (4 g, 6.55 mmol, 1 equiv.) and 1,1,2,2-tetracyano-1,2-bis(trimethylsiloxy)ethane (4 g, 13.1 mmol, 2 equiv.) were placed into a Schlenk flask. A magnetic stirrer was added and the compounds were dissolved in 50 ml thf. The mixture was heated to reflux for 18 hours and refluxing was stopped when the signal at 7.9 ppm in the  $^{11}\text{B}$  NMR spectrum disappeared. The solvent was removed and the resulting solid was washed two times with 20 ml  $\text{CH}_2\text{Cl}_2$ . The washed raw product was dissolved in 7 ml thf. After addition of 25 ml  $\text{Et}_2\text{O}$  the product crystallized. The crystals were separated and dried at  $10^{-3}$  mbar and 120 °C for 2 hours to give the solvent free borate. Yield: 3.4 g (73 %).  $T_{\text{Dec}}$  304.8 °C. Anal. calc. % (found): C, 40.72 (38.63); H, 0 (1.04); N, 31.66 (29.11).  $^{13}\text{C}$  NMR (DMSO- $d_6$ , 300 MHz, 25 °C, ppm):  $\delta$  = 112.12 (s,  $-\underline{\text{C}}\text{N}$ , 8C); 72.42 (s,  $-\underline{\text{C}}-\text{CN}$ , 4C).  $^{11}\text{B}$  NMR (DMSO- $d_6$ , 300 MHz, 25°C):  $\delta$  = 11.94 (s). IR (ATR,  $\text{cm}^{-1}$ ):  $\tilde{\nu}$  = 2271 (w), 2254 (w), 1624 (w), 1198 (w), 1174 (m), 1071 (vs), 1054 (vs), 974 (s), 957 (vs), 928 (s), 814 (w), 717 (m), 683 (w), 634 (m), 568 (m), 531 (w). Raman (784 nm, 65 mW, 25 °C, 4 scans,  $\text{cm}^{-1}$ ):  $\tilde{\nu}$  = 2273 (1), 2256 (1), 1270 (1), 1198 (2), 979 (1), 816 (1), 1101 (1), 1045 (1), 979 (3), 816 (1), 662 (2), 572 (1), 494 (1), 486 (1), 476 (1), 468 (1), 431 (1), 425 (1), 323 (1), 268 (1), 237 (1), 174 (1), 161 (2), 142 (4), 129 (10), 105 (4), 68 (2), 66 (2).

**General procedure for the synthesis of imidazolium and ammonium salts.** A Schlenk flask was loaded with Na[B(tceg) $_2$ ] (1.95 g, 5.5 mmol, 1.1 equiv.) and dissolved in 10 ml  $\text{CH}_3\text{CN}$ . The imidazolium or ammonium chlorides (5 mmol, 1 equiv.) were dissolved in 10 ml  $\text{CH}_3\text{CN}$  and added to this solution. Except for  $\text{Me}_4\text{NCl}$ , which was suspended in  $\text{CH}_3\text{CN}$ , then the borate in  $\text{CH}_3\text{CN}$  was added and the suspension was heated to reflux for 3 h. The reaction mixture was stirred over night and the precipitated NaCl was filtered off. The solvent was removed *in vacuo*. The residual oils or solids were dissolved in 5 ml  $\text{CH}_3\text{CN}$ , filtrated and the solvent was removed again. The excess of Na[B(tceg) $_2$ ] was removed by dissolving the product in 5 ml  $\text{CH}_2\text{Cl}_2$  and filtering off the sodium salt. After removal of the solvents *in vacuo* the products were dried for 2 h at 80 °C and  $10^{-3}$  mbar. Yields: 88 – 93 %.

**EMIm[B(tceg) $_2$ ] (5).**  $T_{\text{Mp}}$  (onset) 64.1 °C, (peak) 66.4 °C.  $T_{\text{Dec}}$  (onset) 222.3 °C. Anal. calc. % (found): C, 48.90 (48.81); H, 2.51 (3.14); N, 31.68 (30.65).  $^1\text{H}$  NMR (DMSO- $d_6$ , 300 MHz, 25°C):  $\delta$  = 9.10 (s,  $\text{MeN}-\underline{\text{C}}\text{H}-\text{NEt}$ , 1H); 7.77 (t,  $\text{MeN}-\underline{\text{C}}\text{H}-\text{CH}$ , 1H,  $^3J_{\text{CHCH}} = 1.77$  Hz); 7.68 (t,  $\text{EtN}-\underline{\text{C}}\text{H}-\text{CH}$ , 1H,  $^3J_{\text{CHCH}} = 1.77$  Hz); 4.19 (q,  $-\text{N}-\underline{\text{C}}\text{H}_2-\text{CH}_3$ , 2H),  $^3J_{\text{CHCH}} = 7.30$  Hz); 3.84 (s,  $-\text{N}-\underline{\text{C}}\text{H}_3$ , 3H); 1.41 (t,  $-\text{N}-\text{CH}_2-\underline{\text{C}}\text{H}_3$ , 3H,  $^3J_{\text{CHCH}} = 7.30$  Hz).  $^{13}\text{C}$  NMR (DMSO- $d_6$ , 300 MHz, 25 °C, ppm):  $\delta$  = 136.21 (s,  $\text{MeN}-\underline{\text{C}}\text{H}-\text{NEt}$ ); 123.56 (s,  $\text{MeN}-\underline{\text{C}}\text{H}-\text{CH}$ ); 121.96 (s,  $\text{EtN}-\underline{\text{C}}\text{H}-\text{CH}$ ); 112.12 (s,  $-\underline{\text{C}}\text{N}$ , 8C); 72.42 (s,  $-\underline{\text{C}}-\text{CN}$ , 4C); 44.12 (s,  $-\text{N}-\underline{\text{C}}\text{H}_2-\text{CH}_3$ ); 35.68 (s,  $-\text{N}-\underline{\text{C}}\text{H}_3$ ); 15.08 (s,  $-\text{N}-\text{CH}_2-\underline{\text{C}}\text{H}_3$ ).  $^{11}\text{B}$  NMR (DMSO- $d_6$ , 300 MHz, 25°C):  $\delta$  = 11.96 (s). IR (ATR,  $\text{cm}^{-1}$ ):  $\tilde{\nu}$  = 3175 (w), 3157 (w), 3138 (w), 3102 (w), 2962 (w), 2251 (m), 1603 (w), 1574 (m), 1564 (m), 1462 (w), 1435 (w), 1392 (w), 1347 (w), 1319 (w), 1259 (m), 1164 (s), 1136 (m), 1060 (vs), 993 (s), 961 (vs), 925 (s), 843 (m), 828 (s), 798 (s), 744 (s), 718 (s), 698 (m), 667 (m), 646 (m), 619 (s), 560 (m). Raman (784 nm, 32.5 mW, 25 °C, 4 scans,  $\text{cm}^{-1}$ ):  $\tilde{\nu}$  = 3181 (1), 3133 (1), 2994 (1), 2973 (1), 2953 (1), 2247 (6), 1576 (1), 1463 (2), 1451 (1), 1413 (3), 1388 (2), 1349 (1), 1333 (1), 1294 (1), 1269 (1), 1186 (1), 1156 (1), 1113 (1), 1090 (1), 1037 (1), 1025 (2), 997 (3), 986 (2), 967 (1), 859 (1), 719 (1), 700 (1), 672 (4), 597 (1), 561 (1), 497 (1), 480 (2), 450 (1), 430 (3), 411 (1), 374 (1), 336 (1), 291 (2), 284 (2), 242 (1), 230 (4), 178 (1), 138 (10), 74 (4).

**BMIm[B(tceg) $_2$ ] (6).**  $T_{\text{G}}$  (onset) -37.4 °C, (peak) -34.3 °C.  $T_{\text{Mp}}$  (onset) 44.2 °C, (peak) 45.4 °C.  $T_{\text{Dec}}$  (onset) 241.5 °C. Anal. calc. % (found): C, 51.09 (50.78); H, 3.22 (3.24); N, 29.79 (28.96).  $^1\text{H}$  NMR (DMSO- $d_6$ , 300 MHz, 25°C):  $\delta$  = 9.10 (s,  $\text{MeN}-\underline{\text{C}}\text{H}-\text{NBu}$ , 1H); 7.76 (t,  $\text{MeN}-\underline{\text{C}}\text{H}-\text{CH}$ , 1H,  $^3J_{\text{CHCH}} = 1.76$  Hz); 7.69 (t,  $\text{BuN}-\underline{\text{C}}\text{H}-\text{CH}$ , 1H,  $^3J_{\text{CHCH}} = 1.76$  Hz); 4.15 (t,  $-\text{N}-\underline{\text{C}}\text{H}_2-\text{CH}_2$ , 2H,  $^3J_{\text{CHCH}} = 7.17$  Hz); 3.84 (s,  $-\text{N}-\underline{\text{C}}\text{H}_3$ , 3H); 1.71–1.82 (m,  $-\text{N}-\text{CH}_2-\underline{\text{C}}\text{H}_2$ , 2H); 1.20–1.33 (m,  $-\text{CH}_2-\underline{\text{C}}\text{H}_2-\text{CH}_3$ , 2H); 0.90 (t,  $-\text{CH}_2-\underline{\text{C}}\text{H}_3$ , 3H,  $^3J_{\text{CHCH}} = 7.35$  Hz).  $^{13}\text{C}$  NMR (DMSO- $d_6$ , 300 MHz, 25 °C, ppm):  $\delta$  = 136.49 (s,  $\text{MeN}-\underline{\text{C}}\text{H}-\text{NEt}$ ); 123.61 (s,  $\text{MeN}-\underline{\text{C}}\text{H}-\text{CH}$ ); 122.61 (s,  $\text{BuN}-\underline{\text{C}}\text{H}-\text{CH}$ ); 112.13 (s,  $-\underline{\text{C}}\text{N}$ , 8C); 72.42 (s,  $-\underline{\text{C}}-\text{CN}$ , 4C); 48.49 (s,  $-\text{N}-\underline{\text{C}}\text{H}_2-\text{CH}_2$ ); 35.74 (s,  $-\text{N}-\underline{\text{C}}\text{H}_3$ ); 31.34 (s,  $-\text{N}-\text{CH}_2-\underline{\text{C}}\text{H}_2$ ); 18.76 (s,  $-\text{CH}_2-\underline{\text{C}}\text{H}_2-\text{CH}_3$ ); 13.24 (s,  $-\text{CH}_2-\underline{\text{C}}\text{H}_3$ ).  $^{11}\text{B}$  NMR (DMSO- $d_6$ , 300 MHz, 25°C):  $\delta$  = 11.92 (s). IR (ATR,  $\text{cm}^{-1}$ ):  $\tilde{\nu}$  = 3159 (w), 3120 (w), 2966 (w), 2938 (w), 2878 (w), 2251 (w), 1595 (w), 1566 (m), 1466 (w), 1428 (w), 1384 (w), 1337 (w), 1164 (m), 1066 (vs), 959 (vs), 923 (s), 833 (m), 743 (m), 716 (m), 696 (w), 671 (w), 649 (m), 622 (s), 561 (m). Raman (632 nm, 120  $\mu\text{W}$ , 25 °C, 4 scans,  $\text{cm}^{-1}$ ):  $\tilde{\nu}$  = 2255 (2), 2247 (2), 1568 (1), 1449 (1), 1428 (1), 1418 (1), 1388 (1), 1340 (1), 1280 (1), 1189 (1), 1162 (1), 1154 (1), 1114 (1), 1106 (1), 1029 (1), 1019 (2), 981 (2), 977 (2), 902 (1), 880 (1), 717 (1), 658 (5), 619 (1), 579 (1), 504 (1), 481 (2), 439 (2), 425 (2), 419 (1), 319 (2), 286 (2), 269 (1), 238 (2), 228 (10), 219 (4).



**OMIm[B(tcgg)] (7).**  $T_G$  (onset)  $-52.2$  °C, (peak)  $-46.8$  °C.  $T_{Dec}$  (onset)  $257.1$  °C. **Anal. calc. % (found):** C, 54.77 (54.32); H, 4.40 (4.18); N, 26.61 (25.83).  **$^1H$  NMR** (DMSO- $d_6$ , 300 MHz, 25 °C):  $\delta$  = 9.14 (s, MeN- $\underline{CH}$ -NOct, 1H); 7.76 (t, MeN- $\underline{CH}$ -CH, 1H,  $^3J_{CHCH}$  = 1.75 Hz); 7.69 (t, OctN- $\underline{CH}$ -CH, 1H,  $^3J_{CHCH}$  = 1.75 Hz); 4.15 (t, -N- $\underline{CH_2}$ -CH $_2$ , 2H,  $^3J_{CHCH}$  = 7.23 Hz); 3.85 (s, -N- $\underline{CH_3}$ , 3H); 1.72–1.83 (m, -N-CH $_2$ - $\underline{CH_2}$ , 2H); 1.18–1.33 (m, - $\underline{CH_2}$ - $\underline{CH_2}$ - $\underline{CH_2}$ - $\underline{CH_2}$ - $\underline{CH_2}$ -CH $_3$ , 10H); 0.86 (t, -CH $_2$ - $\underline{CH_3}$ , 3H,  $^3J_{CHCH}$  = 6.74 Hz).  **$^{13}C$  NMR** (DMSO- $d_6$ , 300 MHz, 25 °C, ppm):  $\delta$  = 136.50 (s, MeN- $\underline{CH}$ -NOct); 123.59 (s, MeN- $\underline{CH}$ -CH); 122.45 (s, OctN- $\underline{CH}$ -CH); 112.11 (s, - $\underline{CN}$ , 8C); 72.42 (s, - $\underline{C}$ -CN, 4C); 48.77 (s, -N- $\underline{CH_2}$ -CH $_2$ ); 35.73 (s, -N- $\underline{CH_3}$ ); 31.14 (s, -N-CH $_2$ - $\underline{CH_2}$ ); 29.37 (s, -N-CH $_2$ -CH $_2$ - $\underline{CH_2}$ ); 28.45 (s, -N-CH $_2$ -CH $_2$ -CH $_2$ - $\underline{CH_2}$ ); 28.31 (s, - $\underline{CH_2}$ -CH $_2$ -CH $_2$ -CH $_3$ ); 25.48 (s, - $\underline{CH_2}$ -CH $_2$ -CH $_3$ ); 22.03 (s, - $\underline{CH_2}$ -CH $_3$ ); 13.90 (s, -CH $_2$ - $\underline{CH_3}$ ).  **$^{11}B$  NMR** (DMSO- $d_6$ , 300 MHz, 25 °C):  $\delta$  = 11.96 (s). **IR** (ATR,  $cm^{-1}$ ):  $\tilde{\nu}$  = 3159 (w), 3118 (w), 2956 (w), 2929 (m), 2857 (w), 2250 (w), 1713 (w), 1593 (w), 1568 (m), 1466 (w), 1427 (w), 1377 (w), 1337 (w), 1162 (m), 1067 (vs), 960 (s), 921 (m), 833 (m), 743 (m), 716 (m), 695 (w), 684 (w), 649 (m), 622 (m), 561 (w). **Raman** (632 nm, 1.2 mW, 25 °C, 4 scans,  $cm^{-1}$ ):  $\tilde{\nu}$  = 2964 (1), 2934 (2), 2856 (1), 2240 (2), 1416 (10), 1386 (10), 1108 (1), 1085 (1), 1021 (2), 871 (1), 840 (1), 811 (1), 783 (1), 660 (1), 643 (2), 622 (2), 598 (2), 552 (1), 482 (1), 419 (2), 364 (1), 291 (1).

**Me $_4$ N[B(tcgg)] (8).**  $T_{Mp}$  (onset)  $169.6$  °C, (peak)  $172.6$  °C.  $T_{Dec}$  (onset)  $270.3$  °C. **Anal. calc. % (found):** C, 47.43 (47.20); H, 2.99 (3.12); N, 31.12 (30.49).  **$^1H$  NMR** (DMSO- $d_6$ , 300 MHz, 25 °C):  $\delta$  = 3.09 (s, -N- $\underline{CH_3}$ , 12H).  **$^{13}C$  NMR** (DMSO- $d_6$ , 300 MHz, 25 °C, ppm):  $\delta$  = 112.13 (s, - $\underline{CN}$ , 8C); 72.42 (s, - $\underline{C}$ -CN, 4C); 54.39 (t, -N- $\underline{CH_3}$ ,  $^1J_{CN}$  = 3.94 Hz).  **$^{11}B$  NMR** (DMSO- $d_6$ , 300 MHz, 25 °C):  $\delta$  = 11.98 (s). **IR** (ATR,  $cm^{-1}$ ):  $\tilde{\nu}$  = 3053 (w), 2313 (w), 2253 (w), 1486 (s), 1454 (w), 1420 (w), 1189 (w), 1162 (m), 1132 (m), 1100 (s), 1064 (vs), 961 (vs), 947 (vs), 816 (w), 738 (w), 715 (m), 696 (w), 676 (m), 633 (m), 559 (w), 540 (w). **Raman** (784 nm, 65 mW, 25 °C, 4 scans,  $cm^{-1}$ ):  $\tilde{\nu}$  = 2253 (2), 2243 (2), 1448 (2), 1258 (1), 1184 (1), 977 (2), 971 (2), 951 (1), 945 (2), 748 (5), 711 (1), 656 (6), 566 (2), 560 (1), 473 (2), 432 (4), 412 (1), 367 (1), 363 (1), 313 (2), 305 (1), 285 (3), 275 (1), 268 (1), 237 (1), 222 (10), 172 (2), 155 (6), 152 (6), 146 (5), 119 (10).

**Et $_4$ N[B(tcgg)] (9).**  $T_{Mp}$  (onset)  $135.7$  °C, (peak)  $140.0$  °C.  $T_{Dec}$  (onset)  $248.3$  °C. **Anal. calc. % (found):** C, 52.08 (51.76); H, 4.37 (4.45); N, 27.33 (27.88).  **$^1H$  NMR** (DMSO- $d_6$ , 300 MHz, 25 °C):  $\delta$  = 3.20 (q, -N- $\underline{CH_2}$ -CH $_3$ , 8H,  $^3J_{CHCH}$  = 7.28 Hz); 1.16 (tt, -N-CH $_2$ - $\underline{CH_3}$ , 12H,  $^3J_{CHCH}$  = 7.28 Hz,  $^3J_{CHCN}$  = 1.81 Hz).  **$^{13}C$  NMR** (DMSO- $d_6$ , 300 MHz, 25 °C, ppm):  $\delta$  = 112.13 (s, - $\underline{CN}$ , 8C); 72.42 (s, - $\underline{C}$ -CN, 4C); 51.37 (t, -N- $\underline{CH_2}$ -CH $_3$ ,  $^1J_{CN}$  = 2.99 Hz); 7.05 (s, -N-CH $_2$ - $\underline{CH_3}$ ).  **$^{11}B$  NMR** (DMSO- $d_6$ , 300 MHz, 25 °C):  $\delta$  = 11.94 (s). **IR** (ATR,  $cm^{-1}$ ):  $\tilde{\nu}$  = 3018 (w), 2996 (w), 2956 (w), 2248 (w), 1485 (m), 1456 (w), 1441 (m), 1394 (m), 1365 (w), 1173 (m), 1136 (w), 1087 (vs), 1063 (vs), 998 (s), 954 (vs), 923 (s), 783 (m), 715 (m), 698 (w), 667 (w), 647 (w), 635 (w), 561 (w). **Raman** (632 nm, 12 mW, 25 °C, 4 scans,  $cm^{-1}$ ):  $\tilde{\nu}$  = 2255 (10), 1485 (1), 1455 (4), 1385 (1), 1291 (2), 1178 (2), 1134 (1), 1110 (3), 1062 (1), 994 (2), 885 (1), 806 (1), 778 (1), 669 (7), 592 (1), 552 (1), 474 (3), 427 (3), 424 (3), 410 (4), 330 (1), 282 (2), 221 (5), 214 (5), 166 (2), 147 (2), 132 (2), 107 (3).

**Bu $_4$ N[B(tcgg)] (10).**  $T_{Mp}$  (onset)  $90.9$  °C, (peak)  $95.0$  °C.  $T_{Dec}$  (onset)  $270.0$  °C. **Anal. calc. % (found):** C, 58.64 (58.82); H, 6.33 (6.42); N, 21.98 (21.44).  **$^1H$  NMR** (DMSO- $d_6$ , 300 MHz, 25 °C):  $\delta$  = 3.11 – 3.21 (m, -N- $\underline{CH_2}$ , 8H); 1.49 – 1.64 (m, -N-CH $_2$ - $\underline{CH_2}$ , 8H); 1.31 (hex, - $\underline{CH_2}$ -CH $_3$ , 8H,  $^3J_{CHCH}$  = 7.28 Hz); 0.94 (t, -CH $_2$ - $\underline{CH_3}$ , 12H,  $^3J_{CHCH}$  = 7.28 Hz).  **$^{13}C$  NMR** (DMSO- $d_6$ , 300 MHz, 25 °C, ppm):  $\delta$  = 112.13 (s, - $\underline{CN}$ , 8C); 72.42 (s, - $\underline{C}$ -CN, 4C); 57.50 (s, -N- $\underline{CH_2}$ -CH $_3$ ); 23.04 (s, -N-CH $_2$ - $\underline{CH_3}$ ); 19.19 (s, - $\underline{CH_2}$ -CH $_3$ ); 13.47 (s, -CH $_2$ - $\underline{CH_3}$ ).  **$^{11}B$  NMR** (DMSO- $d_6$ , 300 MHz, 25 °C):  $\delta$  = 11.96 (s). **IR** (ATR,  $cm^{-1}$ ):  $\tilde{\nu}$  = 2968 (m), 2937 (m), 2878 (m), 2250 (w), 1470 (m), 1459 (m), 1380 (w), 1320 (w), 1241 (w), 1153 (w), 1133 (w), 1063 (vs), 1003 (s), 943 (s), 908 (m), 894 (m), 887 (m), 875 (m), 813 (m), 757 (w), 736 (m), 716 (m), 692 (w), 679 (w), 659 (w), 630 (w), 568 (w), 555 (w), 537 (w). **Raman** (784 nm, 65 mW, 25 °C, 4 scans,  $cm^{-1}$ ):  $\tilde{\nu}$  = 3003 (1), 2976 (1), 2940 (1), 2879 (1), 2248 (4), 1459 (3), 1447 (2), 1353 (1), 1322 (2), 1271 (1), 1188 (2), 1153 (1), 1132 (1), 1109 (4), 1063 (2), 1033 (1), 1001 (2), 975 (1), 925 (1), 904 (2), 877 (1), 798 (1), 758 (1), 717 (1), 679 (1), 660 (5), 634 (1), 596 (1), 571 (1), 537 (1), 520 (1), 506 (1), 476 (2), 423 (4), 399 (1), 325 (1), 294 (1), 264 (3), 230 (10).

## Acknowledgement

Financial support by the DFG is gratefully acknowledged. We gratefully thank the Lonza AG (Switzerland) for the provision of trimethylsilyl cyanide utilized for this work. We are indebted to Fabian Reiß (University Rostock) and Dr. Ronald Wustrack (University Rostock) for the measurement of Raman spectra.

## References

- [1] J. S. Wilkes, *Green Chemistry* **2002**, *4*, 73–80.
- [2] R. P. Swatloski, S. K. Spear, J. D. Holbrey, R. D. Rogers, *J. Am. Chem. Soc.* **2002**, *124*, 4974–4975.
- [3] a) M. E. Van Valkenburg, R. L. Vaughn, M. Williams, J. S. Wilkes, *Thermochimica Acta* **2005**, *425*, 181–188; b) M. Zhang, R. G. Reddy, *ECS Transactions* **2007**, *2*, 27–34.
- [4] D. Zhao, M. Wu, Y. Kou, E. Min, *Catalysis Today* **2002**, *74*, 157–189.
- [5] N. Madriaa, T. A. Arunkumar, N. G. Nair, A. Vadapalli, Y.-W. Huang, S. C. Jones, V. P. Reddy, *Journal of Power Sources* **2013**, *234*, 277–284.
- [6] X. Li, D. Zhao, Z. Fei, L. Wang, *Science in China Series B: Chemistry* **2006**, *49*, 385–401.
- [7] a) D. Zhao, Z. Fei, T. J. Geldbach, R. Scopelliti, P. J. Dyson, *J. Am. Chem. Soc.* **2004**, *126*, 15876–15882; b) Z. Fei, D. Zhao, D. Pieraccini, W. H. Ang, T. J. Geldbach, R. Scopelliti, C. Chiappe, P. J. Dyson, *Organometallics* **2007**, *26*, 1588–1598; c) C. Premi, N. Jain, *Eur. J. Org. Chem.* **2013**, *78*, 5493–5499; d) C. Chiappe, D. Pieraccini, D. Zhao, Z. Fei, P. J. Dyson, *Adv. Synth. Catal.* **2006**, *348*, 68–74.
- [8] K. Sasaki, S. Matsumura, K. Toshima, *Tetrahedron Letters* **2004**, *45*, 7043–7047.
- [9] H. Bönemann, R. Brinkmann, S. Kinge, T. O. Ely, M. Armand, *Fuell Cells* **2004**, *4*, 289–296.
- [10] M. Karsch, H. Lund, A. Schulz, A. Villinger, K. Voss, *Eur. J. Inorg. Chem.* **2012**, *33*, 5542–5553.
- [11] J. Harloff, M. Karsch, H. Lund, A. Schulz, A. Villinger, *Eur. J. Inorg. Chem.* **2013**, *24*, 4243–4250.
- [12] M. Becker, J. Harloff, T. Jantz, A. Schulz, A. Villinger, *Eur. J. Inorg. Chem.* **2012**, *34*, 5658–5667.
- [13] I. Alkorta, O. Picazo, J. Elguero, *Tetrahedron Asymmetry* **2005**, *16*, 755–760.
- [14] M. T. Mock, R. G. Potter, D. M. Camaioni, J. Li, W. G. Dougherty, W. S. Kassel, B. Twamley, D. L. DuBois, *J. Am. Chem. Soc.* **2009**, *131*, 14454–14465.
- [15] a) M. M. Aminia, M. Sharbatdaran, M. Mirzaee, P. Mirzaei, *Polyhedron* **2006**, *25*, 3231–3237; b) S. Heřmánek, O. Kříž, J. Fusek, Z. Černý, B. Čáseňský, *J. Chem. Soc. Perkin Trans. II* **1989**, 987–992; c) R.-M. Ho, T.-C. Wang, C.-C. Lin, T.-L. Yu, *Macromolecules* **2007**, *40*, 2814–2821; d) D. S. McGuinness, A. J. Rucklidge, R. P. Tooze, A. M. Slawin, *Z. Organometallics* **2007**, *26*, 2561–2569; e) K. Tabatabaieian, M. Mamaghani, A. Pourahamad, *Russ. J. Org. Chem.* **2001**, *37*, 1287–1288; f) S. Gou, J. Wang, X. Liu, W. Wang, F.-X. Chen, X. Feng, *Adv. Synth. Catal.* **2007**, *349*, 343–349; g) E. Keller, N. Veldman, A. L. Spek, B. L. Feringa, *Tetrahedron: Asymmetry* **1997**, *8*, 3403–3413.
- [16] N. Malek, T. Maris, M. Simard, J. D. Wuest, *J. Am. Chem. Soc.* **2005**, *127*, 5910–5916.
- [17] E. Bernhardt, G. Henkel, H. Willner, *Z. Anorg. Allgem. Chem.* **2000**, *626*, 560–568.
- [18] a) Y. Y. Karabach, M. Fatima, C. Guedes da Silva, M. N. Kopylovich, B. Gil-Hernandez, J. Sanchiz, A. M. Kirillov, A. J. L. Pombeiro, *Inorg. Chem.* **2010**, *49*, 11096–11105; b) H. Dan, S. Nishikiori, O. Yamamuro, *Dalton Trans.* **2011**, *40*, 1168–1174; c) P. K. Thallapally, R. Kishan Motkuri, C. A. Fernandez, B. P. McGrail, G. S. Behrooz, *Inorg. Chem.* **2010**, *49*, 4909–4915; d) B. F. Hoskins, R. Robson, *J. Am. Chem. Soc.* **1990**, *112*, 1546–1554.
- [19] a) S. R. Batten, B. F. Hoskins, R. Robson, *New J. Chem.* **1998**, 173–175; b) B. F. Abrahams, S. R. Batten, B. F. Hoskins, R. Robson, *Inorg. Chem.* **2003**, *42*, 2654–2664.
- [20] a) F.-Q. Liu, T. D. Tilley, *Inorg. Chem.* **1997**, *36*, 5090–5096; b) F.-Q. Liu, T. D. Tilley, *Chem. Commun.* **1998**, 103–104.
- [21] I. M. Malkowsky, R. Fröhlich, U. Griesbach, H. Pütter, S. R. Waldvogel, *Eur. J. Inorg. Chem.* **2006**, *8*, 1690–1697.
- [22] C. A. Angell, W. Xu, US2004/0034253 A1.
- [23] W. Lidy, W. Sundermeyer, *Chem. Ber.* **1973**, *106*, 587–593.
- [24] P. Pyykkö, M. Atsumi, *Chem. Eur. J.* **2009**, *15*, 12770–12779.
- [25] a) V. M. Goldschmidt, *Chem. Ber.* **1927**, *60*, 1263–1296; b) R. D. Shannon, *Acta Cryst.* **1976**, *A32*, 751–767; c) L. Glasser, H. D. B. Jenkins, *Inorg. Chem.* **2008**, *47*, 6195–6202.
- [26] a) H. D. B. Jenkins, L. Glasser, T. M. Klapötke, M.-J. Crawford, K. K. Bhasin, J. Lee, G. J. Schrobilgen, L. S. Sunderlin, J. F. Liebman, *Inorg. Chem.* **2004**, *43*, 6238–6248; b) H. D. Jenkins, J. F. Liebman, *Inorg. Chem.* **2005**, *44*, 6359–6372.
- [27] A. Bernsdorf, H. Brand, R. Hellmann, M. Köckerling, A. Schulz, A. Villinger, K. Voss, *J. Am. Chem. Soc.* **2009**, *131*, 8958–8970.
- [28] D. W. M. Hofmann, *Acta Cryst.* **2002**, *B58*, 489–493.
- [29] U. Preiss, J. M. Slattey, I. Krossing, *Ind. Eng. Chem. Res.* **2009**, *48*, 2290–2296.

## 6 Anhang

### **Coordination Networks Based on Nitrile Functionalized Borate Anions**

Jörg Harloff, Markus Karsch, Henrik Lund, Axel Schulz, Alexander Villinger.

*Z. Anorg. Allg. Chem.* **2013**, eingereicht.

Eine weitere Publikation, deren Ergebnisse ebenfalls im 4. Kapitel aufgeführt sind, steht noch zur Veröffentlichung aus. In dieser bereits eingereichten Arbeit wurden, bis auf die Synthese und Charakterisierung des 5-Hydroxy-isophthalonitrils, sämtliche experimentellen Arbeiten von mir durchgeführt. Mit Ausnahme von 5-Hydroxy-isophthalonitril wurden alle Verbindungen, von denen im Manuskript die Kristallstruktur beschrieben ist, von mir für die Röntgenstrukturanalytik kristallisiert.

Das vorliegende Manuskript zur Publikation wurde von mir als Erstautor verfasst. Zudem wurde von mir ein Supporting verfasst, das sämtliche Darstellungen der Verbindungen und die analytischen Daten beinhaltet. Der eigene Anteil liegt bei ca. 80 %.

## Coordination Networks Based on Nitrile Functionalized Borate Anions

Jörg Harloff,<sup>[a]</sup> Markus Karsch,<sup>[a]</sup> Henrik Lund,<sup>[a]</sup> Axel Schulz,<sup>[a,b]\*</sup>, Alexander Villinger<sup>[a]</sup>

Dedicated to Prof. Ingo-Peter Lorenz on the occasion of his 70<sup>th</sup> birthday

**Abstract.** Salts of cyano borates bear potential of forming coordination polymers with solvent filled voids as a source for porous materials. Herein we describe the synthesis and properties of novel cyano borates Na[H–B(O–C<sub>12</sub>H<sub>8</sub>–CN)<sub>3</sub>], Na[B(O–C<sub>12</sub>H<sub>8</sub>–CN)<sub>4</sub>] (C<sub>12</sub>H<sub>8</sub> = biphenyl) and Na[B{O–C<sub>6</sub>H<sub>3</sub>–(CN)<sub>2</sub>}<sub>4</sub>], as well as a new modification of Na[B(O–C<sub>6</sub>H<sub>4</sub>–CN)<sub>4</sub>]. Crystal structures of the sodium borates and the starting materials HO–C<sub>6</sub>H<sub>3</sub>–(CN)<sub>2</sub> and HO–C<sub>12</sub>H<sub>8</sub>–CN (new modification) are discussed as well. Data of nitrogen sorption experiments revealed a notable surface area in solvent free Na[H–B(O–C<sub>12</sub>H<sub>8</sub>–CN)<sub>3</sub>].

**Keywords:** borates / coordination chemistry / sorption experiments / porous materials / structure

[a] Institut für Chemie  
Universität Rostock  
18059 Rostock, A.-Einstein-Str. 3a  
Fax: (+)49-(0)381/498-6381  
E-mail: axel.schulz@uni-rostock.de

[b] Leibniz-Institut für Katalyse e.V.  
18059 Rostock, A.-Einstein-Str. 29a  
Fax: (+)49-(0)381/498-6381

## Introduction

Coordination polymers offer a wide range of applications in diverse fields due to their potential of specific and interesting properties, such as luminescence, magnetism or tunable porosity.<sup>[1]</sup> Combined with their high thermal stability, this provides them as perfect materials in LED's, superconductors or molecular storage media. However, cyanide is one of the most applied ligands for the formation of coordination polymers. Furthermore, nitrile functionalized ligands show their potential as suitable building units in coordination polymers.<sup>[2]</sup> For example cyanide bridged copper was found to form coordination polymers with luminescence properties of a wide spectroscopic range depending on a co-ligand.<sup>[3]</sup> Also materials with ferromagnetic properties are accessible through coordination polymers with cyano bridged transition metals. Some of them show changes in magnetic ordering as well as their color depending on solvation and can be utilized as magnetic color sensors.<sup>[4]</sup> Nevertheless, the capability of uptaking small molecules is one of the most favorable abilities researched in coordination polymer chemistry. For example porous coordination polymers are attracting attention in molecular separation, heterogeneous catalysis, solvent and gas storage, while additional functions in porous coordination polymers like gas sensing, chiral separation and the already mentioned magnetic molecular sensing offer special applications in diverse fields.<sup>[2c,5]</sup> Prussian blue and its analogues, for example  $\text{Ni}_3[\text{Re}_6\text{Se}_8(\text{CN})_6]_2$ , show a large uptake of solvent molecules which can be easily removed, remaining porous material as well as magnetic properties.<sup>[6]</sup>

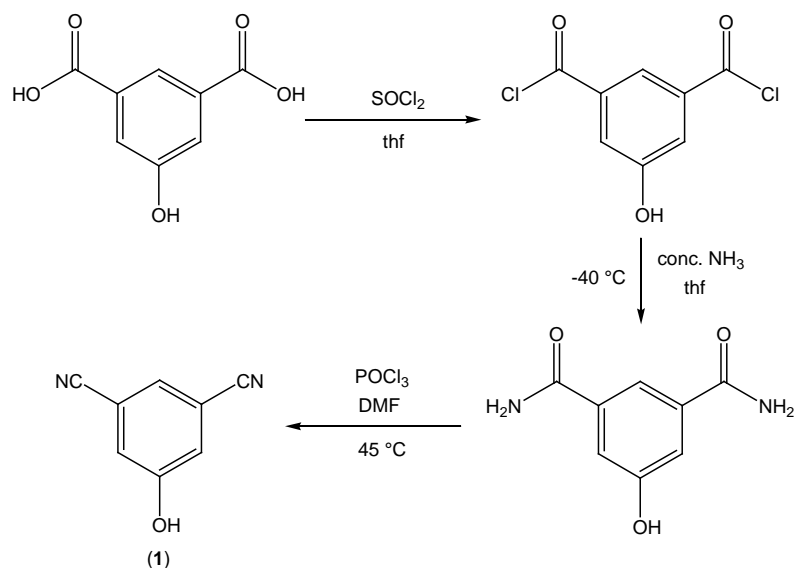
We recently studied the synthesis, structures and properties of several coordination polymers based on cyano borates of the type  $\text{Na}[\text{B}(\text{O}-\text{X}-\text{CN})_4]$  ( $\text{X} = \text{C}_6\text{H}_4, \text{C}_2\text{H}_4$ )<sup>[7,8]</sup> as well as the nitrile rich borates  $\text{Na}[\text{B}(\text{tceg})_2]$  and  $\text{Na}_2[\text{B}_2(\text{OMe})_2(\text{tceg})_3]$  (tceg = tetracyanoethylene glycolate).<sup>[9]</sup> These studies examined the potential in cyanoborates for the formation of porous coordination networks, however, to the best of our knowledge cyano borates with the large CN substituted biphenoxy ligand  $[\text{B}(\text{O}-\text{C}_{12}\text{H}_8-\text{CN})_4]^-$  or the dicyano-phenoxy ligand  $[\text{B}\{\text{O}-\text{C}_6\text{H}_3-(\text{CN})_2\}_4]^-$  are not known yet. The only known cyano-borates are of the type  $[\text{B}(\text{C}_6\text{H}_4-\text{CN})_4]^-$ ,<sup>[10]</sup> and  $[\text{B}(\text{CN})_4]^-$ <sup>[11]</sup> or with the mentioned para-cyano-phenoxy and tceg ligands. Besides there is a great wealth of coordination polymers based on polycyanometallates,<sup>[12]</sup>  $[\text{C}(\text{CN})_3]^-$ <sup>[13]</sup> or  $\text{Si}(p-\text{C}_6\text{H}_4-\text{CN})_4$ .<sup>[14]</sup>

Herein we describe the syntheses, structures and physical properties of coordination polymers bearing the novel  $[\text{H}-\text{B}(\text{O}-\text{C}_{12}\text{H}_8-\text{CN})_3]^-$  and  $[\text{B}\{\text{O}-\text{C}_6\text{H}_3-(\text{CN})_2\}_4]^-$  anions, just like a new modification of  $\text{Na}[\text{B}(\text{O}-\text{C}_6\text{H}_4-\text{CN})_4]$ . The synthesis and physical properties of

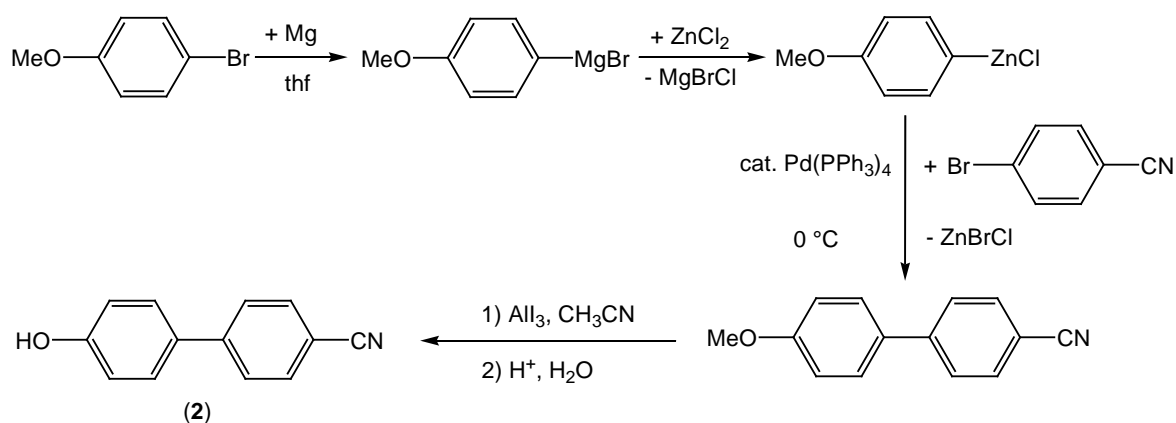
Na[B(O-C<sub>12</sub>H<sub>8</sub>-CN)<sub>4</sub>] are described as well. Two of the three utilized hydroxynitriles were synthesized and characterized by spectroscopic studies and X-ray diffractometry.

## Results and Discussion

**Synthesis.** For the synthesis of cyano-group functionalized borates different synthetic routes are well studied and described in literature.<sup>[7-11]</sup> One of the most common synthetic methods to generate borates is the treatment of NaBH<sub>4</sub> with four equivalents of the desired hydroxynitriles, a method which was also applied here. Two of the three utilized hydroxynitriles were synthesized in modified reactions according to literature. 5-Hydroxy-isophthalonitrile, HO-C<sub>6</sub>H<sub>3</sub>-(CN)<sub>2</sub> (**1**), was prepared in a two-step reaction starting from 5-hydroxy-isophthalic acid (Scheme 1).<sup>[15]</sup> The first reaction step was the amination of the acid by conversion with thionyl chloride to the acyl chloride and a secondary reaction with ammonium affording 5-hydroxy-benzene-1,3-dicarbonylamide in moderate yields up to 52 %. Dehydration of the amide with phosphoryl chloride in a second reaction step gave raw 5-Hydroxy-isophthalonitrile (**1**) which was sublimed twice at 120 °C and 10<sup>-3</sup> mbar affording a pure product in good yields (74 %). In a two-step reaction 4-hydroxy-4'-cyano-1,1'-biphenyl, HO-C<sub>12</sub>H<sub>8</sub>-CN (**2**), was synthesized according to literature (Scheme 2).<sup>[16]</sup> In the first reaction step 4-methoxy-4'-cyano-1,1'-biphenyl, MeO-C<sub>12</sub>H<sub>8</sub>-CN, was prepared from 4-bromoanisole and 4-bromobenzonitrile via Negishi coupling reaction utilizing Pd(PPh<sub>3</sub>)<sub>4</sub> as catalyst in good yields (74 %). The methyl group was split off by AlI<sub>3</sub> in a second reaction step, followed by hydrolysis and sublimation at 150 °C and 10<sup>-3</sup> mbar leading to **2** in moderate yields (67 %).



**Scheme 1.** Synthesis of HO-C<sub>6</sub>H<sub>3</sub>-(CN)<sub>2</sub> (**1**).



**Scheme 2.** Synthesis of HO-C<sub>12</sub>H<sub>8</sub>-CN (**2**).

Na[B(O-C<sub>6</sub>H<sub>4</sub>-CN)<sub>4</sub>] was synthesized as reported in our previous studies by conversion of NaBH<sub>4</sub> with 4.25 equivalents of HO-C<sub>6</sub>H<sub>4</sub>-CN in thf under refluxing. After concentration of the reaction mixture Na[B(O-C<sub>6</sub>H<sub>4</sub>-CN)<sub>4</sub>]·4.5thf crystallized at room temperature. The solvent molecules were removed *in vacuo* from the isolated crystals to give solvent free Na[B(O-C<sub>6</sub>H<sub>4</sub>-CN)<sub>4</sub>] (**3**). A new modification was obtained after crystallization from CH<sub>3</sub>CN which was determined by X-ray diffractometry as Na[B(O-C<sub>6</sub>H<sub>4</sub>-CN)<sub>4</sub>]·CH<sub>3</sub>CN (**3**·CH<sub>3</sub>CN). The crystals were dried for 5 hours at 120 °C and 10<sup>-3</sup> mbar to obtain solvent free **3** in moderate yields (58 %). The synthesis of Na[B{O-C<sub>6</sub>H<sub>3</sub>-(CN)<sub>2</sub>}]<sub>4</sub> analogue to the synthesis of **5** by reacting NaBH<sub>4</sub> with 4.25 equivalents of HO-C<sub>6</sub>H<sub>3</sub>-(CN)<sub>2</sub> in thf under refluxing led not to full hydride substitution, which was achieved after refluxing in CH<sub>3</sub>CN. After removal





show also good solubility in thf and CH<sub>3</sub>CN, while **5** is almost insoluble in thf and slightly soluble in CH<sub>3</sub>CN at room temperature. Sodium borate **6** is better soluble in thf, but less soluble in CH<sub>3</sub>CN than **5**. Interestingly, additions of **2** were found to increase the solubility of **5** in CH<sub>3</sub>CN. Also the sodium borates form colorless solids and decompose at temperatures between 298 °C and 318 °C without melting (Table 1). In presence of water the sodium borates (**3-6**) form B<sub>2</sub>O<sub>3</sub>·*n*H<sub>2</sub>O as revealed by <sup>11</sup>B NMR studies and the respective hydroxynitriles according to <sup>1</sup>H NMR experiments. Decomposition in other protic solvents like MeOH, EtOH etc. was also observed, resulting in the respective hydroxynitriles and transesterification products. In an approach to crystallize Na[B(O-C<sub>12</sub>H<sub>8</sub>-CN)<sub>4</sub>] from dry EtOH a new modification of HO-C<sub>12</sub>H<sub>8</sub>-CN crystallized from solution. Nevertheless, all borates can be synthesized in bulk and are infinitely stable when stored under argon in sealed tubes. Sodium borates **3**, **4** and **5** precipitate often as solvates, in which solvent can be removed by thermal treatment *in vacuo*. The uncoordinated acetonitrile molecules in **5**·**3**CH<sub>3</sub>CN can be completely removed at room temperature *in vacuo*, while the coordinated thf molecules in **4**·**2**thf·**x**solvent as well as the entrapped CH<sub>3</sub>CN molecules in **3**·**3**CH<sub>3</sub>CN require prolonged thermal treatment up to 120 °C *in vacuo* for full removal. Data from TGA-DSC measurements of the crystalline compounds **3**·**3**CH<sub>3</sub>CN, **4**·**2**thf·**x**solvent and **5**·**3**CH<sub>3</sub>CN validate these results, although higher temperatures were required for the removal of the guest molecules as a result of the higher pressure (see Supporting Information).

**Table 1.** Thermal analysis: Melting and decomposition points (from DSC measurements); spectroscopic data: IR, Raman, and <sup>13</sup>C NMR data of **1-6**.

	T <sub>mp</sub> /°C	T <sub>dec</sub> /°C	<sup>13</sup> C NMR/ppm CN	<sup>11</sup> B NMR/ppm	IR/cm <sup>-1</sup> ν <sub>CN</sub>	Raman/cm <sup>-1</sup> ν <sub>CN</sub>
<b>1</b>	251	-	117.1	-	2236, 2250	2247
<b>2</b>	198	-	119.1	-	2228	2237
<b>3</b>	-	292	119.5	2.6	2220, 2231	2220, 2234, 2243
<b>4</b>	-	318	117.3	2.3	2235	2238
<b>5</b>	-	314	119.2	4.3*	2224, 2238	2233, 2249
<b>6</b>	-	301	119.2	2.8	2224	2219, 2237

\* broad signal

**Spectroscopic studies.**  $^{13}\text{C}$  and  $^{11}\text{B}$  NMR data along with IR/Raman data for compounds described in this work are listed in Table 1. The IR and Raman data of all considered CN group containing compounds show bands in the expected region between 2219-2250  $\text{cm}^{-1}$ , which can be assigned to the  $\nu_{\text{CN}}$  stretching frequencies. Interestingly, most bands of the  $\nu_{\text{CN}}$  stretching frequencies appear with at lower wave numbers in IR than in Raman. Most of the synthesized compounds exhibit two different  $\nu_{\text{CN}}$  stretching frequencies for the uncoordinated and the sodium coordinated, respectively hydrogen bonded, cyano groups in both the IR and Raman spectra. Solvent free  $\text{Na}[\text{B}(\text{O}-\text{C}_6\text{H}_4-\text{CN})_4]$  crystallized from  $\text{CH}_3\text{CN}$ , shows three different  $\nu_{\text{CN}}$  stretching frequencies in Raman, which can be assigned to various coordination modes of the sodium at the CN group and/or the oxygen atom in the ligand. The  $^{13}\text{C}$  NMR resonances of the *ortho* cyano groups in **1** and **4** are detected slightly upfield shifted (117.1-117.3 ppm) than the *para* cyano groups (119.1-119.5 ppm). As expected the  $^{11}\text{B}$  NMR resonances in the  $\text{BO}_4$  moieties containing borates (**3**, **4** and **5**) occur at similar shifts between 2.3 and 2.8 ppm, which lie well compared to our results from previously studied cyano borates.<sup>[7,8]</sup> Exceptionally, the  $^{11}\text{B}$  NMR spectrum of sodium borate **5**, which contains a residual hydride at the boron atom, shows a broad signal around 4.3 ppm due to the coupling between boron and hydrogen. This coupling affects also the  $^1\text{H}$  NMR resonance for the hydride, resulting in a broad signal.

**X-ray structure analysis.** X-ray quality crystals of all considered species were selected in Kel-F-oil (Riedel-de Haen) or Fomblin YR-1800 (Alfa Aesar) at ambient temperature. All samples were cooled to  $-100(2)$  °C during the measurement. More details are found in the supporting information file. The structures of compounds **1-5**, as well as MeO–C<sub>12</sub>H<sub>8</sub>–CN, have been determined. The structure of MeO–C<sub>12</sub>H<sub>8</sub>–CN is already known and not discussed, but structure details are attached in supporting information. Due to the poor quality of X-ray crystallographic data of **4** and **5** only the discussion of connectivity in the networks is feasible. Table 2 presents the X-ray crystallographic data of species **1-3**.

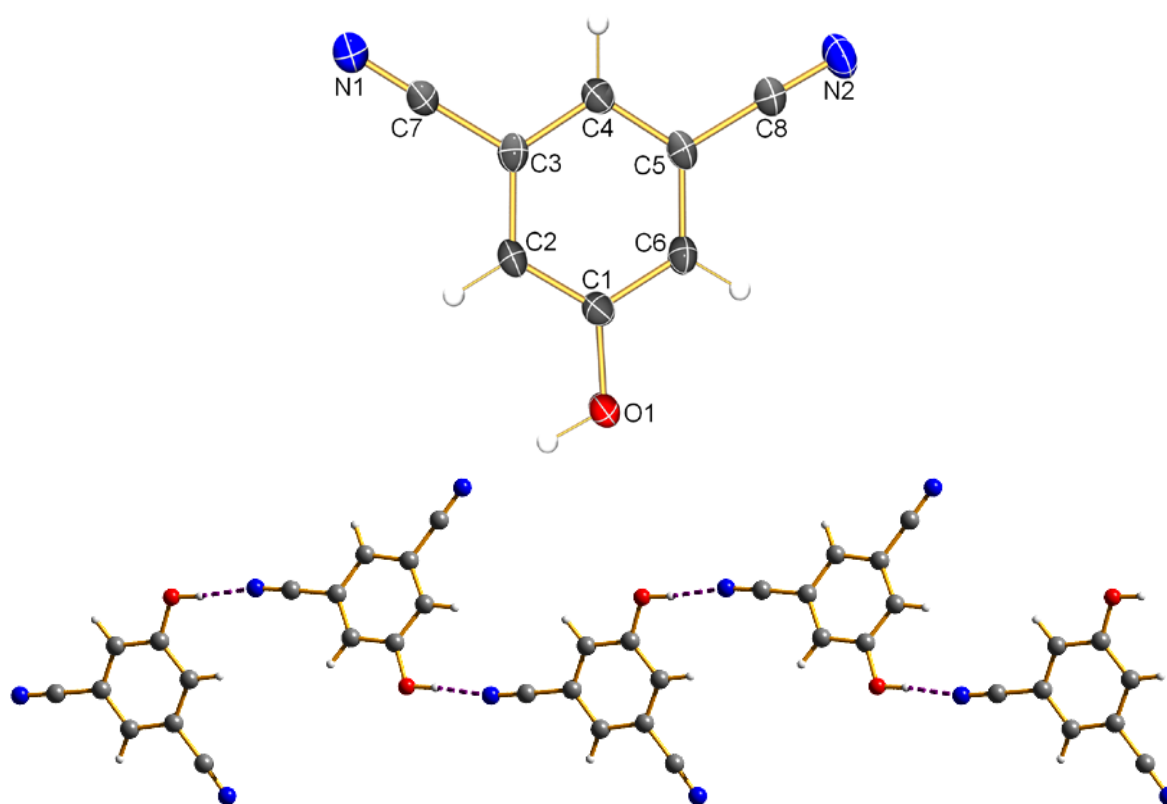


**Figure 1.** Top: ORTEP drawing of the molecular structure of **1**. Thermal ellipsoids with 50 % probability at 173 K; Bottom: Ball-and-stick drawing of the molecular strings formed by hydrogen bonding. View along *a*-axis. Selected bond lengths (Å) and angles (°): N1–C7 1.141(2), N2–C8 1.141(2), O1–C1 1.360(2); N1–C7–C3 178.9(2), N2–C8–C5 178.2(2), O1–C1–C6 116.6(1), O1–C1–C2 123.2(1), C1–O1–H1 113(1); O1–C1–C2–C3 179.0(1), C6–C1–C2–C3  $-1.2(2)$ , C1–C2–C3–C4 1.3(2), C1–C2–C3–C7  $-178.1(1)$ , C2–C3–C4–C5  $-0.3(2)$ , C7–C3–C4–C5 179.1(1), C3–C4–C5–C6  $-0.8(2)$ , C3–C4–C5–C8 178.7(1), O1–C1–C6–C5 179.9(1), C2–C1–C6–C5 0.1(2), C4–C5–C6–C1 0.9(2), C8–C5–C6–C1  $-178.6(1)$ .

*HO–C<sub>6</sub>H<sub>3</sub>–(CN)<sub>2</sub>* (**1**). Crystals suitable for X-ray crystallography were obtained by crystallisation from a hot saturated CH<sub>3</sub>CN solution. 5-Hydroxy-isophthalonitrile crystallizes in the monoclinic space group *P2<sub>1</sub>/c* with four formula units per unit cell. The 5-hydroxy-isophthalonitrile, displayed in Figure 1, has a nearly planar molecular structure with torsion angles deviating maximal 1.9° from perfect planarity. In the crystals the molecules are

intermolecularly hydrogen bonded between one cyano and the hydroxyl group forming molecular chains. The N $\cdots$ H distance is 1.92 Å which is larger than the sum of the covalent radii for N–H bonds (1.03 Å), but significantly shorter than the sum of the van-der-Waals radii (2.65 Å). The CN groups with average CN bond lengths of 1.141 Å are lying well within the sum of the covalent radii for CN triple bonds,  $\Sigma r_{\text{cov}}(\text{C}\equiv\text{N}) = 1.14$  Å.<sup>[17]</sup>

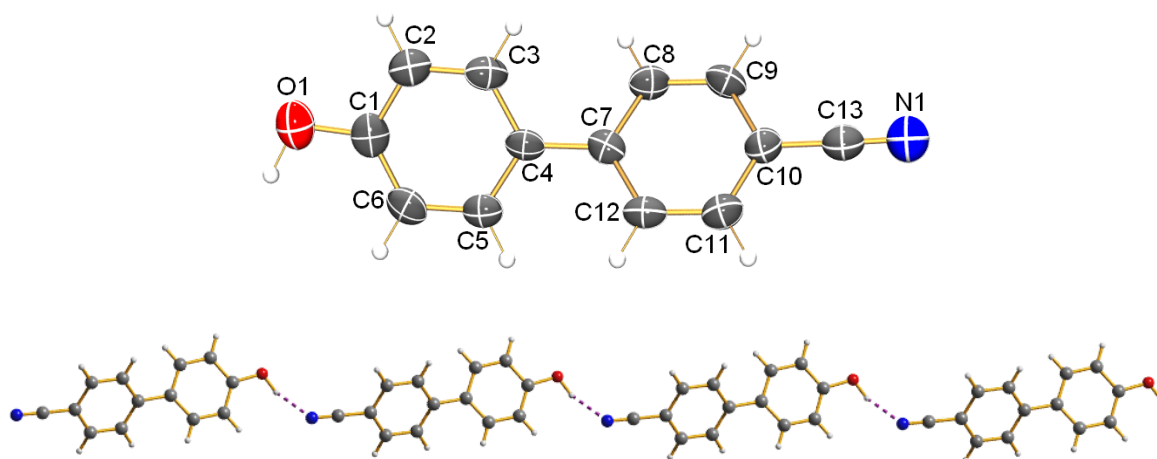


**Figure 2.** Top: ORTEP drawing of the molecular structure of **2**. Thermal ellipsoids with 50 % probability at 173 K; Bottom: Ball-and-stick drawing of the molecular strings formed by hydrogen bonding. Selected bond lengths (Å) and angles (°): N1–C13 1.145(4), O1–C1 1.370(4), C4–C7 1.469(5), O1–H1 0.98(5); N1–C13–C10 178.9(5), O1–C1–C2 116.0(4), O1–C1–C6 124.0(4); C3–C4–C7–C8 –37.5(5), C3–C4–C7–C12 141.8(4), C5–C4–C7–C12 –38.5(6), C5–C4–C7–C8 142.2(4).

*HO–C<sub>12</sub>H<sub>8</sub>–CN* (**2**). Crystals suitable for X-ray crystallography were obtained from an EtOH solution of Na[B(O–C<sub>12</sub>H<sub>8</sub>–CN)<sub>4</sub>] after storage at room temperature for 3 days. 4-Hydroxy-4'-cyano-biphenyl crystallized in the triclinic space group *P*-1. Four molecules of **2** make up the asymmetric unit which takes place four times in the unit cell. Only one independent molecule of **2** is depicted in Figure 2 since the structural parameters are all similar. Comparable to **1** the molecules in **2** form molecular chains with intermolecularly hydrogen bonding between the cyano and the hydroxyl group. The hydrogen bond with a H1 $\cdots$ N1 distance of 1.87 Å lies between the sum of the covalent radii for N–H bonds (1.03 Å) and the sum of the van-der-Waals radii (2.65 Å). Torsion was found in the molecule between both phenyl rings with a torsion angle of 38.5°. The average bond length of the cyano groups is 1.145 Å in accord with the sum of the covalent radii for CN triple bonds (vide supra).

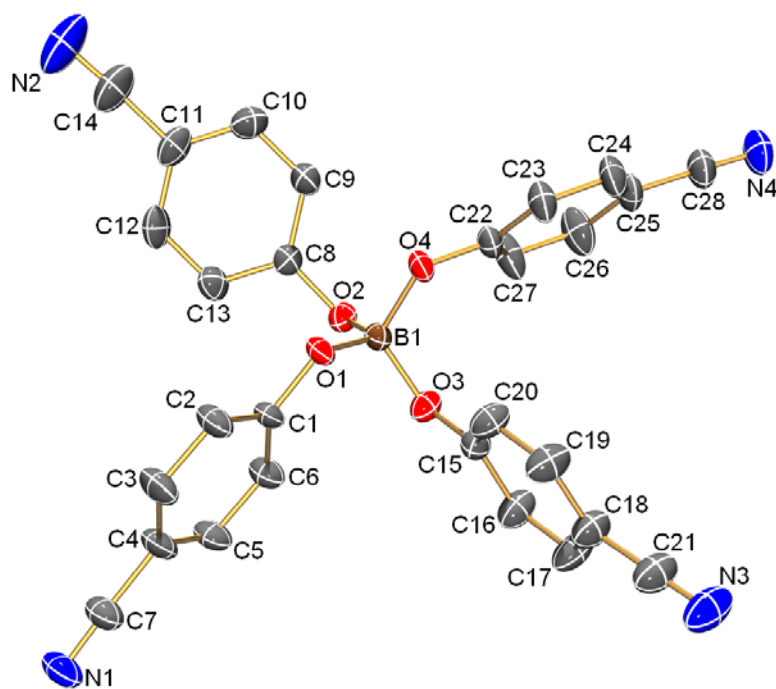


**Figure 3.** ORTEP drawing of the molecular structure of the anion in  $3 \cdot \text{CH}_3\text{CN}$ . Thermal ellipsoids with 50% probability at 173 K. Selected bond lengths ( $\text{\AA}$ ) and angles ( $^\circ$ ): B1–O2 1.452(2), B1–O3 1.452(2), B1–O4 1.485(2), B1–O1 1.482(2), N1–C7 1.141(2), N2–C14 1.134(3), N3–C21 1.144(2), N4–C27 1.142(2), O2–C8 1.370(2), O3–C15 1.348(2), O4–C22 1.359(2), O1–C1 1.351(2); C1–O1–B1 124.1(1), C8–O2–B1 116.9(1), C15–O3–B1 125.1(1), C22–O4–B1 122.5(1), O1–B1–O2 112.3(1), O1–B1–O3 114.3(1), O1–B1–O4 99.2(1), O2–B1–O3 104.2(1), O2–B1–O4 113.6(1), O3–B1–O4 113.7(1), N1–C7–C4 178.1(2), N2–C14–C11 176.9(3), N3–C21–C18 179.7(2), N4–C27–C25 178.7(2).

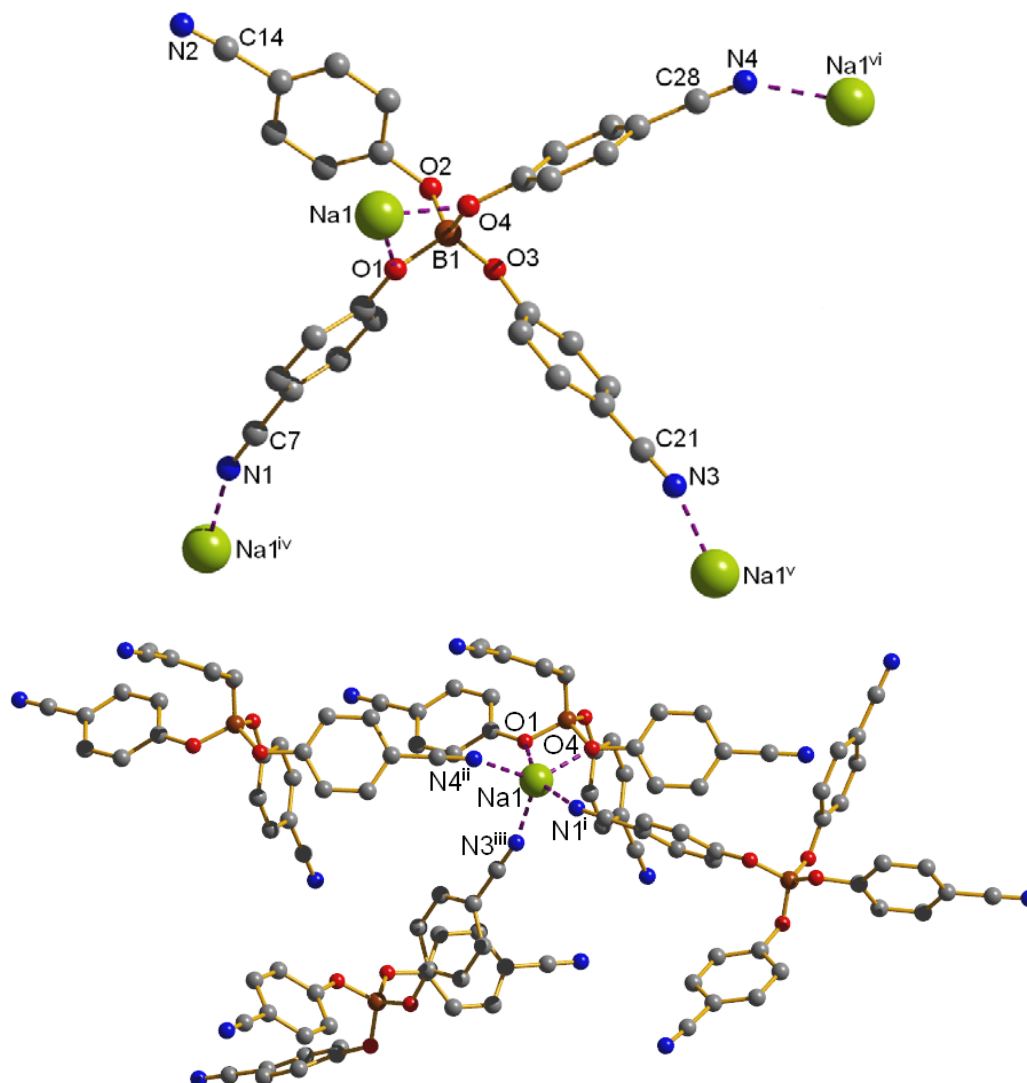


**Figure 4.** Top: Ball-and-stick drawing of the local environment around the anion center in **3·CH<sub>3</sub>CN**. Symmetry codes: (iv)  $-x+1/2, y+1/2, z-1/2$ ; (v)  $-x+1, -y+2, z+1/2$ ; (vi)  $x, y, z+1$ ; Bottom: Ball-and-stick drawing of the local environment about the sodium centers in **3·CH<sub>3</sub>CN** (Hydrogen atoms omitted for clarity). Symmetry codes: (i)  $-x+1/2, y-1/2, z+1/2$ ; (ii)  $x, y, z-1$ ; (iii)  $-x+1, -y+2, z-1/2$ . Selected bond lengths (Å) and angles (°): Na1 $\cdots$ O1 2.406(1), Na1 $\cdots$ O4 2.345(1), Na1 $\cdots$ N1<sup>i</sup> 2.348(2), Na1 $\cdots$ N3<sup>iii</sup> 2.376(2), Na1 $\cdots$ N4<sup>ii</sup> 2.362(2), N1<sup>i</sup> $\cdots$ Na1 $\cdots$ O1 155.48(5), N3<sup>iii</sup> $\cdots$ Na1 $\cdots$ O1 87.09(5), N4<sup>ii</sup> $\cdots$ Na1 $\cdots$ O1 98.56(5), O4 $\cdots$ Na1 $\cdots$ O1 56.77(3), O4 $\cdots$ Na1 $\cdots$ N1<sup>i</sup> 98.72(5), O4 $\cdots$ Na1 $\cdots$ N3<sup>iii</sup> 106.73(6), O4 $\cdots$ Na1 $\cdots$ N4<sup>ii</sup> 138.09(5), N1<sup>i</sup> $\cdots$ Na1 $\cdots$ N3<sup>iii</sup> 102.51(6), N1<sup>i</sup> $\cdots$ Na1 $\cdots$ N4<sup>ii</sup> 100.62(6), N4<sup>ii</sup> $\cdots$ Na1 $\cdots$ N3<sup>iii</sup> 104.82(7), C7–N1 $\cdots$ Na1<sup>iv</sup> 160.7(2), C21–N3 $\cdots$ Na1<sup>v</sup> 163.8(2), C27–N4 $\cdots$ Na1<sup>vi</sup> 147.4(2).

*Na*[*B*(*O*–*C*<sub>6</sub>*H*<sub>4</sub>–*CN*)<sub>4</sub>]*·CH*<sub>3</sub>*CN* (**3·CH<sub>3</sub>CN**). X-ray quality crystals were obtained from a cold saturated CH<sub>3</sub>CN solution after warming up to room temperature. Sodium-tetrakis(4-cyano-phenoxy)-borate crystallized with an acetonitrile molecule in the orthorhombic space group *Pna*2<sub>1</sub> with four formula units per unit cell. As depicted in Figure 4, each anion coordinates three sodium cations with three of its four cyano groups and a fourth one is chelated by its oxygen atoms. According to that, the sodium cation is coordinated by three anions via nitrile groups and additionally chelated by two oxygen atoms from a fourth anion resulting in a distorted square pyramidal coordination sphere. With N3<sup>iii</sup> on top of the pyramid

and sodium located slightly out of the square area there are angles between the corners and the top of the pyramid of  $N3^{iii}\cdots Na1\cdots O1$   $87.09(5)^\circ$ ,  $O4\cdots Na1\cdots N3^{iii}$   $106.73(6)^\circ$ ,  $N1^i\cdots Na1\cdots N3^{iii}$   $102.51(6)^\circ$  and  $N4^{ii}\cdots Na1\cdots N3^{iii}$   $104.82(7)^\circ$ . Additionally, a close contact between sodium and a carbon atom of the phenyl ring ( $Na1\cdots C8$   $3.541 \text{ \AA}$ ) from the chelating anion is found, which lies well within the sum of the van-der-Waals radii [ $\Sigma r_{vdw}(Na\cdots C) = 3.97 \text{ \AA}$ ]. Including this interaction, the square pyramidal coordination sphere can be expanded to an octahedrally, which explains best the situation around the  $Na^+$  cation, finally forming a 3d network with the acetonitrile molecules placed in the voids (Figure 5). The boron atom is in a slightly distorted tetrahedral coordination environment (Figure 3) with two smaller [ $O1-B1-O4$   $99.2(1)$ ,  $O2-B1-O3$   $104.2(1)^\circ$ ] and four larger angles [ $O1-B1-O2$   $112.3(1)$ ,  $O1-B1-O3$   $114.3(1)$ ,  $O2-B1-O4$   $113.6(1)$ ,  $O3-B1-O4$   $113.7(1)^\circ$ ]. The average B–O distance is  $1.466 \text{ \AA}$  [*cf.*  $\Sigma r_{cov}(B-O) = 1.48 \text{ \AA}$ ],<sup>[17]</sup> which is similar to those values that were found in tetraalkoxyborates.<sup>[7-9]</sup> The  $BO_4$  tetrahedron displays a bent structure with B–O–C angles between  $116.9(1)$ - $125.1(1)^\circ$ . For the uncoordinated cyano group a slightly shorter bond length with  $N2-C14$   $1.134(3) \text{ \AA}$  is found compared to the coordinated nitrile groups [ $N1-C7$   $1.141(2)$ ,  $N3-C21$   $1.144(2)$ ,  $N4-C27$   $1.142(2) \text{ \AA}$ ], however, the bond lengths lie well within the sum of the covalent radii for CN triple bonds [*cf.*  $\Sigma r_{cov}(C\equiv N) = 1.14 \text{ \AA}$ ].<sup>[17]</sup>

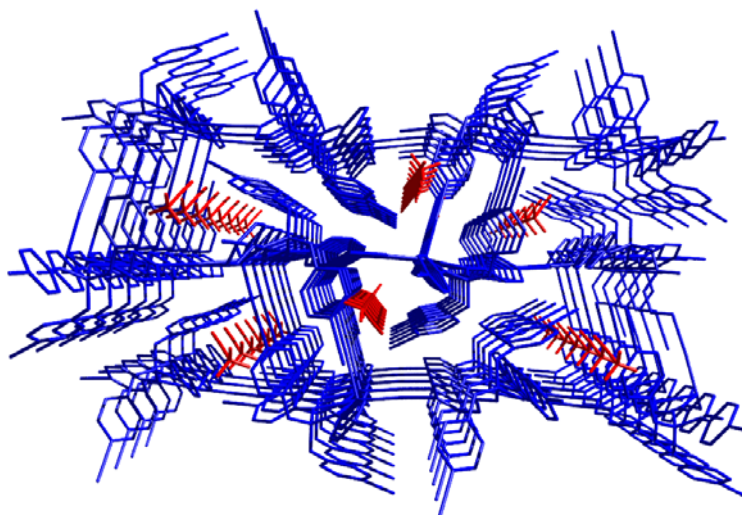


**Figure 5.** Inclusion of  $CH_3CN$  (red) within the three dimensional coordination network (blue) in the crystal structure of  $3 \cdot CH_3CN$ . Hydrogen atoms in the network omitted for clarity. View along  $c$ -axis.

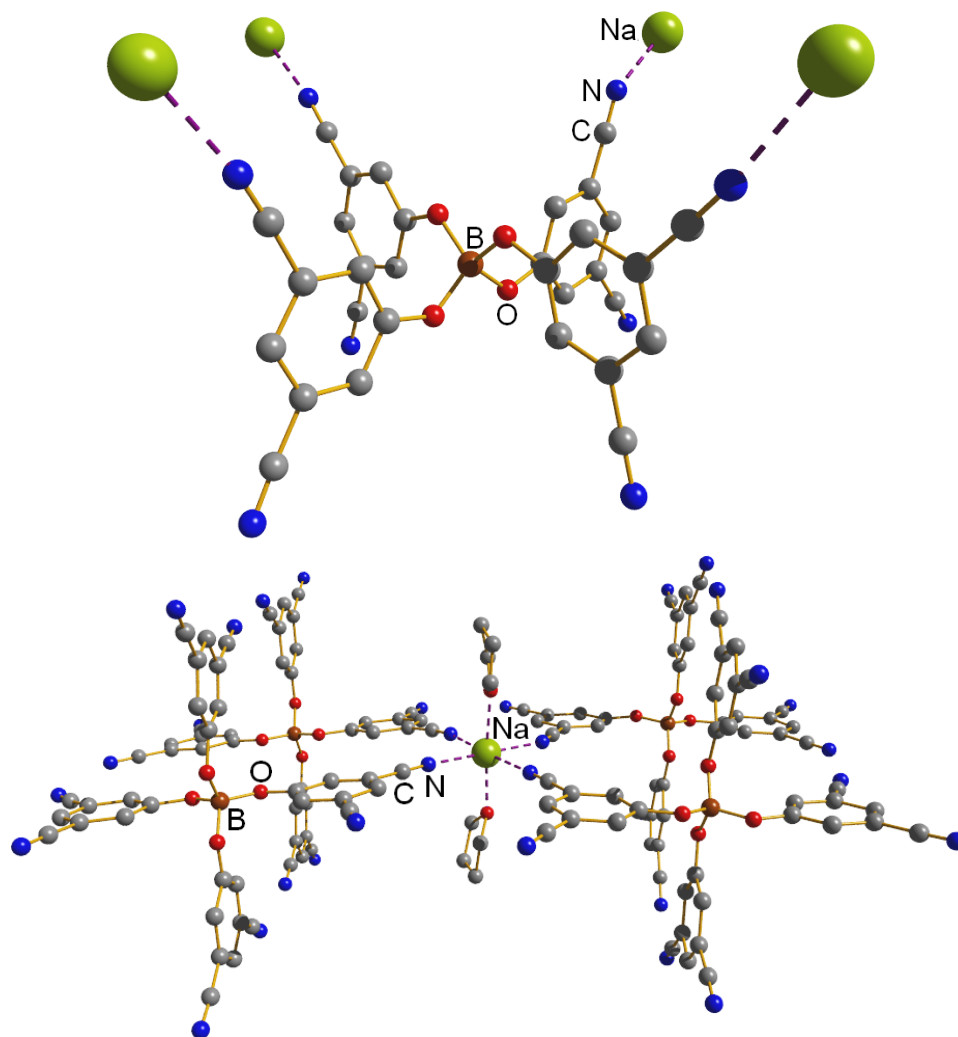


**Figure 6.** Top: Ball-and-stick drawing of the local environment around the anion center in **4**·2thf·xsolvent. Bottom: Ball-and-stick drawing of the local environment around the sodium centers in **4**·2thf·xsolvent (Hydrogen atoms omitted for clarity).

*Na[B{O–C<sub>6</sub>H<sub>3</sub>–(CN)<sub>2</sub>]<sub>4</sub>·2thf·xsolvent* (**4**·2thf·xsolvent). Crystals of **4** with entrapped solvent molecules were obtained from a mixture of thf/CH<sub>2</sub>Cl<sub>2</sub> after storage over night at –40 °C and analysed by X-ray crystallography. Sodium borate **4** crystallizes along with an undefinable number of solvent molecules in the orthorhombic space group *Pbca* with 8 formula units per unit cell. In the anions each of the two opposing ligands along with the boron center are coplanar, leading to a perpendicular configuration of the four ligands. The para-carbon atoms of the phenyl ligands and the boron center make up a coplanarity, resulting in an arrangement of half of the cyano groups above, respectively under, this planar. As shown in Figure 6, the anion [B{O–C<sub>6</sub>H<sub>3</sub>–(CN)<sub>2</sub>]<sub>4</sub><sup>–</sup> coordinates four Na<sup>+</sup> cations via four nitrile groups, that are located one sided to the anion. Interestingly, those four sodium cations are also coordinated to four nitrile groups of a second anion. Thereby, each Na<sup>+</sup> cation is coordinated octahedrally by four independent borate anions through their nitrile groups and



the oxygen atoms of two thf molecules, that are arranged in trans-position. Consequentially, a coordination network with a two dimensionally extension is formed with two borate anions as the nodes of square pores (Figure 7). The pores are filled with solvent molecules, whereas every solvent position is partially occupied by thf and CH<sub>2</sub>Cl<sub>2</sub>. However, the number of solvent molecules can be estimated by the number of residual electrons obtained by X-ray crystallographic data divided by the number of electrons in thf, and CH<sub>2</sub>Cl<sub>2</sub> respectively, which leads to a range between 55 and 58 solvent molecules per unit cell.

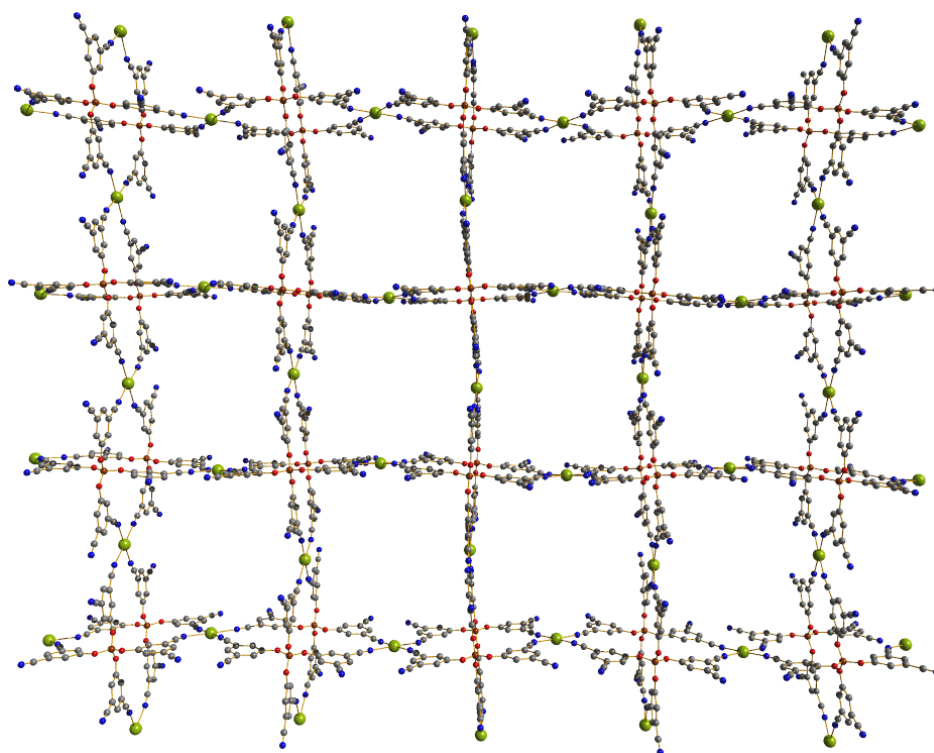


**Figure 7.** Two dimensional extension of the coordination network in **4·2thf·xsolvent**. Solvent molecules and hydrogen omitted for clarity. View along *c*-axis.

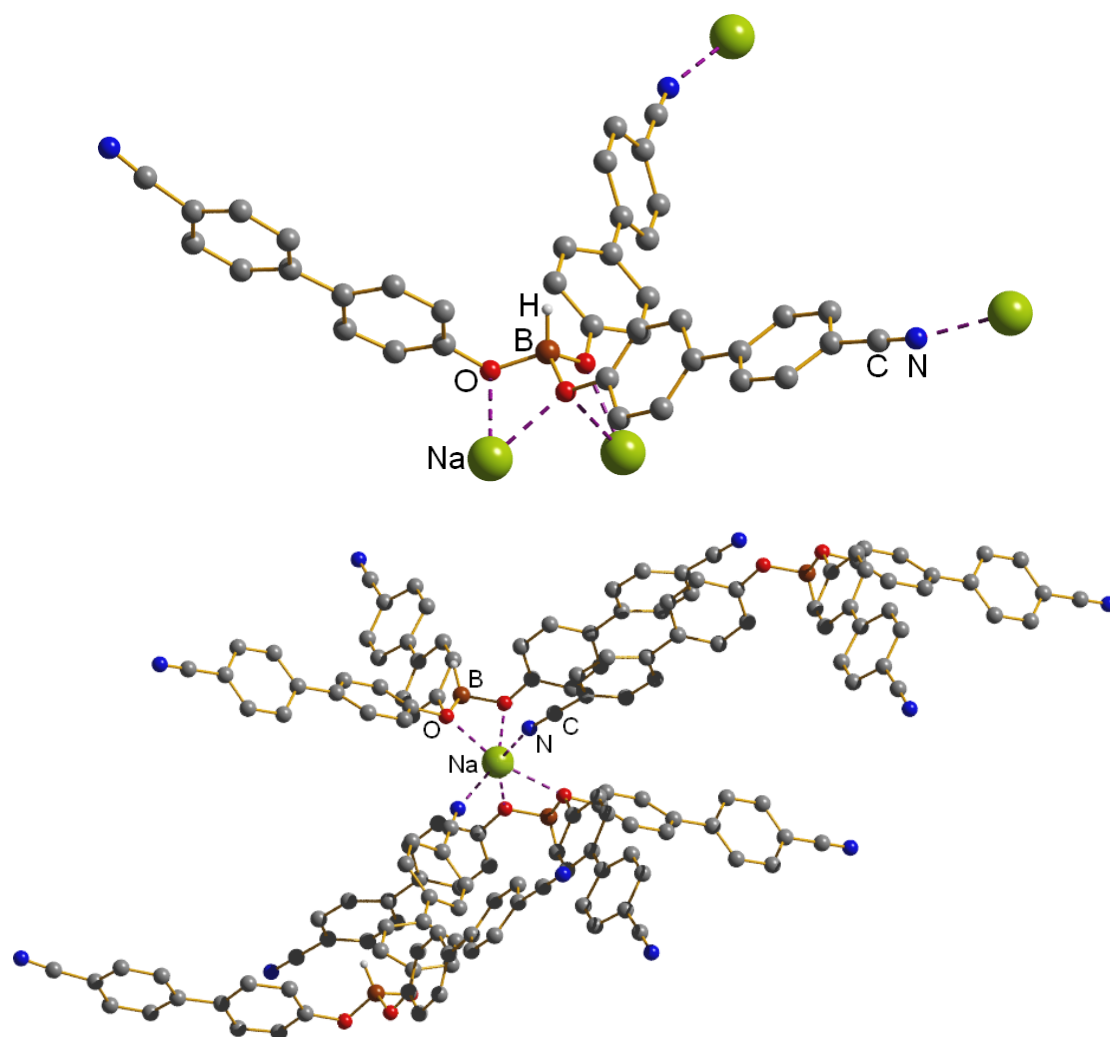


**Figure 8.** Top: Ball-and-stick drawing of the local environment of the anion; Bottom: Ball-and-stick drawing of the local environment of the  $\text{Na}^+$  ion in  $5 \cdot 3\text{CH}_3\text{CN}$  (Hydrogen atoms at biphenyl groups omitted for clarity).

$\text{Na}[\text{H}-\text{B}(\text{O}-\text{C}_{12}\text{H}_8-\text{CN})_3] \cdot 3\text{CH}_3\text{CN}$  ( $5 \cdot 3\text{CH}_3\text{CN}$ ) crystallized at 7 °C from a hot saturated solution in  $\text{CH}_3\text{CN}$ . Sodium borate  $5 \cdot 3\text{CH}_3\text{CN}$  crystallizes in the monoclinic space group  $P2_1/n$  with four formula units per unit cell. The boron center is bonded by three cyano-biphenoxy ligands and a residual hydrogen atom (Figure 8). From a viewing direction along the B–H bond the ligands in the anion display a three pointed star. The hydride sits in a pocket formed by the cyano-biphenyl groups along with the borate center. The anion in  $5 \cdot 3\text{CH}_3\text{CN}$  coordinates to four sodium cations, whereby two  $\text{Na}^+$  cations are coordinated by the cyano groups and each remaining cation chelated by two oxygen atoms originating from the borate center. The third nitrile group remains uncoordinated. Both chelated sodium cations are additionally chelated by a second anion with its oxygen atoms. Two further coordinations by nitrile groups, coming from a third and fourth anion, results in a distorted octahedrally coordination environment around the  $\text{Na}^+$  cations. As displayed in Figure 9 the sodium borate forms a porous coordination network with three-dimensional extension, whereas three

acetonitrile molecules per borate remain uncoordinated. Expressed by the two shades of blue there are two interpenetrated networks in the crystal structure of  $5 \cdot 3\text{CH}_3\text{CN}$ , while the acetonitrile molecules (red) are located within the triangular shaped pores. In viewing direction along the  $c$ -axis the interpenetrating networks alternate consecutively.

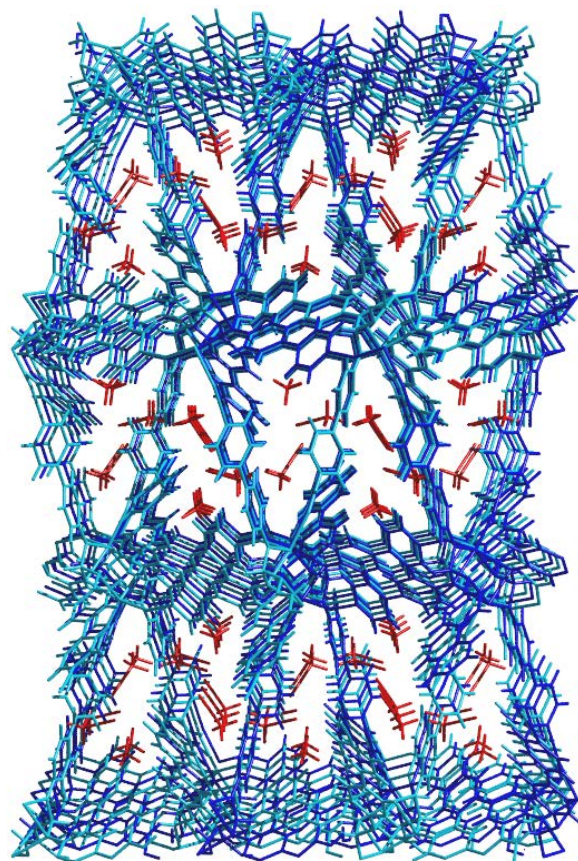


**Figure 9.** Inclusion of  $\text{CH}_3\text{CN}$  (red) in the interpenetrating coordination networks (blue and light blue) with three dimensional extension in the crystal structure of  $5 \cdot 3\text{CH}_3\text{CN}$ . View along  $c$ -axis.

**Table 2.** Crystallographic details of HO–C<sub>6</sub>H<sub>3</sub>–(CN)<sub>2</sub> (**1**), HO–C<sub>12</sub>H<sub>8</sub>–CN (**2**), Na[B(O–C<sub>6</sub>H<sub>4</sub>–CN)<sub>4</sub>]·CH<sub>3</sub>CN (**3**).

	<b>1</b>	<b>2</b>	<b>3</b>
Chem. Formula	C <sub>8</sub> H <sub>4</sub> N <sub>2</sub> O	C <sub>13</sub> H <sub>9</sub> NO	C <sub>30</sub> H <sub>19</sub> BN <sub>5</sub> NaO
Form. Wght. [g·mol <sup>-1</sup> ]	144.13	195.21	547.30
Colour	colourless	colourless	colourless
Cryst. System	monoclinic	triclinic	orthorhombic
Space Group	<i>P</i> 2 <sub>1</sub> / <i>c</i>	<i>P</i> -1	<i>P</i> na2 <sub>1</sub>
a [Å]	3.8070(2)	10.6030(8)	14.9581(5)
b [Å]	12.9698(8)	11.7875(9)	18.9313(6)
c [Å]	13.4362(9)	17.973(1)	10.6249(4)
α [°]	90	103.015(3)	90
β [°]	92.101(4)	100.210(3)	90
γ [°]	90	109.815(4)	90
V [Å <sup>3</sup> ]	662.98(7)	1978.7(3)	3008.7(2)
Z	4	8	4
μ [mm <sup>-1</sup> ]	0.10	0.08	0.09
λ <sub>MoKα</sub> [Å]	0.71073	0.71073	0.71073
T [K]	173	173	173
Measured Reflections	8593	24288	29343
Independent Reflections	1588	5206	9818
Reflections with I > 2σ(I)	1109	2679	7118
R <sub>int</sub> .	0.056	0.112	0.034
F(000)	296	816	1128
R <sub>1</sub> (R[F <sub>2</sub> > 2σ(F <sub>2</sub> )])	0.041	0.052	0.045
wR <sub>2</sub> (all data)	0.104	0.137	0.096
GooF	1.05	0.98	1.02
Parameters	104	558	382

**Nitrogen Sorption Experiments.** Sorption experiments were done on a Thermo Sorptomatic 1990 measuring at  $-196\text{ }^{\circ}\text{C}$  using a volumetric experimental setup. The solvent free samples of **3**, **5** and **6** (approximately 500 to 600 mg) were weight into a glass burette in a glove box and activated at  $70\text{ }^{\circ}\text{C}$  in high vacuum over night. As revealed by the nitrogen sorption experiments the presence of permanent porosity was found in the solvent free and activated samples of  $\text{Na}[\text{H}-\text{B}(\text{O}-\text{C}_{12}\text{H}_8-\text{CN})_3]$  (**5**), while almost no uptake of nitrogen was observed at samples of  $\text{Na}[\text{B}(\text{O}-\text{C}_{12}\text{H}_8-\text{CN})_4]$  (**3**) and  $\text{Na}[\text{B}(\text{O}-\text{C}_6\text{H}_4-\text{CN})_4]$  (**6**). The type I isotherm of **5** is typical for pore diameters in the microporous region,<sup>[18]</sup> which lies well with the data of the X-ray diffractometric experiments of  $\mathbf{5}\cdot\mathbf{3CH}_3\text{CN}$ . The pore volumes at  $p/p^0 = 0.95$  amount to  $0.0735\text{ cm}^3\text{ g}^{-1}$  (**5**),  $0.0253\text{ cm}^3\text{ g}^{-1}$  (**6**) and  $0.0094\text{ cm}^3\text{ g}^{-1}$  (**3**) according to Gurvich's rule.<sup>[19]</sup> The surface areas were calculated according to BET theory with 3 parameter fit. As well as the pore volumes the surface areas decrease along the series  $\text{Na}[\text{H}-\text{B}(\text{O}-\text{C}_{12}\text{H}_8-\text{CN})_3]$  ( $131.3\text{ m}^2\text{ g}^{-1}$ ),  $\text{Na}[\text{B}(\text{O}-\text{C}_{12}\text{H}_8-\text{CN})_4]$  ( $17.2\text{ m}^2\text{ g}^{-1}$ ) and  $\text{Na}[\text{B}(\text{O}-\text{C}_6\text{H}_4-\text{CN})_4]$  ( $7.1\text{ m}^2\text{ g}^{-1}$ ).

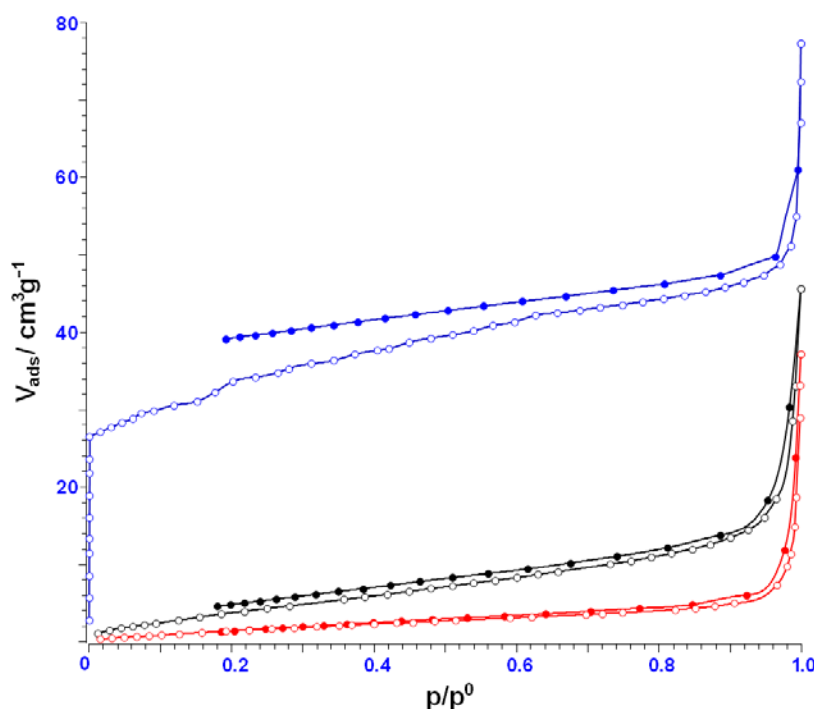


**Figure 10.**  $\text{N}_2$  adsorption isotherms of **3** (red), **5** (blue) and **6** (black) at  $-196\text{ }^{\circ}\text{C}$ .

**Thermodynamics.** The principles of Volume-Based Thermodynamics (VBT), introduced by Jenkins, Glasser and Passmore, can be used to estimate the lattice potential energy ( $U_{\text{POT}}$ ), lattice enthalpy ( $\Delta H_L$ ) and the standard entropy ( $S^\circ_{298}$  in  $\text{J mol}^{-1} \text{K}^{-1}$  at 298.15 K and 101 kPa) of the new sodium borates from its molecular volume.<sup>[20,21]</sup> To investigate the influence of the anion in the formation of coordination polymers we have studied the sodium borates **3**, **4**, **5** and **6**, along with the well known sodium tetracyanidoborate for comparison (Table 6).<sup>[22]</sup> Molecular volumes can be calculated by summing up the volume contributions from each atom in the molecular formula as described by Hofmann.<sup>[23]</sup> For the estimation of ionic volumes Hofmann's approach is not always the best method. For instance the anion and cation volumes are equal since no charge considerations are made. Jenkins and Liebman's isomegetic rule can be referred to as the theoretical basis of Hofmann's approach. The isomegetic rule's different approach offers another way to ion volumes. Krossing *et al.* found that  $V_{\text{Hofmann}}$  correlates linearly with the experimental cation volumes according to  $V_{\text{exp}} = 0.964V_{\text{Hofmann}} - 7 \text{ \AA}^3$  and for the anion according to  $0.946V_{\text{Hofmann}} + 27 \text{ \AA}^3$ .<sup>[24]</sup> for the estimation of volumes.

*Anion size and lattice enthalpies.* As expected the anion volumes increase along the series  $[\text{B}(\text{CN})_4]^-$  ( $137 \text{ \AA}^3$ ) <  $[\text{B}(\text{O}-\text{C}_6\text{H}_4-\text{CN})_4]^-$  ( $572 \text{ \AA}^3$ ) <  $[\text{B}\{\text{O}-\text{C}_6\text{H}_3-(\text{CN})_2\}_4]^-$  ( $605 \text{ \AA}^3$ ) <  $[\text{H}-\text{B}(\text{O}-\text{C}_{12}\text{H}_8-\text{CN})_3]^-$  ( $737 \text{ \AA}^3$ ) and  $[\text{B}(\text{O}-\text{C}_{12}\text{H}_8-\text{CN})_4]^-$  ( $963 \text{ \AA}^3$ ). While each phenoxy spacer contributes approximately  $109 \text{ \AA}^3$  to the anion volume, each biphenoxy group increases the anion volume by  $207 \text{ \AA}^3$  in respect of  $[\text{B}(\text{CN})_4]^-$ . From X-ray diffraction data of **3**· $\text{CH}_3\text{CN}$  the anion volume of  $[\text{B}(\text{O}-\text{C}_6\text{H}_4-\text{CN})_4]^-$  can be calculated by subtracting the volumes of the acetonitrile molecule [ $V(\text{CH}_3\text{CN}) = 54.8 \text{ \AA}^3$ ] and the sodium cation [ $V(\text{Na}^+) = 18.1 \text{ \AA}^3$ ] from the cell volume. With a cell volume of  $3008.7 \text{ \AA}^3$  and  $Z = 4$ , considering the volume of a  $\text{CH}_3\text{CN}$  molecule and the sodium cation, an anion volume  $V([\text{B}(\text{O}-\text{C}_6\text{H}_4-\text{CN})_4]^-) = 679.3 \text{ \AA}^3$  is calculated. The discrepancies between the anion volume based on Hofmann's approach and the anion volume derived from X-ray data are estimated to be ca. 18.6 %. Thus results can be explained with the disorder of the acetonitrile molecule in the crystal structures, which takes more space than calculated for  $\text{CH}_3\text{CN}$ , as well as the dead volume between the spherical atom volumes, that is not included in the calculations. As expected the insertion of phenoxy-spacer, respectively biphenoxy-spacer, results in a decrease of the lattice potential energy regarding to the enlargement of the anions.

**Table 3.** Ionic volumes of cyano-substituted borate anions and thermodynamic data derived from volume-based thermodynamics (VBT) for the sodium salts ( $V(\text{Na}^+) = 18.1 \text{ \AA}^3$ ).

	$V_{\text{anion}} (\text{\AA}^3)$	$U_{\text{pot}} (\text{kJ mol}^{-1})$	$\Delta H_L (\text{kJ mol}^{-1})$	$S_{298}^\circ (\text{J K}^{-1} \text{mol}^{-1})$
$[\text{B}(\text{CN})_4]^-$	136.7	540.8	542.0	225.4
$[\text{B}(\text{O}-\text{C}_6\text{H}_4-\text{CN})_4]^-$ (3)	571.6	383.6	384.8	816.9
$[\text{B}\{\text{O}-\text{C}_6\text{H}_3-(\text{CN})_2\}_4]^-$ (4)	604.8	378.5	379.7	862.1
$[\text{H}-\text{B}(\text{O}-\text{C}_{12}\text{H}_8-\text{CN})_3]^-$ (5)	737.2	361.4	362.6	1042.2
$[\text{B}(\text{O}-\text{C}_{12}\text{H}_8-\text{CN})_4]^-$ (6)	963.4	339.9	341.1	1349.7

$$U_{\text{pot}} = 2 \cdot 1 \left( \frac{117.3}{\sqrt[3]{V_m}} + 51.9 \text{ kJ mol}^{-1} \right), \quad \Delta H_L = U_{\text{pot}} + 1 \left( \frac{3}{2} - 2 \right) RT + 1 \left( \frac{6}{2} - 2 \right) RT, \quad S_{298}^\circ = 1360V_m + 15 \text{ J K}^{-1} \text{mol}^{-1},$$

corrected Hoffmann's volumina are used.<sup>[52]</sup>

As expected with increasing anion volumes of the new sodium borates the lattice potential energies ( $U_{\text{pot}}$ ), as well as the lattice enthalpies ( $\Delta H_L$ ), decrease. The standard entropies ( $S_{298}^\circ$ ), which are proportional to the anion volumes, increase along the series  $[\text{B}(\text{CN})_4]^-$  ( $225.4 \text{ J K}^{-1} \text{mol}^{-1}$ ) <  $[\text{B}(\text{O}-\text{C}_6\text{H}_4-\text{CN})_4]^-$  ( $816.9 \text{ J K}^{-1} \text{mol}^{-1}$ ) <  $[\text{B}\{\text{O}-\text{C}_6\text{H}_3-(\text{CN})_2\}_4]^-$  ( $862.1 \text{ J K}^{-1} \text{mol}^{-1}$ ) <  $[\text{H}-\text{B}(\text{O}-\text{C}_{12}\text{H}_8-\text{CN})_3]^-$  ( $1042.2 \text{ J K}^{-1} \text{mol}^{-1}$ ) and  $[\text{B}(\text{O}-\text{C}_{12}\text{H}_8-\text{CN})_4]^-$  ( $1349.7 \text{ J K}^{-1} \text{mol}^{-1}$ ).

## Conclusions

Four different cyano-functionalized borates with aromatic spacer groups were synthesized from  $\text{NaBH}_4$  and their respective hydroxynitriles. Beside the already known  $\text{Na}[\text{B}(\text{O}-\text{C}_6\text{H}_4-\text{CN})_4]$ , the sodium borates  $\text{Na}[\text{B}\{\text{O}-\text{C}_6\text{H}_3-(\text{CN})_2\}_4]$ ,  $\text{Na}[\text{H}-\text{B}(\text{O}-\text{C}_{12}\text{H}_8-\text{CN})_3]$  and  $\text{Na}[\text{B}(\text{O}-\text{C}_{12}\text{H}_8-\text{CN})_4]$  are accessible via this reaction method. It was shown that two of the three utilized starting compounds are easily preparable in bulk. The crystal structure of  $\text{HO}-\text{C}_6\text{H}_3-(\text{CN})_2$  as well as a new modification of  $\text{HO}-\text{C}_{12}\text{H}_8-\text{CN}$  in the crystal phase were also characterized by X-ray diffractometry. Coordination polymer networks without solvent molecules coordinating at the cation and a three-dimensional extension were obtained from the sodium salts of  $[\text{B}(\text{O}-\text{C}_6\text{H}_4-\text{CN})_4]^-$  and the novel  $[\text{H}-\text{B}(\text{O}-\text{C}_{12}\text{H}_8-\text{CN})_3]^-$ , while  $\text{Na}[\text{B}\{\text{O}-\text{C}_6\text{H}_3-(\text{CN})_2\}_4]$  results in a two-dimensional network that is coordinated by thf molecules. The phenyl-, respectively biphenyl-, groups were found as dominant structure-directing units that generate potential voids in the coordination networks. It was found that the anions coordinate the sodium cations preferably with strong dative metal $\cdots$ nitrogen ( $\text{M}\cdots\text{NC}$ ) bonds.

Crystallization from thf results in an additional coordination of the solvent to the cation, while acetonitrile was found to remain uncoordinated in the crystal structures, which promotes coordination of the borate oxygen atoms to the cation. As shown by nitrogen sorption experiments, the solvent filled voids in the three-dimensional networks of Na[B(O-C<sub>6</sub>H<sub>4</sub>-CN)<sub>4</sub>] collapse after removal of the guest molecules, whereas Na[H-B(O-C<sub>12</sub>H<sub>8</sub>-CN)<sub>3</sub>] represents a porous coordination network with a surface area up to 131 m<sup>2</sup> g<sup>-1</sup>. Therefore, salts of extended cyano borates offer a new class of porous coordination polymers.

## Experimental

**General Information.** All manipulations were carried out under oxygen- and moisture-free conditions under argon using standard Schlenk or drybox techniques.

Dichloromethane and acetonitrile were refluxed over CaH<sub>2</sub>, thf and Et<sub>2</sub>O were dried over Na/benzophenone and freshly distilled prior to use. DMF was dried over molecular sieves and distilled prior to use. Thionyl chloride (ACROS) and phosphoryl chloride (Merck) were distilled under argon atmosphere prior to use. 5-Hydroxyisophthalic acid (ABCR) and ZnCl<sub>2</sub> (Riedel-de-Haën) were dried *in vacuo* at 120 °C and stored under argon. 4-Bromobenzonitrile (Fluorochem) and 4-hydroxybenzonitrile (Alfa Aeser) were sublimated *in vacuo* at 80 °C and stored under argon. Aluminium powder (Laborchemie Apolda), magnesium (Merck), iodine (Laborchemie Apolda), NaBH<sub>4</sub> (Merck), PPh<sub>3</sub> (Fluka), PdCl<sub>2</sub> (ABCR) and ammonia solution (25%, Th. Geyer) were used as received.

**NMR:** <sup>1</sup>H, <sup>11</sup>B and <sup>13</sup>C spectra were obtained on Bruker AVANCE 250 (250 MHz), AVANCE 300 (300 MHz) spectrometer and were referenced externally. CDCl<sub>3</sub> and DMSO-d<sub>6</sub> were dried over CaH<sub>2</sub>.

**IR:** Nicolet 380 FT-IR with a Smart Orbit ATR device was used.

**Raman:** Bruker VERTEX 70 FT-IR with RAM II FT-Raman module, equipped with a Nd:YAG laser (1064 nm), or Kaiser Optical Systems RXN1-785 nm was used.

**CHN analyses:** Analysator Flash EA 1112 from Thermo Quest or C/H/N/S-Mikronalysator TruSpec-932 from Leco was used.

**DSC:** DSC 823e from Mettler-Toledo (Heating-rate 5 °C/min) was used.

A sample of approximately 3 to 5 mg was placed in an aluminium crucible. The closed crucible was placed in the furnace. The closed furnace was flushed with nitrogen and the sample was measured using a heating rate of 5 °C per minute. The heat flow is calculated based on a two point calibration (melting points of In and Zn) using the Mettler-Toledo STARe Software.

Decomposition Temperatures in the experimental part are in relation to the measurements done this way.

**Melting Point-Measurement.** Melting points were detected on EZ-Melt MPA120 (Heating-rate 5 °C/min).

**TGA-Measurement** was done on Setaram LapSys 1600 TGA-DSC under Argon atmosphere (Heating-rate 5 °C/min).

**Nitrogen Sorption** experiments were done on a Thermo Sorptomatic 1990 at -196 °C. The sample (approximately 500 to 600 mg) was weight into a glass burette in a glove box and was activated at 70 °C in high vacuum over night. Measurements were done at -196 °C using a volumetric experimental setup.



**X-ray Structure Determination:** X-ray quality crystals were selected in Fomblin YR-1800 perfluoroether (Alfa Aesar) at ambient temperatures. The samples were cooled to 173(2) K during measurement. The data were collected on a Bruker Apex Kappa-II CCD diffractometer using graphite-monochromated Mo K $\alpha$  radiation ( $\lambda = 0.71073$  Å). The structures were solved by direct methods (*SHELXS-97*) and refined by full-matrix least squares procedures (*SHELXL-97*). Semi-empirical absorption corrections were applied (*SADABS*). All non hydrogen atoms were refined anisotropically, hydrogen atoms were included in the refinement at calculated positions using a riding model.

The position of an acetonitrile molecule in **3** was found to be disordered and was split in two parts. The occupancy of each part was refined freely (C29/C30/N5: 0.765(8)/0.235(8)).

**Synthesis of HO-C<sub>6</sub>H<sub>3</sub>-(CONH<sub>2</sub>)<sub>2</sub>.** 5-Hydroxyisophthalic acid (5.46 g, 30 mmol, 1 equiv.) was placed into a Schlenk flask and dissolved in 150 ml thf. To this solution thionyl chloride (30 ml, 49.2 mmol, 1.64 equiv.) and 1 ml DMF were added. A reflux condenser with a bubble counter was fixed upon the flask and the reaction mixture was heated to reflux until the evolution of gaseous by-product fades. Afterwards the solvent was removed *in vacuo* and the resulting oil was dissolved in 100 ml thf and dried *in vacuo* again. After drying for 30 min *in vacuo* a slightly greenish oil of raw 5-Hydroxy-benzene-1,3-dicarbonylchloride was obtained. The raw 5-Hydroxy-benzene-1,3-dicarbonylchloride was dissolved in 75 ml thf and placed into a dropping funnel. An aqueous ammonia solution (150 ml) was cooled to -40 °C and the thf solution of 5-Hydroxy-benzene-1,3-dicarbonylchloride was added dropwise under stirring. After addition of the ammonia a white precipitate was obtained at -40 °C. The suspension was allowed to warm up to -25 °C and stirred for further two hours without cooling. Removal of the solvents *in vacuo* results in a white solid. The precipitate was washed with 100 ml dist. water, three times with 20 ml CH<sub>2</sub>Cl<sub>2</sub> and three times with 20 ml thf. In the organic solvents a significant amount of the product was dissolved. For optimized yields the combined organic solutions were concentrated, the precipitated solid was filtered off and washed again with water, CH<sub>2</sub>Cl<sub>2</sub> and thf. The combined solid fractions were dried at 60 °C over night. Yield: 2.81 g (53 %). **T<sub>Mp</sub>** 306 °C. **Anal. calc. % (found):** C, 48.48 (48.12); H, 5.09 (4.88); N, 14.14 (13.76). **<sup>1</sup>H NMR** (DMSO-d<sub>6</sub>, 300 MHz, 25 °C, ppm):  $\delta = 9.85$  (s, br, -OH, 1H); 7.89 (s, br, -N-H, 2H); 7.79 (t, H<sub>2</sub>NCO-C-CH-C-CONH<sub>2</sub>, 1H, <sup>4</sup>J<sub>H-H</sub> = 1.43 Hz); 7.37 (d, -CH-C-OH, 2H, <sup>4</sup>J<sub>H-H</sub> = 1.45 Hz); 7.35 (s, br, -N-H, 2H). **<sup>13</sup>C NMR** (DMSO-d<sub>6</sub>, 250 MHz, 25 °C, ppm):  $\delta = 167.9$  (s, -CONH<sub>2</sub>, 2C); 157.3 (s, -C-OH, 1C); 135.9 (s, -C-CONH<sub>2</sub>, 2C); 117.5 (s, -CH-C-OH, 2C); 117.2 (s, H<sub>2</sub>NCO-C-CH-C-CONH<sub>2</sub>, 1C). **IR** (ATR, cm<sup>-1</sup>):  $\tilde{\nu} = 3340$  (m), 3188 (s), 3070 (s), 2845 (m), 2725 (m), 2594 (w), 1686 (m), 1660 (s), 1622 (s), 1579 (s), 1504 (s), 1441 (s), 1392 (s), 1352 (s), 1304 (s), 1275 (s), 1234 (s), 1153 (m), 1117 (s), 1090 (s), 1039 (m), 999 (m), 968 (s), 920 (m), 883 (s), 760 (s), 677 (s), 631 (vs), 555 (vs). **Raman** (250 mW, 30 °C, 1000 scans, cm<sup>-1</sup>):  $\tilde{\nu} = 3202$  (2), 3102 (2), 3052 (4), 1661 (4), 1455 (9), 1432 (10), 1281 (5), 1131 (6), 1110 (8), 967 (5), 915 (2), 901 (4), 780 (3), 695 (5), 641 (3), 612 (3), 556 (4), 471 (5), 421 (3), 383 (4), 363 (7), 267 (6), 219 (8), 192 (9), 151 (10).

**Synthesis of HO-C<sub>6</sub>H<sub>3</sub>-(CN)<sub>2</sub> (1).** In a Schlenk flask 20 ml DMF was cooled with an ice bath to 0 °C. Freshly distilled phosphoryl chloride (3.3 ml, 36 mmol, 3 equiv.) was added dropwise under stirring. To this stirred mixture 5-Hydroxy-benzene-1,3-dicarbonylamide (2.16 g, 12 mmol, 1 equiv.) dissolved in 30 ml DMF was added dropwise via dropping funnel. The solution was stirred for one hour at room temperature and three hours at 45 °C. The red coloured solution was poured into ice. A white precipitate was obtained and filtered off. The crude product was sublimated twice at 120 °C and 10<sup>-3</sup> mbar to obtain analytical pure product of 5-Hydroxyisophthalonitrile. Yield: 1.28 g (74 %). **T<sub>Mp</sub>** 251 °C. **Anal. calc. % (found):** C, 66.67 (66.17); H, 2.80 (3.20); N, 19.44 (18.81). **<sup>1</sup>H NMR** (DMSO-d<sub>6</sub>, 300 MHz, 25 °C, ppm):  $\delta = 11.01$  (s, br, -OH, 1H); 7.48 (t, NC-C-CH-C-CN, 1H, <sup>4</sup>J<sub>H-H</sub> = 1.42 Hz); 7.48 (d, -CH-C-OH, 2H, <sup>4</sup>J<sub>H-H</sub> = 1.26 Hz). **<sup>13</sup>C NMR** (DMSO-d<sub>6</sub>, 300 MHz, 25 °C, ppm):  $\delta = 158.3$  (s, -C-OH, 1C); 126.2 (s, NC-C-CH-C-CN, 1C); 123.5 (s, -CH-C-OH, 2C); 117.1 (s, -CN, 2C); 113.7 (s, -C-CN, 1C). **IR** (ATR, cm<sup>-1</sup>):  $\tilde{\nu} = 3283$  (s), 3093 (m), 3067 (m), 3051 (m), 2250 (m), 2236 (m), 1790 (w), 1715 (w), 1602 (s), 1589 (s), 1558 (s), 1483 (m), 1434 (s), 1325 (m), 1308 (s), 1224 (s), 1165 (s), 1113 (m), 1005 (m), 880 (s), 815 (w), 769 (w), 671 (s), 657 (m), 605 (m), 548 (m). **Raman** (1500 mW, 30 °C, 500 scans, cm<sup>-1</sup>):  $\tilde{\nu} = 3098$  (1), 3069 (1), 3052 (1), 2247 (10), 1650 (1), 1594 (1), 1482 (1), 1324 (1), 1312 (1), 1227 (1), 1164 (1), 1003 (1), 980 (1), 938 (1), 631 (1), 614 (1), 554 (1), 523 (1), 471 (1), 458 (1), 438 (1), 389 (1), 241 (1), 205 (1), 180 (1), 163 (1), 91 (6).

**Synthesis of MeO-C<sub>12</sub>H<sub>8</sub>-CN.** Magnesium (5.98 g, 0.246 mol, 1.5 equiv.) was placed into a three-necked flask with an argon inlet. A magnetic stirrer and freshly distilled thf (500 ml) were added to the magnesium. On the three-necked flask a reflux condenser with bubble counter and a dropping funnel were fixed. The dropping funnel was loaded with 4-Bromoanisole (45.93 g, 0.246 mol, 1.5 equiv.) dissolved in 50 ml thf. The mixture was slowly added to the suspension of magnesium in thf. While some of the magnesium fades the mixture warms up

to 50 °C after full addition. Full conversion to the Grignard-compound was achieved after heating to reflux for 3 h. The mixture was cooled to room temperature and anhydrous ZnCl<sub>2</sub> (66.96 g, 0.491 mol, 3 equiv.) was added slowly. The resulting suspension was stirred for 1 h and afterwards cooled with an ice bath to 0 °C. Addition of 4-Bromobenzonitrile (29.80 g, 0.164 mol, 1 equiv.) and Pd(PPh<sub>3</sub>)<sub>4</sub> (1.91 g, 1.65 mmol, 0.1 equiv.) results in a greyish yellow suspension that was stirred for 30 min at 0 °C. Thereafter it was stirred at room temperature for 3 h followed by refluxing for another 30 min. The reaction mixture was poured into a mixture of ice and diluted HCl (250 ml). After warming up to room temperature CH<sub>2</sub>Cl<sub>2</sub> was added until two phases appear with a yellow colouring in the CH<sub>2</sub>Cl<sub>2</sub>-phase and the aqueous phase was extracted further two times with 50 ml CH<sub>2</sub>Cl<sub>2</sub>. The isolated CH<sub>2</sub>Cl<sub>2</sub> phases were combined and dried *in vacuo*. The resulting precipitate was recrystallized from a mixture of 1:1 CH<sub>2</sub>Cl<sub>2</sub>/MeOH to give the crude product. Pure compound for analytical experiments was obtained after three times recrystallization. Yield of crude product: 25.37 g (74 %). **T<sub>mp</sub>** 101 °C. **Anal. calc. % (found):** C, 80.36 (81.07); H, 5.30 (5.43); N, 6.69 (6.22). **<sup>1</sup>H NMR** (CDCl<sub>3</sub>, 300 MHz, 25 °C, ppm): δ = 7.61-7.71 (m, –CH–CH–C–CN + –CH–C–CN, 4H); 7.51-7.57 (m, –CH–CH–C–OMe, 2H); 6.98-7.04 (m, –CH–C–OMe, 2H); 3.86 (s, –O–CH<sub>3</sub>, 3H). **<sup>13</sup>C NMR** (CDCl<sub>3</sub>, 300 MHz, 25 °C, ppm): δ = 160.3 (s, –C–OMe, 1C); 145.3 (s, –C–CH–CH–C–CN, 1C); 132.7 (s, –C–CH–C–CN, 2C); 131.6 (s, –C–CH–CH–C–OMe, 1C); 128.5 (s, –CH–CH–C–CN, 2C); 127.2 (s, –CH–CH–C–OMe, 2C); 119.2 (s, –CN, 1C); 114.7 (s, –CH–C–OMe, 2C); 110.2 (s, –C–CN, 1C); 55.5 (s, –O–CH<sub>3</sub>, 1C). **IR** (ATR, cm<sup>-1</sup>):  $\tilde{\nu}$  = 2958 (w), 2920 (m), 2842 (w), 2223 (m), 1605 (s), 1575 (w), 1515 (w), 1494 (s), 1470 (m), 1446 (m), 1396 (m), 1313 (w), 1306 (w), 1294 (m), 1275 (m), 1241 (s), 1176 (s), 1109 (m), 1036 (s), 1020 (s), 999 (m), 854 (m), 822 (vs), 810 (vs), 783 (m), 769 (m), 737 (m), 718 (m), 636 (m), 627 (m), 563 (s), 552 (s), 536 (s). **Raman** (500 mW, 25 °C, 500 scans, cm<sup>-1</sup>):  $\tilde{\nu}$  = 3078 (1), 2231 (2), 1611 (10), 1586 (1), 1524 (1), 1321 (1), 1302 (2), 1295 (2), 1249 (1), 1187 (4), 845 (1), 819 (1), 779 (1), 749 (1), 657 (1), 645 (1), 528 (1), 490 (1), 427 (1), 423 (1), 340 (1), 243 (1), 178 (1).

**Synthesis of HO–C<sub>12</sub>H<sub>8</sub>–CN (2).** A three-necked flask was loaded with aluminium powder (6.54 g, 0.242 mol, 2 equiv.). The powder was suspended in 500 ml freshly distilled CH<sub>3</sub>CN. A reflux condenser with bubble counter and a magnetic stirrer were added to the flask. Iodine (92.32 g, 0.364 mol, 3 equiv.) was slowly added in 5 g portions while the mixture was cooled with an ice bath. At the beginning a yellowish brown suspension was formed and the reaction mixture heats up. After full addition of the iodine the brown precipitate faded resulting in a red solution that was refluxed for 30 min. At room temperature 4-Methoxy-4'-cyano-1,1'-biphenyl (25 g, 0.119 mol, 1 equiv.) was added and the reaction mixture was heated to reflux for 4 h. The mixture was poured into ice/water and acidified with diluted H<sub>2</sub>SO<sub>4</sub> to pH = 0-1. A white precipitate was formed and filtered off and washed with water. The precipitate was dissolved in Et<sub>2</sub>O while a grey byproduct remains. The solution was washed with an aqueous Na<sub>2</sub>S<sub>2</sub>O<sub>3</sub>-solution and water. After removal of the solvent *in vacuo* a white precipitate was obtained that was washed with 25 ml of CHCl<sub>3</sub>. Sublimation at 10<sup>-3</sup> mbar and 150 °C gives the crystalline product. Yield: 15.64 g (67 %). **T<sub>mp</sub>** 198 °C. **Anal. calc. % (found):** C, 79.98 (79.99); H, 4.65 (4.61); N, 7.17 (6.49). **<sup>1</sup>H NMR** (DMSO-d<sub>6</sub>, 300 MHz, 25 °C, ppm): δ = 9.78 (s, –OH, 1H); 7.74-7.85 (m, –CH–CH–C–CN + –CH–C–CN, 4H); 7.56-7.61 (m, –CH–CH–C–OH, 2H); 6.86-6.92 (m, –CH–C–OH, 2H). **<sup>13</sup>C NMR** (CDCl<sub>3</sub>, 300 MHz, 25 °C, ppm): δ = 158.4 (s, –C–OH, 1C); 144.6 (s, –C–CH–CH–C–CN, 1C); 132.7 (s, –CH–C–CN, 2C); 128.8 (s, –C–CH–CH–C–OH, 1C); 128.3 (s, –CH–CH–C–CN, 2C); 126.5 (s, –CH–CH–C–OH, 2C); 119.1 (s, –CN, 1C); 116.0 (s, –CH–C–OH, 2C); 108.7 (s, –C–CN, 1C). **IR** (ATR, cm<sup>-1</sup>):  $\tilde{\nu}$  = 3377 (m), 2228 (m), 1602 (m), 1588 (m), 1557 (w), 1520 (w), 1493 (m), 1437 (m), 1403 (w), 1356 (w), 1342 (m), 1296 (w), 1275 (m), 1204 (s), 1179 (s), 1122 (m), 1106 (m), 1004 (w), 975 (w), 957 (w), 938 (w), 857 (m), 827 (vs), 813 (vs), 779 (m), 738 (m), 716 (m), 599 (s), 561 (vs), 533 (vs). **Raman** (500 mW, 25 °C, 500 scans, cm<sup>-1</sup>):  $\tilde{\nu}$  = 3076 (1), 2237 (3), 1609 (10), 1597 (2), 1529 (1), 1298 (3), 1288 (1), 1217 (1), 1190 (4), 1182 (1), 852 (1), 841 (1), 833 (1), 787 (1), 747 (1), 645 (1), 496 (1), 452 (1), 427 (1), 412 (1), 328 (1), 280 (1), 239 (1), 205 (1), 160 (1).

**Synthesis of Na[B(O–C<sub>6</sub>H<sub>4</sub>–CN)<sub>4</sub>] (3).** 4-Hydroxy-benzonitrile (3.5 g, 29.4 mmol, 5 equiv.) dissolved in thf (20 ml) was rapidly added to a stirred suspension of NaBH<sub>4</sub> (0.223 g, 5.9 mmol, 1 equiv.) in thf (40 ml) at room temperature. The resulting suspension was heated to reflux for three hours. A colourless solid was received after filtering the suspension and the removal of the solvent *in vacuo*. This crude product was washed two times with 10 ml of Et<sub>2</sub>O to remove the excess of 4-Hydroxy-benzonitrile. Pure product of Na[B(O–C<sub>6</sub>H<sub>4</sub>–CN)<sub>4</sub>]-4.5thf was obtained after recrystallization from a hot saturated solution in thf. After isolation and drying of the crystals at 10<sup>-3</sup> mbar and 120 °C for four hours pure solvent free Na[B(O–C<sub>6</sub>H<sub>4</sub>–CN)<sub>4</sub>] was obtained. Yield: 2.35 g (78 %). Crystals of the coordination polymer Na[B(O–C<sub>6</sub>H<sub>4</sub>–CN)<sub>4</sub>]-CH<sub>3</sub>CN, suitable for X-ray crystallography, were obtained from a cold saturated solution in CH<sub>3</sub>CN that was allowed to warm up to room temperature. For analysis guest molecules of CH<sub>3</sub>CN were removed *in vacuo* under slow heating up to 150 °C with a heat grow of 25 °C/hour. Yield: 1.75 g (58 %). **T<sub>Dec</sub>** 292 °C (DSC). **Anal. calc. % (found):** C 66.43 (66.01); H 3.19 (3.23); N 11.07 (10.41). **<sup>1</sup>H NMR** (DMSO-d<sub>6</sub>, 300 MHz, 25 °C, ppm): δ = 7.57-7.48 (m, –CH–C–CN, 8H); 7.13-7.02 (m, –CH–C–O, 8H). **<sup>13</sup>C NMR** (DMSO-d<sub>6</sub>, 300 MHz, 25 °C, ppm): δ = 165.4 (s, –C–O, 1C); 133.1 (s, –C–C–CN, 1C); 119.5 (s, –CN, 1C); 119.1 (s, –C–C–O, 1C); 100.5 (s, –C–CN, 1C). **<sup>11</sup>B-NMR** (DMSO-d<sub>6</sub>, 300 MHz, 25 °C, ppm): δ = 2.57 (s). **IR** (ATR, cm<sup>-1</sup>):  $\nu$  = 2231 (m), 2220 (m), 1599 (s), 1504 (s), 1420 (w), 1290 (m), 1258 (vs),

1167 (m), 1107 (w), 1017 (s), 988 (s), 961 (s), 931 (vs), 872 (m), 839 (vs), 809 (s), 747 (m), 729 (m), 699 (m), 677 (m), 659 (m), 633 (w), 604 (m), 546 (vs). **Raman** (100 mW, 250 Scans, 25 °C, cm<sup>-1</sup>):  $\tilde{\nu}$  = 3204 (1), 3081 (2), 3064 (1), 3000 (1), 2577 (1), 2243 (7), 2234 (9), 2220 (10), 1611 (8), 1601 (10), 1519 (1), 1421 (1), 1320 (1), 1298 (1), 1199 (5), 1175 (7), 1108 (1), 998 (2), 946 (1), 935 (1), 903 (7), 873 (1), 852 (1), 837 (1), 817 (1), 776 (6), 729 (1), 719 (1), 699 (1), 679 (1), 651 (1), 634 (1), 619 (1), 607 (1), 551 (1), 498 (2), 434 (1), 410 (1), 386 (1), 267 (1), 244 (2).

**Synthesis of Na[B{O-C<sub>6</sub>H<sub>3</sub>(CN)<sub>2</sub>]<sub>4</sub>] (4).** 5-Hydroxy-isophthalonitrile (1.06 g, 8.67 mmol, 4.25 equiv.) was dissolved in 20 ml thf and added to a suspension of NaBH<sub>4</sub> (66 mg, 1.75 mmol, 1 equiv.) in 30 ml thf. The reaction mixture was heated to reflux for three hours until no more hydrogen evolution was observable. The solvent was removed *in vacuo* and 40 ml CH<sub>3</sub>CN were added. Heating to reflux for further four hours led to full exchange of the hydride. The excess of 5-hydroxy-isophthalonitrile was separated from the reaction mixture by crystallization from a cold concentrated CH<sub>3</sub>CN solution. The solvent of the residual solution was removed *in vacuo*. Recrystallization from a thf/CH<sub>2</sub>Cl<sub>2</sub>-2:1-mixture obtains solvated Na[B{O-C<sub>6</sub>H<sub>3</sub>(CN)<sub>2</sub>]<sub>4</sub>. Removal of the guest molecules took place at 10<sup>-3</sup> mbar and 150 °C. Yield: 0.667 g (63 %). **T<sub>Dec</sub>** (onset) 318 °C. **Anal. calc. % (found):** C, 63.39 (62.75); H, 1.99 (2.03); N, 18.48 (17.86). **<sup>1</sup>H NMR** (DMSO-d<sub>6</sub>, 300 MHz, 25 °C, ppm):  $\delta$  = 7.76 (t, NC-C-CH-C-CN, 1H, <sup>4</sup>J<sub>H-H</sub> = 1.43 Hz); 7.70 (d, -CH-C-O, 2H, <sup>4</sup>J<sub>H-H</sub> = 1.43 Hz). **<sup>13</sup>C NMR** (DMSO-d<sub>6</sub>, 300 MHz, 25 °C, ppm):  $\delta$  = 157.1 (s, -C-O, 1C); 126.4 (s, NC-C-CH-C-CN, 1C); 123.6 (s, -CH-C-OH, 2C); 117.3 (s, -CN, 2C); 113.4 (s, -C-CN, 1C). **<sup>11</sup>B NMR** (DMSO-d<sub>6</sub>, 300 MHz, 25 °C, ppm):  $\delta$  = 2.34 (s). **IR** (ATR, cm<sup>-1</sup>):  $\tilde{\nu}$  = 3083 (w), 2235 (m), 1580 (s), 1553 (w), 1432 (s), 1321 (s), 1309 (s), 1255 (m), 1159 (s), 1017 (vs), 997 (s), 984 (s), 942 (s), 921 (vs), 871 (s), 671 (s), 618 (m), 576 (m). **Raman** (1500 mW, 30 °C, 500 scans, cm<sup>-1</sup>):  $\tilde{\nu}$  = 3078 (1), 2238 (10), 1588 (3), 1452 (1), 1439 (1), 1351 (3), 1331 (1), 1313 (1), 1255 (1), 1125 (1), 1177 (2), 1030 (1), 997 (5), 983 (6), 932 (1), 614 (2), 573 (1), 549 (1), 521 (1), 467 (2), 440 (1), 379 (2), 207 (1).

**Synthesis of Na[H-B(O-C<sub>12</sub>H<sub>8</sub>-CN)<sub>3</sub>] (5).** In a Drybox one Schlenk flask was loaded with NaBH<sub>4</sub> (0.064 g, 1.69 mmol, 1 equiv.) and a second one with HO-C<sub>12</sub>H<sub>8</sub>-CN (1.35 g, 6.94 mmol, 4.1 equiv.). The 4-Hydroxy-4'-cyano-1,1'-biphenyl was dissolved in 25 ml thf and this solution added to the NaBH<sub>4</sub>. A reflux condenser with a bubble counter was fixed on the flask and the reaction mixture was heated to reflux for 4 h until no more hydrogen evolution was observable. When the reaction is over a white precipitate was obtained suspended in a yellow solution. The crude product was filtered off and washed two times with 10 ml thf. Pure compound for analytical experiments was obtained after recrystallization from acetonitrile. Drying of the crystals at 10<sup>-3</sup> mbar and 70 °C for 1 hour gave solvent free Na[H-B(O-C<sub>12</sub>H<sub>8</sub>-CN)<sub>3</sub>]. Yield: 0.669 g (64 %). **T<sub>Dec</sub>** (onset) 314 °C. **Anal. calc. % (found):** C, 75.87 (75.45); H, 4.08 (4.04); N, 6.45 (6.21). **<sup>1</sup>H-NMR** (DMSO-d<sub>6</sub>, 300 MHz, 25 °C, ppm):  $\delta$  = 7.74-7.84 (m, -CH-CH-C-CN + -CH-C-CN, 12H); 7.50-7.57 (m, -CH-CH-C-O-B, 6H); 6.97-7.04 (m, -CH-C-O-B, 6H); 3.91 (br, -B-H, 1H). **<sup>13</sup>C NMR** (DMSO-d<sub>6</sub>, 300 MHz, 25 °C, ppm):  $\delta$  = 161.46 (s, -C-O-B, 3C); 145.36 (s, -C-CH-CH-C-CN, 3C); 132.60 (s, -CH-C-CN, 6C); 127.46 (s, -CH-CH-C-CN, 6C); 126.46 (s, -C-CH-CH-C-O-B, 3C); 126.17 (s, -CH-CH-C-O-B, 6C); 119.24 (s, -CN, 3C); 118.70 (s, -CH-C-O-B, 6C); 107.92 (s, -C-CN, 3C). **<sup>11</sup>B NMR** (DMSO-d<sub>6</sub>, 300 MHz, 25 °C, ppm):  $\delta$  = 4.34 (br). **IR** (ATR, cm<sup>-1</sup>):  $\tilde{\nu}$  = 3034 (w), 2238 (m), 2224 (m), 1596 (s), 1558 (w), 1538 (w), 1520 (m), 1505 (w), 1489 (s), 1456 (w), 1424 (w), 1403 (w), 1311 (w), 1260 (s), 1178 (m), 1145 (s), 1097 (s), 1023 (m), 1004 (w), 903 (s), 866 (s), 853 (s), 817 (vs), 774 (s), 735 (s), 715 (s), 682 (m), 665 (m), 649 (m), 632 (m), 561 (m), 548 (s), 531 (s). **Raman** (500 mW, 25 °C, 500 scans, cm<sup>-1</sup>):  $\tilde{\nu}$  = 2249 (2), 2233 (2), 1622 (1), 1609 (10), 1538 (1), 1326 (1), 1297 (3), 1290 (2), 1190 (4), 1155 (1), 1103 (1), 1026 (1), 1013 (1), 930 (1), 880 (1), 821 (1), 793 (1), 745 (1), 645 (1), 426 (1), 410 (1).

**Synthesis of Na[B(O-C<sub>12</sub>H<sub>8</sub>-CN)<sub>4</sub>] (6).** A Schlenkflask was loaded with Na[H-B(O-C<sub>12</sub>H<sub>8</sub>-CN)<sub>3</sub>] (1.5 g, 2.43 mmol, 1 equiv.) and HO-C<sub>12</sub>H<sub>8</sub>-CN (0.95 g, 4.87 mmol, 2 equiv.) dissolved in 50 ml CH<sub>3</sub>CN was added. A reflux condenser with a bubble counter was fixed on the flask. The reaction mixture was refluxed for 7 h until the forming of hydrogen faded. The resulting suspension was filtered and the solvent of the filtrate was removed *in vacuo* and dried at 100 °C. After washing three times with 50 ml Et<sub>2</sub>O the product was dried at 70 °C *in vacuo* for 3 h. Yield: 1.53 g (78 %). **T<sub>Dec</sub>** (onset) 301 °C. **Anal. calc. % (found):** C, 77.05 (76.56); H, 3.98 (4.29); N, 6.91 (6.73). **<sup>1</sup>H NMR** (DMSO-d<sub>6</sub>, 300 MHz, 25 °C, ppm):  $\delta$  = 7.69-7.81 (m, -CH-CH-C-CN + -CH-C-CN, 16H); 7.43-7.51 (m, -CH-CH-C-O-B, 8H); 7.16-7.23 (m, -CH-C-O-B, 8H). **<sup>13</sup>C NMR** (DMSO-d<sub>6</sub>, 300 MHz, 25 °C, ppm):  $\delta$  = 159.19 (s, -C-O-B, 4C); 145.14 (s, -C-CH-CH-C-CN, 4C); 132.55 (s, -CH-C-CN, 8C); 127.43 (s, -CH-CH-C-CN, 8C); 127.22 (s, -C-CH-CH-C-O-B, 4C); 126.26 (s, -CH-CH-C-O-B, 8C); 119.18 (s, -CH-C-O-B + -CN, 12C); 108.09 (s, -C-CN, 4C). **<sup>11</sup>B NMR** (DMSO-d<sub>6</sub>, 300 MHz, 25 °C, ppm):  $\delta$  = 2.87 (s). **IR** (ATR, cm<sup>-1</sup>):  $\tilde{\nu}$  = 2224 (m), 1597 (m), 1557 (w), 1536 (w), 1489 (s), 1457 (w), 1421 (w), 1391 (w), 1309 (w), 1285 (m), 1249 (s), 1175 (m), 1109 (m), 1026 (m), 1011 (m), 945 (vs), 934 (vs), 880 (m), 853 (m), 821 (vs), 770 (m), 737 (m), 714 (m), 645 (m), 562 (s), 533 (vs). **Raman** (1000 mW, 25 °C, 500 scans, cm<sup>-1</sup>):  $\tilde{\nu}$  = 2237 (2), 2219 (1), 1615 (1), 1598 (10), 1326 (1), 1287 (4), 1179 (4), 911 (1), 784 (1), 520 (1), 414 (1), 398 (1), 304 (1), 207 (1), 105 (1).

## Acknowledgement

Financial support by the DFG is gratefully acknowledged. We are indebted to Fabian Reiß (University Rostock) and Dr. Ronald Wustrack (University Rostock) for the measurement of Raman spectra.

## References

- 
- [1] a) B. Chen, Y. Yang, F. Zapata, G. Lin, G. Qian, E. B. Lobkovsky, *Adv. Mater.* **2007**, *19*, 1693–1696; b) S. M. Holmes, G. S. Girolami, *J. Am. Chem. Soc.* **1999**, *121*, 5593–5594; c) V. Niel, J. M. Martinez-Agudo, M. C. Muñoz, A. B. Gaspar, J. A. Real, *Inorg. Chem.* **2001**, *40*, 3838–3839; d) S. Kitagawa, R. Kitaura, S. Noro, *Angew. Chem. Int. Ed.* **2004**, *43*, 2334–2375.
- [2] a) B. F. Hoskins, R. Robson, *J. Am. Chem. Soc.* **1990**, *112*, 1546–1554; b) L. G. Beauvais, J. R. Long, *J. Am. Chem. Soc.* **2002**, *124*, 12096–12097; c) B. F. Hoskins, R. Robson, *J. Am. Chem. Soc.* **1989**, *111*, 5962–5964; d) S. Shimomura, R. Matsuda, T. Tsujino, T. Kawamura, S. Kitagawa, *J. Am. Chem. Soc.* **2006**, *128*, 16416–16417; e) T. Küppers, E. Bernhardt, H. Willner, H. W. Rohm, M. Köckerling, *Inorg. Chem.* **2005**, *44*, 1015–1022.
- [3] M. D. Dembo, L. E. Dunaway, J. S. Jones, E. A. Lepekhina, S. M. McCullough, J. L. Ming, X. Li, F. Baril-Robert, H. H. Patterson, C. A. Bayse, R. D. Pike, *Inorg. Chim. Acta* **2010**, *364*, 102–114.
- [4] a) Y. Sato, S. Ohkoshi, K. Arai, M. Tozawa, K. Hashimoto, *J. Am. Chem. Soc.* **2003**, *125*, 14590–14595; b) S. Ohkoshi, K. Arai, Y. Sato, K. Hashimoto, *Nat. Mater.* **2004**, *3*, 857–861; c) B. Nowicka, M. Rams, K. Stadnicka, B. Sieklucka, *Inorg. Chem.* **2007**, *46*, 8123–8125.
- [5] a) G. J. Halder, C. J. Kepert, B. Moubaraki, K. S. Murray, J. D. Cashion, *Science* **2002**, *298*, 1762–1765; b) K. Biradha, M. Fujita, *Angew. Chem. Int. Ed.* **2002**, *41*, 3392–3395; c) K. W. Chapman, P. J. Chupas, E. R. Maxey, J. W. Richardson, *Chem. Commun.* **2006**, 4013–4015.
- [6] M. V. Bennett, L. G. Beauvais, M. P. Shores, J. R. Long, *J. Am. Chem. Soc.* **2001**, *123*, 8022–8032.
- [7] M. Karsch, H. Lund, A. Schulz, A. Villinger, K. Voss, *Eur. J. Inorg. Chem.* **2012**, *33*, 5542–5553.
- [8] J. Harloff, M. Karsch, H. Lund, A. Schulz, A. Villinger, *Eur. J. Inorg. Chem.* **2013**, *24*, 4243–4250.
- [9] J. Harloff, M. Karsch, A. Schulz, A. Villinger, *Eur. J. Inorg. Chem.* **2013**, accepted.
- [10] N. Malek, T. Maris, M. Simard, J. D. Wuest, *J. Am. Chem. Soc.* **2005**, *127*, 5910–5916.
- [11] E. Bernhardt, G. Henkel, H. Willner, *Z. Anorg. Allgem. Chem.* **2000**, *626*, 560–568.
- [12] a) Y. Y. Karabach, M. Fatima, C. Guedes da Silva, M. N. Kopylovich, B. Gil-Hernandez, J. Sanchiz, A. M. Kirillov, A. J. L. Pombeiro, *Inorg. Chem.* **2010**, *49*, 11096–11105; b) H. Dan, S. Nishikiori, O. Yamamuro, *Dalton Trans.* **2011**, *40*, 1168–1174; c) P. K. Thallapally, R. Kishan Motkuri, C. A. Fernandez, B. P. McGrail, G. S. Behrooz, *Inorg. Chem.* **2010**, *49*, 4909–4915.
- [13] a) S. R. Batten, B. F. Hoskins, R. Robson, *New J. Chem.* **1998**, 173–175; b) B. F. Abrahams, S. R. Batten, B. F. Hoskins, R. Robson, *Inorg. Chem.* **2003**, *42*, 2654–2664.
- [14] a) F.-Q.Liu, T. D. Tilley, *Inorg. Chem.* **1997**, *36*, 5090–5096; b) F.-Q.Liu, T. D. Tilley, *Chem. Commun.* **1998**, 103–104.
- [15] a) M. Mazik, W. Sicking, *Chem. Eur. J.* **2001**, *7*, 664–670; b) W. Thiel, R. Mayer, E.-A. Jauer, H. Modrow, H. Dost, *J. f. prakt. Chemie* **1986**, *328*, 497–514.
- [16] B. Heinrich, D. Guillon, *Mol. Cryst. Liq. Cryst.* **1995**, *268*, 21–43.
- [17] P. Pyykkö, M. Atsumi, *Chem. Eur. J.* **2009**, *15*, 12770–12779.
- [18] K. S.W. Sing, D. H. Everett, R. A. W. Haul, L. Mouscou, R. A. Pierotti, J. Rouquerol, T. Siemieniowska, *Pure Appl. Chem.* **1985**, *57*, 603–619.
- [19] a) F. Rouquerol, J. Rouquerol, K. S. W. Sing, *Adsorption by Powders and Porous Solids*, Academic Press, London, UK, **1999**; b) S. Lowell, J. Shields, M. A. Thomas, M. Thommes, *Characterization of Porous Solids and Powders: Surface Area, Pore Size and Density*, Springer, The Netherlands, **2004**.
- [20] a) V. M. Goldschmidt, *Chem. Ber.* **1927**, *60*, 1263–1296; b) R. D. Shannon, *Acta Cryst.* **1976**, *A32*, 751–767; c) L. Glasser, H. D. B. Jenkins, *Inorg. Chem.* **2008**, *47*, 6195–6202.
- [21] a) H. D. B. Jenkins, L. Glasser, T. M. Klapötke, M.-J. Crawford, K. K. Bhasin, J. Lee, G. J. Schrobilgen, L. S. Sunderlin, J. F. Liebman, *Inorg. Chem.* **2004**, *43*, 6238–6248; b) H. D. Jenkins, J. F. Liebman, *Inorg. Chem.* **2005**, *44*, 6359–6372.
- [22] A. Bernsdorf, H. Brand, R. Hellmann, M. Köckerling, A. Schulz, A. Villinger, K. Voss, *J. Am. Chem. Soc.* **2009**, *131*, 8958–8970.

---

[23] D. W. M. Hofmann, *Acta Cryst.* **2002**, B58, 489–493.

[24] U. Preiss, J. M. Slattery, I. Crossing, *Ind. Eng. Chem. Res.* **2009**, 48, 2290–2296.

## Liste der Publikationen

1. Markus Karsch, Henrik Lund, Axel Schulz, Alexander Villinger, Karsten Voss.  
*Eur. J. Inorg. Chem.* **2012**, 5542-5553.
2. Jörg Harloff, Markus Karsch, Henrik Lund, Axel Schulz, Alexander Villinger.  
*Eur. J. Inorg. Chem.* **2013**, 4243-4250.
3. Jörg Harloff, Markus Karsch, Axel Schulz, Alexander Villinger.  
*Eur. J. Inorg. Chem.* **2014**, 896-907.
4. Jörg Harloff, Markus Karsch, Henrik Lund, Axel Schulz, Alexander Villinger.  
*Z. Anorg. Allg. Chem.* **2014**, angenommen.

## Posterbeiträge

1. New CN-functionalized Ionic Liquids Based on Borate Anions.  
Frühjahrssymposium Rostock, März 2012.  
M. Karsch, A. Villinger, J. Harloff, A. Schulz.
2. A Nitrile-rich Borate Anion – Application in Ionic Liquids.  
Norddeutsches Doktorandenkolloquium Bremen, September 2013.  
M. Karsch, A. Villinger, J. Harloff, A. Schulz.

## **Wissenschaftlicher Lebenslauf**

### **Persönliche Daten**

Name: Markus Karsch  
Geburtsdatum: 06.11.1985  
Geburtsort: Rostock  
Staatsangehörigkeit: Deutsch

### **Studium**

10/2010 – 04/2014 Promotion im Arbeitskreis von Prof. Dr. Axel Schulz an der Universität Rostock  
10/2008 – 09/2010 Chemie – Studium an der Universität Rostock  
Diplomarbeit „Synthese neuer schwach koordinierender Lewis-Säure-Lewis-Base-Addukt-Anionen“  
Abschluss: Diplom  
10/2005 – 09/2008 Chemie – Studium an der Universität Rostock  
Abschluss: Vordiplom

### **Schulausbildung**

08/2002 – 07/2005 Fachgymnasium für Wirtschaft in Rostock Schmarl  
Abschluss: Allgemeine Hochschulreife  
08/1996 – 07/2002 Realschule Dummerstorf  
Abschluss: qualifizierter Realschulabschluss  
01/1996 – 07/1996 Grundschule Kavelstorf  
08/1992 – 12/1995 Grundschule Gehlsdorf

### **Berufstätigkeit**

07/2008 – 08/2008 Studentische Hilfskraft bei Dr. Detlef Heller, Leibniz-Institut für Katalyse e.V.  
10/2010 – 12/2013 Wissenschaftlicher Mitarbeiter am Institut für Chemie der Universität Rostock, Lehrstuhl für Anorganische und Elementorganische Chemie, Arbeitskreis Prof. Dr. Axel Schulz